Fatty Acid Profiling in Pharmaceutical Products by Liquid Chromatography-Mass Spectrometry-based Approaches

Dissertation

der Mathematisch-Naturwissenschaftlichen Fakultät

der Eberhard Karls Universität Tübingen

zur Erlangung des Grades eines

Doktors der Naturwissenschaften

(Dr. rer. nat.)

vorgelegt von

Matthias Olfert

aus Olpe

Tübingen

2024

Gedruckt mit Genehmigung der Mathematisch-Naturwissenschaftlichen Fakultät der Eberhard Karls Universität Tübingen.

Tag der mündlichen Qualifikation:	17.07.2024
Dekan:	Prof. Dr. Thilo Stehle
1. Berichterstatter/-in:	Prof. Dr. Michael Lämmerhofer
2. Berichterstatter/-in:	Prof. Dr. Matthias Gehringer

Table of Contents

Summary

Appropriate sensitive and selective analytical techniques and methods are of crucial importance for the in-depth characterization of unknown compounds in pharmaceutical drug substances and products, in order to prevent harm to patient's health. Even though the power of analytical methods are continuously evolving, unexpected and uncontrolled impurities continue to regularly lead to scandals in pharmaceutical manufacturing and show the ongoing lack of comprehensive quality control of drug substances and products. For this, liquid chromatography in form of (high)-performance liquid chromatography has been established as one of the most versatile analytical techniques in all stages of the product life cycle, from development to routine analysis. (U)HPLC analysis allows fast and efficient separation of drug substances, matrix components and impurities. Coupling with various detection techniques that are precisely tailored to the chemical properties of the respective compounds and analytical task is of utmost importance. Even though, mass spectrometric detection is often considered as the gold standard and all-in-one solution of many analytical problems, it often lacks in selectivity especially for isobaric and isomeric compounds which do not display characteristic fragmentation patterns. Therefore, this work shows how the utilization of different derivatization techniques and the implementation of orthogonal stationary phases and detectors improves identification of unknown compounds by further increasing sensitivity and selectivity.

The first part of the thesis shows the significance of lipid oxidation in pharmaceutical lipid formulations, generating a huge variety of oxidation products, which require comprehensive characterization as they are classified as impurities. For this, the combination of commonly used reversed-phase columns with innovative chiral polysaccharide stationary phases in a full-comprehensive two-dimensional liquid chromatography setup was established. This setup shows excellent shape-selectivity for isomers of conjugated fatty acids, compatibility and orthogonality of the used chiral and reversed-phase stationary phases. In this context, chiral polysaccharide columns show immaculate shape selectivity for fatty acid isomers under reversed-phase conditions, probably due to their complex three-dimensional structure. Furthermore, the complementarity of UV-detection to MS-detection is demonstrated, which allows double bond characterization of conjugated fatty acid isomers (distinction of di-, tri-, and tetraenes as well as E/Z isomerism) by UV spectra and identification of unknown oxylipins by characteristic MS2-spectra.

The second part displays the importance of chirality-determination for impurity profiling and for in-depth characterization of biotechnologically produced substances like teicoplanin. This has relevance, as for example in case of Teicoplanin, its antibacterial efficacy can be affected by its fatty acid sidechains. State-of-the-art chiral polysaccharide columns in combination with 1-naphthylamine-derivatization make the enantiomeric separation by liquid chromatography feasible. Thus, the enantiomeric separation of the *anteiso*-methyl branched fatty acid side-chain of Teicoplanin RS3 and hence its stereochemistry determination with custom synthesized standards is possible. Additionally, the excellent selectivity for achiral compounds is presented for the conformation and identification of previously unknown constitutional isomers.

The third part is focused in the development of a workflow for the determination of double bond positions by liquid chromatography coupled with tandem mass spectrometry. The derivatization with dimethyldisulfide allows the proposal of characteristic fragment ions of different (poly)unsaturated fatty acids and utilizes electrospray-ionization in negative mode. To obtain higher sensitivity and flexibility with regard to ionization-modes, 2,2'-dipyridyldisulfide was introduced as derivatization reagent, which allows detection of ω-end and carboxyl-end fragments in positive ion mode of fatty acids with up to two double bonds. This approach could be considered as a starting point for further optimization and investigation of other disulfide-based derivatization reagents.

Zusammenfassung

Zur Gewährleistung der Patientensicherheit ist die Verwendung von geeigneten analytischen Techniken und Methoden zur Charakterisierung unbekannter Veunreinigungen in Wirkstoffen und pharmazeutischen Produkten von immenser Bedeutung. Vor allem Änderungen in Synthese- und Herstellungsprozessen führten in den letzten Jahrzehnten gehäuft zu Skandalen in der pharmazeutischen Industrie, vor allem wenn die Überwachung durch die entsprechende Analytik nicht angepasst wurde. Flüssigchromatographische Techniken wie (Ultra)-Hochleistungsflüssigkeitschromatographie ((U)HPLC) hat sich aufgrund ihrer Vielseitigkeit als Standard für die Analytik über den gesamten „product life cycle“, beginnend mit der Entwicklung bis hin zur Routineanalytik, etabliert. (U)HPLC-Analysen erlauben eine schnelle und effiziente Trennung von Wirkstoffen, Hilfsstoffen und Verunreinigungen. Die Kopplung mit verschiedenen Detektionstechniken, die anhand der chemischen Eigenschaften der zu untersuchenden Analyte ausgewählt und angepasst wurden, ist von großer Bedeutung. Auch wenn die massenspektrometrische (MS) Detektion als Goldstandard und „Lösung für alles“ für viele analytische Probleme angesehen wird, zeigt sich oft die fehlende Selektivität für isobare und isomere Analyte, die keine charakteristische MS2-Fragmentierung zeigen. Ziel dieser Arbeit ist es Konzepte aufzuzeigen, wie die Verwendung unterschiedlicher Derivatisierungstechniken und die Implementierung von orthogonalen stationären Phasen und Detektoren die Identifizierung unbekannter Analyte, durch Erhöhung der Sensitivität und Selektivität, verbessert.

Der erste Teil dieser Arbeit zeigt die Relevanz von Oxidationsreaktionen in pharmazeutischen Lipidformulierungen, welche eine große Vielfalt von Oxidationsprodukten generieren. Diese Oxidationsprodukte benötigen eine möglichst umfassende Charakterisierung, da sie als Verunreinigungen klassifiziert werden müssen. Hierfür wurde eine Kombination aus klassischer Umkehrphasen-Säule und einer innovativen chiralen Polysaccharidsäule in einem „full-comprehensive“ zweidimensionalen Flüssigchromatographie-Aufbau entwickelt. Diese Kombination zeigt exzellente Selektivität anhand der dreidimensionalen Struktur der konjugierten Fettsäureisomere, Kompatibilität und Orthogonalität der chiralen und Umkehrphasen-Säule. Diese hohe Selektivität für konjugierte Fettsäureisomere wurde vor allem bei den chiralen Polysaccharidsäulen beobachtet und kann vermutlich auf die komplexe dreidimensionale Struktur der stationären Phasen selbst zurückgeführt werden. Ebenfalls konnte gezeigt werden, dass sich UV- und MS-Detektion komplementär zueinander verhalten, weshalb durch die Kopplung beider Detektoren eine Charakterisierung der Doppelbindungen durch UV-Spektren und die Identifizierung unbekannter Oxylipine durch charakteristische MS2-Spektren möglich war.

Der zweite Teil beschäftigt sich mit der Relevanz der Chiralitätsbestimmung in der Verunreinigungsanalytik und in der detaillierten Charakterisierung von biotechnologisch hergestellten Wirkstoffen, am Beispiel von Teicoplanin. Teicoplanin weist eine unterschiedlich starke antibakterielle Wirksamkeit, in Abhängigkeit zur vorliegenden Fettsäureseitenkette, auf. Diese unterscheiden sich bezüglich ihrer Chiralität (bei verzweigten Fettsäuren), Länge und Verzweigung. Mittels moderner chiraler Polysaccharidsäulen und 1-Naphthylamin-Derivatisierung ist die Enantiomerentrennung durch Flüssigchromatographie möglich. Hierdurch wird die Enantiomerentrennung der anteiso-methyl verzweigten Fettsäureseitenkette von Teicoplanin RS3 möglich und durch Verwendung eines selbst-synthetisierten enantiomeren-reinen Standards kann die Stereochemie bestimmt werden. Zusätzlich wird die exzellente Selektivität der chiralen Polysaccharidsäulen für achirale Substanzen anhand der Identifizierung von, zuvor unbekannten, Konstitutionsisomeren gezeigt.

Der dritte Teil der Arbeit beschäftigt sich mit der Entwicklung eines kostengünstigen Workflows zur Doppelbindungspositionsbestimmung mittels Flüssigchromatographie in Kombination mit MS-Detektion. Die Derivatisierung mit Dimethyldisulfid erlaubt den Vorschlag von charakteristischen Fragmenten von (mehrfach) ungesättigten Fettsäuren und verwendete Elektrosprayionisation im negativen Ionisationsmodus. Für höhere Sensitivität und Flexibilität der Methode wurde 2,2‘-Dipyridyldisulfid als Derivatisierungsreagenz eingeführt, welches eine Ionisierung im positiven Ionisationsmodus ermöglicht. Damit können charakeristische Fragmentionen von Omega- und Carboxyende für Fettsäuren mit bis zu zwei Doppelbindungen im positiven Ionisatonsmodus detektiert werden. Diese Methode könnte als Startpunkt für weitere Optimierungen und Untersuchung weiterer Disulfid-basierten Derivatisierungsreagenzien verwendet werden.

Abbreviations

^{1}D	First Dimension
^{2}D	Second Dimension
1D	One dimensional
1D-LC	One-dimensional Liquid Chromatography
2D-LC	Two-dimensional Liquid Chromatography
APCI	Atmospheric Pressure Chemical Ionization
API	Active Pharmaceutical Ingredient
ASM	Active Solvent Modulation
CAD	Charged Aerosol Detection
CDA	Chiral Derivatizing Agent
CLA	Conjugated Linoleic Acid
CSP	Chiral Stationary Phase
DAD	Diode Array Detector
DF	Dilution Factor
EEA	European Economic Area
EMA	European Medicines Agency
EP	European Pharmacopoeia
ESI	Electron Spray Ionization
EU	European Union
GC	Gas Chromatography
HOMO	Highest Occupied Molecular Orbital
HPLC	High Performance Liquid Chromatography
HRMS	High Resolution Mass Spectrometry
ICH	International Council for Harmonisation of Technical Requirements for Pharmaceuticals for Human Use
JP	Japanese Pharmacopoeia
LBDDS	Lipid Based Drug Delivery System
LC	Liquid Chromatography
LDL	Low Density Lipoprotein

LUMO	Lowest Unoccupied Molecular Orbital
mLC-LC	Multiple heartcutting 2D-LC
MS	Mass spectrometry
NP	Normal Phase
PAH	Polycyclic Aromatic Hydrocarbons
PEG	Polyethylene glycol
PUFA	Polyunsaturated Fatty Acid
RP	Reversed Phase
SCFA	Short-chain fatty acid
LC×LC	Full-comprehensive 2D-LC
sLC×LC	Selective Comprehensive 2D-LC
UHPLC	Ultra High-Performance Liquid Chromatography
USP	United States Pharmacopoeia
UV	Ultraviolet
WHO	World Health Organization

List of publications

Publication I:

M. Olfert, S. Bäurer, M. Wolter, S. Buckenmaier, E. Brito-de la Fuente, M. Lämmerhofer

Comprehensive profiling of conjugated fatty acid isomers and their lipid oxidation products by two-dimensional chiral RP×RP liquid chromatography hyphenated to UV- and SWATH-MS-detection

Analytica Chimica Acta 1202, 2022

DOI: 10.1016/j.aca.2022.339667

Publication II:

C. Geibel*, **M. Olfert***, C. Knappe, K. Serafimov, M. Lämmerhofer

Branched medium-chain fatty acid profiling and enantiomer separation of *anteiso*-forms of teicoplanin fatty acyl side chain RS3 using UHPLC-MS/MS with polysaccharide columns

Journal of Pharmaceutical and Biomedical Analysis 224, 2023

DOI: 10.1016/j.jpba.2022.115162

* These authors contributed equally

Publication III:

M. Olfert, C. Knappe, A. Sievers-Engler, B. Masberg, M. Lämmerhofer

Determination of double bond positions in unsaturated fatty acids by pre-column derivatization with dimethyl and dipyridyl disulfide followed by LC-SWATH-MS analysis

Analytical and Bioanalytical Chemistry, 2024

DOI: 10.1007/s00216-024-05542-z

Publications not included in this dissertation:

Publication IV:

M. Wolter, C. Geibel, **M. Olfert**, M. Su, W. Bicker, M. Kramer, W. Lindner, M. Lämmerhofer
Development and chromatographic exploration of stable-bonded cross-linked amino silica against classical amino phases
Journal of Separation Science 45, 3286-3300, 2022
DOI: 10.1002/jssc.202200268

Publication V:

S. Vaas, M. O. Zimmermann, D. Schollmeyer, J. Stahlecker, M. U. Engelhardt, J. Rheinganz, B. Drotleff, **M. Olfert**, M. Lämmerhofer, M. Kramer, T. Stehle, F. M. Böckler
Principles and Applications of CF2X Moieties as Unconventional Halogen Bond Donors in Medicinal Chemistry, Chemical Biology, and Drug Discovery
Journal of Medicinal Chemistry 66, 10202-10225, 2023
DOI: 10.1021/acs.jmedchem.3c00634

Publication VI:

P. Flury, J. Breidenbach, N. Krüger, R. Voget, L. Schäkel, Y. Si, V. Krasniqi, S. Calistri, **M. Olfert**, K. Sylvester, C. Rocha, R. Ditzinger, A. Rasch, S. Pöhlmann, T. Kronenberger, A. Poso, K. Rox, S. A. Laufer, C. E. Müller, M. Gütschow, T. Pillaiyar
Cathepsin-Targeting SARS-CoV-2 Inhibitors: Design, Synthesis, and Biological Activity
ACS Pharmacology & Translational Science, 7, 2, 493-514, 2024
DOI (original): 10.1021/acsptsci.3c00313
DOI (correction): 10.1021/acsptsci.4c00095

Author contributions

Publication I:

Comprehensive profiling of conjugated fatty acid isomers and their lipid oxidation products by two-dimensional chiral RP×RP liquid chromatography hyphenated to UV- and SWATH-MS-detection

Analytica Chimica Acta 1202, 2022
DOI: 10.1016/j.aca.2022.339667

Matthias Olfert
Investigation, Methodology, Data curation, Visualization, Formal analysis, Writing: original draft

Stefanie Bäurer
Investigation, Methodology, Data curation, Supervision, Writing: Review & editing

Marc Wolter
Formal analysis, Writing: Review & editing

Stephan Buckenmaier
Conceptualization, Writing: Review & editing

Edmundo Brito-de la Fuente
Conceptualization, Writing: Review & editing, Resources

Michael Lämmerhofer
Conceptualization, Methodology, Supervision, Resources, Writing: Review & editing

Publication II:

Branched medium-chain fatty acid profiling and enantiomer separation of *anteiso*-forms of teicoplanin fatty acyl side chain RS3 using UHPLC-MS/MS with polysaccharide columns

Journal of Pharmaceutical and Biomedical Analysis 224, 2023
DOI: 10.1016/j.jpba.2022.115162

Christian Geibel*
Investigation, Methodology, Formal analysis, Data curation, Visualization, Writing: original draft

Matthias Olfert*
Investigation, Methodology, Formal analysis, Writing: review & editing

Cornelius Knappe
Investigation, Writing: review & editing

Kristian Serafimov
Investigation, Writing: review & editing

Michael Lämmerhofer
Conceptualization, Methodology, Supervision, Resources, Writing: Review & editing

* These authors contributed equally

Publication III:

Determination of double bond positions in unsaturated fatty acids by pre-column derivatization with dimethyl and dipyridyl disulfide followed by LC-SWATH-MS analysis

Analytical and Bioanalytical Chemistry, 2024
DOI: 10.1007/s00216-024-05542-z

Matthias Olfert

Investigation, Methodology, Data curation, Visualization, Formal Analysis, Writing: Original Draft

Cornelius Knappe

Methodology, Writing: Review & Editing

Adrian Sievers-Engler

Methodology, Writing: Review & Editing

Benedikt Masberg

Formal Analysis, Writing: Review & Editing

Michael Lämmerhofer

Conceptualization, Methodology, Supervision, Resources, Writing: Review & Editing

Contribution to Conferences & Meetings

Poster presentations

Jahrestagung der Deutschen Pharmazeutischen Gesellschaft 2021

Virtual Meeting; September 28 – October 01, 2021

UV-spectra evaluation and RPxRP 2D-LC-MS method development for the characterisation and separation of conjugated fatty acid isomers

Matthias Olfert, Stefanie Bäurer, Michael Lämmerhofer

17th International Symposium on Hyphenated Techniques in Chromatography and Separation Technology 2022

Ghent, Belgium; May 18 – May 20, 2022

Full comprehensive chiral × RP 2D-LC-MS analysis of conjugated fatty acid isomers

Matthias Olfert, Stefanie Bäurer, Marc Wolter, Stephan Buckenmaier, Edmundo Brito-de la Fuente, Michael Lämmerhofer

26th International Symposium on Separation Sciences 2022

Ljubljana, Slovenia; June 28 – July 01, 2022

Comprehensive profiling of conjugated fatty acid isomers and lipid oxidation products by two-dimensional chiral RP×RP LC-UV-MS

Matthias Olfert, Stefanie Bäurer, Marc Wolter, Stephan Buckenmaier, Edmundo Brito-de la Fuente, Michael Lämmerhofer

Jahrestagung der Deutschen Pharmazeutischen Gesellschaft 2022

Marburg, Germany; September 13 – September 16, 2022

Two-dimensional chiral RP×RP LC-UV-MS analysis of lipid oxidation products and determination of double bond positions in fatty acids

Matthias Olfert, Michael Lämmerhofer

ANAKON 2023

Vienna, Austria; April 11 – April 14, 2023

Teicoplanin - Profiling of branched medium-chain fatty acids and enantiomer separation of *anteiso*-forms of fatty acyl side chain RS3

Matthias Olfert, Christian Geibel, Cornelius Knappe, Kristian Serafimov, Michael Lämmerhofer

51st International Symposium on High Performance Liquid Phase Separations and Related Techniques 2023

Düsseldorf, Germany; June 18 – June 22, 2023

Two-dimensional chiral RP×RP LC-UV-MS method development for characterization of conjugated fatty acid isomers and lipid oxidation products

Matthias Olfert, Stefanie Bäurer, Michael Lämmerhofer

Jahrestagung der Deutschen Pharmazeutischen Gesellschaft 2023

Tübingen, Germany; October 07 – October 10, 2023

Determination and enantiomeric separation of branched medium-chain fatty acids in Teicoplanin

Matthias Olfert, Christian Geibel, Cornelius Knappe, Kristian Serafimov, Michael Lämmerhofer

Oral presentations

34. Doktorandenseminar des AK Separation Science

Hohenrhoda, Germany; January 07 – January 09, 2024

Fettsäuren in der Verunreinigungsanalytik: Strategien zur Charakterisierung von fettsäurehaltigen Formulierungen

Matthias Olfert

1 Introduction

1.1 Impurities in pharmaceutical products – a quality issue

The European Pharmacopoeia (EP) is the fundamental literature in regard to legal and scientific advice for manufacturers of pharmaceutical products for the European market and is designed with the intention to ensure the highest possible quality of pharmaceuticals, and therefore protecting public health [1, 2]. This can be achieved by introduction of harmonized quality standards for materials used in the production of pharmaceuticals [1]. Although the European Pharmacopeia is the most important guideline for the European market, the global harmonization with guidelines like the USP (United States Pharmacopoeia) and JP (Japanese Pharmacopoeia) gains more and more in importance [3, 4]. For this harmonization, especially documents from the WHO (World Health Organization) and the ICH (International Council for Harmonisation of Technical Requirements for Pharmaceuticals for Human Use) should be taken into consideration [4]. Implementation of ICH guidelines is not mandatory, but is expected from members of the ICH [5]. The European Medicines Agency (EMA) is responsible for the implementation and publication of ICH-guidelines for members of the European Union (EU). ICH guidelines are accordingly, besides the EP, a regulatory standard in the European Economic Area (EEA).

For ensuring proper quality of pharmaceuticals a major aspect is the control of impurities, as they are considered as a quality issue that often lead to either adverse effects or reduced efficacy of the drug substance (active pharmaceutical ingredient) [6]. The EP specifies tests for impurities for most of the listed drugs [7] and the ICH released several guidelines specifying the handling of impurities in pharmaceutical products. Herein they differentiate between: (1) impurities in the drug substances: any component which is not the chemical entity of the drug substance [8] and (2) impurities in the drug product: any component which is not the drug substance nor an excipient [9]. Since physiological properties, both biological activities and toxicities, of newly discovered impurities are typically unknown [10], those definitions cannot distinguish between impurities with negative, positive or no effects on the health of patients.

Furthermore, impurities can be classified into the three main groups: organic impurities, inorganic impurities and residual solvents. Each of these groups is regulated and information can be found in the respective ICH quality guidelines: (1) Q3A Impurities in New Drug Substances [8]; (2) Q3B Impurities in New Drug Products [9]; (3) Q3C Guideline for Residual Solvents [11]; (4) Q3D Guideline for Elemental Impurities [12]; (5) M7 Guideline on assessment and control of DNA reactive (mutagenic) impurities [13]. A guideline for extractable and leachables is under

development by ICH (ICH Q3E) and is expected to reach step 4 adoption of an ICH harmonized guideline according to the EWG workplan in Q4 2026 [14].

Organic impurities can be further differentiated in degradation related impurities (degradation of API, interaction of API with e.g. excipients or primary packaging material) and process related impurities (e.g. intermediates and by-products from API-synthesis) [6].

Organic impurities like API-related impurities are typically accompanied by decrease of API and increase of impurities in the pharmaceutical formulation. Because of their chemically related structure to the API, those impurities can bear one of the highest pathophysiological risks [6]. A prominent example for this is p-aminophenol which results from synthesis or degradation reactions of paracetamol, a commonly used analgesic and antipyretic drug. It has been shown that p-aminophenol can display nephrotoxicity and teratogenicity [15]. Paracetamol is just one of many examples that illustrate the necessity of suitable quality control methods at manufacturing sites of drug substances and products. More recently the “Valsartan-Scandal” has shown that lack of comprehensive control can result in severe cases of adverse effects [16].

Quality control methods have to be specifically tailored for the analyzed drug substance and product, allowing qualification and quantification of all relevant analytes and, in the Common Technical Document (CTD) specified, impurities [17, 18]. For this purpose, ICH Guideline Q14 should be used as a guidance for proper development of analytical procedures [19]. Sufficiently high selectivity, sensitivity, accuracy/precision and robustness of the method are essential and need to be shown during the method validation, according to ICH Q2 Guideline [20]. This can be challenging, as in the majority of cases impurities are present in low amounts in the (complex) sample matrix and have to be reported, identified and/or qualified once the respective threshold is exceeded. Those thresholds for impurities in pharmaceuticals are dependent of the maximum daily dose of the drug substance and are further defined either as percentage of the drug substance or as maximum total daily intake of the degradation product [9].

The Reporting Threshold defines the amount of impurity at which the occurrence of the impurity must be reported to the authorities, whilst amounts above the Identification Threshold require structural elucidation of the impurity. Qualification describes the process of testing the degradation product for biological safety and can even include clinical studies regarding the toxicity [9]. This resembles quite an effort and therefore exceeding the Qualification Threshold should be avoided if possible, e.g. by alteration of storage conditions [9] or optimization of the analytical separation. Table 1 summarizes the legally binding thresholds.

In the context of DNA-reactive (i.e., mutagenic) impurities in drug substances and drug products, additional guidance has been established with ICH guideline M7. With this guideline, the Threshold of Toxicological Concern (TTC) was specifically established for any unstudied compound to reach a negligible risk of cancer for patients. For drug products with intended long-term treatment (> 10 years), this might address impurities which have no carcinogenic data available (i.e., defined as class 2 or 3 in context of the guideline), here the TTC limits the daily intake of these impurities to 1.5 µg per day [13].

The theoretical prediction of degradation patterns/products is only possible to a certain degree [21, 22]. Functional groups can act as possible reaction sites for degradation, thus APIs with multiple functional groups and complex sample matrices can result in complex degradation patterns. Although in-silico prediction of degradation reactions gives a good idea of possible products, stability studies and impurity profiling during the development and quality control are indispensable [23]. Even the use of accelerated conditions or forced degradation could be beneficial during development or impurity profiling to provoke the formation of impurities, typically present in low quantities [24].

Table 1: Thresholds for Degradation Products in New Drug Products, reproduced from ICH guideline Q3B(R2) [9].

Reporting Thresholds				
MDD	≤ 1 g		> 1 g	
Threshold	0.1 %		0.05 %	
Identification Thresholds				
MDD	< 1 mg	1 mg – 10 mg	> 10 mg – 2 g	> 2g
Threshold*	1.0 % or 5 µg TDI	0.5 % or 20 µg TDI	0.2 % or 2 mg TDI	0.10 %
Qualification Thresholds				
MDD	< 10 mg	10 mg – 100 mg	> 100 mg – 2 g	> 2 g
Threshold*	1.0 % or 50 µg TDI	0.5 % or 200 µg TDI	0.2 % or 3 mg TDI	0.15 %

MDD: Maximum Daily Dose | TDI: Total Daily Intake| *whichever threshold is lower

In the European Pharmacopoeia the “Test for Related Substances” (Impurities) is typically performed with chromatographic methods like thin layer-, gas- or liquid chromatography, which mostly replaced colorimetric/spectrophotometric methods [1]. The listed LC-methods in the EP are typically described quite vague, often utilizing columns which are not state of the art anymore due to larger inner diameter and large particle sizes. This leaves room for optimization of the exact

column chemistry and herein, technological developments in software assisted method optimization [25], Liquid Chromatography (UHPLC-systems, Columns: smaller particles, core shell, new selectors…) and detection [26] bear a huge potential for the improvement of established quality control methods, possibly resulting in faster separations, higher resolution [25, 26] or separation of isomers and enantiomers [27]. This emphasizes the importance of modern analytical techniques and approaches to tackle impurity profiling in pharmaceuticals, especially if the analytical problem is of complex nature. For increasingly complex analytical questions, the analyst´s toolbox offers plenty of parameters and strategies for optimizing methods, like chemical derivatization, optimized mobile phases, different chemical entities of stationary phases, orthogonal separations, combinations of different detectors and separation techniques and many more.

1.2 Lipids

1.2.1 Definition & Classification

Lipids can be defined as organic molecules which are insoluble in water and soluble in organic solvents. This rough definition already implies the structural and physiological diversity of this group of biomolecules [28]. To overview this enormous group of molecules different classification systems and databases have been suggested, but especially the classification system of the LIPID MAPS consortium and their underlying database for lipids enjoys great popularity in the Lipidomics community [29]. Herein lipids are differentiated based on the fundamental molecules used in their biosynthesis, ketoacyl or isoprene units. By this, lipids can be assigned to one of the following main groups: fatty acyls, glycerolipids, glycerophospholipids, sphingolipids, saccharolipids and polyketides are based on condensation reaction of ketoacyl groups, whilst sterol and prenol lipids are based on condensation reaction of isoprene groups [28]. The group of fatty acyls contains besides fatty acids also compounds like alcohols, aldehydes and esters [28], whereas fatty acids will be the main focus of this work. Fatty acyls have various biological functions on their own but are also one of the fundamental building blocks for larger lipids, for example fatty acids for triglycerides or alcohols for wax esters [30, 31].

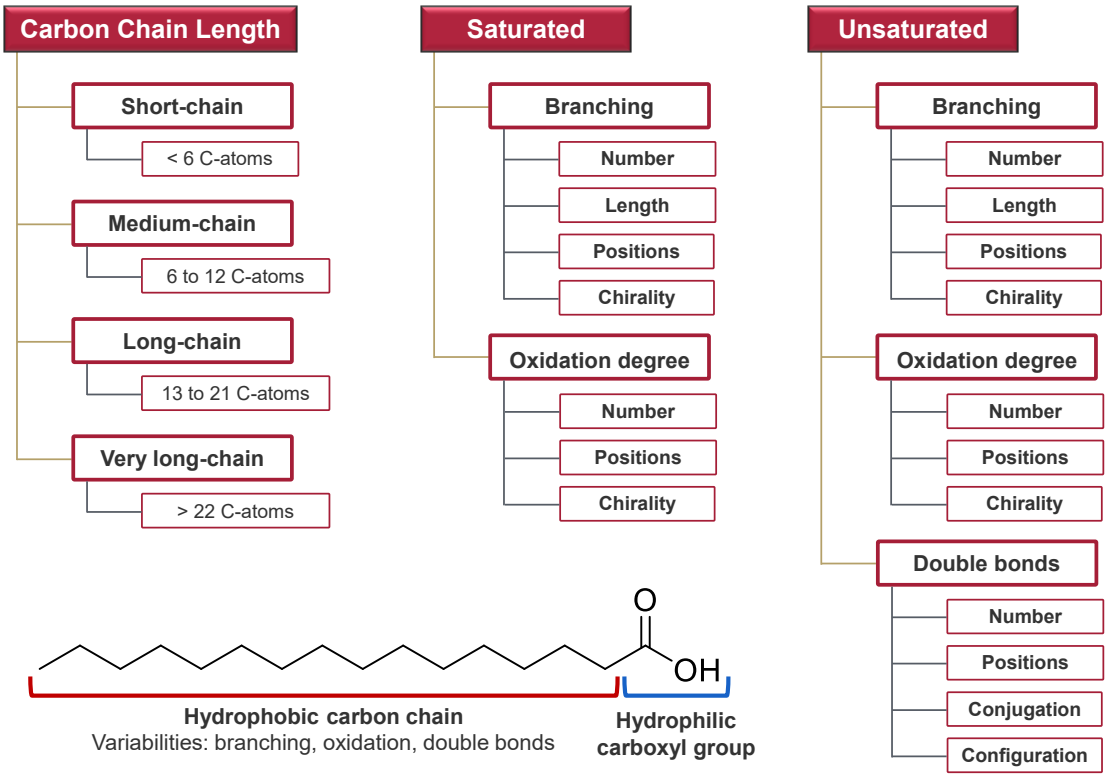

Figure 1: Possible characterization parameters and general structure of fatty acids.

Fatty acids generally consist of a hydrophilic carboxylic group and a hydrophobic carbon chain. Hence the hydrophobicity of fatty acids depends on the carbon chain length and its degree of oxidation, whereas longer carbon chains equal higher hydrophobicity. In contrast, multiple oxidations (e.g. hydroxyl, peroxyl-groups…) lead to higher hydrophilicity of the carbon chain, however this usually only occurs in polyunsaturated fatty acids, due to their bisallylic methylene groups [32]. The structural diversity of fatty acids is visualized in Figure 1, whereas features from the first column can be combined with features from the second or third column, depending on whether it is a saturated or unsaturated fatty acid. Saturated and unsaturated fatty acids can be further differentiated by the occurrence of branching or oxidation.

The human body can produce most of the required fatty acids for the metabolism, by condensation of acetyl-CoA and malonyl-CoA followed by elongation with more acetyl-CoA units, catalyzed by fatty acyl synthase [33]. Fatty acids that cannot be synthesized and therefore need to be substituted by dietary intake are called essential fatty acids. The two essential polyunsaturated fatty acids are called α-linolenic acid (C18:3, ω-3) and linoleic acid (C18:2, ω-6) [34] and are necessary for the synthesis of other ω-3 and ω-6 fatty acids (see Figure 2).

It is more likely to find hydroxy or branched chain fatty acids instead of polyunsaturated fatty acids in bacteria than in humans [30, 35]. Branched chain fatty acids are therefore likely to be found in the pharmaceutical field as part of biotechnologically produced pharmaceuticals, e.g. as part of antibiotics like teicoplanin [27, 36]. Their biosynthesis can occur by decarboxylation and elongation of branched chain amino acids, leading to *anteiso* fatty acids in case of isoleucine and *iso* fatty acids in case of valine and leucine [37].

1.2.2 Biological functions of fatty acids in humans

The biological functions of fatty acids in humans are heterogenic and can be grouped in the following categories: Regulation of membrane structure and function, intracellular signaling, transcription factor activities, gene expression and production of bioactive lipid mediators [38].

As part of phospholipids, phosphosphingolipids, sphingolipids or gangliosides fatty acids impact properties of cellular membranes, whereas all parameters mentioned in Figure 1 influence the fluidity of the membrane. For example mono-unsaturated fatty acids, ω-3- or ω-6- fatty acids in cell membranes contribute to higher fluidity, especially if they bear double bonds in cis configuration [39, 40]. Relevance of this topic is given as multiple organism have shown that the adaptability of their membrane fluidity is part of a coping strategy to deal with temperature changes [41, 42]. Polyunsaturated fatty acids (PUFAs) allow insertion of proteins by disturbing the arrangement of the cell membrane lipids, influencing membrane permeability and elasticity and also have pathophysiological relevance [39, 43]. For example, low levels of long-chain PUFAs in cell membranes has been shown to play a role in the occurrence of diabetes-related microvascular complications [39, 44].

To avoid disturbing membrane integrity, fatty acids are usually stored as triglycerides in adipocytes, where they can be utilized for energy production [39]. Once energy is needed the fatty acids are cleaved by lipase-activity and transported via albumin through the blood to the energy requiring tissue, where they are converted to Coenzyme A derivatives and transferred via carnitine shuttle in the mitochondria [45]. Here, β-oxidation takes place, during which multiple enzymes lead to generation of NADH and $FADH_2$ and the scission of one acetyl-CoA per cycle, which is then available to the citric cycle, generating ATP. β-oxidation of unsaturated fatty acids results in less ATP than their saturated equivalent due to the required conversion of β-γ-double bonds [46]. Further functions are dependent on the respective fatty acids and include signaling, gene- and receptor-interactions and protein acylation [47].

1.2.3 Health concerns of fatty acids

In addition, to the previously described general functions of fatty acids, extensive research has been done to investigate additional physiological or pathophysiological effects. Especially since cardiovascular diseases have risen over the last few decades in first-world countries at an alarming rate. Specifically the increased intake of saturated fatty acids and trans fatty acids are suspected to play a major pathophysiological role [48].

Saturated fatty acids

As described previously saturated fatty acids can be synthesized by the human body and serve in form of phospholipids, ceramides, sphingolipids or gangliosides important physiological functions. Depending on the carbon chain length the functions in the human body vary. For example myristic and palmitic acid are involved in protein anchoring and trafficking, whilst several fatty acids could be involved in gene expression by e.g. influencing transcription factors or promote inflammation by inducing the NF-κB pathway [38]. Animal-derived products are considered as the major source of saturated fatty acids, but also plant oils (e.g. palm oil, coconut oil) contain high levels of saturated fatty acids [38, 48]. High intake of saturated fatty acids, especially lauric, myristic and palmitic acid, is correlated with increased LDL cholesterol and may be correlated with increased coagulation, insulin resistance and inflammation, which in turn are linked to many “first-world diseases”, like type 2 diabetes or cardiovascular and coronary heart disease [38, 49]. Thus, a reduction or substitution with unsaturated fatty acids can be beneficial for the human health.

Mono-unsaturated fatty acids

The most common mono-unsaturated cis fatty acids palmitoleic (C16:1, ω-7) and oleic acid (C18:1, ω-9) can be obtained by de-novo synthesis or by consumption of plant oils (e.g. olive oil) or animal fats [38]. In studies most of the health benefits for oleic acid could either be assigned to the reduction of consumption of saturated fatty acids or the polyphenols in the consumed olive oil or mediterranean diet. For palmitoleic acid research still has to be intensified, but an increase in insulin sensitivity could already be shown [38, 50]. Trans fatty acids like elaidic acid (C18:1, ω-9) can be generated by partial hydrogenation of vegetable oils and are commonly used in the food industry to extend shelf life and for its semi-solid properties. In contrast, trans fatty acids are known to increase the risk of cardiovascular and metabolic diseases, thus a reduction in the diet is strongly recommended [51, 52].

Polyunsaturated fatty acids: omega-3/omega-6

Polyunsaturated fatty acids (PUFAs) exhibit multiple double bonds which can be conjugated or isolated. They can be further differentiated based on the position of the first double bond, counted from the ω-end, resulting in the classes of ω-3 fatty acids and ω-6 fatty acids [53].

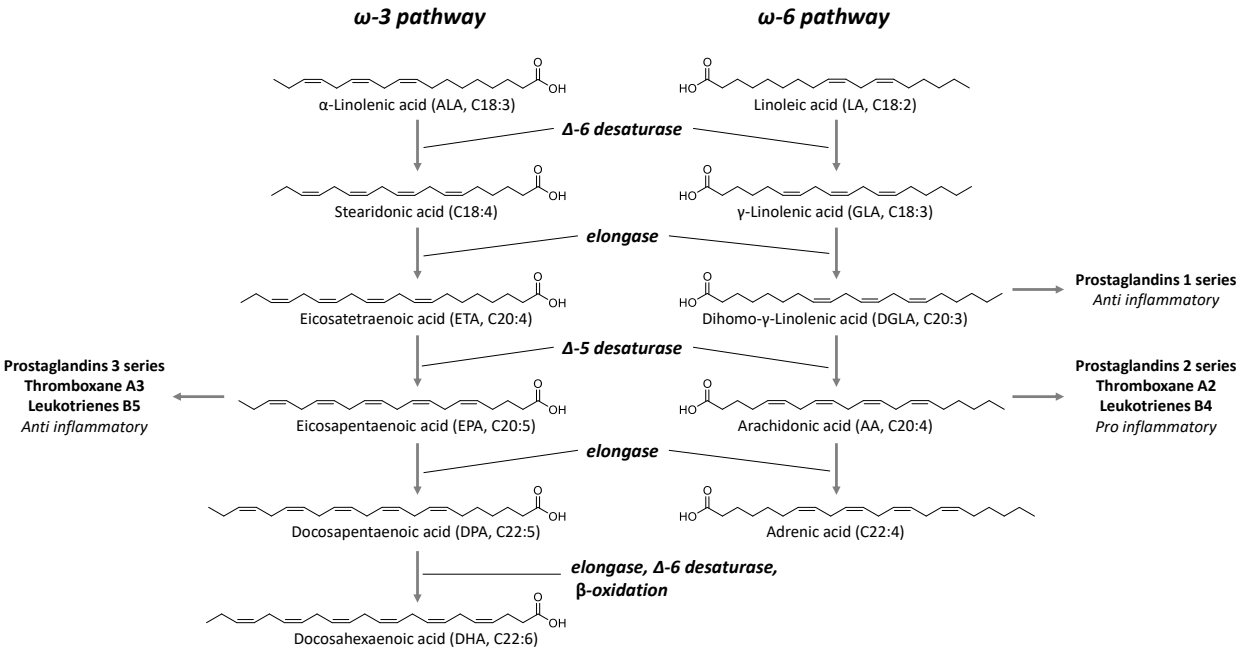

Figure 2: Overview of omega-3 and omega-6 pathway for the biosynthesis of PUFAs, Thromboxanes, Prostaglandins and Leukotrienes; visualized with information from Nagy et al. [40] and Rustan et al. [53].

The unconjugated essential fatty acids α-linolenic acid (C18:3, ω-3) and linoleic acid (C18:2, ω-6) are indispensable for the proper functioning of the human body, as they are used as "starting material" for further biosynthesis of PUFAs according to the ω-3-/ω-6-pathway, shown in Figure 2 [53]. Since both pathways share the same enzymes, if one is extensively used by a respective diet (ω-3-or ω-6-rich), the other one is less active since the enzymes are already occupied. In this process, dihomo-γ-linolenic acid plays a central role as precursor of either prostaglandin 1 (anti-inflammatory) in a ω-3-PUFA rich diet or arachidonic acid in a ω-6-PUFA rich diet, which can be converted into proinflammatory prostaglandin 2, thromboxane A2 and leukotriene B4 [40].

Since saturated fatty acids and trans fatty acids are mainly associated with negative influence on the human health, a substitution of them with unsaturated fatty acids is always beneficial [38]. For polyunsaturated fatty acids many health benefits with regard to cardiovascular, inflammatory and metabolic diseases have been noticed, especially for ω-3-PUFAs eicosapentaenoic acid and docosahexaenoic acid effects are well researched [38, 54]. Although ω-6-PUFAs linoleic acid and arachidonic acid are precursors for inflammatory mediators (see Figure 2), supplementation had

only minimal effect on inflammatory biomarkers [54]. While linoleic acid is known for its LDL-cholesterol lowering effect, arachidonic acid is an important precursor for different mediators, involved in many biological functions (e.g. inflammation, platelet aggregation, vascular tonus) [38, 54]. A generalized statement about ω-6-PUFA is not possible, due to their role in physiological and pathophysiological processes, thus further research is necessary.

Conjugated fatty acids exhibit at least two double bonds in conjugation, which can occur on different positions and each double bond can display either cis (*Z*) or trans (*E*) configuration [55]. Conjugated linoleic acids can naturally be found in animal-derived products (e.g. milk or ruminant meat) or produced by alkaline isomerization of linoleic acid, while others were found in plant seed oils (e.g. conjugated linolenic acid) [56]. In general, a lot of different positive health effects have been reported, ranging from anti-obesity, anti-inflammatory to anti-carcinogenic [55, 56]. These physiological properties differ between the different conjugated fatty acid isomers and it has been reported that double bond position and configuration has an influence on their health effects [56, 57]. For example, the main isomers of commercial conjugated linoleic acid (CLA) are 10t,12c-CLA and 9c,11t-CLA, both showed anti-carcinogenic effects, whereas mainly 10t,12c-CLA showed anti-obese and anti-hypertensive effects [57]. Meaning, the exact determination of the conjugated fatty acids is crucial for the discussion of possible health benefits.

1.2.4 Isomerism of fatty acids

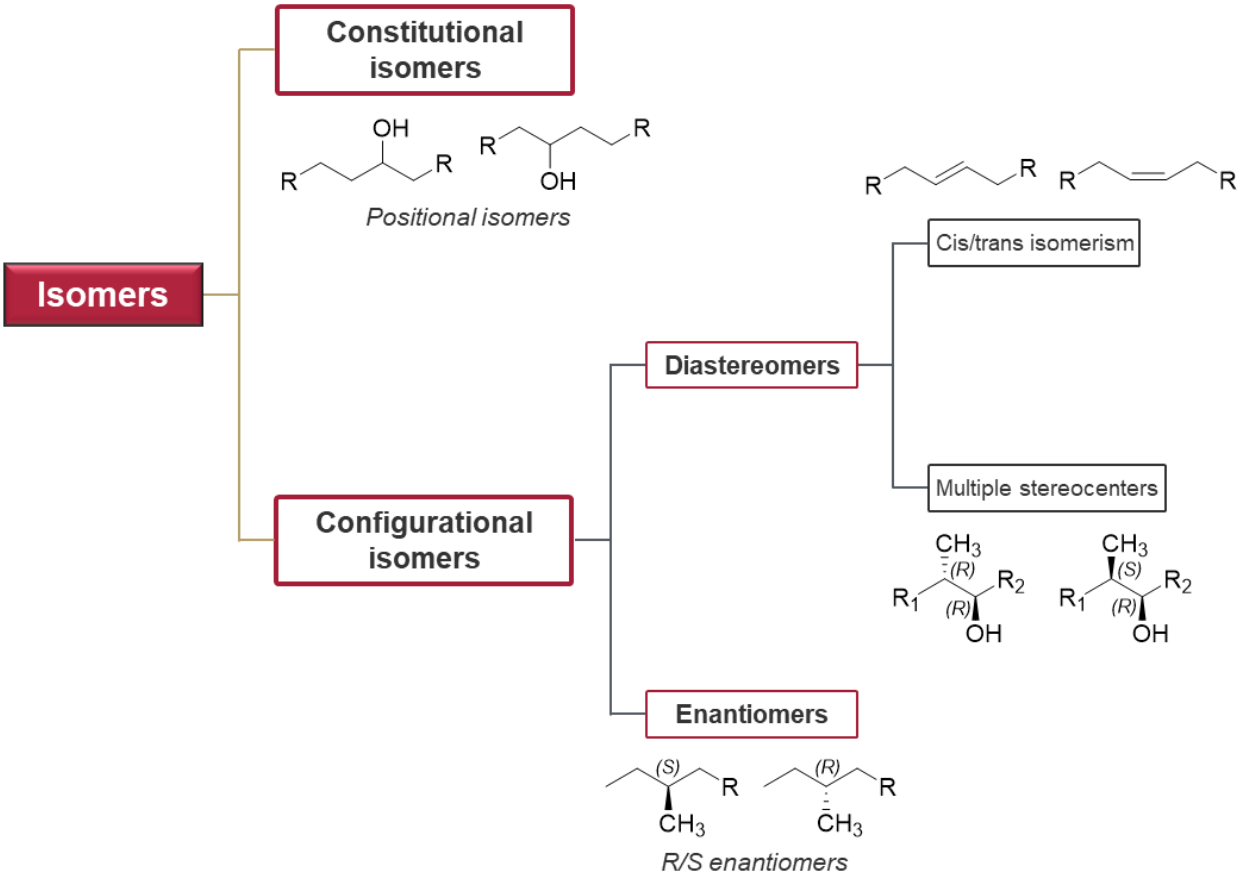

Figure 3: Overview of different types of isomerism which can also be found in different fatty acids.

Isomerism describes the phenomenon of two or more molecules to share the same atomic compositions but differ in the arrangement of bonds or orientation of atoms in space. While constitutional or positional isomers differ in the arrangement of their atomic bonds, diastereomers and respectively enantiomers share the same arrangement but differ in the geometric relationship of some atoms and the isomers are not convertible into each other without cleavage of covalent bonds. Additionally, enantiomers are chiral and hence not super imposable to each other [58].

Examples like the “Contergan-scandal” show that isomerism of an active pharmaceutical ingredient can dramatically impact its pharmacodynamics and pharmacokinetics [58]. In this case the teratogenic S-enantiomer led to over ten thousand malformations of newborns [59]. The concept of different (patho)physiological effects of isomers also applies for fatty acids. As discussed above, health benefits of ω-3/ω-6 fatty acids differ (constitutional isomers) and cis fatty acids are considered as healthier than trans fatty acids (diastereomers) [51]. Fatty acid

enantiomers might be relevant during in-depth characterization of biotechnologically produced pharmaceuticals, like teicoplanin (*anteiso* fatty acid side-chains) [27].

Hence, the determination of efficacy and toxicity during the development of a new drug substance should additionally consider the effects of potential enantiomers and might even justify the launch of the final drug product with a single stereoisomer as API, as advised in the scientific guideline “Investigation of chiral active substances” by the European-Medicines Agency [60].

Based on the similar physicochemical properties of isomers, advanced analytical methods may be necessary during drug-development, quality control and impurity profiling to achieve comprehensive characterization.

1.3 Lipid-based pharmaceuticals

1.3.1 Relevance and different types

An increasing number of newly developed drug substances are poorly soluble in water, therefore exhibiting poor bioavailability and fluctuations in their pharmacokinetics when taken orally. Addressing this issue, lipid-based drug delivery systems (LBDDS) have been extensively researched and applied for the formulation of many structurally diverse APIs [61]. The formulations can be classified according to the use of oils (e.g. triglycerides), water soluble/insoluble surfactants and/or cosolvents (e.g. polyethyleneglycol) [62].

Propofol is a famous example for a drug substance, requiring formulation as LBDDS, known for its abuse potential and possible correlation with the death of Michael Jackson [63]. Due to its lipophilicity a formulation with a hydrophobic solvent (e.g. oils) makes sense but requires emulsification to allow intravenous application due to the risk of life-threatening fat embolies. To achieve this, different lipids can be found in the formulation: soybean-oil (PUFA-rich triglycerides) and medium-chain triglycerides for dissolving the API; phospholipids as emulsifier [64]. In general, intravenous application of drugs is often undesirable due to disadvantages like required sterility, possible infections and thrombosis [65]. Therefore, oral administration is preferred, but requires appropriate formulation [61]. The huge variety of approved oral lipid-based pharmaceutical was summarized by Savla et al. [61].

The COVID-19 pandemic showed the utilization of lipids in form of lipid nanoparticles as a way to encapsulate and deliver labile pharmaceuticals to their target cells. In case of the COVID-19 vaccines, encapsulation of the immunity-inducing mRNA ensured stability against degradation by nucleases in physiological fluids as well as the immune system and allowed direct delivery into target cells by internalization. The complex encapsulation formulation consisted of cationic/ionizable lipids, phospholipids, cholesterol and polyethylene glycol containing lipids (PEG-lipids) [66].

Further applications of lipids with regard to human health are: (1) supplementation of malnutrition or for improvement of diseases [67], (2) necessity of enteral or parenteral nutrition e.g. as energy source and source of essential fatty acids due to current health state of patients like inability for ingestion or digestion, e.g. in intensive care units [68], (3) basic component of skin care products or dermal pharmaceuticals, (4) transdermal drug delivery systems [69].

1.3.2 Lipid degradation in pharmaceuticals

Most of the mentioned applications do not contain free fatty acids, instead larger lipids like triglycerides (as energy carrier) or phospholipids (as emulsifier) are being used. During production or storage free fatty acids can be generated by hydrolysis from those larger lipids in the lipid formulation or starting materials (see Figure 4) [70], of course also only partial hydrolysis can occur. This process can be accelerated by temperature, basic or acidic conditions [71].

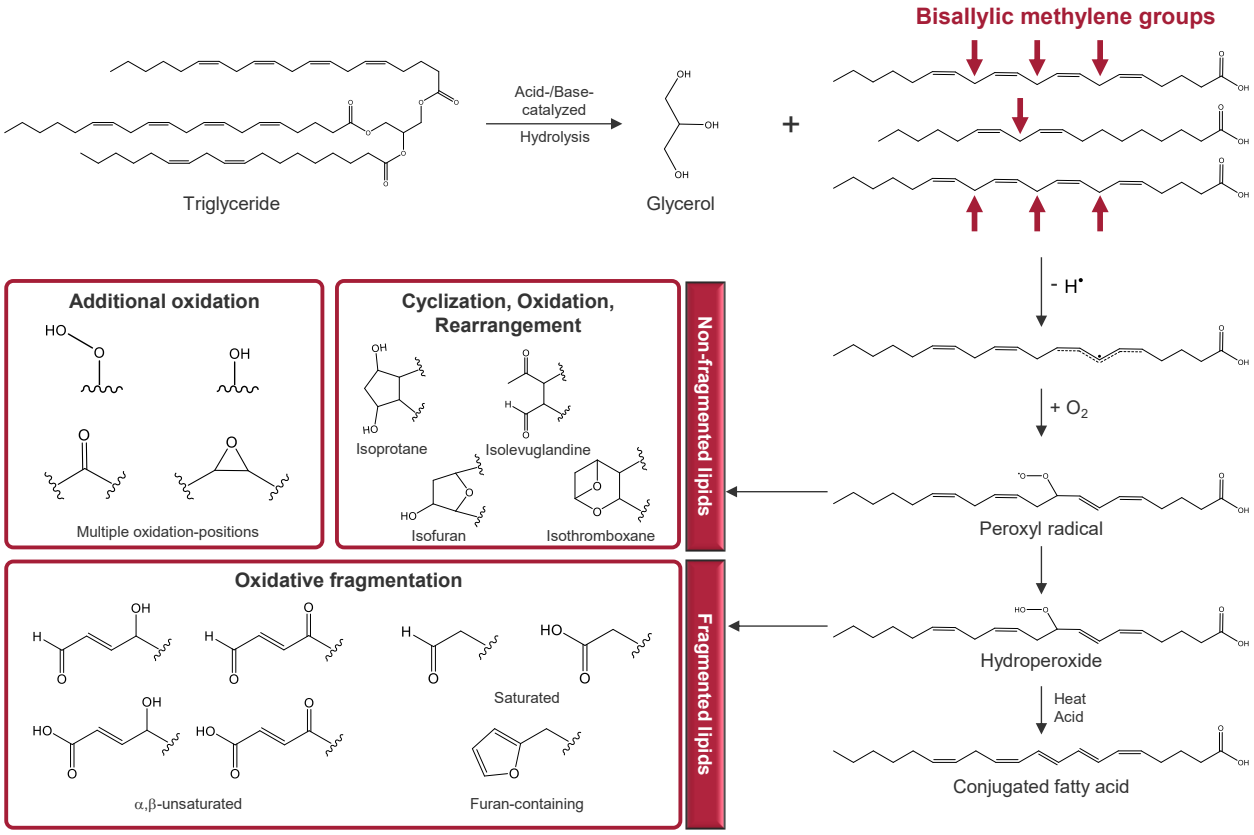

Figure 4: Degradation pathway of triglycerides or other larger lipids into free fatty, followed by lipid autoxidation and further degradation into (non)-fragmented lipids. Visualized with information from Bochkov et al. [72] and Gong et al. [73].

Especially PUFAs are prone to autoxidation due to their bisallylic methylene groups, resulting in degradation of the free fatty acids into instable peroxyl-radicals and hydroperoxides. Those two species will further react into a multitude of different fragmented or non-fragmented lipids (Figure 4) [72], including conjugated fatty acids [73]. This oxidation process of PUFAs is not limited to free acids but can also simultaneously occur while still being part of the larger lipids, which increases the complexity of the resulting sample even more due to the number of different compounds which can be generated from the initial larger lipid (e.g. triglyceride, phospholipid…).

Oxidized phospholipids are suspected to play a role in many (pathological) inflammatory and cardiovascular processes [72], additionally many of the oxidation products are generally considered to be toxic, as they are known to react with many biomolecules (e.g. DNA, proteins, amino acids) and can thus, in the worst case, exhibit mutagenic or carcinogenic properties [74]. Especially aldehydes, generated by e.g. hock-cleavage or β-scission [72], are known for their toxicity due to their high electrophilicity, which allows reactions with nucleophilic biomolecules [75].

Hence, even though some degradation products (e.g. conjugated PUFAs) may bear health benefits, it is more than justified that oxidation products have to be considered as impurity and must be reported, identified or qualified once the respective threshold is exceeded.

1.4 Liquid chromatography

Liquid chromatography describes the separation of analytes between a liquid (mobile) and solid (stationary) phase, based on different strength of interactions. (Ultra)-High-Performance Liquid Chromatography ([U]HPLC) is considered as the gold standard for routine analysis of many pharmaceuticals and benefits from an unlimited number of possible phase systems (i.e. stationary phase/mobile phase combinations) and the possibility of a variety of different detectors (e.g. Diode Array Detector, Mass spectrometry, Fluorescence Light Detector) [76]. Nowadays, despite higher costs, UHPLC is often preferred due to the option of using columns with smaller diameters and particle sizes, which results in increased sensitivity, higher resolution and faster methods [77].

1.4.1 Shape selectivity in reversed phase liquid chromatography

Reversed phase (RP) chromatography utilizes nonpolar stationary phases and more polar mobile phases, allowing the separation of nonpolar analytes. The fully porous or superficially porous silica particles are typically covalently modified with linear alkanes (e.g. C8, C18, C30), although the variety is enormous and unusual moieties like cholesteryl, phenyl-hexyl and biphenyl are also being used [78]. Mobile phases typically consist of water and an organic solvent like acetonitrile or methanol, which can be altered to modify retention and selectivity. One of the most famous example being the cancellation of π-π-interactions by acetonitrile in phenyl-based columns [79]. Especially if columns are not end-capped, free silanol groups can interfere with separations, additives (buffers, acids, bases) can be used to decrease unwanted silanol activity of the modified silica particles [80]. Separation of analytes is mainly caused by the different hydrophobicity of the molecules and therefore varying interactions with the alkyl chains of the stationary phase, governed by partitioning and/or adsorption processes [78, 81]. Based on this principle, analytes with only small differences in polarity are typically more difficult to separate. In case of fatty acids stronger retention with increased carbon chain length and weaker retention with increased number of double bonds and oxidation-degree can be expected [82]. Chemical properties like position of oxidation or double bond position and configuration might only have a small impact on their hydrophobicity but can still result in retention shifts [82]. Therefore, retention can also be influenced by the three-dimensional structure of analytes.

Columns which are particularly good in separating structurally similar analytes based on their three-dimensional structure, are characterized by the term “shape selectivity”. This is limited for analytes with conformational restrictions, meaning the rotatability of bonds is limited e.g. due to double bonds, fused ring systems or steric hindrance [83, 84]. This limited rotatability changes

the three-dimensional structure of the molecule, which can be described by different descriptors: The length to breadth ratio (L / B ratio) two-dimensionally describes the side-ratio of the van der Waals radii of the planar molecule depiction [83, 85]. The three-dimensional descriptor “minimum cross-sectional area” is a more suitable for non-planar molecules as a box is drawn around the three dimensional depiction of the molecule [83, 86]. The chromatographic determination of shape selectivity can be performed by column selectivity test mixture SRM869 which consists of different polycyclic aromatic hydrocarbons (PAHs) [84], the Tanaka test differentiates planar and non-planar PAHs [84, 87] and Lesellier et al. evaluated it by separation of carotenoid isomers [84, 88]. A higher degree of shape selectivity can be observed for columns with higher bonding densities of selectors (e.g. alkyl-chains) on the silica particle, this typically results in higher selectivity of polymeric stationary phases when compared with monomeric stationary phases [83]. Planar molecules are stronger retained than nonplanar molecules and the retention increases with higher L / B ratio [83, 84]. This leads to earlier elution of coiled-up molecules, while more oblong molecules are stronger retained, which could be due to deeper penetration of the “pockets” formed by the ordered alkyl-chains. This model is often described as slot model [84]. Reversed phase columns with longer alkyl-chain modifications (C8 < C18 < C30) [84, 89] and lower column temperatures, due to higher degree of order, enhance the shape selectivity [90]. This knowledge can be translated to different molecule types and be exploited in LC method development.

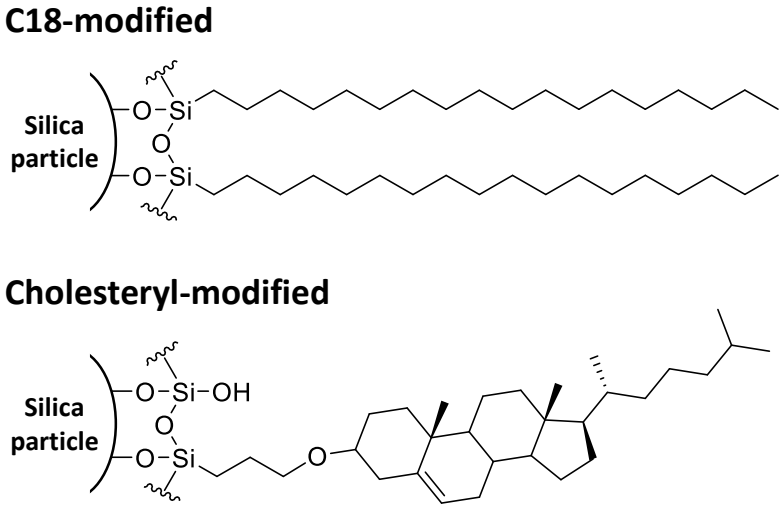

Figure 5: Schematic stationary phase structure of C18 and cholesteryl-modified reversed phase silica particles.

In the category of reversed phase columns, cholesteryl-modified stationary phases show very high shape selectivity, which has been mainly attributed to its highly ordered structure on the silica particles and is referred to as liquid crystal structure [91, 92]. Those columns typically consist of silica particles with cholesterol covalently bond by a variable linker, which increases the mobility

of the cholesterol (see Figure 5) [92]. Compared to common reversed phase columns, cholesteryl-modified stationary phases show better shape discrimination of many analytes, including diastereomers [82, 91] and sometimes even enantiomers [91], despite having lower bonding density, compared to a C18-phase [92]. Enantiomeric separations are probably caused by the formation of pockets and the chirality of the selector itself. Additionally, the cholesteryl-columns are capable withstanding high percentages of water in the mobile phase, without collapse of the respective moieties [91].

1.4.2 Enantioselective liquid chromatography

In case of single enantiomer drugs, the respective other enantiomer can have different pharmacological properties (e.g. pharmacodynamics) and thus has to be considered as impurity [93, 94], resulting in the need for appropriate analytical methods. The separation of chiral analytes by liquid chromatography (LC) is typically not possible with commonly used reversed phase columns, as enantiomers are only differentiable by not being super imposable. Hence, different approaches have been suggested for the distinction of chiral compounds, which can be differentiated into indirect and direct approaches [95].

Indirect enantiomer separation

Indirect enantiomer separations are based on generation of (permanent) diastereomers prior to LC-analysis by reaction of both enantiomers with a chiral derivatization agent (CDA) [95]. Hereby, two diastereomers are being formed, which are characterized by different physicochemical properties and thus can be separated with achiral columns (e.g. reversed-phase columns). This approach requires: (1) a possible reaction site on enantiomers and derivatization agent, (2) ideally 100 % enantiomeric purity of the derivatization agent, (3) derivatization conditions that should not chemically alter the enantiomers and CDA (including racemization) [96]. Additionally, the derivatization product should bear respective groups which give appropriate properties suitable for the chosen LC mode and detector [95, 96].

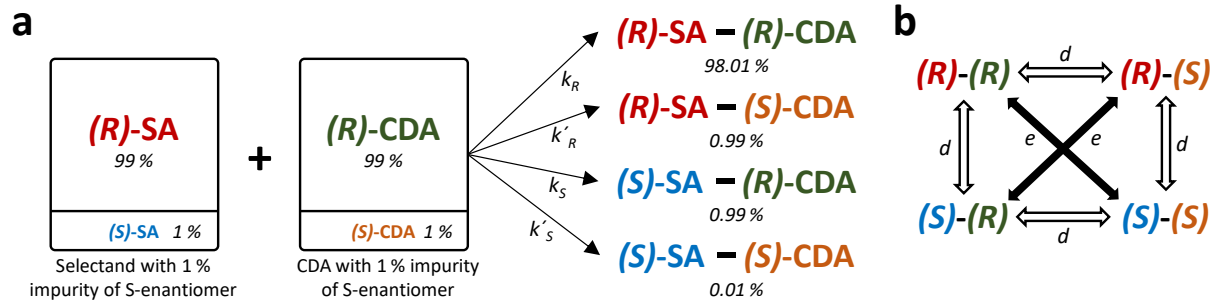

Figure 6: Reaction scheme for indirect enantiomer separation, a: reaction scheme of R-enantiomer of the selectand (with 1% impurity) with R-enantiomer of the derivatization agent (with 1% impurity), leading to the four respective products; b: enantiomeric/diastereomeric relation between the products, this leads on an achiral column to the coelution of (R)-(R) with (S)-(S) and (R)-(S) with (S)-(R), which leads to the overestimation of the impurity (S)-SA. “e” symbolizes enantiomeric compounds, “d” symbolizes diastereomeric compounds. Visualized with information from W. Lindner [97].

Derivatization reactions should always be conducted until completion, as in case of “kinetic racemate resolution” the reaction constants from R-and S-enantiomers differ. For example if a racemate is derivatized with reaction constant k_R being higher than k_S, an incomplete reaction may lead to the over-assumption of R-enantiomer [97]. Commonly used reagents are (±)-1-(9-

fluorenyl)ethyl chloroformate [98], OPA (*o*-phthalaldehyde) with chiral thiols and Marfey´s reagent [96, 99], bearing reactive functional groups like acyl chlorides. The determination of enantiomeric purity of CDAs is especially important in impurity profiling: Impure CDAs lead to generation of two diastereomeric products for each S- and R-analyte, which in total results in two coeluting enantiomers and two (separated) diastereomers, leading to lower enantiomeric excess levels than the true value (see Figure 6) [97]. Since higher levels of impurities suggest a higher relevance, this overestimation would result in more thorough analytics and higher costs.

Direct enantiomeric separation

Direct enantiomer separation does not require derivatization prior to chromatographic analysis, instead the enantiomers are being separated by formation of transient (non-covalent) diastereomeric complexes with a chiral selector, added either to the mobile phase or adsorptively or covalently immobilized on silica, leading to a chiral stationary phases [100].

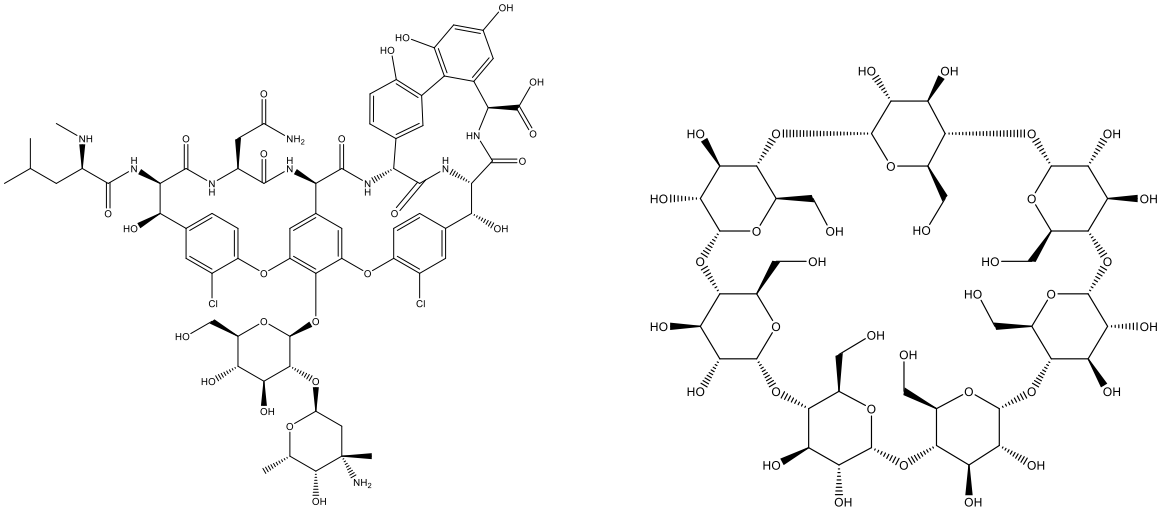

Figure 7: Structure of chiral mobile phase additives vancomycin (left) and β-cyclodextrin (right).

In the first instance diastereomers are formed between chiral mobile phase additives and enantiomeric analytes, yielding different association and dissociation constants [101]. This is often explained with the three-point-attachment model, explained in this chapter. Additionally, the distribution of these complexes between stationary and mobile phase can differ and thus contribute to the enantioseparation [101]. Since diastereomers differ in their physical properties a separation can be achieved with an achiral stationary phase. Nevertheless, the chromatographic method still has to be optimized, as the type of stationary phase, temperature, mobile phase pH and composition can greatly influence the separation [101]. Also, the used chiral additive has to

be selected according to the analytical problem, a screening of several chiral additives may be necessary. Examples for chiral additives are ligand-exchanger (e.g. ternary complex between copper, amino acids and enantiomer of interest), macrocyclic antibiotics (e.g. vancomycin, Figure 7) and cyclodextrin (e.g. β-cyclodextrin, Figure 7) [101]. This approach has only low significance in HPLC/UHPLC as the (pricey) additives are being consumed during analysis and interferences in the detection of the analytes are common [101, 102]. Additionally, detection principle and LC-methods can be restricted in the choice of chromatographic mode due to limitations from the used additive [101]. Also, (semi-)preparative separation of the enantiomers is only achievable with significant effort, since the chiral additive has to be removed after the collection.
Some of these problems can be circumvented by the use of chiral stationary phases (CSPs), although to some extent even the same selectors are being used. CSPs typically consist of porous silica particles with covalently bound or physically adsorbed chiral selectors [102], which are responsible for the chiral recognition. The formed diastereomers can exhibit different association and/or dissociation constants [97]. Depending on the fit and strength of interaction the association constant is higher for an “ideal fit” of one enantiomer in the interaction site, whilst it is lower for a “non-ideal fit” of the other enantiomer [102]. This ideally results in chromatographic separation of the enantiomers.

This chiral recognition can be explained in a simplified manner by the “three-point attachment model” from Easson and Stedman [103], who postulated that at least three configuration dependent interaction points between chiral molecule and its interaction site are required for chiral recognition. This was highly discussed and refined with the following adjustments [102]: multipoint-interactions (dipole stacking, π-π-interactions) can count as more than one interaction site [104]; not all three interactions are needed (one strong interaction could be enough to generate the diastereomeric complex); molecule with stereocenters in rigid structures require less interactions [105]; solvent molecules and the environment on the adsorbent´s surface can influence chiral recognition [102], thus the mobile phase composition should be carefully considered during method development. Further the steric accessibility of the interaction site of the CSP can play a significant role in enantio-recognition, since bulky residues of the chiral stationary phase may “shield” the access to the interaction site for one enantiomer [102].

Over the past decades a huge diversity of chiral stationary phases has been researched and/or commercialized (see Figure 8) [102, 106]. Especially, (immobilized) chiral polysaccharide columns have been established as the state-of-the-art phases for enantiomer separation [107, 108]. Here, amylose- or cellulose-derivatives with phenylcarbamate- or benzoate-residues are

synthesized and either coated or immobilized (covalently bound [109] or crosslinked [110]) on silica particles [102], resulting in complex three-dimensional structures (see Figure 9). The interactions leading to the extraordinary enantio-selectivity of these columns are quite manifold and can be grouped in molecular chirality (stereocenters of glucopyranose units), conformational chirality and supramolecular chirality [102].

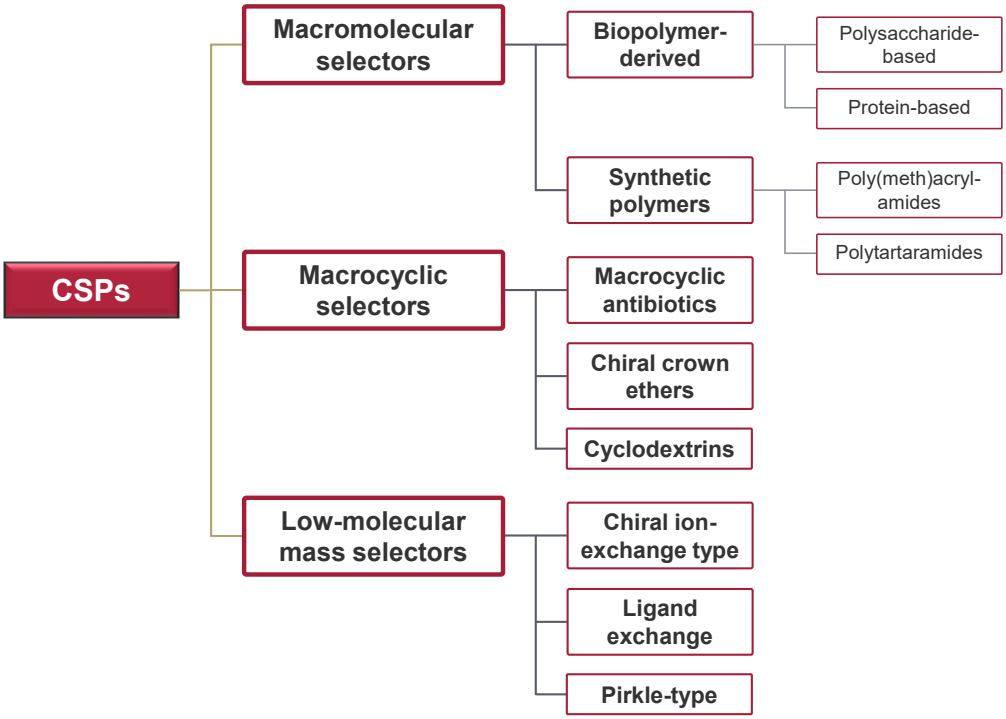

Figure 8: Classification of chiral stationary phases in macromolecular, macrocyclic and low-molecular mass selectors, visualized with information from M. Lämmerhofer [102] & J. Teixeira et al. [106].

The conformational chirality is influenced by the different helicity of amylose (left-handed 4/3) and cellulose (left-handed 3/2) in the polymer backbone, due to α- or β-1,4 glycosidic bonds [111-113]. The modification of the polysaccharides with phenylcarbamates or benzoates results in a polar layer close to the polymer-backbone (carbamates/benzoates) and a hydrophobic layer in the periphery [111], here the substituents (e.g. chlorine and/or methyl) and positions on the phenyl-ring modify the polar interactions of the polar layer [111, 114, 115]. In total this results in a chiral groove (see Figure 9) with, by the substituents limited access, which is able to host and differentiate chiral molecules due to complex combinations of interactions [111]. This, also allows problematic separations of achiral molecules like α-/γ-linolenic acid [111, 116]. These fatty acids only differ in their double bond positions and thus in their three-dimensional structure, some conformations could result in more favorable three-dimensional structures, allowing penetration of the grooves and stronger interactions. The drastic influence of variations in the used backbone and selectors were also shown for achiral fatty acid isomers [82]. The supramolecular chirality is

explained by the formation of ordered regions from the alignment of polymer-chains and is for example influenced by the used solvents during coating procedure (in case of coated phases) [102, 117].

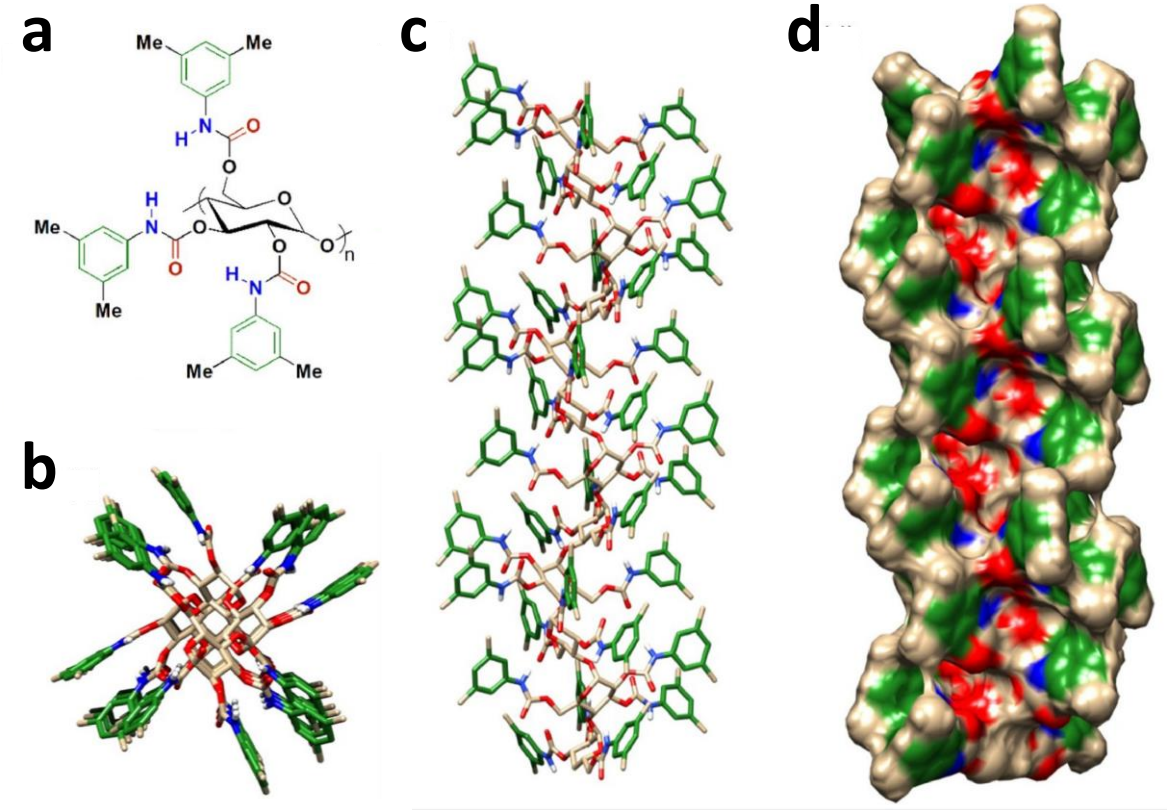

Figure 9: Amylose tris(3,5-dimethylphenylcarbamate); a: structural formula; b: three-dimensional structure, viewpoint along the backbone axis; c three-dimensional structure, viewpoint perpendicular to the backbone axis; d: three-dimensional structure with electron densities (phenyl: green, N-H: blue, C=O: red), viewpoint perpendicular to the backbone axis. Reprinted from Journal of Chromatography A, 1623 (2020), P. Peluso, V. Mamane, R. Dallocchio, A. Dessì, S. Cossu, Noncovalent interactions in high-performance liquid chromatography enantioseparations on polysaccharide-based chiral selectors, Copyright (2020), with permission from Elsevier (Ref. [111]).

Changes of the polymer´s chain conformation and therefore selectivity changes are possible by temperature-changes [118], mobile phase solvents [119] and additives [120]. Coated phases are prone to swelling and bleeding of the polysaccharides, when used with certain solvents, diminishing its performance [102]. Compared to coated phases, immobilized phases exhibit reduced enantioselectivity due to the immobilization when used with standard solvents, which can be compensated by the use of non-standard solvents due to its remarkable solvent compatibility [121, 122]. The dominance of chiral polysaccharide columns for enantiomer separation has been strengthened over the past decades more and more by developments like the immobilization, allowing separations in basically all chromatographic modes with excellent solvent compatibility, new phenylcarbamate/benzoate-residues and sub-2µm particles.

1.5 Multidimensional Liquid Chromatography

1.5.1 Basics and different approaches

During the validation of analytical methods, according to ICH, proper selectivity should be proven by either absence of interferences or by comparing with results, obtained with an orthogonal procedure [20]. Thereby the analytical methods should be able to distinguish similar compounds with closely related structures [94]. Depending on the sample this can be very challenging, as complex samples, like lipid-based pharmaceuticals, typically display impurities in low concentrations but exhibit high numbers of other components in high concentrations (APIs or matrix). Especially degradation related impurities, due to their structural similarities, can show similar chromatographic behavior to the precursor-API, possibly resulting in coelution and altering the mass balance [123, 124]. For proper determination the use of multiple orthogonal LC methods and detectors (e.g. LC-MS) has been suggested [94, 123].

It is generally known that coelutions can result in detection interferences, possibly leading to wrong assumptions regarding the molecule´s quantity or structure, e.g. by added UV-spectra or ion-suppression in MS-detection [125]. Therefore, LC-methods with high resolving power are required, where two-dimensional LC (2D-LC) could be considered superior to one-dimensional LC (1D-LC) due to its higher peak capacity and orthogonal separation dimensions [126].

Multidimensional Liquid Chromatography in general describes the use of more than one chromatographic dimension for a specific analytical problem and can be performed “offline” or “online”. In case of offline multidimensional liquid chromatography, the collection step is often followed by some kind of concentration of the analytes (e.g. solvent evaporation, extraction) before injection into the next dimension. The concentration and reinjection step doesn’t have to be done directly after collection [127]. This approach is characterized by its simplicity, since only one chromatographic system without any further instrumentation is needed (implementation of automated fraction collection is optional) and all separation dimensions can be fully optimized without making compromises in regards of analysis time [127, 128]. Downsides include the increased risk of degradation or contamination during collection and concentration of the analytes [127-129], high degree of manual steps and long analysis time, making it unsuitable for large number of samples [130].

In online multidimensional liquid chromatography, the collection and transfer to the next chromatographic dimension is performed with an interface (valve system), which differs from manufacturer to manufacturer. This approach to multidimensional LC is much more expensive

than the offline approach, as it requires at least one valve system and pump for each additional dimension. Typically, this minimalistic setup is extended by a column compartment and detector for each dimension [127]. Further, during the more time consuming method development, besides LC-method optimization also different bottlenecks have to be addressed (discussed in 1.5.4), which are especially present in full-comprehensive 2D-LC [131]. Nevertheless, online multidimensional methods in general offer many advantages, like reduced risk of sample contamination, degradation or loss during collection and no extraction/evaporation step after collection [129].

Most commonly online two-dimensional setups are being used, even though some research groups reported on “online three-dimensional-LC”. Those approaches apply for example a serial coupled (tandem) column, consisting of two columns with different selectivities in the first dimension [132]. Thus, it cannot be considered as “real” 3D-LC with utilization of three separation dimensions, as discussed by Stoll et al. for 2D-LC. The approach of tandem-columns will not drastically increase the resolving power like a coupling of those columns with an interface would. Also, the elution order in the second column could be opposite to the one in the first, thus diminishing the separation achieved in the first dimension [127].

1.5.2 Interfaces and different modes of online 2D-LC

Until the 2000´s direct transfer was the preferred way to transfer fractions from first to second dimension, where analytes eluting from the first dimension (^{1}D) are being focused on the second dimension (^{2}D) column. Nowadays, it has been largely replaced by loop transfer, due to increased popularity of gradient elution. Loop transfer requires an interface comprising of at least one valve and one loop, in which the collected fraction from the ^{1}D is stored until analysis in the second dimension [94]. Dependent on the analytical problem, the 2D-LC interface and operation mode can be selected, whereas exact interface-design and principle differ from manufacturer to manufacturer. For further information regarding this the reader is referred to Reference [133].

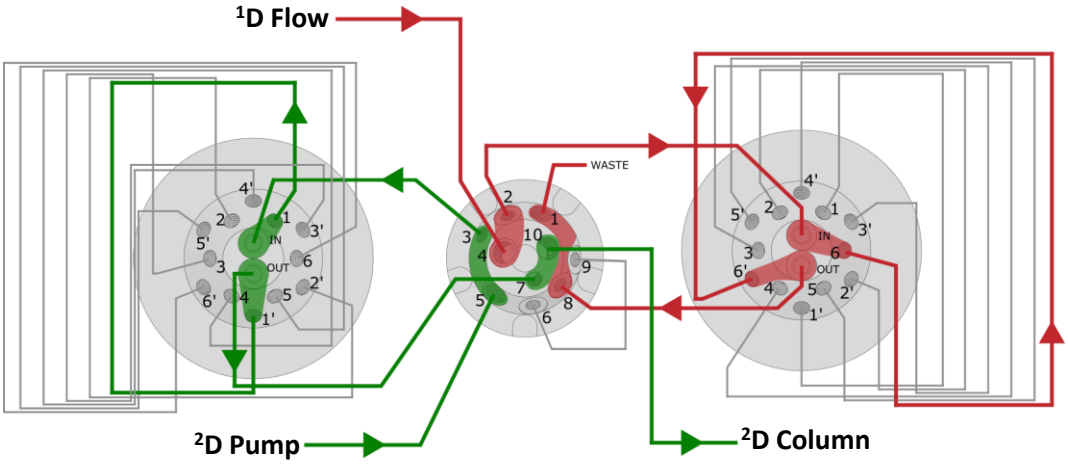

Figure 10: Heartcutting 2D-LC interface from Agilent Technologies (Waldbronn, Germany) consisting of an ASM (active solvent modulation)-valve connected with two deck valves with six deck loops each. Eluent flow from the ^{1}D is symbolized in red (collection-position), Eluent flow from the ^{2}D is symbolized in green (analyzing-position). Grey capillary in the ASM-valve (port 6 to 9) is used for active solvent modulation.

In heartcutting 2D-LC (LC-LC) a single fraction of the ^{1}D mobile phase is being collected in a loop (capillary), followed by a valve switch that transfers the fraction into the second dimension (^{2}D), allowing further separation of analytes which are not separated in the ^{1}D [127]. After completion of the ^{2}D method the next fraction can be transferred.

Multiple heartcutting 2D-LC (mLC-LC) can be performed if multiple fractions/peaks of the ^{1}D are of interest, but requires a more sophisticated valve-setup (example shown in Figure 10). Here, the deck loops can be utilized for “peak parking” before respective valve-switches, of the deck valves and ASM-valve (in this case), transfer the collected eluent to the ^{2}D [127, 134].

In Selective comprehensive 2D-LC (sLC×LC) multiple fractions of one peak group are collected and transferred to the ^{2}D, allowing the comprehensive analysis of one ^{1}D fraction (also possible with valve-setup in Figure 10) [127, 135].

In all of these modes both dimensions are independent of each other in regards of method length, as the stored fractions can be transferred into the ^{2}D at a later point in time, resulting in more optimal separation conditions in both dimensions and thus better peak resolution [134, 136]. Only if more fractions are of interest than storage-capillaries available the method lengths have to be revisited. The collection-start of these methods is either triggered time- or peak-based, where typically both approaches need at least one screening run to optimize the cut times or trigger limits for proper collection.

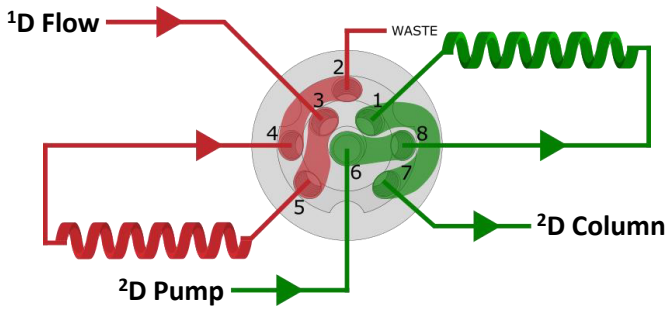

Figure 11: Full comprehensive valve (2-position/8 port) from Agilent Technologies (Waldbronn, Germany); Eluent flow from the ^{1}D is symbolized in red, Eluent flow from the ^{2}D is symbolized in green.

In contrast, full comprehensive 2D-LC can be considered as “untargeted” approach as it can be used, after method development, on unknown samples as it does not require a trigger to initiate the collection. Instead, all of the eluent from the ^{1}D is transferred in fractions to the ^{2}D [127]. Here the 2D-LC valve is equipped with two identical loops (see Figure 11), during the analysis of the first loop in the ^{2}D, the second loop is being filled with ^{1}D eluent. One of the challenges of this approach is that ^{1}D and ^{2}D analysis time are coupled, hence to avoid information loss, the ^{2}D separation has to be finished before the other loop is filled with ^{1}D eluent [127, 137]. This can be achieved by usage of low flow rates and narrow columns in the ^{1}D and fast ^{2}D separations (e.g. < 60 seconds) [136], e.g. by use of short columns with wider inner diameter and high flow rates [137].

In pharmaceutical analysis (multiple) heart-cutting is more commonly applied than comprehensive 2D-LC. This might be due to: (1) the simplicity of (m)LC-LC in development and application [94], (2) the complexity of LC×LC in data analysis and method optimization [129], (3) since robust, fast and orthogonal methods are required, yet simple methods are preferred [130]. The most common applications in the pharmaceutical field are: (m)LC-LC and sLC×LC for trace analysis [138, 139] and enantiomeric separations [94, 140]; LC×LC for impurity profiling [94, 141]. To lesser extent online 2D-LC is used for desalting, which allows coupling of existing MS-incompatible routine analysis methods with an MS-compatible ^{2}D, thereby enabling MS-detection [94, 134].

1.5.3 Peak capacity

The term peak capacity (n_c) was first described by Giddings to put the separation capabilities of columns and methods into numbers. Peak capacity describes the theoretical number of peaks which can be placed between the first (void time) and last eluting peak, exhibiting a constant resolution [129, 142]. In one-dimensional gradient elution this simplified equation from Dolan et al. in regards to the used separation space is commonly applied [143]:

$$n_c = \frac{t_{last} - t_{first}}{W} \quad (1)$$

Here t_{last} stands for the retention time of the last eluting peak, t_{first} for the first eluting peak and W is the average baseline peak width, implicating that long methods with narrow peaks will lead to high peak capacity. Since this approach assumes peak widths being constant, modified versions with regards to changing peak widths in reversed phase and ion-exchange chromatography have been introduced by Neue [144].

Giddings explained the necessity of multidimensional systems in relationship to the sample dimensionality. He stated simple samples (low sample dimensionality) do not require separation techniques with high dimensionality, but complex (multidimensional) samples (e.g. “omics” samples or pharmaceutical multicomponent formulation) need separation methods with high system dimensionality, resulting in high peak capacities as illustrated in Figure 12 [131, 145]. Complex samples with a large number of compounds will require high peak capacities to obtain a chromatogram, ideally without coelution and interference of other compounds [131].

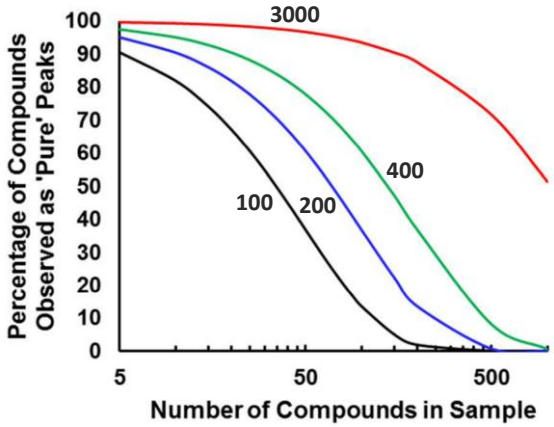

Figure 12: Relationship between number of compounds in the sample, effective peak capacity of the method (red: 3000, green: 400, blue: 200, black: 100) and the resulting number of compounds which will be visible as “pure” peaks (resolution ≥ 1). Based on calculations of Statistical Theory of peak Overlap [146]. Reprinted with permission from American Chemical Society from D. R. Stoll, P. W. Carr, Two-Dimensional Liquid Chromatography: A State of the Art Tutorial, Analytical Chemistry, 89 (2017), 519-531 (Ref. [131]). Copyright 2017 American Chemical Society.

Stoll defined this failure of resolving complex mixtures by 1D-LC, based on too low peak capacities, as type-A problems. Although many developments (e.g. superficially porous and smaller particles) in one-dimensional liquid chromatography (1D-LC) have increased the overall performance and therefore the peak capacity, the limits are fairly often reached with complex samples. While for 1D-LC peak capacities of 3000 are far from reachable, they can be achieved with two-dimensional liquid chromatography (2D-LC), as peaks "profit" from the peak capacities of both dimensions due to complementary separation mechanisms [131].

The theoretical peak capacity of a two-dimensional separation can be obtained by multiplication of the peak capacity of the first dimension (^1n_c) with the peak capacity of the second dimension (^2n_c) and is referred to as the product rule [147]:

$$n_{c,2D} = {}^1n_c \cdot {}^2n_c \tag{2}$$

Based on this equation offline 2D-LC would be ideal in regards of maximization of peak capacity as the length of the second dimension is not limited. However, this would result in extremely long runtimes, therefore online LC×LC is often preferred [129, 131]. But even here it should be seen as a theoretical concept, as it is based on ideal assumptions like complete orthogonality and the absence of undersampling, whilst in reality these factors play a significant role in the development of 2D-LC methods. For this, respective correction factors (<β> correction factor for undersampling; $f_{coverage}$: utilization of separation space) can be applied, resulting in the more realistic "effective peak capacity" [129, 148]:

$$n_{c,2D} = {}^1n_c \cdot {}^2n_c \cdot \frac{1}{<\beta>} * f_{coverage} \tag{3}$$

1.5.4 Online comprehensive 2D-LC method development

An analyst is often confronted with samples which contain mixtures of analytes that are difficult to separate (e.g. isomers or enantiomers). With such samples and limited analysis time 1D-LC often reaches its limit due to incomplete separation of “resistant” peak pairs (Figure 13, Column A, critical analyte pair red-green). Changing to another column with different selectivity may be able to separate this critical peak, but other peaks might coelute (Figure 13, Column B). Stoll refers to this problem as type-B problem [131]. Type-B problems and, the above mentioned, type-A problems can be solved by proper utilization of two-dimensional LC (Figure 13, Column A × Column B). In order to benefit from 2D-LC, proper method-development in consideration of the four main issues is necessary: (1) orthogonality issue, (2) compatibility issue, (3) undersampling issue and (4) sensitivity issue. Although these issues also occur to certain extent in offline 2D-LC, the focus of this chapter will be on the significance in online 2D-LC, as they occur more frequently and solutions are not that trivial.

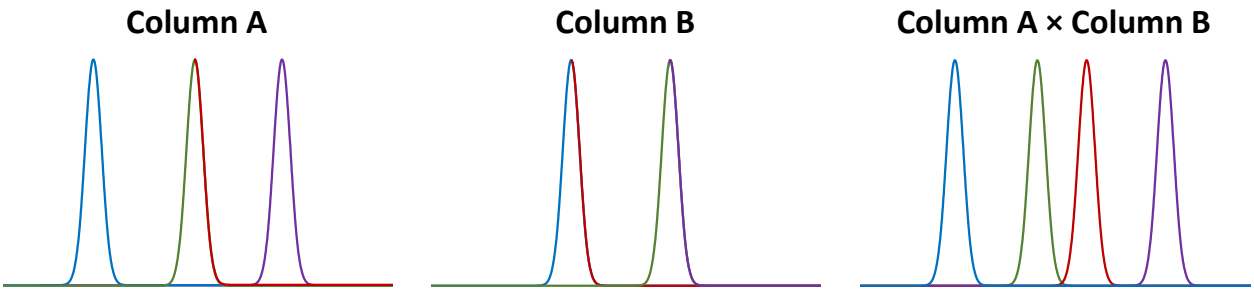

Figure 13: Visualization of type-B problems [131] in 1D-LC (Column A, Column B) and its solution by two-dimensional coupling of Column A and B (Column A × Column B). Column A cannot separate green/red analytes, while Column B can separate green and red analytes, but cannot separate blue/red and green/violet. Each color represents one analyte, bicolored peaks symbolize coeluting analytes while uni-color peaks symbolize resolved analytes.

The orthogonality issue

In two dimensional LC the used separation space should be maximized by coupling two separation dimensions with (ideally) completely unrelated separation mechanisms, resolving unseparated peaks from the first dimension in the second dimension and vice versa. Combining columns with similar separation mechanisms will not give any additional separation, when compared with one-dimensional LC (see Figure 14a). This is known as the orthogonality issue [131]. For this, Giddings proposed selecting the separation modes based on the type and number of intermolecular interactions of the investigated analyte mixture with mobile or stationary phase, also known as sample dimensionality [145, 149]. For example, in a mixture of *anteiso*-methyl-alkanes with different chain lengths, the hydrophobicity and the configuration of the stereocenter contribute to the dimensionality. Hence, it would be necessary that one dimension's separation mechanism is based on hydrophobicity and the other dimension's separation mechanism on chirality, which in reality is very unlikely as columns mostly exhibit multiple interaction types. This characteristic can either be exploited, in case of mixed-mode columns or, if necessary, inhibited by proper selection of mobile phase and thus reducing some interactions while increasing others [149]. Overall, combinations of two dimensions with significant differences in the separation mechanism are desirable. For this purpose, orthogonality metrics can be used for quantification of those differences, improving the decision-making process. Many approaches have been proposed and discussed on the search for the "ideal" orthogonality metric [150, 151].

Here, Schure et al. differentiated between discretizing and non-discretizing methods and even suggested the use of "product orthogonality metrics", composing of one discretizing method combined with the convex hull relative area. Discretizing methods divide the separation space into bins or boxes and calculate the orthogonality metric according to the rules of the respective method [150]. Gilar first described the discretizing concept of geometric surface coverage (SC_G) as orthogonality metric by a visualization of the two-dimensional separation space, divided into bins/boxes, whereas the total amount of bins should be (ideally) equal to the number of analytes in the sample (Figure 14b). The normalized retention times of the analytes from the first and second column are displayed in the grid and the orthogonality is calculated by counting occupied bins (∑bins) in relationship to the total peak capacity (equals total number of bins; P_{max}) [152]:

$$O = \frac{\sum bins - \sqrt{P_{max}}}{0.63 \cdot P_{max}} \quad (4)$$

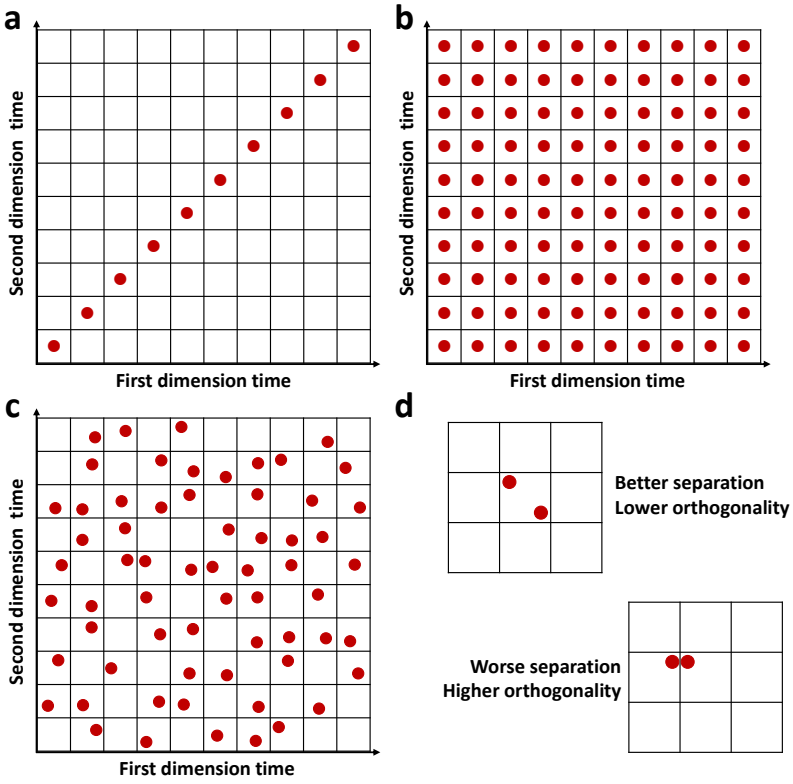

Figure 14: Visualization of the two-dimensional separation space, analytes are symbolized by red dots; a: strong correlation of separation mechanisms of first and second dimension, no benefit from the two-dimensional coupling, b: no correlation of separation mechanism of first and second dimension, 100 % of bins are occupied, ideal, unrealistic; c: no correlation of first and second dimension separation mechanism, 63 % of bins are occupied, realistic, random; d: problem of the bin-counting approach: individual distribution of analytes in relation to each other are not considered, thus better separated peaks can result in lower orthogonality due to presence in the same bin. Figure a, b and c are reproduced with permission from American Chemical Society from M. Gilar, P. Olivova A. E. Daly, J. C. Gebler, Orthogonality of Separation in Two-Dimensional Liquid Chromatography, Analytical Chemistry, 77 (2005), 6426-6434 (Ref. [152]). Copyright 2005 American Chemical Society.

Gilar stated that complete utilization of separation space (Figure 14b) is an unrealistic notion. More likely a full-orthogonal realistic random system has area coverage of 63 % in the separation space, which was accounted in equation 4 and is displayed in Figure 14c [152]. Gilar´s approach is a fast and simple method calculating orthogonalities for comparison, but it received criticism, as the resulting orthogonalities are strongly dependent on the selected bin-sizes [153] and the concept of setting the total number of bins equal to the amount of analytes is often not possible for complex mixtures with unknown number of analytes and overlapping peaks [148]. Also, the selection of bin sizes may be a weak point: e.g. for an analyte mixture of 23 analytes a 5x5 grid could lead to an underestimation.

Stoll modified the approach of geometrical surface coverage by focusing on the dimensionality of separation space, instead of the sample space [148]. In this method (SC_S, known as Gilar-Stoll surface coverage) the separation space is divided into bins of user-selected size, which will be

closer to reality as some combinations of peak-capacities in the first and second dimension are easier to achieve than others [154]. After plotting, a line is drawn around the utilized separation space including unoccupied bins (Figure 15a), followed by fractional coverage calculation. The inclusion of unoccupied bins assumes that even if the investigated sample does not fill this empty bin it is still plausible that a compound in a different sample could, based on the separation mechanism [148, 154]. This metric is less influenced by bin-size compared to SC_G, but can lead to overestimation of orthogonality due to the inclusion of empty bins [151]. Additionally, it is hardly automatable and thus the inclusion or exclusion of empty bins is highly subjective [148]. Other discretizing methods are: box-counting dimension D_{BC} [151, 155], Two-dimensional entropy H_{12} [150, 156] and mutual information MI [150, 151].

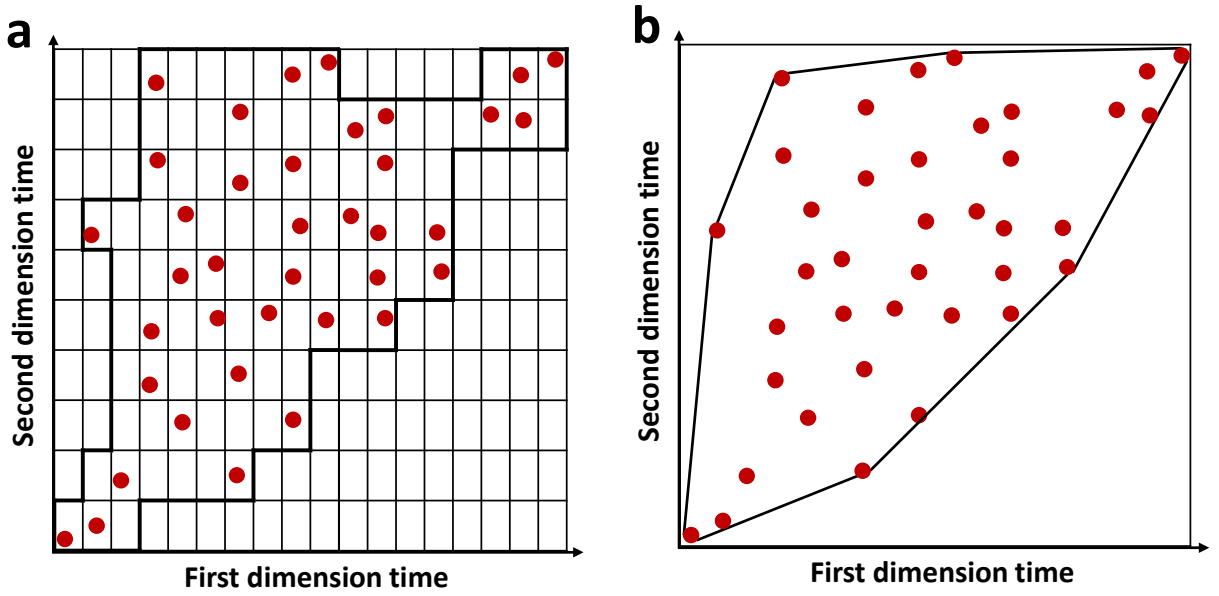

Figure 15: a: Schematic representation of Gilar-Stoll surface coverage SC_S [154]; b: Schematic representation of the convex hull method [148].

Non-discretizing methods include, among others, nearest neighbour statistics [157], convex hull [158] and asterisk method [159]. The convex hull surface coverage method is based on the calculation of convex hull relative area A_H, where the peaks at the margin of the separation space plot are connected by straight lines, resulting in an area which can be related to the total separation space [148, 150]. This results in comparable surface coverage values as the Gilar-Stoll method and also includes areas of the separation space which are less occupied, both leading in general to higher orthogonalities than SC_G and due to its non-discretizing character the guess-work of whether or not including empty bins is removed. But it seems to be prone to outliers since even one will significantly alter the area utilized [151].

The orthogonality determination in general becomes more accurate with increasing number of analytes/peaks, as variability increases with smaller sample sets [150, 151]. Therefore the use of model mixtures is often proposed instead of using the sample for which the 2D-separation is being optimized [151]. Correct selection of the model mixture is not trivial, as representative compounds must be chosen, but exact compositions of samples may not be known [151] and real samples show finite number of analytes [150], therefore the exact transferability to other samples may be criticized.

Especially SC_G can be disadvantageous for samples with low number of analytes, as it does not account for empty bins, which could lead to similar orthogonalities, although the distribution in separation space is completely different [151]. Also, due to the fixed bin-sizes two or more peaks could display low resolution, but due to the elution in different bins the orthogonality is higher than for better separations eluting in the same bin (Figure 14d). Therefore, other quality-parameters (e.g. resolution) should not be neglected in the determination of separation dimensions.

The compatibility issue

Correct selection of mobile phases in liquid chromatography is of high relevance, as the chosen mobile phases have great influence on the separations in 1D-LC and 2D-LC. Different mobile phases can enhance or decrease interaction of analytes and stationary phases, as for example known from acetonitrile decreasing π-π-interactions [160, 161]. In 2D-LC the compatibility issue often defines the order of the separation dimensions, as the compatibility of transferred ^{1}D mobile phase in the second dimension is of major concern [161]. The most prominent compatibility issue is: Viscous fingering, caused by viscosity differences between ^{1}D and ^{2}D mobile phase, resulting in penetration of low viscosity ^{2}D mobile phase through the high viscosity sample plug (e.g. isopropanol, transferred from the first dimension) [161, 162]. This results in reduced chromatographic performance and may even lead to peak splitting. The phenomenon of viscous fingering is rarely observed in 1D-LC, as the volume of sample plugs are rather small, which is not the case in 2D-LC due to the larger transfer volume [161, 163].

The usage of isopropanol in the ^{1}D mobile phase (e.g. in RPLC×RPLC) or any other solvent with high elution strength in the respective chromatographic mode, can also lead to breakthrough after transfer to the second dimension, caused by large injection volume and high elution strength. [161, 164]. Hereby, the resulting chromatogram can exhibit two peaks for each analyte, one eluting close to dead volume, due to being dragged through the ^{2}D column by the solvent plug and a smaller one at the expected position, due to some analyte-molecules still being able to

interact with the column [165]. Under certain circumstances total breakthrough can occur, where the second peak is symmetrical (no deformed peak shape) [164].

Active solvent modulation in the 2D-LC interface reduces solvent strength and viscosity of collected ^{1}D mobile phase, thus focusing the analytes in the ^{2}D column head and improving peak-shape, allowing larger transfer volumes in the second dimension [161, 166]. Alternatively, the use of trap columns instead of collection capillaries is possible and allows reduced ^{2}D transfer volume and a variety of new applications, like desalting or enrichment of analytes [167, 168]. NPLC×RPLC is the extreme case for incompatibility, as the mobile phases are typically completely immiscible and show very high elution strength in the contrary dimension. Therefore, solutions like thermal modulation on trap columns [169], vacuum-evaporation-interface [170] and thermal evaporation assisted adsorption interface [171] have been proposed for removal of normal-phase solvent, but are less frequently used in routine LC×LC analysis [161]. Also, the solubility of ^{1}D buffer salts in the second dimension and MS-compatibility should be considered during method development, especially phosphate buffers are generally known for precipitation in solvents with high organic content and being incompatible with MS-detection.

The orthogonality issue and the compatibility issue typically represent the bottlenecks, making certain combination more easily achievable than others, which have been summarized by Pirok et al. [161].

The Undersampling issue

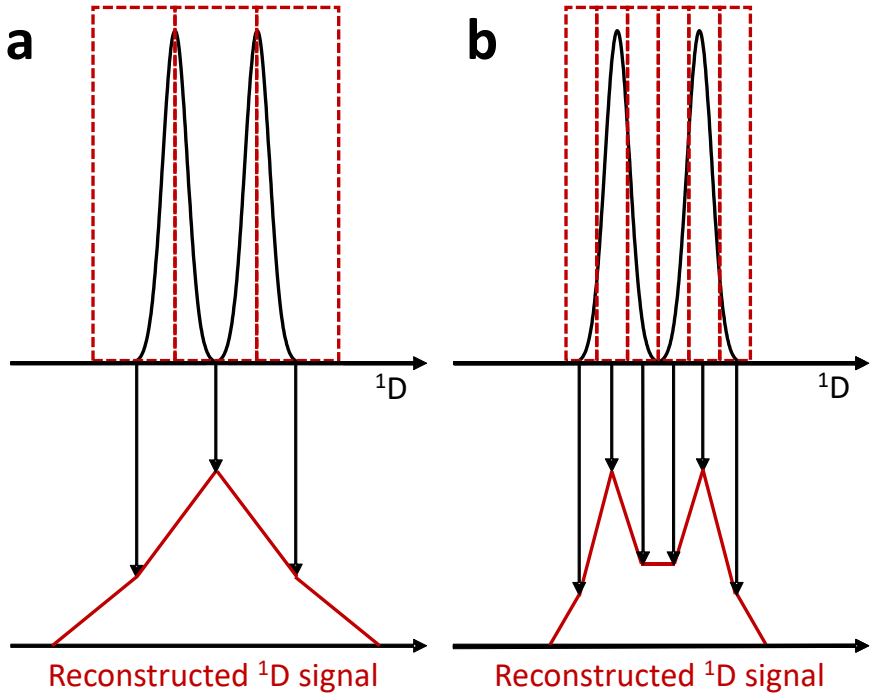

Figure 16: Schematic representation of the undersampling phenomenon in a 2D-LC setup. The chromatogram in the top shows the ^{1}D detector signal, while the bottom shows the (from the ^{2}D signal) reconstructed signal of the first dimension. Red boxes symbolize the transferred fractions. a: three fractions over the width of both peaks result in loss of ^{1}D separation, b: Six fractions over the width of both peaks taken. ^{1}D separation is preserved but still a bit of undersampling is visible, as the peaks in the reconstructed signal are not baseline separated. Reprinted & modified with permission from S. Bäurer [172].

Undersampling describes the loss of resolution of ^{1}D separations due to remixing of separated analytes during the collection or transfer to the second dimension, which is typically caused by low sampling rates (fraction collection rates) in the first dimension [131]. This will lead to complete loss of separation if the second dimension doesn't show selectivity for the respective peak pair [153]. This is illustrated in Figure 16a. The first dimension chromatogram, reconstructed from the second dimension, only displays one peak. In practice this will lead to reduced peak capacities of the 2D-method, as the prerequisite of the product rule of not losing any resolution from the first dimension is not fulfilled, thus reducing the number of separated peaks dramatically [131, 173].

To prevent this loss of resolution Murphy, Schure and Foley stated that a minimum of three fractions for in-phase sampling and four fractions for out of phase sampling per 8σ peak width have to be collected [131, 174]. Visualized in Figure 16b the collection of three fractions per peak leads to a visible separation in the reconstructed signal. Nevertheless, complete prevention of undersampling is rarely achievable and can be accounted for by broadening factor <β> (Equation (*5*, constant κ=0.21 if $0.2 < (t_s/^{1}\sigma) < 16$; t_s: sampling time, $^{1}\sigma$: standard deviation of the first

dimension peak before sampling; according to [175]). The broadening factor is used in the calculation of the effective peak capacity (Equation (*3* and to correct the first dimension´s peak capacity (Equation (*6*, according to [175]) [131].

$$< \beta > = \sqrt{1 + \kappa * \left(\frac{t_s}{{}^1\sigma}\right)^2} \tag{5}$$

$${}^1n_c{}' = \frac{{}^1n_c}{< \beta >} \tag{6}$$

As shown above, long sampling times in the ^{1}D increase the risk of undersampling and thus can reduce the ^{1}D peak capacity to the extent that the relevance of a LC×LC in comparison to 1D-LC might be questioned [126, 131]. Intuitively, one could think that the simple solution for the prevention of undersampling would be the use of short ^{1}D sampling times. Unfortunately, this has only limited applicability as the ^{1}D sampling times in LC×LC are dependent on the ^{2}D analysis time. Therefore, the reduction of ^{1}D sampling time might correlate with a loss of ^{2}D peak capacity, up to the point, where the reduction of undersampling will not benefit the total peak capacity enough to overrule the loss of ^{2}D peak capacity [131, 176].

The sensitivity issue

The detection sensitivity issue in 2D-LC is driven by the subsequent dilution of the analyte on the ^{1}D and ^{2}D column, due to the continuous diffusion of the analytes, resulting in peak broadening and loss of sensitivity [131]. Compared to 1D-LC this phenomenon is more prominent in 2D-LC due to the additional dilution in the second dimension [175, 177]. Several researchers reported on this problem and introduced the dilution factor [175, 178, 179], which in 2D-LC is formed by the multiplication of ^{1}D dilution factor (^{1}DF) and ^{2}D dilution factor (^{2}DF) [179].

Special interest is paid to ^{2}DF as a metric for estimating sample dilution (^{2}DF > 1) or concentration (^{2}DF < 1) by the ^{2}D dimension, which suggests minimizing ^{2}D peak widths and increasing the transfer volume to ^{2}D [175]. Here $c_{transfer}/V_{transfer}$ and c_{det}/V_{det} are the concentrations or volumes of transfer and detection in the ^{2}D, while $\sigma_{v,col}$ resembles the standard deviation of the ^{2}D peak in volume units (see Equation (7).

$$^2DF = \frac{c_{transfer}}{c_{det}} = \frac{V_{transfer}}{V_{det}} = \frac{\sqrt{2\pi} * \sigma_{v,col}}{V_{transfer}} \quad (7)$$

The accessibility of ^{2}DF < 1 is strongly dependent on the used combination of separation dimensions, as the elution strength and amount of solvent transferred from the first dimension has significant impact on the peak width and height in the second dimension [163, 180]. While some combinations do not need any adjustments to achieve low ^{2}DF values, some could be incompatible, not allowing transfer of large volumes, due to the risk of ^{2}D peak broadening [163, 175]. For example, in RPLC×RPLC the transfer of small volumes of a strong eluent into the ^{2}D could still work (depending on the conditions in the ^{2}D), due to the subsequent dilution of the small sample puck by ^{2}D mobile phase.

In case of rather incompatible approaches a multitude of modifications to the 2D-interface can be used to minimize negative effects. Some examples have already been discussed above as solution of “The compatibility issue”. Probably the most important being active solvent modulation, which dilutes the collected ^{1}D solvent with ^{2}D mobile phase, thus allowing focusing of analytes in the ^{2}D column head [166]. Another factor contributing to reduced sensitivity in 2D-LC is the development of fast ^{2}D methods, which usually involves the use of short columns with relatively wide inner diameter, allowing high flow rates [137]. In case of mass spectrometric (MS) detection, the mobile phase fraction reaching the ion source often has to be reduced (e.g. by flow splitters), as the ESI sources of most mass spectrometers are not build for high flow rates and could lead to incomplete evaporation of solvent. Reducing the mobile phase fraction reaching the detector also reduces the amount of analyte reaching it, thus reducing its sensitivity.

1.6 Detection issues of fatty acids in liquid chromatography

Especially in the past decades the main focus of fatty acid analysis lied on GC-analysis, which in general requires derivatization of non-volatile analytes (e.g. to respective methyl esters) to achieve volatility [181]. This increases the risk of sample-alteration, e.g. facilitated oxidation reactions especially in polyunsaturated fatty acids by heating or the use of sulphuric acid during derivatization [182]. Due to the focus of this work on liquid chromatography the reader is referred to Ref [183, 184] for more information regarding GC-analysis of fatty acids. Also, other detection techniques like charged-aerosol-detection (CAD) should not be forgotten in impurity profiling, due to its possibility of quantification without respective standards as different analytes will have similar detector responses [185, 186], but will not be discussed here. Especially LC has been implemented as one of the most important analytical techniques in pharmaceutical analysis, due to short analysis times by ongoing advances in this field (e.g. UHPLC-instruments, smaller and core-shell particles, innovative stationary phases) [187] and its versatility regarding usable detection techniques.

1.6.1 Mass spectrometry detection

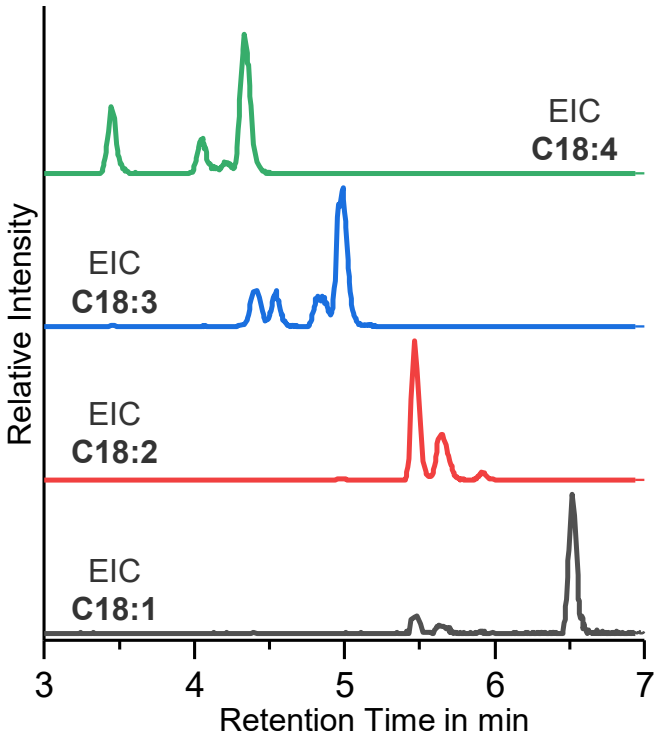

Figure 17: Extracted ion chromatograms of LC-QTOF measurements of a PUFA mixture. EICs of different m/z values correspond to C18:1, C18:2, C18:3 and C18:4 fatty acids. For most of the EICs multiple peaks with the same m/z value are visible, which cannot be further differentiated with MS-analysis alone. Visualized with data from own measurements.

Mass spectrometric detection is often considered as the gold-standard of analytical detection techniques. It is popular in various sectors from research to routine analysis in almost all industries from quality control to forensics. Mass spectrometry is based on the ionization of analytes, followed by separation and detection according to their mass-to-charge ratio [188]. Many different variations (e.g. high/low resolution, time-of-flight detection) exist and different ionization techniques (e.g. Atmospheric Pressure Chemical Ionization (APCI), Electrospray Ionization (ESI)) can be employed. Disadvantages like high initial and operating costs and the necessity of a qualified operator often make, especially HRMS (High Resolution Mass Spectrometry), uneconomical for routine analysis, but can give great advantage in impurity profiling, degradation product determination and development of the quality control methods of pharmaceuticals as non-isobaric coelutions can be easily determined [189].

Mass spectrometric detection is characterized by high sensitivity, making it first choice from a regulatory point of view for quantification of genotoxic impurities [189], but in case of fatty acids sensitivity can be limited due to necessity of detection in negative mode [190]. Additionally, the correct quantification of analytes can be hindered by “matrix effects” due to coelution of compounds and thus interference with each other’s ionization efficiency (enhancement or suppression) [191, 192]. The differences in ionization efficiency due to matrix effects requires the use of (expensive) isotope-labeled internal standards for quantitative analysis [191]. This especially applies to complex samples, like lipid-based pharmaceuticals which are composed of APIs and numerous different matrix components, as coelutions are more likely to be expected. In this case, the use of 2D-LC could be advised, as its high separation power can reduce matrix effects [192].

In case of selectivity mass spectrometric detection is often superior to other detection techniques due to its high mass resolution and possibility to fragment the analyte of interest, enabling the exact identification based on *m/z* value (MS1-level) and the occurrence of characteristic fragments (MS2-level) [82]. Unfortunately, a differentiation of isomeric/isobaric compounds is not possible on MS1-level, leaving the analyst with the scientific question: “Which of visible MS1-peaks belongs to my analyte and what are the other peaks?” (see Figure 17). In this case, a differentiation is only possible in case of characteristic fragmentation behavior (MS2-level), which is typically not observed for fatty acid isomers, that predominantly only display uncharacteristic decarboxylation [193, 194]. Thus, a determination of conjugation, position or configuration (cis/trans) of double bonds by MS alone is not possible, but could be feasible for example in combination with chemical modification and ion mobility dimension [195-197].

1.6.2 UV-detection

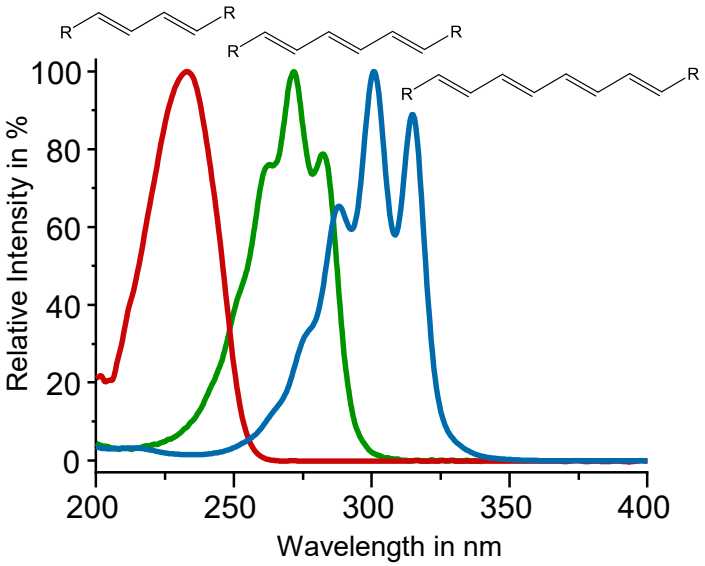

Figure 18: UV-spectra of conjugated C18 fatty acids, recorded during LC-DAD analysis. Normalized UV-spectra of conjugated dienes, trienes and tetraenes, showing bathochromic shift. Visualized with data from own measurements.

UV-detectors are one of the most widely used detectors in combination with (U)HPLC systems. DADs (diode array detectors) are particularly useful due to simultaneous detection of absorbance at multiple wavelengths [198] and recording of UV-spectra. Since they are based on the measurement of UV-light absorbance of the LC eluent (containing analytes) in a flow-cell after Beer-Lambert´s law, their sensitivity is dependent on the extinction coefficients of analytes [199]. Compared to MS-detection, UV-detectors display lower selectivity and are often less sensitive, which has already been discussed in many publications [189, 200, 201]. Nevertheless, HPLC-UV is commonly applied in the quality control for quantification of APIs and impurities, as it reliably meets the specifications of the ICH [8, 189]. Furthermore UV-detection is quite inexpensive, robust, requires minimal maintenance and, in contrast to MS, can be used to reliably quantify structurally similar analytes without respective standards [189].

The different absorbance maxima of molecules can be explained by the different energy gaps between HOMO (highest occupied molecule orbital) and LUMO (lowest unoccupied molecule orbital), which translates to the amount of energy needed to achieve e.g. a $\pi \rightarrow \pi^*$ transition [202]. In case of saturated and unconjugated fatty acids the energy gap is quite large, resulting in absorbance < 210 nm [82, 203]. This can be used to explain the lower selectivity of UV-detectors, as many different analytes absorb in this region [202]. Therefore, coelutions with other analytes or solvent impurities, which absorb in a similar region, can lead to overestimation during

quantification and therefore in impurity profiling maybe even exceeding the thresholds defined by the ICH.

Also, those analytes are more likely affected by the UV-cut-off of the used eluents (e.g. ethanol 210 nm), resulting in lower sensitivity [204]. In comparison conjugated fatty acids bear conjugated π -electron systems of different sizes which results in smaller energy gaps due to delocalization of HOMO and LUMO, resulting in a bathochromic shift towards higher wavelengths [202]. This results due to bigger conjugated π -electron systems of the fatty acids, in the following order of λ_{max}: dienes (approx. 230 nm) < trienes (approx. 270 nm) < tetraenes (approx. 300 nm); see Figure 18 [82]. Therefore, a differentiation between conjugated/unconjugated isomers and configurational isomers, based on number of Z-configured double bonds is possible [82].

The coupling of UV- with MS-detectors can really benefit the analytical method due to their complementarity in regards to sensitivity and selectivity, especially in case of isomeric/isobaric compounds without characteristic fragments (e.g. conjugated fatty acid isomers [82]) [141, 189]. This could be even more advisable when LC×LC is applied, as the high flow from ^{2}D eluent to the MS-detector usually has to be splitted anyway. The use of methods with high separation power (like LC×LC) when using UV-detection is important as UV-spectra are additive, thus coelutions could lead to misidentification.

1.6.3 Chemical derivatization of fatty acids

Derivatizations are typically not the first choice when considering ways to improve performance of analytical methods, as they lengthen the sample preparation, may introduce degradation products or might impact the sensitivity by unwanted side reactions [205]. Also, in context of "green chemistry", derivatization reactions are rather unwanted and should be avoided if possible [206, 207] or at least efforts should be made to achieve more environmentally friendly derivatizations. Therefore, the possibility for miniaturization, automatization and the use of "greener" solvents and reagents should be considered [206].

Nevertheless, during highly demanding analytical problems one may reach the limitations of common detection techniques, increasing the necessity of chemically altering the properties of the analytes. Therefore, chemical derivatization can be applied to achieve: (1) feasibility of the analytes for certain detection techniques (e.g. derivatization with chromophores or fluorophores for UV-/fluorescence-detection [205]), (2) to reduce volatility of analytes for ESI-MS or CAD (e.g. aldehydes or short fatty acids [27]) or increase it for gas chromatography, (3) to increase sensitivity/selectivity [190, 205], (4) to gain more information of unknown compounds during impurity determination (e.g. double bonds position determination [208]). Typically, derivatization solves multiple problems at once, e.g. derivatization of medium-chain *anteiso* fatty acids with 1-naphthylamine reduces volatility, increases retention and selectivity (e.g. chromatographic selectivity), and allows detection in positive mode [27]. The chemoselectivity of the derivatization reaction is also contributing to the selectivity of the analytical method, as only specific functional groups react with the derivatization agent, thus allowing group-type selection (i.e. if the reagent reacted with the analyte, the analyte needs to bear a functional group which is able to react with the derivatization reagent, e.g carboxylic groups react with 1-napthylamine) [27].

Pre-column derivatization is considered to be more flexible than post-column derivatization in regards of optimizing reaction conditions, can be performed without hardware modifications [205, 209] and influences the chromatographic properties of the analytes, thus may be improving separations [27]. The change in the chromatographic properties could be unwanted due to the change of elution pattern, which may lead to the necessity of changing an already established LC-method [209]. Pre-column derivatizations requires stable derivatives if sample preparation is performed batch-wise, while the reaction-speed is not a priority [209]. Of course, this does not necessarily have to be the case if automated sample preparation is being used, allowing analysis of each sample after exactly the same incubation time, e.g. by autosampler derivatization.

Enhancing sensitivity and selectivity

The analytical problems of fatty acids which can be overcome by derivatization are: (1) volatility (especially SCFA [27, 210]), (2) weak interactions with RP-stationary phases (especially SCFA [27, 210]), (3) low UV-absorbance (unconjugated FAs, see chapter 1.6.2), (4) sensitivity and selectivity issue [190]. Derivatization of fatty acids is often considered in combination with LC-MS analysis, although they can be analyzed without derivatization in negative mode (e.g. ESI negative), it is often characterized by low ionization efficiency or low sensitivities [190, 205]. Although this can be improved by appropriate mobile phase composition [205, 211], an increase in sensitivity and selectivity, especially in complex samples is highly desirable. This typically involves charge switching by derivatization of the carboxylic group with a, in positive mode ionizable, reagent [190, 212].

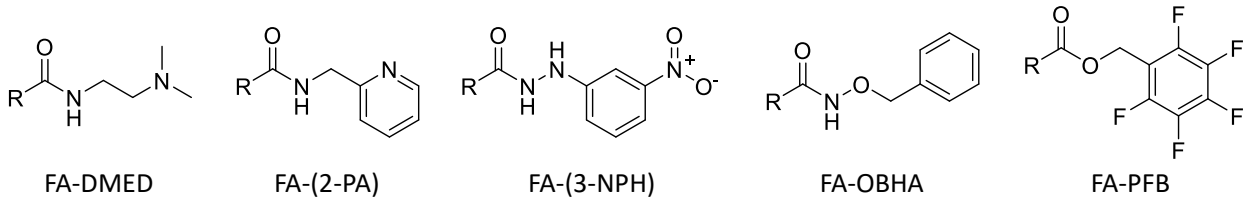

Figure 19: Reaction products of fatty acids with commonly used derivatization reagents DMED: N,N-dimethylethane-1,2-diamine; 2-PA: 2-picolylamine; 3-NPH: (3-nitrophenyl)hydrazine; OBHA: O-benzylhydroxylamine; PFB: pentafluorobenzylbromide. Visualized with information from Meckelmann et al. [213] and Jankech et al. [205].

Reagent and reaction conditions should be considered carefully before applying to the sample, as derivatization reactions can also alter the matrix composition [210] or in case of lipid formulation may increase the fatty acid content by facilitating degradation of the matrix (e.g. hydrolysis from triglycerides, see chapter 1.3.2). Caused by the low reactivity of carboxylic acids, most derivatization procedures require activation of fatty acids by the use of coupling agents, to achieve the formation of derivatives under mild conditions. One of the most commonly used activators is EDC (1-Ethyl-3-[3-dimethylaminopropyl]carbodiimide), which forms o-acylisourea-derivatives with the carboxylic acids, exhibiting a good leaving group [205]. Due to the reactivity of activators it is likely that undesirable by-products are being generated [214]. After activation, derivatization with amines (primary, secondary, aromatic), hydrazines, hydrazides and hydroxylamines can be utilized, resulting in amides, hydrazides or hydroxamic acid-derivatives, respectively (see Figure 19). In contrast, during derivatizations by esterification the activation with acidic or basic conditions is sufficient, which is more likely applied for UV-detection, as many reagents do not contain an easily ionizable group [205, 213].

In case of LC-MS analysis the presence of an easy ionizable group in the reagent is a must [190], while sensitivity in UV-detection really profits from reagents with extended chromophores, as discussed above. The presence of additional highly hydrophobic structures (e.g. phenyl rings) are optional for sufficiently retained analytes, but may be necessary e.g. for fatty acids with low hydrophobicity [215]. Therefore, with a good reagent selection immense sensitivity-improvements are possible, as shown by Calvigioni et al., who achieved quantification of SCFAs in the pg/mL range by 3-NPH-derivatization and MS-detection [216].

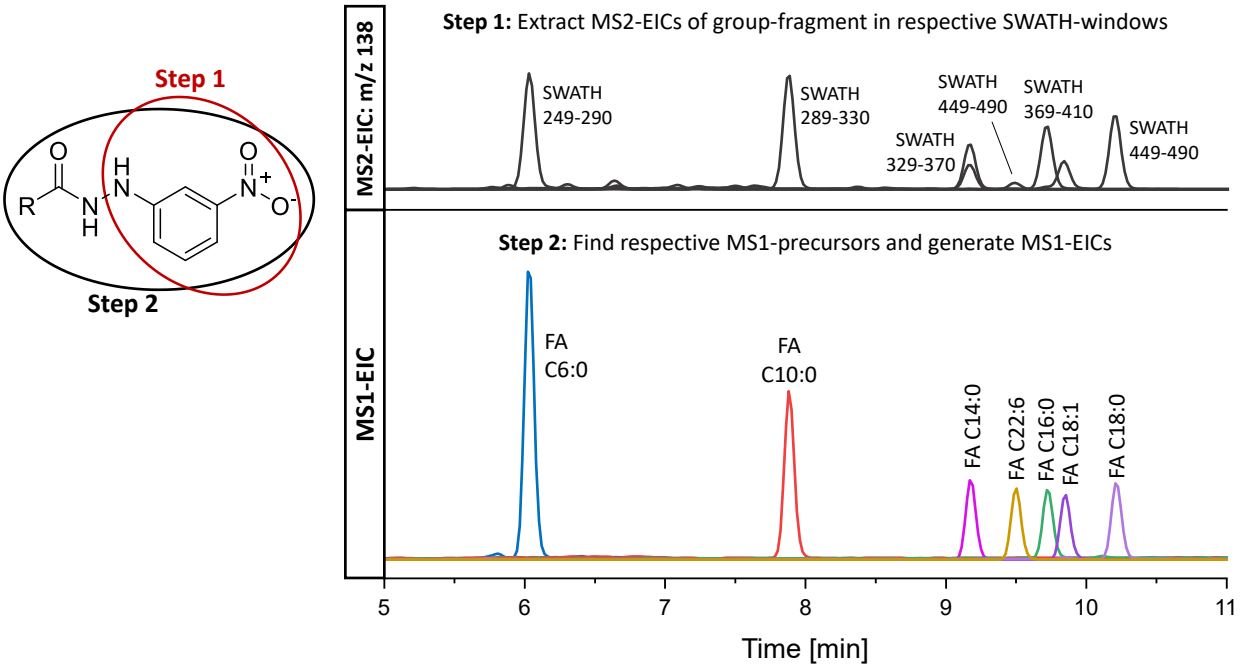

Figure 20: Workflow for untargeted identification of fatty acids (FA) by derivatization with 3-nitrophenylhydrazine. In Step 1 MS2-EICs of the derivatization-tag can be generated and give a quick overview where reacted FAs elute, subsequent evaluation of MS1-spectra and corresponding MS1-EICs (Step 2) give the respective precursor mass. Hence, an identification of the derivatized FA is possible. Visualized with data from own measurements.

Further, the derivatization of fatty acids and other compounds increases the selectivity of the respective analytical methods [190, 194]. In the structural elucidation of unknowns, it gives valuable information, as derivatized analytes most likely have the same functional group. In MS/MS, fatty acid fragments are typically not observed [194], therefore the identification of those analytes by the derivatization tag (derivatization reagent fragment) in the MS2-spectra is a huge advantage in regards of selectivity [194]. In untargeted LC-MS analysis, this opens the opportunity to conveniently identify compounds with carboxylic groups by MS2 extracted ion chromatograms (shown in Figure 20).

The use of isotope labeled derivatization reagents (e.g. $^{13}C_6$-3-NPH) enables an easy synthesis of standards for quantification of compounds in LC-MS for which no standards are available [217].

Further, it was shown for short/medium *anteiso*-branched chain fatty acids, that derivatization can help the enantiomeric recognition by increasing the interactions with the stationary phase [27, 215]. And enantiomeric separation can be performed with achiral columns by derivatization with chiral reagents (see chapter 1.4.2).

Determination of double bond positions

For the positional determination of double bonds in liquid-chromatography two main strategies are available: (1) use of specific hardware or hardware modifications and (2) chemical derivatization of double bonds followed by fragmentation during ionization or by collision-induced-dissociation (CID) to yield characteristic fragment ions. Hardware-based approaches, which can be used for double bond distinction is possible by ultraviolet photo-dissociation (UVPD) [218], ozone-induced dissociation (ozID) [219] or electron-induced dissociation [220]. Those setups are based on reactions in the gas-phase and therefore can be employed as alternative fragmentation mode to, the widely employed, CID. They partly have been commercialized, e.g. EAD in the ZenoTOF 7600 mass spectrometer (Sciex) and UVPD in the Orbitrap Fusion Lumos mass spectrometer (Thermo Fisher Scientific) [221], but are typically quite expensive. In UVPD, fragmentation at double bond positions are caused by absorbance of photons by the C-C-double bond in form of UV-light, while in electron-induced dissociation fragmentation is caused by interaction with an electron beam [221]. The concept of ozonolysis for double bond localization is based on the formation of ozonides, which decompose to characteristic fragments (aldehyde and Criegee ion, see Figure 21) [208]. Off-line approaches [222] and the implementation in different sections of the mass spectrometers, starting from the electrospray ion source (OzESI-MS) [223] to ozone-induced dissociation (ozID) in the ion trap of a respective mass spectrometer [219], have been proposed.

Two of the most commonly applied chemical derivatization approaches are Paternò-Büchi or epoxidation reaction, but many more have been suggested. The Paternò Büchi reaction of the double bond with aldehyde or ketone containing reagents involves activation of the aldehyde/ketone by UV-radiation leading to the formation of an oxetane ring at the double bond´s position [224, 225]. Two positional isomers of the oxetane ring are formed for each double bond. Fragmentation is possible by CID under C-C-bond cleavage of the initial double bond position and C-O-bond cleavage of the reagent (see Figure 21). For each double bond this results in two characteristic fragments, in case of acetone as reagent with a mass difference of 26 Da [208]. The original method with acetone had low yields, side reactions and *m/z*-overlap with underivatized lipids [208, 226]. The selection of reagent dramatically impacts the reaction. For

instance, trifluoroacetophenone leads to higher yields (20 – 30 %), fewer side reactions and no overlap with unreacted lipids [208, 227], while acetylpyridine introduces charge switching, thus allowing signal enhancement in positive mode [228]. Paternò-Büchi reactions can be performed off-line and on-line ("pre-source" or in-source) and therefore might require specific hardware (depending on the setup, e.g. fused silica capillaries, nanoESI-tips, microflow-reactors, low pressure mercury lamps) [224, 227, 229].

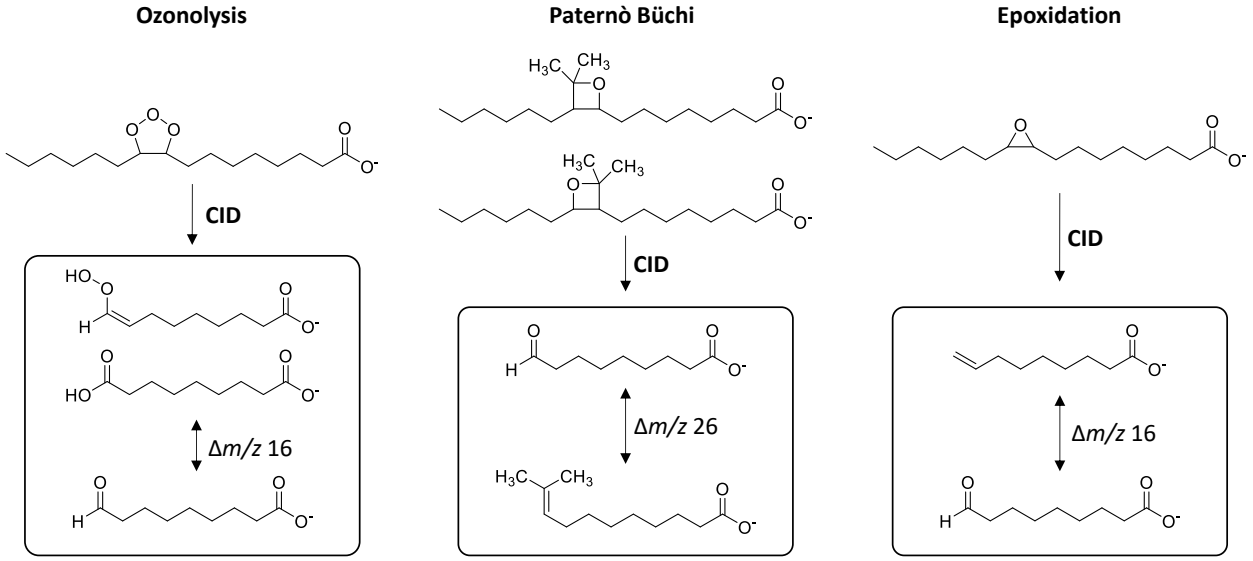

Figure 21: Overview of different derivatization products and CID-fragments of common methods for positional determination of double bonds in palmitoleic acid (Ozonolysis, Paternò Büchi and Epoxidation) Visualized with information from Chen et al. [208].

Epoxidation of double bonds can be performed by low temperature plasma [230], m-CPBA [231] or oxone (potassium peroxymonosulfate) [232]. Hereby, stable epoxides are introduced at the double bond positions, which can be fragmented by CID, resulting in two detectable products per double bond (aldehyde or ethylene on the carboxylic-end fragment; see Figure 21) [208]. Low temperature plasma can be directly introduced in the sample solution [230] or paper-based analytical devices can be utilized [233]. The drawbacks of this method (hardware requirements and overoxidized by-products) can be overcome by epoxidation with m-CPBA (meta-chloroperoxybenzoic acid), which is characterized by high specificity, high reaction rate and less overoxidation [208, 231]. Oxone (potassium peroxymonosulfate) can also be utilized for epoxidation, which is favourable because of its fast reaction, high yield (close to 100%) and in case of polyunsaturated FAs only one (fully epoxidized) reaction product [208, 232].

A new approach to LC-MS double bond position determination by derivatization with disulfide-reagents is discussed in publication III.

1.7 References

[1] A.-S. Bouin, M. Wierer, Quality standards of the European Pharmacopoeia, Journal of Ethnopharmacology 158 (2014) 454-457. https://doi.org/10.1016/j.jep.2014.07.020.

[2] European Directorate for the Quality of Medicines & Healthcare (EDQM), European Pharmacopoeia: Introduction, 11th edition, Strasbourg, 2024.

[3] D.S. Belz, Das Arzneibuch, Bundesgesundheitsblatt - Gesundheitsforschung - Gesundheitsschutz 49(12) (2006) 1205-1211. https://doi.org/10.1007/s00103-006-0090-9.

[4] USP Council of the Convention Section on Global Public Health, USP Council of Experts International Health Expert Committee, USP Regionalization Team, M.L. Heyman, R.L. Williams, Ensuring global access to quality medicines: Role of the US pharmacopeia, Journal of Pharmaceutical Sciences 100(4) (2011) 1280-1287. https://doi.org/10.1002/jps.22391.

[5] The International Council for Harmonisation of Technical Requirements for Pharmaceuticals for Human Use, Implementation of ICH Guidelines, in Rules of Procedure of the Assembly, 2023. https://admin.ich.org/sites/default/files/inline-files/AssemblyRoP_Approved_v14.0_2023_1031_0.pdf. (Accessed 5th May 2024).

[6] L. Kung-Tien, C. Chien-Hsin, Determination of Impurities in Pharmaceuticals: Why and How?, in: P. Paulo, X. Sandra (Eds.), Quality Management and Quality Control, IntechOpen, Rijeka, 2019, p. Ch. 7. https://doi.org/10.5772/intechopen.83849.

[7] European Directorate for the Quality of Medicines & Healthcare (EDQM), European Pharmacopoeia, 11th edition, Strasbourg, 2024.

[8] International Conference on Harmonisation of Technical Requirements for Registration of Pharmaceuticals for Human Use, ICH Harmonised Tripartite Guideline: Impurities in New Drug Substances Q3A (R2), 2006. https://database.ich.org/sites/default/files/Q3A%28R2%29%20Guideline.pdf. (Accessed 14th May 2024).

[9] International Conference on Harmonisation of Technical Requirements for Registration of Pharmaceuticals for Human Use, ICH Harmonised Tripartite Guideline: Impurities in New Drug Products Q3B (R2), 2006. https://database.ich.org/sites/default/files/Q3B%28R2%29%20Guideline.pdf. (Accessed 15th May 2024).

[10] L. Müller, R.J. Mauthe, C.M. Riley, M.M. Andino, D.D. Antonis, C. Beels, J. DeGeorge, A.G.M. De Knaep, D. Ellison, J.A. Fagerland, R. Frank, B. Fritschel, S. Galloway, E. Harpur, C.D.N. Humfrey, A.S. Jacks, N. Jagota, J. Mackinnon, G. Mohan, D.K. Ness, M.R. O'Donovan, M.D. Smith, G. Vudathala, L. Yotti, A rationale for determining, testing, and controlling specific impurities in pharmaceuticals that possess potential for genotoxicity, Regulatory Toxicology and Pharmacology 44(3) (2006) 198-211. https://doi.org/10.1016/j.yrtph.2005.12.001.

[11] International Council for Harmonisation of Technical Requirements for Pharmaceuticals for Human Use, ICH Harmonised Guideline - Impurities: Guideline for Residual Solvents Q3C(R9), 2021. https://database.ich.org/sites/default/files/ICH_Q3C%28R9%29_Guideline_MinorRevision_2024_2024_Approved.pdf. (Accessed 14th May 2024).

[12] International Council for Harmonisation of Technical Requirements for Pharmaceuticals for Human Use, ICH Harmonised Guideline: Guideline for Elemental Impurities Q3D(R2), 2022. https://database.ich.org/sites/default/files/Q3D-R2_Guideline_Step4_2022_0308.pdf. (Accessed 14th May 2024).

[13] International Council for Harmonisation of Technical Requirements for Pharmaceuticals for Human Use, ICH Harmonised Guideline: Assessment and Control of DNA reactive (mutagenic) Impurities in Pharmaceuticals to limit potential carcinogenic risk M7 (R2), 2023. https://database.ich.org/sites/default/files/ICH_M7%28R2%29_Guideline_Step4_2023_0216_0.pdf. (Accessed 15th May 2024).

[14] ICH Official Website - Quality guidelines, Q3E EWG: Impurity: Assesment and Control of Extractables and Leachables for Pharmaceuticals and Biologics. https://www.ich.org/page/quality-guidelines. (Accessed 28th april 2024).

[15] U.B.R. Khandavilli, L. Keshavarz, E. Skořepová, R.R.E. Steendam, P.J. Frawley, Organic Salts of Pharmaceutical Impurity p-Aminophenol, Molecules 25(8) (2020) 1910.

[16] I. Mansouri, J. Botton, L. Semenzato, N. Haddy, M. Zureik, N-nitrosodimethylamine-Contaminated Valsartan and Risk of Cancer: A Nationwide Study of 1.4 Million Valsartan Users, Journal of the American Heart Association 11(24) (2022) e8067. https://doi.org/10.1161/JAHA.122.026739.

[17] International Conference on Harmonisation of Technical Requirements for Registration of Pharmaceuticals for Human Use, ICH Harmonised Tripartite Guideline: Impurities in New Drug Substances Q3A (R2), 2006. https://database.ich.org/sites/default/files/Q3A%28R2%29%20Guideline.pdf. (Accessed 15th May 2024).

[18] International Conference on Harmonisation of Technical Requirements for Registration of Pharmaceuticals for Human Use, ICH Harmonised Tripartite Guideline: The Common Technical Document for the Registration of Pharmaceuticals for Human Use: Quality - M4Q(R1), Quality Overall Summary of Module 2, Module 3: Quality, 2002. https://database.ich.org/sites/default/files/M4Q_R1_Guideline.pdf. (Accessed 22nd May 2024).

[19] International Council for Harmonisation of Technical Requirements for Pharmaceuticals for Human Use, ICH Harmonised Guideline: Analytical Procedure Development Q14 2023. https://database.ich.org/sites/default/files/ICH_Q14_Guideline_2023_1116.pdf. (Accessed 28th april 2024).

[20] International Council for Harmonisation of Technical Requirements for Pharmaceuticals for Human Use, ICH Harmonised Guideline: Validation of Analytical Procedures Q2(R2) 2023. https://database.ich.org/sites/default/files/ICH_Q2%28R2%29_Guideline_2023_1130.pdf. (Accessed 28th april 2024).

[21] M.H. Kleinman, S.W. Baertschi, K.M. Alsante, D.L. Reid, M.D. Mowery, R. Shimanovich, C. Foti, W.K. Smith, D.W. Reynolds, M. Nefliu, M.A. Ott, In Silico Prediction of Pharmaceutical Degradation Pathways: A Benchmarking Study, Molecular Pharmaceutics 11(11) (2014) 4179-4188. https://doi.org/10.1021/mp5003976.

[22] C. Foti, K. Alsante, G. Cheng, T. Zelesky, M. Zell, Tools and workflow for structure elucidation of drug degradation products, TrAC Trends in Analytical Chemistry 49 (2013) 89-99. https://doi.org/10.1016/j.trac.2013.06.005.

[23] M.H. Kleinman, D. Elder, A. Teasdale, M.D. Mowery, A.P. McKeown, S.W. Baertschi, Strategies To Address Mutagenic Impurities Derived from Degradation in Drug Substances and Drug Products, Organic Process Research & Development 19(11) (2015) 1447-1457. https://doi.org/10.1021/acs.oprd.5b00091.

[24] M. Blessy, R.D. Patel, P.N. Prajapati, Y.K. Agrawal, Development of forced degradation and stability indicating studies of drugs—A review, Journal of Pharmaceutical Analysis 4(3) (2014) 159-165. https://doi.org/10.1016/j.jpha.2013.09.003.

[25] R. Kormány, I. Molnár, J. Fekete, Renewal of an old European Pharmacopoeia method for Terazosin using modeling with mass spectrometric peak tracking, Journal of Pharmaceutical and Biomedical Analysis 135 (2017) 8-15. https://doi.org/10.1016/j.jpba.2016.11.050.

[26] O. Wahl, S. Jorajuria, Development and validation of a new UHPLC method for related proteins in insulin and insulin analogues as an alternative to the European Pharmacopoeia RP-HPLC method, Journal of Pharmaceutical and Biomedical Analysis 166 (2019) 71-82. https://doi.org/10.1016/j.jpba.2018.12.034.

[27] C. Geibel, M. Olfert, C. Knappe, K. Serafimov, M. Lämmerhofer, Branched medium-chain fatty acid profiling and enantiomer separation of anteiso-forms of teicoplanin fatty acyl side chain RS3 using UHPLC-MS/MS with polysaccharide columns, Journal of Pharmaceutical and Biomedical Analysis 224 (2023) 115162. https://doi.org/10.1016/j.jpba.2022.115162.

[28] E. Fahy, D. Cotter, M. Sud, S. Subramaniam, Lipid classification, structures and tools, Biochimica et Biophysica Acta (BBA) - Molecular and Cell Biology of Lipids 1811(11) (2011) 637-647. https://doi.org/10.1016/j.bbalip.2011.06.009.

[29] M. Sud, E. Fahy, D. Cotter, A. Brown, E.A. Dennis, C.K. Glass, A.H. Merrill, Jr, R.C. Murphy, C.R.H. Raetz, D.W. Russell, S. Subramaniam, LMSD: LIPID MAPS structure database, Nucleic Acids Research 35(suppl_1) (2006) D527-D532. https://doi.org/10.1093/nar/gkl838.

[30] D. Voet, J.G. Voet, C.W. Pratt, Klassifizierung der Lipide, Lehrbuch der Biochemie - Dritte, vollständig überarbeitete und erweiterte Auflage, WILEY-VCH, Weinheim, Germany, 2019, pp. 299-315.

[31] W.B. Rizzo, Fatty aldehyde and fatty alcohol metabolism: Review and importance for epidermal structure and function, Biochimica et Biophysica Acta (BBA) - Molecular and Cell Biology of Lipids 1841(3) (2014) 377-389. https://doi.org/10.1016/j.bbalip.2013.09.001.

[32] H. Yin, L. Xu, N.A. Porter, Free Radical Lipid Peroxidation: Mechanisms and Analysis, Chemical Reviews 111(10) (2011) 5944-5972. https://doi.org/10.1021/cr200084z.

[33] D. Voet, J.G. Voet, C.W. Pratt, Fettsäurebiosynthese, Lehrbuch der Biochemie - Dritte, vollständig überarbeitete und erweiterte Auflage, WILEY-VCH, Weinheim, Germany, 2019, pp. 839-851.

[34] U.N. Das, Essential fatty acids: biochemistry, physiology and pathology, Biotechnology Journal 1(4) (2006) 420-439. https://doi.org/10.1002/biot.200600012.

[35] Y. Cao, X. Zhang, Production of long-chain hydroxy fatty acids by microbial conversion, Applied Microbiology and Biotechnology 97(8) (2013) 3323-3331. https://doi.org/10.1007/s00253-013-4815-z.

[36] O. Yushchuk, B. Ostash, A.W. Truman, F. Marinelli, V. Fedorenko, Teicoplanin biosynthesis: unraveling the interplay of structural, regulatory, and resistance genes, Applied Microbiology and Biotechnology 104(8) (2020) 3279-3291. https://doi.org/10.1007/s00253-020-10436-y.

[37] H. Oku, T. Kaneda, Biosynthesis of branched-chain fatty acids in Bacillus subtilis. A decarboxylase is essential for branched-chain fatty acid synthetase, Journal of Biological Chemistry 263(34) (1988) 18386-18396. https://doi.org/10.1016/S0021-9258(19)81371-6.

[38] P.C. Calder, Functional Roles of Fatty Acids and Their Effects on Human Health, Journal of Parenteral and Enteral Nutrition 39(1S) (2015) 18S-32S. https://doi.org/10.1177/0148607115595980.

[39] C.C.C.R. De Carvalho, M.J. Caramujo, The Various Roles of Fatty Acids, Molecules 23(10) (2018) 2583.

[40] K. Nagy, I.-D. Tiuca, Importance of Fatty Acids in Physiopathology of Human Body, in: C. Angel (Ed.), Fatty Acids, IntechOpen, Rijeka, 2017, p. Ch. 1. https://doi.org/10.5772/67407.

[41] T. Farkas, E. Fodor, K. Kitajka, J.E. Halver, Response of fish membranes to environmental temperature, Aquaculture Research 32(8) (2001) 645-655. https://doi.org/10.1046/j.1365-2109.2001.00600.x.

[42] M. Suutari, K. Liukkonen, S. Laakso, Temperature adaptation in yeasts: the role of fatty acids, Microbiology 136(8) (1990) 1469-1474. https://doi.org/10.1099/00221287-136-8-1469.

[43] J.M. Smaby, M.M. Momsen, H.L. Brockman, R.E. Brown, Phosphatidylcholine acyl unsaturation modulates the decrease in interfacial elasticity induced by cholesterol, Biophysical Journal 73(3) (1997) 1492-1505. https://doi.org/10.1016/S0006-3495(97)78181-5.

[44] R. N.M. Weijers, Lipid Composition of Cell Membranes and Its Relevance in Type 2 Diabetes Mellitus, Current Diabetes Reviews 8(5) (2012) 390-400. https://doi.org/10.2174/157339912802083531.

[45] D. Voet, J.G. Voet, C.W. Pratt, Fettsäureoxidation, Lehrbuch der Biochemie - Dritte, vollständig überarbeitete und erweiterte Auflage, WILEY-VCH, Weinheim, Germany, 2019, pp. 820-838.

[46] K. Bartlett, S. Eaton, Mitochondrial β-oxidation, European Journal of Biochemistry 271(3) (2004) 462-469. https://doi.org/10.1046/j.1432-1033.2003.03947.x.

[47] J. Lund, A.C. Rustan, Fatty Acids: Structures and Properties, Encyclopedia of Life Sciences2020, pp. 283-292. https://doi.org/10.1002/9780470015902.a0029198.

[48] F.M. Sacks, A.H. Lichtenstein, J.H.Y. Wu, L.J. Appel, M.A. Creager, P.M. Kris-Etherton, M. Miller, E.B. Rimm, L.L. Rudel, J.G. Robinson, N.J. Stone, L.V.V. Horn, Dietary Fats and Cardiovascular Disease: A Presidential Advisory From the American Heart Association, Circulation 136(3) (2017) e1-e23. https://doi.org/10.1161/CIR.0000000000000510.

[49] K.-T. Khaw, M.D. Friesen, E. Riboli, R. Luben, N. Wareham, Plasma Phospholipid Fatty Acid Concentration and Incident Coronary Heart Disease in Men and Women: The EPIC-Norfolk Prospective Study, PLOS Medicine 9(7) (2012) e1001255. https://doi.org/10.1371/journal.pmed.1001255.

[50] W. Hu, M. Fitzgerald, B. Topp, M. Alam, T.J. O'Hare, A review of biological functions, health benefits, and possible de novo biosynthetic pathway of palmitoleic acid in macadamia nuts, Journal of Functional Foods 62 (2019) 103520. https://doi.org/10.1016/j.jff.2019.103520.

[51] D. Mozaffarian, M.B. Katan, A. Ascherio, M.J. Stampfer, W.C. Willett, Trans Fatty Acids and Cardiovascular Disease, New England Journal of Medicine 354(15) (2006) 1601-1613. https://doi.org/10.1056/NEJMra054035.

[52] A.-B. Oteng, S. Kersten, Mechanisms of Action of trans Fatty Acids, Advances in Nutrition 11(3) (2020) 697-708. https://doi.org/10.1093/advances/nmz125.

[53] A.C. Rustan, C.A. Drevon, Fatty acids: Structures and Properties, Encyclopedia of Life Sciences (2005). https://doi.org/10.1038/npg.els.0003894.

[54] I. Djuricic, P.C. Calder, Beneficial Outcomes of Omega-6 and Omega-3 Polyunsaturated Fatty Acids on Human Health: An Update for 2021, Nutrients 13(7) (2021) 2421.

[55] A.A. Hennessy, P.R. Ross, G.F. Fitzgerald, C. Stanton, Sources and Bioactive Properties of Conjugated Dietary Fatty Acids, Lipids 51(4) (2016) 377-397. https://doi.org/10.1007/s11745-016-4135-z.

[56] K. Nagao, T. Yanagita, Conjugated fatty acids in food and their health benefits, Journal of Bioscience and Bioengineering 100(2) (2005) 152-157. https://doi.org/10.1263/jbb.100.152.

[57] K. Koba, T. Yanagita, Health benefits of conjugated linoleic acid (CLA), Obesity Research & Clinical Practice 8(6) (2014) e525-e532. https://doi.org/10.1016/j.orcp.2013.10.001.

[58] N. Chhabra, M.L. Aseri, D. Padmanabhan, A review of drug isomerism and its significance, International Journal of Applied and Basic Medical Research 3(1) (2013) 16-18. https://doi.org/10.4103/2229-516x.112233.

[59] N. Vargesson, Thalidomide-induced teratogenesis: History and mechanisms, Birth Defects Research Part C: Embryo Today: Reviews 105(2) (2015) 140-156. https://doi.org/10.1002/bdrc.21096.

[60] European-Medicines-Agency, Scientific guideline, Investigation of chiral active substances, Reference number: 3CC29A, 1993. https://www.ema.europa.eu/en/documents/scientific-guideline/investigation-chiral-active-substances_en.pdf. (Accessed 29th April 2024).

[61] R. Savla, J. Browne, V. Plassat, K.M. Wasan, E.K. Wasan, Review and analysis of FDA approved drugs using lipid-based formulations, Drug Development and Industrial Pharmacy 43(11) (2017) 1743-1758. https://doi.org/10.1080/03639045.2017.1342654.

[62] C.W. Pouton, Formulation of poorly water-soluble drugs for oral administration: Physicochemical and physiological issues and the lipid formulation classification system, European Journal of Pharmaceutical Sciences 29(3) (2006) 278-287. https://doi.org/10.1016/j.ejps.2006.04.016.

[63] C. Wilson, P. Canning, E.M. Caravati, The abuse potential of propofol, Clinical Toxicology 48(3) (2010) 165-170. https://doi.org/10.3109/15563651003757954.

[64] Max T. Baker, M. Naguib, David C. Warltier, Propofol: The Challenges of Formulation, Anesthesiology 103(4) (2005) 860-876. https://doi.org/10.1097/00000542-200510000-00026.

[65] S. Kalepu, M. Manthina, V. Padavala, Oral lipid-based drug delivery systems – an overview, Acta Pharmaceutica Sinica B 3(6) (2013) 361-372. https://doi.org/10.1016/j.apsb.2013.10.001.

[66] X. Hou, T. Zaks, R. Langer, Y. Dong, Lipid nanoparticles for mRNA delivery, Nature Reviews Materials 6(12) (2021) 1078-1094. https://doi.org/10.1038/s41578-021-00358-0.

[67] J.M. Kremer, n−3 Fatty acid supplements in rheumatoid arthritis, The American Journal of Clinical Nutrition 71(1) (2000) 349S-351S. https://doi.org/10.1093/ajcn/71.1.349S.

[68] P.C. Calder, D.L. Waitzberg, S. Klek, R.G. Martindale, Lipids in Parenteral Nutrition: Biological Aspects, Journal of Parenteral and Enteral Nutrition 44(S1) (2020) S21-S27. https://doi.org/10.1002/jpen.1756.

[69] M.B. Brown, G.P. Martin, S.A. Jones, F.K. Akomeah, Dermal and Transdermal Drug Delivery Systems: Current and Future Prospects, Drug Delivery 13(3) (2006) 175-187. https://doi.org/10.1080/10717540500455975.

[70] D.A. Siriwardane, C. Wang, W. Jiang, T. Mudalige, Quantification of phospholipid degradation products in liposomal pharmaceutical formulations by ultra performance liquid chromatography-mass spectrometry (UPLC-MS), International Journal of Pharmaceutics 578 (2020) 119077. https://doi.org/10.1016/j.ijpharm.2020.119077.

[71] M. Grit, W.J.M. Underberg, D.J.A. Crommelin, Hydrolysis of Saturated Soybean Phosphatidylcholine in Aqueous Liposome Dispersions, Journal of Pharmaceutical Sciences 82(4) (1993) 362-366. https://doi.org/10.1002/jps.2600820405.

[72] V.N. Bochkov, O.V. Oskolkova, K.G. Birukov, A.-L. Levonen, C.J. Binder, J. Stöckl, Generation and Biological Activities of Oxidized Phospholipids, Antioxidants & Redox Signaling 12(8) (2009) 1009-1059. https://doi.org/10.1089/ars.2009.2597.

[73] M. Gong, Y. Hu, W. Wei, Q. Jin, X. Wang, Production of conjugated fatty acids: A review of recent advances, Biotechnology Advances 37(8) (2019) 107454. https://doi.org/10.1016/j.biotechadv.2019.107454

[74] S. Kubow, Routes of formation and toxic consequences of lipid oxidation products in foods, Free Radical Biology and Medicine 12(1) (1992) 63-81. https://doi.org/10.1016/0891-5849(92)90059-P.

[75] R.M. LoPachin, T. Gavin, Molecular Mechanisms of Aldehyde Toxicity: A Chemical Perspective, Chemical Research in Toxicology 27(7) (2014) 1081-1091. https://doi.org/10.1021/tx5001046.

[76] R. Martino, M. Malet-Martino, V. Gilard, S. Balayssac, Counterfeit drugs: analytical techniques for their identification, Analytical and Bioanalytical Chemistry 398(1) (2010) 77-92. https://doi.org/10.1007/s00216-010-3748-y.

[77] M. Gumustas, S. Kurbanoglu, B. Uslu, S.A. Ozkan, UPLC versus HPLC on Drug Analysis: Advantageous, Applications and Their Validation Parameters, Chromatographia 76(21) (2013) 1365-1427. https://doi.org/10.1007/s10337-013-2477-8.

[78] P. Žuvela, M. Skoczylas, J. Jay Liu, T. Bączek, R. Kaliszan, M.W. Wong, B. Buszewski, Column Characterization and Selection Systems in Reversed-Phase High-Performance Liquid Chromatography, Chemical Reviews 119(6) (2019) 3674-3729. https://doi.org/10.1021/acs.chemrev.8b00246.

[79] M. Yang, S. Fazio, D. Munch, P. Drumm, Impact of methanol and acetonitrile on separations based on π–π interactions with a reversed-phase phenyl column, Journal of Chromatography A 1097(1) (2005) 124-129. https://doi.org/10.1016/j.chroma.2005.08.028.

[80] V.R. Meyer, Reversed-Phase Chromatography, Practical High-Performance Liquid Chromatography - Fifth Edition, John Wiley & Sons2010, pp. 173-193.

[81] J.L. Rafferty, L. Zhang, J.I. Siepmann, M.R. Schure, Retention Mechanism in Reversed-Phase Liquid Chromatography: A Molecular Perspective, Analytical Chemistry 79(17) (2007) 6551-6558. https://doi.org/10.1021/ac0705115.

[82] M. Olfert, S. Bäurer, M. Wolter, S. Buckenmaier, E. Brito-de la Fuente, M. Lämmerhofer, Comprehensive profiling of conjugated fatty acid isomers and their lipid oxidation products by two-dimensional chiral RP×RP liquid chromatography hyphenated to UV- and SWATH-MS-detection, Analytica Chimica Acta 1202 (2022) 339667. https://doi.org/10.1016/j.aca.2022.339667.

[83] L.C. Sander, M. Pursch, S.A. Wise, Shape Selectivity for Constrained Solutes in Reversed-Phase Liquid Chromatography, Analytical Chemistry 71(21) (1999) 4821-4830. https://doi.org/10.1021/ac9908187.

[84] A.K. Mallik, H. Qiu, M. Takafuji, H. Ihara, High molecular-shape-selective stationary phases for reversed-phase liquid chromatography: A review, TrAC Trends in Analytical Chemistry 108 (2018) 381-404. https://doi.org/10.1016/j.trac.2018.09.003.

[85] S. Wise, W.J. Bonnett, F.R. Guenther, W.E. May, A Relationship Between Reversed-Phase C18 Liquid Chromatographic Retention and the Shape of Polycyclic Aromatic Hydrocarbons*, Journal of Chromatographic Science 19(9) (1981) 457-465. https://doi.org/10.1093/chromsci/19.9.457.

[86] C. Yan, D.E. Martire, Molecular theory of chromatographic selectivity enhancement for blocklike solutes in anisotropic stationary phases and its application, Analytical Chemistry 64(11) (1992) 1246-1253.

[87] N. Tanaka, Y. Tokuda, K. Iwaguchi, M. Araki, Effect of stationary phase structure on retention and selectivity in reversed-phase liquid chromatography, Journal of Chromatography A 239 (1982) 761-772. https://doi.org/10.1016/S0021-9673(00)82036-1.

[88] E. Lesellier, C. West, A. Tchapla, Classification of special octadecyl-bonded phases by the carotenoid test, Journal of Chromatography A 1111(1) (2006) 62-70. https://doi.org/10.1016/j.chroma.2006.01.107.

[89] L.C. Sander, S.A. Wise, Effect of phase length on column selectivity for the separation of polycyclic aromatic hydrocarbons by reversed-phase liquid chromatography, Analytical chemistry 59(18) (1987) 2309-2313.

[90] L.C. Sander, S.A. Wise, Subambient temperature modification of selectivity in reversed-phase liquid chromatography, Analytical Chemistry 61(15) (1989) 1749-1754.

[91] J.J. Pesek, M.T. Matyska, G. Brent Dawson, A. Wilsdorf, P. Marc, M. Padki, Cholesterol bonded phase as a separation medium in liquid chromatography: Evaluation of properties and applications, Journal of Chromatography A 986(2) (2003) 253-262. https://doi.org/10.1016/S0021-9673(02)01958-1.

[92] B. Buszewski, M. Jezierska, M. Wełniak, R. Kaliszan, Cholesteryl-silica stationary phase for liquid chromatography: Comparative study of retention behavior and selectivity, Journal of Chromatography A 845(1) (1999) 433-445. https://doi.org/10.1016/S0021-9673(99)00141-7.

[93] K. Pilaniya, H.K. Chandrawanshi, U. Pilaniya, P. Manchandani, P. Jain, N. Singh, Recent trends in the impurity profile of pharmaceuticals, J Adv Pharm Technol Res 1(3) (2010) 302-10. https://doi.org/10.4103/0110-5558.72422.

[94] M. Iguiniz, S. Heinisch, Two-dimensional liquid chromatography in pharmaceutical analysis. Instrumental aspects, trends and applications, Journal of Pharmaceutical and Biomedical Analysis 145 (2017) 482-503. https://doi.org/10.1016/j.jpba.2017.07.009.

[95] W. Lindner, Chiral Liquid Chromatography, in: G. Helmchen, R. Hoffmann, J. Mulzer, E. Schaumann (Eds.), Methods of organic chemistry (Houben-Weyl): Stereoselective Synthesis, Georg Thieme Verlag, Stuttgart, 1995, pp. 193-224.

[96] C. Calderón, M. Lämmerhofer, Enantioselective metabolomics by liquid chromatography-mass spectrometry, Journal of Pharmaceutical and Biomedical Analysis 207 (2022) 114430. https://doi.org/10.1016/j.jpba.2021.114430.

[97] W. Lindner, Determination of Enantiomeric Purity via Formation of Diastereomers, in: G. Helmchen, R. Hoffmann, J. Mulzer, E. Schaumann (Eds.), Methods of organic chemistry (Houben-Weyl): Stereoselective Synthesis, Georg Thieme Verlag, Stuttgart, 1995, pp. 225-252.

[98] R.-C. Moldovan, E. Bodoki, A.-C. Servais, J. Crommen, R. Oprean, M. Fillet, (+) or (−)-1-(9-fluorenyl)ethyl chloroformate as chiral derivatizing agent: A review, Journal of Chromatography A 1513 (2017) 1-17. https://doi.org/10.1016/j.chroma.2017.07.045.

[99] I. Ilisz, R. Berkecz, A. Péter, Application of chiral derivatizing agents in the high-performance liquid chromatographic separation of amino acid enantiomers: A review, Journal of Pharmaceutical and Biomedical Analysis 47(1) (2008) 1-15. https://doi.org/10.1016/j.jpba.2007.12.013.

[100] G.K.E. Scriba, Chiral Recognition Mechanisms in Analytical Separation Sciences, Chromatographia 75(15) (2012) 815-838. https://doi.org/10.1007/s10337-012-2261-1.

[101] L. Yu, S. Wang, S. Zeng, Chiral Mobile Phase Additives in HPLC Enantioseparations, in: G.K.E. Scriba (Ed.), Chiral Separations: Methods and Protocols, Humana Press, Totowa, NJ, 2013, pp. 221-231. https://doi.org/10.1007/978-1-62703-263-6_13.

[102] M. Lämmerhofer, Chiral recognition by enantioselective liquid chromatography: Mechanisms and modern chiral stationary phases, Journal of Chromatography A 1217(6) (2010) 814-856. https://doi.org/10.1016/j.chroma.2009.10.022.

[103] L.H. Easson, E. Stedman, Studies on the relationship between chemical constitution and physiological action: Molecular dissymmetry and physiological activity, Biochem J 27(4) (1933) 1257-66. https://doi.org/10.1042/bj0271257.

[104] W.H. Pirkle, T.C. Pochapsky, Considerations of chiral recognition relevant to the liquid chromatography separation of enantiomers, Chemical Reviews 89(2) (1989) 347-362.

[105] V.A. Davankov, The nature of chiral recognition: Is it a three-point interaction?, Chirality 9(2) (1997) 99-102. https://doi.org/10.1002/(SICI)1520-636X(1997)9:2<99::AID-CHIR3>3.0.CO;2-B.

[106] J. Teixeira, M.E. Tiritan, M.M.M. Pinto, C. Fernandes, Chiral Stationary Phases for Liquid Chromatography: Recent Developments, Molecules 24(5) (2019) 865.

[107] B. Chankvetadze, Recent trends in preparation, investigation and application of polysaccharide-based chiral stationary phases for separation of enantiomers in high-performance liquid chromatography, TrAC Trends in Analytical Chemistry 122 (2020) 115709. https://doi.org/10.1016/j.trac.2019.115709.

[108] J.M. Padró, S. Keunchkarian, State-of-the-art and recent developments of immobilized polysaccharide-based chiral stationary phases for enantioseparations by high-performance liquid chromatography (2013–2017), Microchemical Journal 140 (2018) 142-157. https://doi.org/10.1016/j.microc.2018.04.017.

[109] J. Shen, T. Ikai, Y. Okamoto, Synthesis and application of immobilized polysaccharide-based chiral stationary phases for enantioseparation by high-performance liquid chromatography, Journal of Chromatography A 1363 (2014) 51-61. https://doi.org/https://doi.org/10.1016/j.chroma.2014.06.042.

[110] E. Francotte, T. Zhang, Preparation and evaluation of immobilized 4-methylbenzoylcellulose stationary phases for enantioselective separations, Journal of Chromatography A 1467 (2016) 214-220. https://doi.org/https://doi.org/10.1016/j.chroma.2016.08.006.

[111] P. Peluso, V. Mamane, R. Dallocchio, A. Dessì, S. Cossu, Noncovalent interactions in high-performance liquid chromatography enantioseparations on polysaccharide-based chiral selectors, Journal of Chromatography A 1623 (2020) 461202. https://doi.org/10.1016/j.chroma.2020.461202.

[112] X. Chen, C. Yamamoto, Y. Okamoto, Polysaccharide derivatives as useful chiral stationary phases in high-performance liquid chromatography, Pure and Applied Chemistry 79(9) (2007) 1561-1573. https://doi.org/10.1351/pac200779091561.

[113] E. Yashima, C. Yamamoto, Y. Okamoto, NMR Studies of Chiral Discrimination Relevant to the Liquid Chromatographic Enantioseparation by a Cellulose Phenylcarbamate Derivative, Journal of the American Chemical Society 118(17) (1996) 4036-4048. https://doi.org/10.1021/ja960050x.

[114] B. Chankvetadze, Recent developments on polysaccharide-based chiral stationary phases for liquid-phase separation of enantiomers, Journal of Chromatography A 1269 (2012) 26-51. https://doi.org/10.1016/j.chroma.2012.10.033.

[115] B. Chankvetadze, E. Yashima, Y. Okamoto, Chloromethylphenylcarbamate derivatives of cellulose as chiral stationary phases for high-performance liquid chromatography, Journal of Chromatography A 670(1) (1994) 39-49. https://doi.org/10.1016/0021-9673(94)80278-5.

[116] F. Ianni, F. Blasi, D. Giusepponi, A. Coletti, F. Galli, B. Chankvetadze, R. Galarini, R. Sardella, Liquid chromatography separation of α- and γ-linolenic acid positional isomers with a stationary phase based on covalently immobilized cellulose tris(3,5-dichlorophenylcarbamate), Journal of Chromatography A 1609 (2020) 460461. https://doi.org/10.1016/j.chroma.2019.460461.

[117] E. Francotte, T. Zhang, Supramolecular effects in the chiral discrimination of meta-methylbenzoyl cellulose in high-performance liquid chromatography, Journal of Chromatography A 718(2) (1995) 257-266. https://doi.org/10.1016/0021-9673(95)00686-9.

[118] T. O'Brien, L. Crocker, R. Thompson, K. Thompson, P.H. Toma, D.A. Conlon, B. Feibush, C. Moeder, G. Bicker, N. Grinberg, Mechanistic Aspects of Chiral Discrimination on Modified Cellulose, Analytical Chemistry 69(11) (1997) 1999-2007. https://doi.org/10.1021/ac961241l.

[119] S. Ma, S. Shen, H. Lee, N. Yee, C. Senanayake, L.A. Nafie, N. Grinberg, Vibrational circular dichroism of amylose carbamate: structure and solvent-induced conformational changes, Tetrahedron: Asymmetry 19(18) (2008) 2111-2114. https://doi.org/10.1016/j.tetasy.2008.08.027.

[120] R.W. Stringham, K.G. Lynam, B.S. Lord, Memory effect of diethylamine mobile phase additive on chiral separations on polysaccharide stationary phases, Chirality 16(8) (2004) 493-498. https://doi.org/10.1002/chir.20066.

[121] A. Ghanem, H. Hoenen, H.Y. Aboul-Enein, Application and comparison of immobilized and coated amylose tris-(3,5-dimethylphenylcarbamate) chiral stationary phases for the enantioselective separation of β-blockers enantiomers by liquid chromatography, Talanta 68(3) (2006) 602-609. https://doi.org/10.1016/j.talanta.2005.04.050.

[122] T. Zhang, D. Nguyen, P. Franco, T. Murakami, A. Ohnishi, H. Kurosawa, Cellulose 3,5-dimethylphenylcarbamate immobilized on silica: A new chiral stationary phase for the analysis of enantiomers, Analytica Chimica Acta 557(1) (2006) 221-228. https://doi.org/10.1016/j.aca.2005.10.017.

[123] S.W. Baertschi, Analytical methodologies for discovering and profiling degradation-related impurities, TrAC Trends in Analytical Chemistry 25(8) (2006) 758-767. https://doi.org/10.1016/j.trac.2006.05.012.

[124] M.A. Nussbaum, A. Kaerner, P.J. Jansen, S.W. Baertschi, Role of "mass balance" in pharmaceutical stress testing, in: S.W. Baertschi, K.M. Alsante, R.A. Reed (Eds.), Pharmaceutical Stress Testing - Predicting Drug Degradation, Informa Healthcare2011, pp. 233-253. https://doi.org/10.3109/9781439801802.

[125] T.M. Annesley, Ion Suppression in Mass Spectrometry, Clinical Chemistry 49(7) (2003) 1041-1044. https://doi.org/10.1373/49.7.1041.

[126] D.R. Stoll, X. Wang, P.W. Carr, Comparison of the Practical Resolving Power of One- and Two-Dimensional High-Performance Liquid Chromatography Analysis of Metabolomic Samples, Analytical Chemistry 80(1) (2008) 268-278. https://doi.org/10.1021/ac701676b.

[127] D.R. Stoll, P.W. Carr, Introduction to Two-Dimensional Liquid Chromatography, in: D.R. Stoll, P.W. Carr (Eds.), Multi-Dimensional Liquid Chromatography: Principles, Practice, and Applications, CRC Press2022, pp. 1-28. https://doi.org/10.1201/9781003090557-1.

[128] G. Guiochon, N. Marchetti, K. Mriziq, R.A. Shalliker, Implementations of two-dimensional liquid chromatography, Journal of Chromatography A 1189(1) (2008) 109-168. https://doi.org/10.1016/j.chroma.2008.01.086.

[129] M. Sarrut, G. Crétier, S. Heinisch, Theoretical and practical interest in UHPLC technology for 2D-LC, TrAC Trends in Analytical Chemistry 63 (2014) 104-112. https://doi.org/10.1016/j.trac.2014.08.005.

[130] A.F.G. Gargano, M. Duffin, P. Navarro, P.J. Schoenmakers, Reducing Dilution and Analysis Time in Online Comprehensive Two-Dimensional Liquid Chromatography by Active Modulation, Analytical Chemistry 88(3) (2016) 1785-1793. https://doi.org/10.1021/acs.analchem.5b04051.

[131] D.R. Stoll, P.W. Carr, Two-Dimensional Liquid Chromatography: A State of the Art Tutorial, Analytical Chemistry 89(1) (2017) 519-531. https://doi.org/10.1021/acs.analchem.6b03506.

[132] V.-A. Duong, J.-M. Park, H. Lee, Review of Three-Dimensional Liquid Chromatography Platforms for Bottom-Up Proteomics, International Journal of Molecular Sciences 21(4) (2020) 1524.

[133] D.R. Stoll, G.M. Leme, Instrumentation for Two-Dimensional Liquid Chromatography, in: D.R. Stoll, P.W. Carr (Eds.), Multi-Dimensional Liquid Chromatography: Principles, Practice, and Applications, CRC Press2022, pp. 115-164. https://doi.org/10.1201/9781003090557-4.

[134] K. Zhang, Y. Li, M. Tsang, N.P. Chetwyn, Analysis of pharmaceutical impurities using multi-heartcutting 2D LC coupled with UV-charged aerosol MS detection, Journal of Separation Science 36(18) (2013) 2986-2992. https://doi.org/10.1002/jssc.201300493.

[135] S.R. Groskreutz, M.M. Swenson, L.B. Secor, D.R. Stoll, Selective comprehensive multi-dimensional separation for resolution enhancement in high performance liquid chromatography. Part I: Principles and instrumentation, Journal of Chromatography A 1228 (2012) 31-40. https://doi.org/10.1016/j.chroma.2011.06.035.

[136] M. Pursch, S. Buckenmaier, Loop-Based Multiple Heart-Cutting Two-Dimensional Liquid Chromatography for Target Analysis in Complex Matrices, Analytical Chemistry 87(10) (2015) 5310-5317. https://doi.org/10.1021/acs.analchem.5b00492.

[137] D.R. Stoll, Guidelines for bioanalytical 2D chromatography method development and implementation, Bioanalysis 2(1) (2010) 105-122. https://doi.org/10.4155/bio.09.131.

[138] C. Lee, J. Zang, J. Cuff, N. McGachy, T.K. Natishan, C.J. Welch, R. Helmy, F. Bernardoni, Application of Heart-Cutting 2D-LC for the Determination of Peak Purity for a Chiral Pharmaceutical Compound by HPLC, Chromatographia 76(1) (2013) 5-11. https://doi.org/10.1007/s10337-012-2367-5.

[139] J.G. Shackman, B.L. Kleintop, Peak purity assessment in a triple-active fixed-dose combination drug product related substances method using a commercial two-dimensional liquid chromatography system, Journal of Separation Science 37(19) (2014) 2688-2695. https://doi.org/10.1002/jssc.201400515.

[140] Q. Liu, X. Jiang, H. Zheng, W. Su, X. Chen, H. Yang, On-line two-dimensional LC: A rapid and efficient method for the determination of enantiomeric excess in reaction mixtures, Journal of Separation Science 36(19) (2013) 3158-3164. https://doi.org/10.1002/jssc.201300412.

[141] M. Iguiniz, F. Rouvière, E. Corbel, N. Roques, S. Heinisch, Comprehensive two dimensional liquid chromatography as analytical strategy for pharmaceutical analysis, Journal of Chromatography A 1536 (2018) 195-204. https://doi.org/10.1016/j.chroma.2017.08.070.

[142] J.C. Giddings, Maximum number of components resolvable by gel filtration and other elution chromatographic methods, Analytical Chemistry 39(8) (1967) 1027-1028. https://doi.org/10.1021/ac60252a025.

[143] J.W. Dolan, L.R. Snyder, N.M. Djordjevic, D.W. Hill, T.J. Waeghe, Reversed-phase liquid chromatographic separation of complex samples by optimizing temperature and gradient time: I. Peak capacity limitations, Journal of Chromatography A 857(1) (1999) 1-20. https://doi.org/10.1016/S0021-9673(99)00765-7.

[144] U.D. Neue, Theory of peak capacity in gradient elution, Journal of Chromatography A 1079(1) (2005) 153-161. https://doi.org/10.1016/j.chroma.2005.03.008.

[145] J.C. Giddings, Sample dimensionality: A predictor of order-disorder in component peak distribution in multidimensional separation, Journal of Chromatography A 703(1) (1995) 3-15. https://doi.org/10.1016/0021-9673(95)00249-M.

[146] J.M. Davis, J.C. Giddings, Statistical theory of component overlap in multicomponent chromatograms, Analytical Chemistry 55(3) (1983) 418-424. https://doi.org/10.1021/ac00254a003.

[147] J.M. Davis, D.R. Stoll, P.W. Carr, Effect of first-dimension undersampling on effective peak capacity in comprehensive two-dimensional separations, Anal Chem 80(2) (2008) 461-73. https://doi.org/10.1021/ac071504j.

[148] S.C. Rutan, J.M. Davis, P.W. Carr, Fractional coverage metrics based on ecological home range for calculation of the effective peak capacity in comprehensive two-dimensional separations, Journal of Chromatography A 1255 (2012) 267-276. https://doi.org/10.1016/j.chroma.2011.12.061.

[149] B.W.J. Pirok, D.R. Stoll, Selecting Separation Modes and Selectivities for Multi-Dimensional LC, in: D.R. Stoll, P.W. Carr (Eds.), Multi-Dimensional Liquid Chromatography: Principles, Practice, and Applications, CRC Press2022, pp. 165-182. https://doi.org/10.1201/9781003090557-5.

[150] M.R. Schure, J.M. Davis, Orthogonal separations: Comparison of orthogonality metrics by statistical analysis, Journal of Chromatography A 1414 (2015) 60-76. https://doi.org/10.1016/j.chroma.2015.08.029.

[151] M. Gilar, J. Fridrich, M.R. Schure, A. Jaworski, Comparison of Orthogonality Estimation Methods for the Two-Dimensional Separations of Peptides, Analytical Chemistry 84(20) (2012) 8722-8732. https://doi.org/10.1021/ac3020214.

[152] M. Gilar, P. Olivova, A.E. Daly, J.C. Gebler, Orthogonality of Separation in Two-Dimensional Liquid Chromatography, Analytical Chemistry 77(19) (2005) 6426-6434. https://doi.org/10.1021/ac050923i.

[153] P.W. Carr, J.M. Davis, S.C. Rutan, D.R. Stoll, Principles of Online Comprehensive Multidimensional Liquid Chromatography, in: E. Grushka, N. Grinberg (Eds.), Advances in Chromatography Volume 50, CRC Press2012, pp. 139-235.

[154] J.M. Davis, Dependence of Effective Peak Capacity in Comprehensive Two-Dimensional Separations on the Distribution of Peak Capacity between the Two Dimensions, Analytical Chemistry 80(21) (2008) 8122-8134. https://doi.org/10.1021/ac800933z.

[155] M.R. Schure, The dimensionality of chromatographic separations, Journal of Chromatography A 1218(2) (2011) 293-302. https://doi.org/10.1016/j.chroma.2010.11.016.

[156] M.R. Pourhaghighi, M. Karzand, H.H. Girault, Orthogonality of Two-Dimensional Separations Based on Conditional Entropy, Analytical Chemistry 83(20) (2011) 7676-7681. https://doi.org/10.1021/ac2017772.

[157] W. Nowik, S. Héron, M. Bonose, M. Nowik, A. Tchapla, Assessment of Two-Dimensional Separative Systems Using Nearest-Neighbor Distances Approach. Part 1: Orthogonality Aspects, Analytical Chemistry 85(20) (2013) 9449-9458. https://doi.org/10.1021/ac4012705.

[158] G. Semard, V. Peulon-Agasse, A. Bruchet, J.-P. Bouillon, P. Cardinaël, Convex hull: A new method to determine the separation space used and to optimize operating conditions for comprehensive two-dimensional gas chromatography, Journal of Chromatography A 1217(33) (2010) 5449-5454. https://doi.org/10.1016/j.chroma.2010.06.048.

[159] M. Camenzuli, P.J. Schoenmakers, A new measure of orthogonality for multi-dimensional chromatography, Analytica Chimica Acta 838 (2014) 93-101. https://doi.org/10.1016/j.aca.2014.05.048.

[160] K. Croes, A. Steffens, D.H. Marchand, L.R. Snyder, Relevance of π–π and dipole–dipole interactions for retention on cyano and phenyl columns in reversed-phase liquid chromatography, Journal of Chromatography A 1098(1) (2005) 123-130. https://doi.org/10.1016/j.chroma.2005.08.090.

[161] B.W.J. Pirok, A.F.G. Gargano, P.J. Schoenmakers, Optimizing separations in online comprehensive two-dimensional liquid chromatography, Journal of Separation Science 41(1) (2018) 68-98. https://doi.org/10.1002/jssc.201700863.

[162] P.G. Saffman, G.I. Taylor, The penetration of a fluid into a porous medium or Hele-Shaw cell containing a more viscous liquid, Proceedings of the Royal Society of London. Series A. Mathematical and Physical Sciences 245(1242) (1958) 312-329. https://doi.org/10.1098/rspa.1958.0085.

[163] K.J. Mayfield, R.A. Shalliker, H.J. Catchpoole, A.P. Sweeney, V. Wong, G. Guiochon, Viscous fingering induced flow instability in multidimensional liquid chromatography, Journal of Chromatography A 1080(2) (2005) 124-131. https://doi.org/10.1016/j.chroma.2005.04.093.

[164] S. Chapel, F. Rouvière, V. Peppermans, G. Desmet, S. Heinisch, A comprehensive study on the phenomenon of total breakthrough in liquid chromatography, Journal of Chromatography A 1653 (2021) 462399. https://doi.org/10.1016/j.chroma.2021.462399.

[165] X. Jiang, A. van der Horst, P.J. Schoenmakers, Breakthrough of polymers in interactive liquid chromatography, Journal of Chromatography A 982(1) (2002) 55-68. https://doi.org/10.1016/S0021-9673(02)01483-8.

[166] D.R. Stoll, K. Shoykhet, P. Petersson, S. Buckenmaier, Active Solvent Modulation: A Valve-Based Approach To Improve Separation Compatibility in Two-Dimensional Liquid Chromatography, Analytical Chemistry 89(17) (2017) 9260-9267. https://doi.org/10.1021/acs.analchem.7b02046.

[167] Z. Lin, Q. Wang, Y. Zhou, J.G. Shackman, Trapping mode two-dimensional liquid chromatography for quantitative low-level impurity enrichment in pharmaceutical development, Journal of Chromatography A 1700 (2023) 464043. https://doi.org/10.1016/j.chroma.2023.464043.

[168] R.J. Vonk, A.F.G. Gargano, E. Davydova, H.L. Dekker, S. Eeltink, L.J. de Koning, P.J. Schoenmakers, Comprehensive Two-Dimensional Liquid Chromatography with Stationary-Phase-Assisted Modulation Coupled to High-Resolution Mass Spectrometry Applied to Proteome Analysis of Saccharomyces cerevisiae, Analytical Chemistry 87(10) (2015) 5387-5394. https://doi.org/10.1021/acs.analchem.5b00708.

[169] H.C. van de Ven, A.F.G. Gargano, S. van der Wal, P.J. Schoenmakers, Switching solvent and enhancing analyte concentrations in small effluent fractions using in-column focusing, Journal of Chromatography A 1427 (2016) 90-95. https://doi.org/10.1016/j.chroma.2015.11.082.

[170] H. Tian, J. Xu, Y. Guan, Comprehensive two-dimensional liquid chromatography (NPLC×RPLC) with vacuum-evaporation interface, Journal of Separation Science 31(10) (2008) 1677-1685. https://doi.org/10.1002/jssc.200700559.

[171] J.-F. Li, X. Yan, Y.-L. Wu, M.-J. Fang, Z. Wu, Y.-K. Qiu, Comprehensive two-dimensional normal-phase liquid chromatography × reversed-phase liquid chromatography for analysis of toad skin, Analytica Chimica Acta 962 (2017) 114-120. https://doi.org/10.1016/j.aca.2017.01.038.

[172] S. Bäurer, Characterization and Application of Mixed Mode Stationary Phases in Pharmaceutical and Biochemical Analysis using One- and Two-Dimensional Liquid Chromatography (Dissertation, Pharmacy), University Tuebingen (Germany), 2020. https://doi.org/10.15496/publikation-50209.

[173] J.C. Giddings, Concepts and comparisons in multidimensional separation, Journal of High Resolution Chromatography 10(5) (1987) 319-323. https://doi.org/10.1002/jhrc.1240100517.

[174] R.E. Murphy, M.R. Schure, J.P. Foley, Effect of Sampling Rate on Resolution in Comprehensive Two-Dimensional Liquid Chromatography, Analytical Chemistry 70(8) (1998) 1585-1594. https://doi.org/10.1021/ac971184b.

[175] D.R. Stoll, P.W. Carr, Theoretical Guiding Principles for Two-Dimensional Liquid Chromatography, in: D.R. Stoll, P.W. Carr (Eds.), Multi-Dimensional Liquid Chromatography: Principles, Practice, and Applications, CRC Press2022, pp. 103-114. https://doi.org/10.1201/9781003090557-3.

[176] Y. Huang, H. Gu, M. Filgueira, P.W. Carr, An experimental study of sampling time effects on the resolving power of on-line two-dimensional high performance liquid chromatography, Journal of Chromatography A 1218(20) (2011) 2984-2994. https://doi.org/10.1016/j.chroma.2011.03.032.

[177] I. François, K. Sandra, P. Sandra, Comprehensive liquid chromatography: Fundamental aspects and practical considerations—A review, Analytica Chimica Acta 641(1) (2009) 14-31. https://doi.org/10.1016/j.aca.2009.03.041.

[178] M.R. Schure, Limit of Detection, Dilution Factors, and Technique Compatibility in Multidimensional Separations Utilizing Chromatography, Capillary Electrophoresis, and Field-Flow Fractionation, Analytical Chemistry 71(8) (1999) 1645-1657. https://doi.org/10.1021/ac981128q.

[179] G. Vivó-Truyols, S. van der Wal, P.J. Schoenmakers, Comprehensive Study on the Optimization of Online Two-Dimensional Liquid Chromatographic Systems Considering Losses in Theoretical Peak Capacity in First- and Second-Dimensions: A Pareto-Optimality Approach, Analytical Chemistry 82(20) (2010) 8525-8536. https://doi.org/10.1021/ac101420f.

[180] K. Horváth, J.N. Fairchild, G. Guiochon, Detection issues in two-dimensional on-line chromatography, Journal of Chromatography A 1216(45) (2009) 7785-7792. https://doi.org/10.1016/j.chroma.2009.09.016.

[181] E.M. Antolín, D.M. Delange, V.G. Canavaciolo, Evaluation of five methods for derivatization and GC determination of a mixture of very long chain fatty acids (C24:0–C36:0), Journal of Pharmaceutical and Biomedical Analysis 46(1) (2008) 194-199. https://doi.org/10.1016/j.jpba.2007.09.015.

[182] H.-H. Chiu, C.-H. Kuo, Gas chromatography-mass spectrometry-based analytical strategies for fatty acid analysis in biological samples, Journal of Food and Drug Analysis 28(1) (2020) 60-73. https://doi.org/10.1016/j.jfda.2019.10.003.

[183] I. Brondz, Development of fatty acid analysis by high-performance liquid chromatography, gas chromatography, and related techniques, Analytica Chimica Acta 465(1) (2002) 1-37. https://doi.org/10.1016/S0003-2670(01)01467-2.

[184] T. Seppänen-Laakso, I. Laakso, R. Hiltunen, Analysis of fatty acids by gas chromatography, and its relevance to research on health and nutrition, Analytica Chimica Acta 465(1) (2002) 39-62. https://doi.org/10.1016/S0003-2670(02)00397-5.

[185] S. Almeling, D. Ilko, U. Holzgrabe, Charged aerosol detection in pharmaceutical analysis, Journal of Pharmaceutical and Biomedical Analysis 69 (2012) 50-63. https://doi.org/10.1016/j.jpba.2012.03.019.

[186] X. Zhao, Y. He, J. Chen, J. Zhang, L. Chen, B. Wang, C. Wu, Y. Yuan, Identification and direct determination of fatty acids profile in oleic acid by HPLC-CAD and MS-IT-TOF, Journal of Pharmaceutical and Biomedical Analysis 204 (2021) 114238. https://doi.org/10.1016/j.jpba.2021.114238.

[187] S. Fekete, I. Kohler, S. Rudaz, D. Guillarme, Importance of instrumentation for fast liquid chromatography in pharmaceutical analysis, Journal of Pharmaceutical and Biomedical Analysis 87 (2014) 105-119. https://doi.org/10.1016/j.jpba.2013.03.012.

[188] J.H. Gross, Introduction, Mass Spectrometry - A Textbook, Springer2017, pp. 1-28. https://doi.org/10.1007/978-3-319-54398-7.

[189] M. Khalikova, J. Jireš, O. Horáček, M. Douša, R. Kučera, L. Nováková, What is the role of current mass spectrometry in pharmaceutical analysis?, Mass Spectrometry Reviews 43(3) (2024) 560-609. https://doi.org/10.1002/mas.21858.

[190] C. Mantzourani, M.G. Kokotou, Liquid Chromatography-Mass Spectrometry (LC-MS) Derivatization-Based Methods for the Determination of Fatty Acids in Biological Samples, Molecules 27(17) (2022) 5717.

[191] A. Cappiello, G. Famiglini, P. Palma, E. Pierini, V. Termopoli, H. Trufelli, Overcoming Matrix Effects in Liquid Chromatography−Mass Spectrometry, Analytical Chemistry 80(23) (2008) 9343-9348. https://doi.org/10.1021/ac8018312.

[192] J. Pól, T. Hyötyläinen, Comprehensive two-dimensional liquid chromatography coupled with mass spectrometry, Analytical and Bioanalytical Chemistry 391(1) (2008) 21-31. https://doi.org/10.1007/s00216-008-1879-1.

[193] E. Koch, M. Wiebel, C. Hopmann, N. Kampschulte, N.H. Schebb, Rapid quantification of fatty acids in plant oils and biological samples by LC-MS, Analytical and Bioanalytical Chemistry 413(21) (2021) 5439-5451. https://doi.org/10.1007/s00216-021-03525-y.

[194] Y. Zhu, P. Deng, D. Zhong, Derivatization methods for LC–MS analysis of endogenous compounds, Bioanalysis 7(19) (2015) 2557-2581. https://doi.org/10.4155/bio.15.183.

[195] X. Xie, Y. Xia, Analysis of Conjugated Fatty Acid Isomers by the Paternò-Büchi Reaction and Trapped Ion Mobility Mass Spectrometry, Analytical Chemistry 91(11) (2019) 7173-7180. https://doi.org/10.1021/acs.analchem.9b00374.

[196] R.C. Murphy, T. Okuno, C.A. Johnson, R.M. Barkley, Determination of Double Bond Positions in Polyunsaturated Fatty Acids Using the Photochemical Paternò-Büchi Reaction with Acetone and Tandem Mass Spectrometry, Analytical Chemistry 89(16) (2017) 8545-8553. https://doi.org/10.1021/acs.analchem.7b02375.

[197] F. Wu, X. Wu, C. Chi, C.-F. Ding, Simultaneous Differentiation of C═C Position Isomerism in Fatty Acids through Ion Mobility and Theoretical Calculations, Analytical Chemistry 94(35) (2022) 12213-12220. https://doi.org/10.1021/acs.analchem.2c02706.

[198] M.R. Siddiqui, Z.A. AlOthman, N. Rahman, Analytical techniques in pharmaceutical analysis: A review, Arabian Journal of Chemistry 10 (2017) S1409-S1421. https://doi.org/10.1016/j.arabjc.2013.04.016.

[199] V.R. Meyer, Detectors, Practical High-Performance Liquid Chromatography - Fifth Edition, John Wiley & Sons2010, pp. 91-115.

[200] N. Barbarin, J.D. Henion, Y. Wu, Comparison between liquid chromatography–UV detection and liquid chromatography–mass spectrometry for the characterization of impurities and/or degradants present in trimethoprim tablets, Journal of Chromatography A 970(1) (2002) 141-154. https://doi.org/10.1016/S0021-9673(02)01035-X.

[201] B.X. Mayer, K. Namiranian, P. Dehghanyar, R. Stroh, H. Mascher, M. Müller, Comparison of UV and tandem mass spectrometric detection for the high-performance liquid chromatographic determination of diclofenac in microdialysis samples, Journal of Pharmaceutical and Biomedical Analysis 33(4) (2003) 745-754. https://doi.org/10.1016/S0731-7085(03)00301-7.

[202] H. Meier, S. Bienz, L. Bigler, T. Fox, Chromophore, Spektroskopische Methoden in der organischen Chemie, Georg Thieme Verlag2012, pp. 13-30.

[203] V. Guarrasi, M.R. Mangione, V. Sanfratello, V. Martorana, D. Bulone, Quantification of Underivatized Fatty Acids From Vegetable Oils by HPLC with UV Detection, Journal of Chromatographic Science 48(8) (2010) 663-668. https://doi.org/10.1093/chromsci/48.8.663.

[204] V.R. Meyer, Solvent Properties, Practical High-Performance Liquid Chromatography - Fifth Edition, John Wiley & Sons2010, pp. 81-89.

[205] T. Jankech, I. Gerhardtova, P. Majerova, J. Piestansky, J. Jampilek, A. Kovac, Derivatization of carboxylic groups prior to their LC analysis – A review, Analytica Chimica Acta 1300 (2024) 342435. https://doi.org/10.1016/j.aca.2024.342435.

[206] I. Lavilla, V. Romero, I. Costas, C. Bendicho, Greener derivatization in analytical chemistry, TrAC Trends in Analytical Chemistry 61 (2014) 1-10. https://doi.org/10.1016/j.trac.2014.05.007.

[207] A. Gałuszka, Z. Migaszewski, J. Namieśnik, The 12 principles of green analytical chemistry and the SIGNIFICANCE mnemonic of green analytical practices, TrAC Trends in Analytical Chemistry 50 (2013) 78-84. https://doi.org/10.1016/j.trac.2013.04.010.

[208] C. Chen, R. Li, H. Wu, Recent progress in the analysis of unsaturated fatty acids in biological samples by chemical derivatization-based chromatography-mass spectrometry methods, Journal of Chromatography B 1215 (2023) 123572. https://doi.org/10.1016/j.jchromb.2022.123572.

[209] C.K. Zacharis, P.D. Tzanavaras, Liquid chromatography coupled to on-line post column derivatization for the determination of organic compounds: A review on instrumentation and chemistries, Analytica Chimica Acta 798 (2013) 1-24. https://doi.org/10.1016/j.aca.2013.07.032.

[210] P. Chalova, A. Tazky, L. Skultety, L. Minichova, M. Chovanec, S. Ciernikova, P. Mikus, J. Piestansky, Determination of short-chain fatty acids as putative biomarkers of cancer diseases by modern analytical strategies and tools: a review, Frontiers in Oncology 13 (2023). https://doi.org/10.3389/fonc.2023.1110235.

[211] C. Monnin, P. Ramrup, C. Daigle-Young, D. Vuckovic, Improving negative liquid chromatography/electrospray ionization mass spectrometry lipidomic analysis of human plasma using acetic acid as a mobile-phase additive, Rapid Communications in Mass Spectrometry 32(3) (2018) 201-211. https://doi.org/10.1002/rcm.8024.

[212] L. Xiang, L. Zhu, Y. Huang, Z. Cai, Application of Derivatization in Fatty Acids and Fatty Acyls Detection: Mass Spectrometry-Based Targeted Lipidomics, Small Methods 4(8) (2020) 2000160. https://doi.org/10.1002/smtd.202000160.

[213] S.W. Meckelmann, S. Hellhake, M. Steuck, M. Krohn, N.H. Schebb, Comparison of derivatization/ionization techniques for liquid chromatography tandem mass spectrometry analysis of oxylipins, Prostaglandins & Other Lipid Mediators 130 (2017) 8-15. https://doi.org/10.1016/j.prostaglandins.2017.02.003.

[214] E. Valeur, M. Bradley, Amide bond formation: beyond the myth of coupling reagents, Chemical Society Reviews 38(2) (2009) 606-631. https://doi.org/10.1039/B701677H.

[215] C. Geibel, L. Zhang, K. Serafimov, H. Gross, M. Lämmerhofer, Towards enantioselective ultrahigh performance liquid chromatography–mass spectrometry-based metabolomics of branched-chain fatty acids and anteiso-fatty acids under reversed-phase conditions using sub-2-μm amylose- and cellulose-derived chiral stationary phases, Chirality 34(3) (2022) 484-497. https://doi.org/10.1002/chir.23413.

[216] M. Calvigioni, A. Bertolini, S. Codini, D. Mazzantini, A. Panattoni, M. Massimino, F. Celandroni, R. Zucchi, A. Saba, E. Ghelardi, HPLC-MS-MS quantification of short-chain fatty acids actively secreted by probiotic strains, Frontiers in Microbiology 14 (2023). https://doi.org/10.3389/fmicb.2023.1124144.

[217] J. Han, K. Lin, C. Sequeira, C.H. Borchers, An isotope-labeled chemical derivatization method for the quantitation of short-chain fatty acids in human feces by liquid chromatography–tandem mass spectrometry, Analytica Chimica Acta 854 (2015) 86-94. https://doi.org/10.1016/j.aca.2014.11.015.

[218] V.R. Narreddula, B.I. McKinnon, S.J.P. Marlton, D.L. Marshall, N.R.B. Boase, B.L.J. Poad, A.J. Trevitt, T.W. Mitchell, S.J. Blanksby, Next-generation derivatization reagents optimized for enhanced product ion formation in photodissociation-mass spectrometry of fatty acids, Analyst 146(1) (2021) 156-169. https://doi.org/10.1039/D0AN01840F.

[219] M.C. Thomas, T.W. Mitchell, D.G. Harman, J.M. Deeley, J.R. Nealon, S.J. Blanksby, Ozone-Induced Dissociation: Elucidation of Double Bond Position within Mass-Selected Lipid Ions, Analytical Chemistry 80(1) (2008) 303-311. https://doi.org/10.1021/ac7017684.

[220] J.L. Campbell, T. Baba, Near-Complete Structural Characterization of Phosphatidylcholines Using Electron Impact Excitation of Ions from Organics, Analytical Chemistry 87(11) (2015) 5837-5845. https://doi.org/10.1021/acs.analchem.5b01460.

[221] W. Zhang, R. Jian, J. Zhao, Y. Liu, Y. Xia, Deep-lipidotyping by mass spectrometry: recent technical advances and applications, Journal of Lipid Research 63(7) (2022) 100219. https://doi.org/10.1016/j.jlr.2022.100219.

[222] K.A. Harrison, R.C. Murphy, Direct Mass Spectrometric Analysis of Ozonides: Application to Unsaturated Glycerophosphocholine Lipids, Analytical Chemistry 68(18) (1996) 3224-3230. https://doi.org/10.1021/ac960302c.

[223] M.C. Thomas, T.W. Mitchell, D.G. Harman, J.M. Deeley, R.C. Murphy, S.J. Blanksby, Elucidation of Double Bond Position in Unsaturated Lipids by Ozone Electrospray Ionization Mass Spectrometry, Analytical Chemistry 79(13) (2007) 5013-5022. https://doi.org/10.1021/ac0702185.

[224] X. Ma, Y. Xia, Pinpointing Double Bonds in Lipids by Paternò-Büchi Reactions and Mass Spectrometry, Angewandte Chemie International Edition 53(10) (2014) 2592-2596. https://doi.org/10.1002/anie.201310699.

[225] L. Yang, J. Yuan, B. Yu, S. Hu, Y. Bai, Sample preparation for fatty acid analysis in biological samples with mass spectrometry-based strategies, Analytical and Bioanalytical Chemistry 416(9) (2024) 2371-2387. https://doi.org/10.1007/s00216-024-05185-0.

[226] X. Ma, X. Zhao, J. Li, W. Zhang, J.-X. Cheng, Z. Ouyang, Y. Xia, Photochemical Tagging for Quantitation of Unsaturated Fatty Acids by Mass Spectrometry, Analytical Chemistry 88(18) (2016) 8931-8935. https://doi.org/10.1021/acs.analchem.6b02834.

[227] J. Zhao, X. Xie, Q. Lin, X. Ma, P. Su, Y. Xia, Next-Generation Paternò–Büchi Reagents for Lipid Analysis by Mass Spectrometry, Analytical Chemistry 92(19) (2020) 13470-13477. https://doi.org/10.1021/acs.analchem.0c02896.

[228] P. Esch, S. Heiles, Charging and Charge Switching of Unsaturated Lipids and Apolar Compounds Using Paternò-Büchi Reactions, Journal of the American Society for Mass Spectrometry 29(10) (2018) 1971-1980. https://doi.org/10.1007/s13361-018-2023-x.

[229] J. Zhao, M. Fang, Y. Xia, A liquid chromatography-mass spectrometry workflow for in-depth quantitation of fatty acid double bond location isomers, Journal of Lipid Research 62 (2021) 100110. https://doi.org/10.1016/j.jlr.2021.100110.

[230] Y. Zhao, H. Zhao, X. Zhao, J. Jia, Q. Ma, S. Zhang, X. Zhang, H. Chiba, S.-P. Hui, X. Ma, Identification and Quantitation of C═C Location Isomers of Unsaturated Fatty Acids by Epoxidation Reaction and Tandem Mass Spectrometry, Analytical Chemistry 89(19) (2017) 10270-10278. https://doi.org/10.1021/acs.analchem.7b01870.

[231] Y. Feng, B. Chen, Q. Yu, L. Li, Identification of Double Bond Position Isomers in Unsaturated Lipids by m-CPBA Epoxidation and Mass Spectrometry Fragmentation, Analytical Chemistry 91(3) (2019) 1791-1795. https://doi.org/10.1021/acs.analchem.8b04905.

[232] C. Song, D. Gao, S. Li, L. Liu, X. Chen, Y. Jiang, Determination and quantification of fatty acid C=C isomers by epoxidation reaction and liquid chromatography-mass spectrometry, Analytica Chimica Acta 1086 (2019) 82-89. https://doi.org/10.1016/j.aca.2019.08.023.

[233] X. Zhao, Y. Zhao, L. Zhang, X. Ma, S. Zhang, X. Zhang, Rapid Analysis of Unsaturated Fatty Acids on Paper-Based Analytical Devices via Online Epoxidation and Ambient Mass Spectrometry, Analytical Chemistry 90(3) (2018) 2070-2078. https://doi.org/10.1021/acs.analchem.7b04312.

1.8 List of Figures

1.9 List of Tables

2 Objective

This work focuses on increasing the variety of the analyst´s toolbox by developing analytical methods for the comprehensive characterization of unknown fatty acids, with particular focus on impurity profiling for pharmaceuticals but also general applicability for other lipid-containing samples. This was determined to be necessary, as commonly mass spectrometric detection alone is considered as the holy grail of detection techniques, leaving the analyst stranded in case of multiple isobaric peaks, that are difficult to distinguish without standards or characteristic MS2-fragments. Therefore, multiple concepts are suggested to increase the versatility of analytical methods and allow identification of compounds that exhibit only slight differences in their molecular structure.

The concept of chiral RPLC×RPLC-UV-MS is presented for the comprehensive profiling of conjugated fatty acid and further oxidation products. The importance of combining complementary detections, i.e. combining the sensitivity of MS detection with the selectivity of UV spectra evaluation and untargeted SWATH-MS2 experiments, was expected to be proven with the chosen experimental set-up. UV-spectra evaluation for conjugated fatty acids (cFA) were expected to unveil the possibility of identification of double bond number and configurations. Shape selectivity of stationary phases with regard to their three-dimensional structure and the resulting selectivity for cFA-isomers was investigated.

Modern approaches to enantiomeric determination of *anteiso*-fatty acids, supported by derivatization and robust chiral polysaccharide stationary phases were under investigation to determine potential benefits of these methods. Derivatization of the free fatty acids was expected to enable analytical accessibility with LC-MS, by utilizing high-performance chiral stationary phases to enhance the compositional understanding of Teicoplanin. Although it is a well-studied antibiotic which is in use since decades, its exact chemical composition is still uncertain.

The possibility of low-effort determination of double bond-position with LC-MS is introduced. The investigated approach can serve as a starting point for further development. For this purpose, a GC-MS approach with dimethyldisulfide as derivatization agent was transferred to LC-MS, expected to allow the use of a variety of different column selectivities and minimizing the risk of sample degradation. By the introduction of pyridine-containing reagents, like 2,2'-dipyridyldisulfide, the possibility of charge-switching is explored, in order to enable positional double bond determination in positive mode.

With this work, the analyst´s toolbox can be further expanded with methods for the comprehensive characterization of fatty acids: from utilization of unusual stationary phases, coupling of selectivities in terms of detectors and stationary phases, to derivatizations, leading to more selectivity. Therefore, an analyst should be motivated to challenge the usual way of thinking in analytical method development.

3 Results and Discussion

3.1 Publication I

Comprehensive profiling of conjugated fatty acid isomers and their lipid oxidation products by two-dimensional chiral RP×RP liquid chromatography hyphenated to UV- and SWATH-MS-detection

Matthias Olfert [a], Stefanie Bäurer [a], Marc Wolter [a], Stephan Buckenmaier [b], Edmundo Brito-de la Fuente [c], Michael Lämmerhofer [a,*]

[a] Institute of Pharmaceutical Sciences, Pharmaceutical (Bio-)Analysis, University of Tübingen, Auf der Morgenstelle 8, 72076 Tübingen, Germany

[b] Agilent Technologies, Research and Development, Hewlett-Packard-Str. 8, 76337 Waldbronn, Germany

[c] Fresenius Kabi Deutschland GmbH, Siemensstraße 27, 61352 Bad Homburg, Germany

* Author for correspondence:
Prof. Dr. Michael Lämmerhofer
michael.laemmerhofer@uni-tuebingen.de

This article was published in Analytica Chimica Acta, Volume 1202 (2022), DOI: 10.1016/j.aca.2022.339667

3.1.1 Graphical Abstract

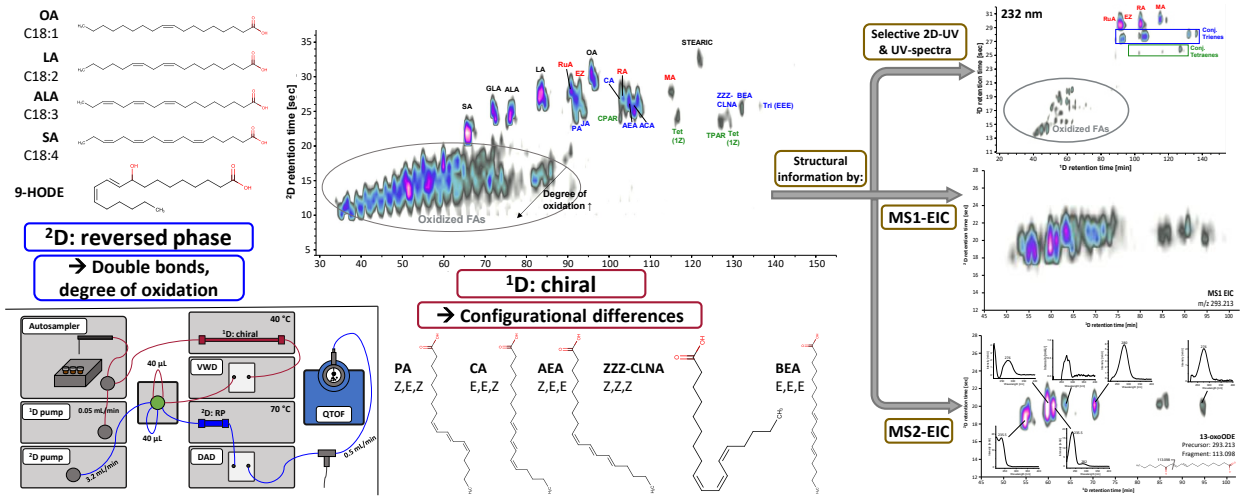

3.1.2 Abstract

This research reports on the development of a comprehensive two-dimensional liquid chromatography (2D-LC) method hyphenated to inline DAD-UV and ESI-QTOF-MS/MS-detection for the separation of conjugated polyunsaturated fatty acid isomers and structurally related (saturated, unconjugated, oxidized) compounds. In pharmaceutical lipid formulations conjugated fatty acids can be found as impurities, generated by oxidation of polyunsaturated fatty acids. Due to the structural complexity of resultant multi-component samples one dimensional liquid chromatography may be suboptimal for quality control and impurity profiling. The screened reversed-phase columns showed a lack of selectivity for the conjugated fatty acid isomers but the resolutions improved with the shape selectivity of the stationary phases (C18- < C30- < cholesteryl-ether-bonded). Further enhanced selectivity for the non-chiral conjugated FAs could be achieved with amylose/cellulose-based chiral stationary phases (CSPs) which harbor cavities for selective inclusion depending on E/Z configurations of the double bonds of the analytes. Amylose-based CSPs showed higher selectivity for conjugated fatty acids than the cellulose-based polysaccharide CSPs. Hyphenating the chiral and reversed-phase columns in a comprehensive 2D-LC-setup was favorable since they showed orthogonality and good compatibility, because both were operated under RP-conditions. The chiral dimension (^{1}D) mainly separated the different isomers, while the reversed-phase dimension (^{2}D) separated according to number of double bonds and degree of oxidation. Using this setup, advanced structural annotation of unknowns was possible based on UV-, MS1- and MS2-spectra. Data-independent acquisition (by SWATH) enabled differentiation of positional isomers of oxidized lipids by characteristic MS2-

fragments and elucidation of co-eluted compounds by selective extracted ion chromatograms of fragment ions (MS2 EICs).

3.1.3 Introduction

Conjugated fatty acids (cFAs) are considered as a subgroup of polyunsaturated fatty acids (PUFAs) and are usually classified based on the respective unconjugated PUFA they "originate" from (e.g. conjugated linoleic acid (CLA), conjugated linolenic acid (CLNA)). Although many positive health benefits are ascribed to cFAs [1], they can be considered as impurities in pharmaceutical lipid-formulations, generated via oxidation of PUFAs [2]. Since impurities, in accordance to guidelines by ICH, have to be identified, quantified, or qualified once the respective thresholds are exceeded, the separation from co-eluting compounds is essential unless specific detection can be employed. This is not trivial because oxidation-reactions or alkaline conditions in PUFA-containing samples can generate a tremendous variety of products, e.g. oxylipins (keto, hydroperoxy-, hydroxyl, epoxy-FAs), further degradation products (e.g. aldehydes) and conjugated FAs [2-4]. Especially the separation of the individual conjugated/unconjugated FA-isomers from each other and from oxidation products can be challenging.

In the field of cFA-research, a lot of studies focused on the separation of positional and geometrical isomers by gas chromatography, e.g. of CLA-isomers [5, 6]. Since derivatization (e.g. to methyl esters) prior to the chromatographic analysis is involved, it may bear some risk of artificially generated impurities in the course of the sample preparation and derivatization step introducing bias in impurity profiling [6].

HPLC-analysis can be performed under milder conditions and allows the identification of double bond configurations in cFAs by UV-detection [7, 8]. Silver-ion chromatography (AgLC) has been suggested as specific LC-mode that can successfully deal with the separation of conjugated fatty acids and CLA-isomers (also as methyl esters) resulting in good resolution, especially when using multiple columns in series [6, 9, 10]. However, bleeding of silver-ions, retention time shifts and build-up of non-conjugated fatty acids is compromising the accurate identification of isomers based on retention times. Oxylipins, some of which represent a subgroup of conjugated FAs, are commonly analyzed by one-dimensional reversed-phase (RP) LC which has reasonable selectivity for many isomers [4, 11-13]. Enantiomers of chiral oxylipins can be separated e.g. by polysaccharide CSPs. Also the separation of different fatty acid groups from each other (saturated, unsaturated, conjugated, unconjugated) has already been reported [14]. In one study, the separation of α- and γ-linolenic acids on a polysaccharide column with enhanced selectivity

over RP was reported [15]. However, one-dimensional liquid chromatographic separations are often limited by their “modest” peak capacity, making the comprehensive analysis of multi-component samples with multiple structurally similar isomers difficult, if not nearly impossible.

Higher peak capacities can be obtained by comprehensive two-dimensional liquid-chromatography (2D-LC) with orthogonal first and second dimensions. In this context RP×RP on distinct RP columns with UV and/or MS-detection is the simplest and most straightforward approach for mobile phase compatibility reasons as discussed by Pirok et al. [16-18]. In a few studies, two dimensional approaches for the separation of lipid oxidation products have already been shown for example by the use of SEC×NPLC [19] or HILIC×RPLC [20]. However, those assays may possess limited selectivity for positional isomers as well as stereoisomers of unsaturated fatty acids, in particular conjugated FAs. The complementary use of AgLC could be of interest from viewpoint of selectivity, but due to its normal-phase elution conditions and solvent incompatibility, respectively, mainly hyphenations with NARP (non-aqueous reversed-phase)-HPLC have been described [19, 21-23], which is problematic for fatty acids/oxylipins. Generic methods which can be applied to many pharmaceutical products are highly desirable in pharmaceutical industry and in this context, 2D-LC has significant potential [24-26]. This may be valid for the impurity profiling of lipid formulations as well. Such methods could be also highly useful for food analysis [19, 27, 28].

To this end, this research focused on the development of a RP×RP-DAD-ESI-QTOF-MS/MS method which enables a comprehensive conjugated fatty acid profiling in lipid samples. Complementary RP and chiral columns are screened using C18 fatty acid mixtures with distinct double bond numbers and E/Z configurations for finding the most orthogonal column combination in ^{1}D and ^{2}D. Finally, a chiral column (Chiralpak IA-U) was selected for ^{1}D separations of the different configurational/positional isomers, coupled via loop modulator interface to a fast ^{2}D reversed-phase separation. The combined information from UV-spectra and MS- as well as MS/MS-detection greatly supports the structural annotation of unknown compounds in this approach.

3.1.4 Experimental

3.1.4.1 Materials

Mass-spectrometry-grade (Rotisolv, Ultra LC-MS grade) methanol, acetonitrile and isopropanol were purchased from Carl Roth (Karlsruhe, Germany). Acetonitrile, methanol and n-hexane, each in HPLC-grade, were obtained from Sigma-Aldrich (Steinheim, Germany). Ultrapure water was produced by additional purification of demineralized water using an Elga LabWater Ultra purification system (Celle, Germany). Acetic acid, hydrochloric acid and potassium hydroxide (KOH) were purchased from Sigma-Aldrich (Steinheim, Germany). Formic acid, acetic acid (Rotipuran > 98%), ammonium acetate and ammonium formate were obtained from Carl Roth (Karlsruhe, Germany). Ethylene glycol was purchased from Merck (Darmstadt, Germany).

Various unconjugated and conjugated fatty acids have been used as test substances. A list of the standards with their suppliers and abbreviations can be found in the Supplemental Material (Table S1).

The chiral columns Chiralpak IA-U, IB-U, IC-U, IG-U, ID-U and IH-U (3.0 x 100 mm, 1.6 µm) were obtained from Chiral Technologies (Illkirch-Graffenstaden, France). The following reversed phase columns were used: Cosmosil Cosmocore 2.6 Cholester (4.6 x 250 mm, 2.6 µm, 90 Å) from Nacalai Tesque (Kyoto, Japan), Acquity UPLC CSH C18 with precolumn (2.1 x 100 mm, 1.7 µm) from Waters (Milford, USA), ProntoSIL 120-5-C30 (2.0 x 200 mm, 5 µm, 120 Å) and ProntoSIL Hypersorb ODS (2.0 x 200 mm, 5 µm, 120 Å) from Bischoff Chromatography (Leonberg, Germany). For the two-dimensional separation Chiralpak IA-3 (2.1 x 150 mm, 3 µm) was obtained from Chiral Technologies (Illkirch-Graffenstaden, France) and the Acquity UPLC CSH C18 (3 x 30 mm, 1.7 µm) was from Waters (Milford, USA).

3.1.4.2 Instrumentation and software

HPLC-system 1: An Agilent 1290 series UHPLC system was equipped with a thermostated autosampler, thermostated column compartment, binary pump and a diode array detector (DAD). The system was controlled using the Agilent OpenLab CDS Acquisition software (Version 2.5) and the data was evaluated with the Agilent OpenLab CDS Data Analysis software (Version 2.5).

HPLC-system 2 (Agilent 2D-LC solution Infinity II): The ^{1}D consisted of a quaternary low-pressure gradient UHPLC pump, thermostated autosampler, thermostated column compartment, and variable wavelength detector (VWD) with 2 µL flow cell; the ^{2}D consisted of a binary high-pressure gradient UHPLC pump, thermostated column compartment, and diode array detector (DAD) with 1 µL flow cell. A pressure-release device was installed between ^{1}D-UV-detector and the ^{1}D/^{2}D-

interface (valve drive with 2-position/8-port 2DLC-valve, loop-size: 40 µL). The system was controlled using Agilent OpenLab CDS ChemStation Edition (Version C.01.10[201]), the same software was used for data evaluation.

For MS-measurements, HPLC-system 2 was hyphenated by a pressure-release valve, T-piece and AB Sciex CDS (calibrant-delivery-system) to an AB Sciex TripleTOF 5600+ system with DuoSpray source for electrospray-ionization from AB Sciex (Concord, Ontario, Canada). The mass spectrometer was controlled by Analyst TF 1.8.1 and MS data evaluation was performed by PeakView 2.2. Origin 2019 (version 9.6) from OriginLab Corporation (Northampton, USA) and LC-Image LC×LC-HRMS (version 2.9r3) from GC Image (Lincoln, NE, USA) were used for data visualization.

3.1.4.3 Preparation of the sample mixtures

For the column-screening five different mixtures of analytes were prepared (tetraene, triene, diene, positional and FA (fatty acid)-mixtures). The composition of the respective mix can be found in Table 1, the concentrations in the supplementary information (Table S2). For the method development on the IA-U, IG-U and RP-column a total mix was prepared, combining aliquots of stock solutions of all five mixtures resulting in the same final concentration (see Table S3).

For the 2D-LC-MS experiments a total mix with 150 µg/mL of each fatty acid, including stearic acid was prepared.

Table 1: Composition of the investigated mixtures of (C18) fatty acids used for the initial column screening and their abbreviations

Mix	Name	DB-Pos.	Configuration	Abbreviation
Triene	Punicic Acid	9,11,13	ZEZ	PA
	Catalpic Acid		EEZ	CA
	alpha-Eleostearic Acid		ZEE	AEA
	beta-Eleostearic Acid		EEE	BEA
	ZZZ-CLNA		ZZZ	ZZZ-CLNA
Diene	Rumenic Acid	9,11	ZE	RuA
	Mangolds Acid		EE	MA
	Ricinenic Acid		ZZ	RA
	10E,12Z-CLA	10,12	EZ	10E,12Z-CLA
FA	Oleic Acid	9	Z	OA
	Linoleic Acid	9,12	ZZ	LA
	alpha-Linolenic Acid	9,12,15	ZZZ	ALA
	gamma-Linolenic Acid	6,9,12	ZZZ	GLA
	Stearidonic Acid	6,9,12,15	ZZZZ	SA
Positional	alpha-Calendic Acid	8,10,12	EEZ	ACA
	Jacaric Acid		ZEZ	JA
	Catalpic Acid	9,11,13	EEZ	CA
	Punicic Acid		ZEZ	PA
Tetraene	cis-Parinaric Acid	9,11,13,15	ZEEZ	CPAR
	trans-Parinaric Acid	9,11,13,15	EEEE	TPAR

3.1.4.4 HPLC-methods

3.1.4.4.1 Column screening

For the column screening HPLC-system 1 was used. Mobile phase A consisted of water with 0.1 % (v/v) acetic acid and mobile phase B of acetonitrile with 0.1 % (v/v) acetic acid. The column temperature was kept at 40 °C. The detection was performed at 210, 232, 260 and 300 nm. Gradient time and flow rate were adjusted to the respective column dimensions.

Chiralpak columns: Gradient profile: 10 to 100 % mobile phase B in 30 min, 100 % B for 5 min, 100 to 10 % B in 0.1 min and hold for 7.9 min. The flow rate was 0.3 mL min^{-1} and the injection volume 10 µL.

Cholester column: Gradient profile: 10 % to 100 % B in 75 min, 12.5 min at 100 % B, 100 % to 10 % B in 0.1 min, 19.75 min reequilibration. The flow rate was 0.705 mL min^{-1} and the injection volume 20 µL.

C18/C30 columns: Gradient profile: 10 % to 100 % B in 60 minutes, 10 min at 100 % B, 100 % to 10 % B in 0.1 min, 15.8 minutes reequilibration. The flow rate was 0.133 mL min^{-1} and the injection volume was 9 µL.

3.1.4.4.2 Final one-dimensional methods for IA-U, IG-U, RP-column

IA-U: ^{1}D from HPLC-system 2 (DAD instead of VWD), mobile phase A: water, 10 mM ammonium acetate and 0.1 % (v/v) acetic acid; mobile phase B: methanol:acetonitrile:water (42.5:42.5:15, v/v/v), 10 mM ammonium acetate, 0.1 % (v/v) acetic acid. Gradient profile: 10 % B for 3 min, 10 % to 75 % B in 0.1 min, 75 % to 100 % B in 26.9 min, 12.9 min at 100 % B, 9 min reequilibration. The flow rate was set to 0.4 mL min^{-1} and the column temperature to 40 °C.

IG-U: ^{1}D from HPLC-system 2 (DAD instead of VWD), mobile phase A: water with 0.1 % (v/v) acetic acid; mobile phase B: methanol:isopropanol (8:2, v/v) + 0.1 % (v/v) acetic acid. Gradient profile: 10 % to 100 % B in 30 min, 5 min at 100 % B, 7.9 min reequilibration. The flow rate was 0.3 mL min^{-1} and the column temperature 30 °C.

Acquity RP-column: ^{2}D from HPLC-system 2 (autosampler from ^{1}D). This method was based on commonly used methods in the lipidomics field [29]. Mobile phase A: acetonitrile:water (3:2, v/v), 10 mM ammonium formate, 0.1 % (v/v) formic acid. Mobile phase B: isopropanol:acetonitrile:water (90:9:1, v/v), 10 mM ammonium formate, 0.1 % (v/v) formic acid. Gradient profile: 2 min 0 % B, 0 % to 82 % B in 11 min, 82 % to 99 % B in 0.5 min, 99 % B for 1.5 min, 99 % to 0% in 0.1 min, reequilibration for 3.9 min. The flow rate was 0.6 mL min^{-1} and the column temperature 65 °C.

3.1.4.4.3 2D-LC-DAD-ESI-MS/MS method with SWATH acquisition

HPLC-system 2 was used. First dimension: column: Chiralpak IA-3, 150 x 3 mm, 3 µm; mobile phase A: water, 10 mM ammonium acetate and 0.1 % (v/v) acetic acid; mobile phase B: methanol:acetonitrile:water (42.5:42.5:15, v/v/v), 10 mM ammonium acetate, 0.1 % (v/v) acetic acid; gradient profile: 10 % B for 17.64 min, 10 % to 75 % B in 0.1 min, 75 % to 100 % B in 118.63 min, 100 % B for 35.63 min, 100 % to 10 % B in 0.1 min, reequilibration for 15 min. The flow rate was 0.05 mL min^{-1} from 0 to 156.4 min and 0.2 mL min^{-1} from 157 to 187.1 min. The column temperature was set to 40 °C.

Second dimension: column: Acquity UPLC CSH C18, 30 x 3 mm, 1.7 µm; mobile phase A: acetonitrile:water (2:8, v/v), 10 mM ammonium formate, 0.1 % (v/v) formic acid. mobile phase B: isopropanol:acetonitrile:water (45:34.5:20.5, v/v), 10 mM ammonium formate, 0.1 % (v/v) formic acid; gradient profile: 0 % B for 0.1 min, 0 % to 60 % B in 0.01 min, 60 % to 100 % B in 0.38 min, 100 % to 0% B in 0.01 min, reequilibration for 0.2 min. The flow rate was set to 3.2 mL min^{-1} and column temperature to 70 °C. The split ratio was adjusted to 0.5 mL min^{-1} to the MS flow path.

Mass spectrometer (MS): Negative mode, cycle time: 960 ms, curtain gas: 35 psi, source gas 1: 30 psi, source gas 2: 50 psi, ion-spray voltage floating: -4500 V, ion source temperature: 400 °C; TOF-MS: accumulation time: 150 ms, scan range: *m/z* 35-1000, collision energy: -5 V, declustering potential: -100 V; SWATH-MS: accumulation time: 40 ms, collision energy: -25 V, collision energy spread: ±5 V, declustering potential: -100 V, SWATH-windows: see Table S4.

3.1.4.5 UV-Spectra comparison

The UV-spectra were recorded during the respective chromatographic analysis with the Agilent DAD-module from 200 to 400 nm in 0.5 nm steps. The spectra were selected at peak apex position with manual references at the beginning/end of the respective peak.

3.1.4.6 Preparation of conjugated PUFAs by alkaline treatment of fatty acids

Stressed arachidonic acid was obtained by alkaline treatment according to the protocol described by M. Igarashi et al. [30], which was based on the AOAC method with slight modifications. 21 % KOH in ethylene glycol (approximately 3.7 N) was bubbled with nitrogen for 5 minutes. 0.5 mL of the solution were subsequently added to 2 mg of arachidonic acid into a hydrolysis vial. After additional bubbling with nitrogen, the closed vials were heated in the oven at 180 °C for 10 min. After cooling down the solution was transferred into a glass vial, 0.5 mL methanol was added and acidified with 1 mL of a 6 N hydrochloric acid solution, leading to precipitation. The mixture was extracted with 2 mL hexane. The two-phase-system was washed using a methanol:water-mixture (3:7, v/v) and water. Fifty (50) µL of the upper layer (hexane phase) were evaporated with nitrogen until dryness. The residue was reconstituted in methanol to achieve a concentration of 0.5 mg mL^{-1}. For LC-UV measurements it was used undiluted.

3.1.5 Results and discussion

3.1.5.1 Column screening

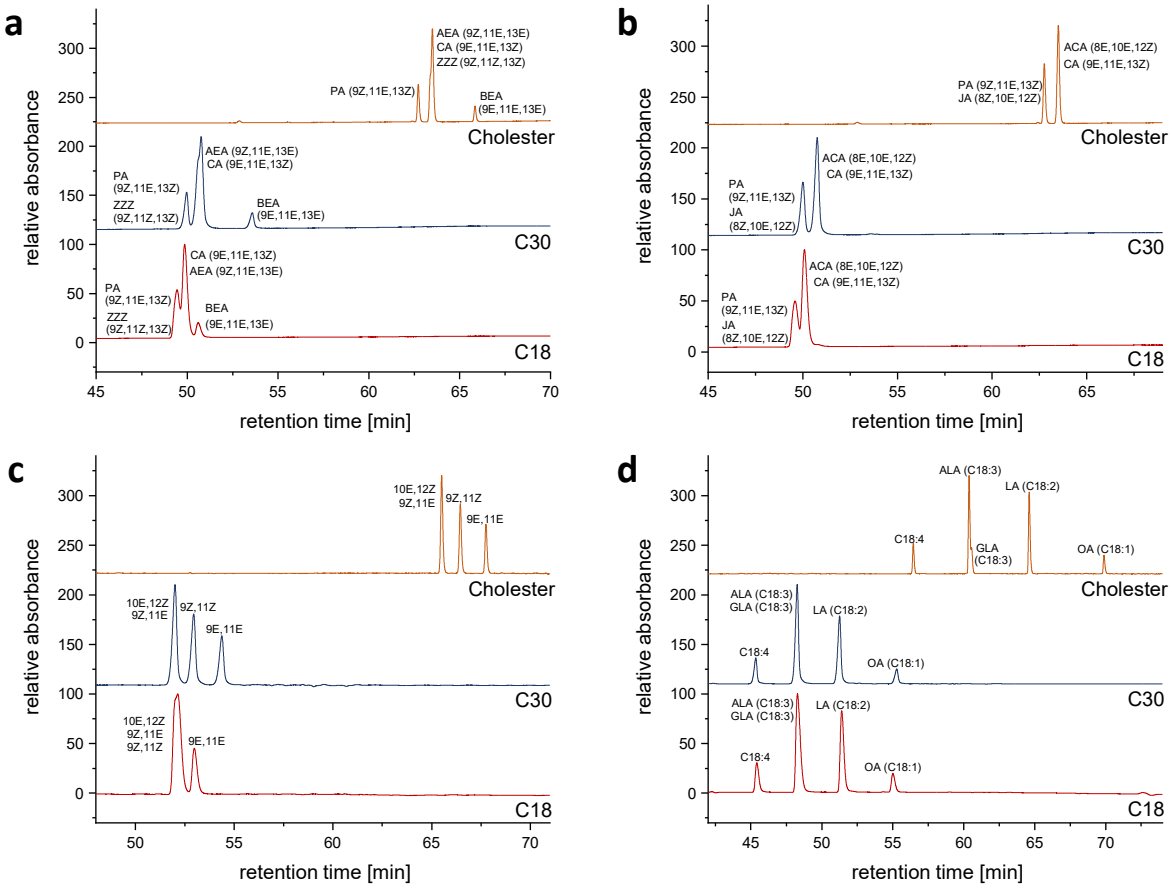

Figure 1: Column screening results: Chromatograms of the investigated fatty acid mixtures on complementary reversed-phase columns (Cholester, C30 and C18). a: triene-mix; b: positional isomers mix; c: diene-mix; d: unconjugated FA-mix; chromatograms of the conjugated tetraene mix can be found in the supplementary information (for conditions see 3.1.4.4.1).

RP chromatography is a commonly used separation mode for the analysis of free fatty acids, fatty acid-derivatives and fatty acid containing samples [29, 31] as well as in lipidomics [32, 33]. Typically, C18-RP-columns are being used to separate FAs furnishing increased retention with carbon number and decreasing retention with double bond number. E/Z-stereoisomers of unsaturated FAs are unfortunately not always well separated. Against this backdrop, different reversed phase-columns were compared to assess whether alternative RP columns have different selectivity and which ones perform best in separating the different FA-groups and the respective isomeric compounds. For this purpose, different fatty acid mixtures (unconjugated FAs, conjugated dienes, conjugated trienes, positional isomers of conjugated trienes, conjugated tetraenes) were analysed. The investigated C18-column showed only poor separation capability

for the isomeric fatty acids, especially for the conjugated dienes, trienes and positional isomers (see Figure 1, red trace). Only the unconjugated C18 PUFAs were sufficiently separated, based on the number of double bonds yet without resolution of α- and γ-linolenic acid (see Figure 1d, red trace). It is well known from the literature that C30-phases exhibit enhanced shape selectivities which has led to unique selectivity for carotenoid isomers and other E/Z isomer mixtures [34, 35]. In fact, the use of a shape-selective C30-RP-stationary phase led to a general improvement of the separations, especially for the conjugated dienes (three out of four isomers were separated; Figure 1c, blue trace). The use of the Cholester-column (based on core-shell silica particles) had similar selectivities (no additional FAs resolved; Figure 1, orange trace) but slightly better resolutions. None of the RP-columns showed a satisfying separation of the isomeric compounds, but the use of stationary phases with enhanced shape selectivity (C18 < C30 < Cholester) resulted in an improvement of the separations.

Chiral stationary phases can also be an attractive choice when isomeric species need to be separated and orthogonal selectivity is required. Polysaccharide CSPs are of particular interest in this context. The Chiralpak columns, which can also be operated under reversed-phase elution conditions, are now available on (sub-2µm) UHPLC supports with immobilized amylose- (IA-U, ID-U, IG-U, IH-U) or cellulose-derivatives (IB-U, IC-U) bearing different substituted phenylcarbamate- or α-methylbenzylcarbamate modifications. The selectivity on these phases typically originates from insertion of analytes into cavities formed by the pendant arylester/arylcarbamate groups at the (slightly) helically wound glucopyranose polymer backbone with different helical twist for cellulose-derivatives (left handed 3/2 helix) and amylose-derivatives (left handed 4/3 helix) [36-39]. The chiral cavities might distinguish between distinct conjugated FAs by steric interactions and thus provide also some sort of shape selectivity. The amylose-based columns, in particular the IG-U-column, showed stronger retention of the analytes than the cellulose-based ones (see Figure 2a and Figure S1). The direct comparison highlights the significantly better separation of the different isomers by the chiral polysaccharide columns, especially by IA-U and IG-U, than on the reversed-phase columns. Compared to IA-U, the IG-U column separated additionally 9Z,11Z,13Z-CLNA and 9E,11E,13E-CLNA of the triene-mix (see Figure 2a) and the positional isomers 9Z,11E,13Z- and 8Z,10E,12Z-CLNA, leading to full separation of all investigated positional isomers. However, the IA-U-column achieved baseline-separation of 9E,11E,13Z and 8E,10E,12Z-CLNA. The diene mix could not be fully separated by any of the columns (co-elution of 9Z,11E and 10E,12Z-CLA), yet the IA-U, ID-U and IG-U columns showed the best results.

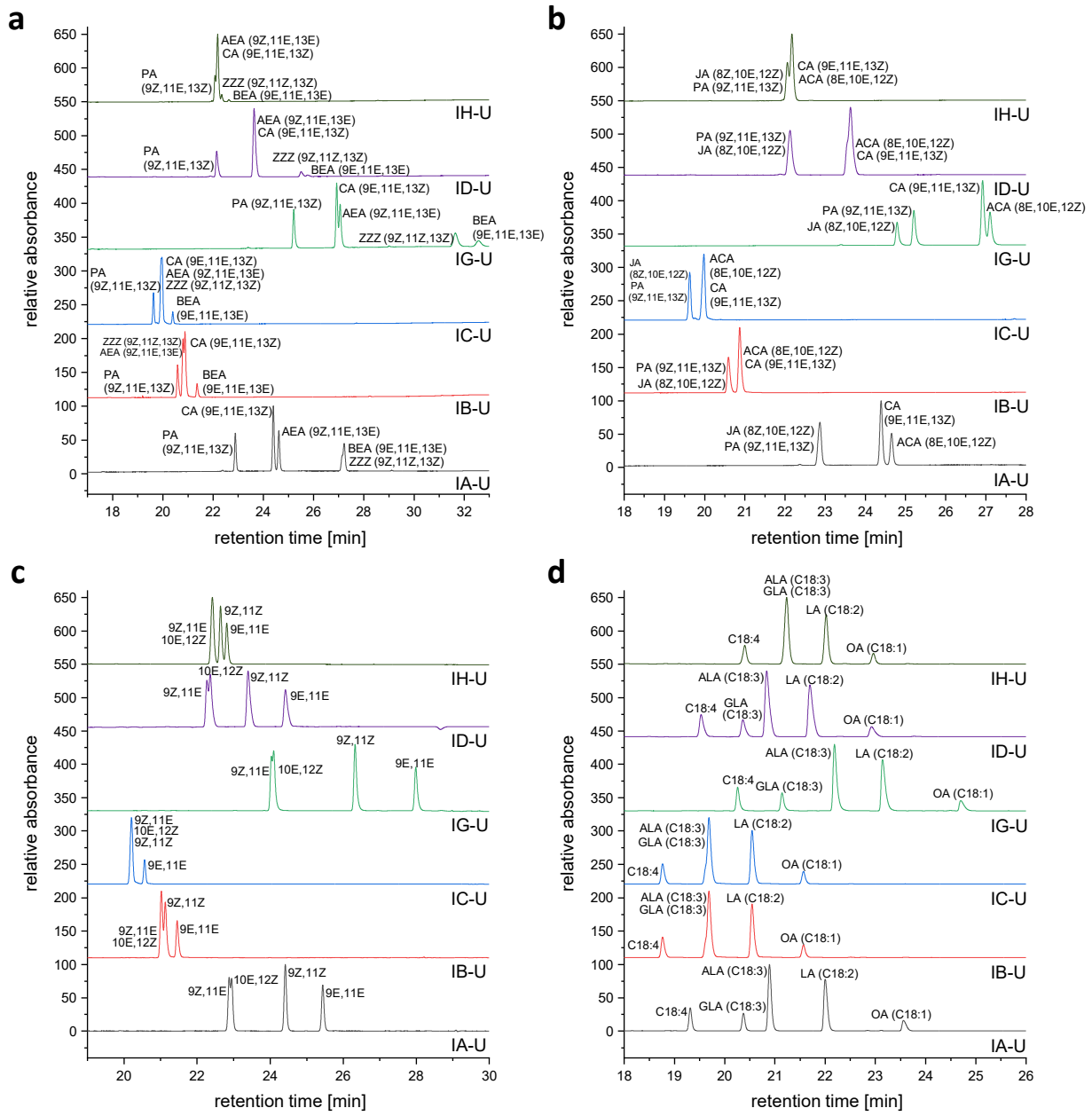

Figure 2: Column screening results: Comparison of the separations on the chiral columns. a: triene mix, b: positional isomers mix, c: diene mix, d: unconjugated FA-mix; chromatograms of the conjugated tetraene mix can be found in the supplementary information (for conditions see 3.1.4.4.1)

For RP- and chiral-columns, the elution order followed a systematic pattern: (a) the higher the number of double bonds, the lower the retention of unconjugated FAs (also applies for cFAs on RP-columns; on chiral columns the elution order of cFAs is reversed); (b) the more double bonds in E-configuration, the higher the retention; (c) on chiral columns the retention windows of conjugated dienes, trienes, tetraenes overlapped while they were separated on the RP-columns. The only compounds that did not follow pattern (b) were the ones which have all double bonds in

Z-configuration (9Z,11Z-CLA and 9Z,11Z,13Z-CLNA, compare Figure 2a, c), since they did not elute in the beginning of their respective series as expected.

3.1.5.2 UV-spectra of conjugated fatty acids

Due to specific absorbance maxima and characteristic shapes [7, 40], the UV-spectra of conjugated dienes/trienes/tetraenes (Figure 3) can be very supportive for identification and differentiation of isobaric fatty acids. The conjugated dienes show the absorbance maximum at around 232 nm (Figure 3a). The conjugated trienes (Figure 3b) feature a trident shape with three local maxima around 270 nm. The spectra of the conjugated tetraenes (Figure 3c) have similar appearance but display four local maxima (at approximately 300 nm), of which the first one is only visible as a shoulder.

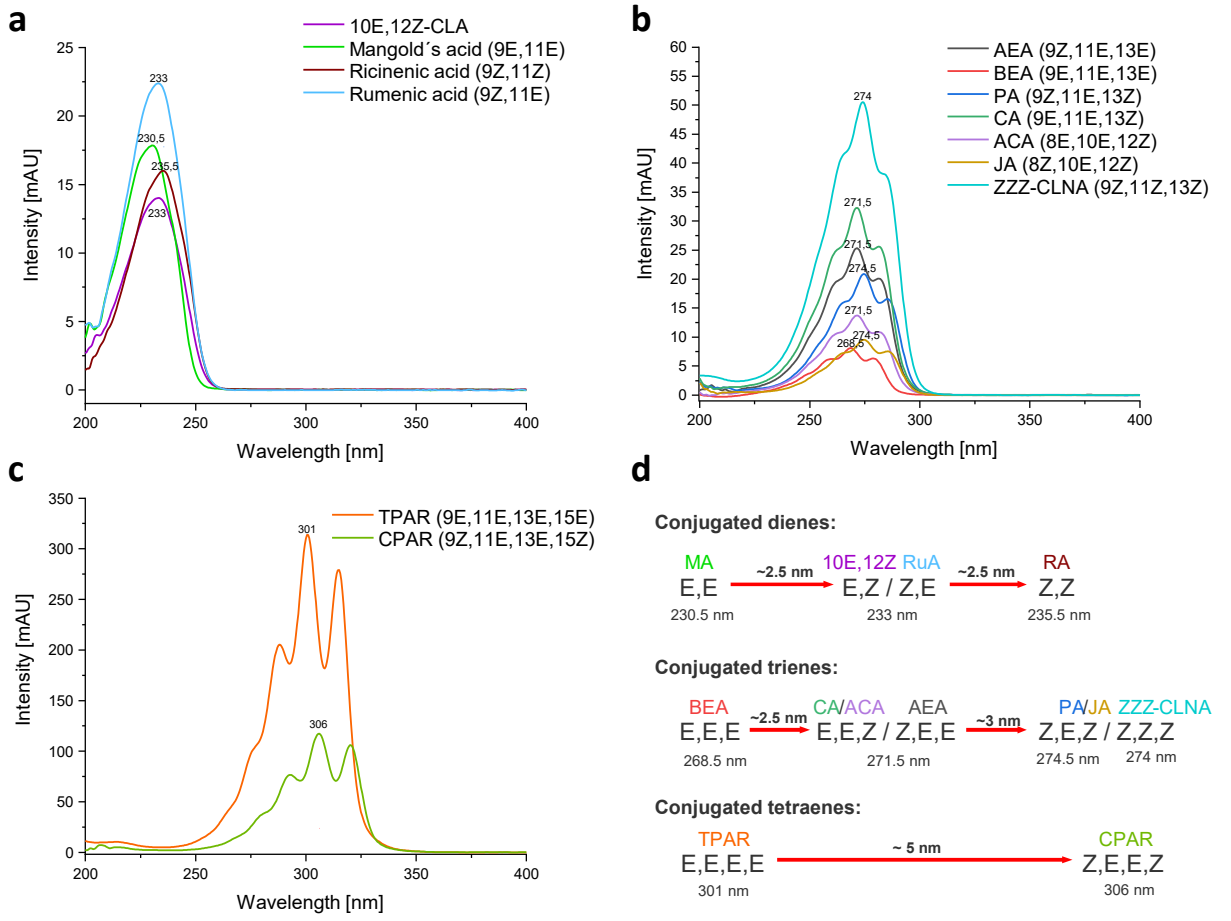

Figure 3: UV spectra of the investigated conjugated fatty acids. a: conjugated dienes, b: conjugated trienes, c: conjugated tetraenes, d: effect of DB configuration and resulting bathochromic shifts, respectively. For better visualization the intensities were normalized.

A closer look into the absorbance maxima allows to derive information about the double bond configurations of cFAs. Thereby, for all investigated cFA-groups it was observed that relative to all-E each double bond in Z-configuration caused a bathochromic shift of approximately 2.5 to 3.0 nm. Neither the position of the conjugated system (see CA/AEA) nor the position of the Z-configuration (compare ACA/CA or JA/PA) had a significant influence on the UV spectra. Hence, the UV spectra can serve as additional identification criteria of unknown isomers. From the herein investigated fatty acids only the 9Z,11Z,13Z-CLNA did not strictly follow this pattern; it showed a slightly lower absorbance maximum (λ_{max} = 274 nm) than the one of 9Z,11E,13Z-CLNA (λ_{max} = 274.5 nm).

Co-elutions in real lipid samples, however, can result in interferences and composite UV-spectra, making an identification via zeroth order UV spectra quite difficult or even impossible. This problem can either be solved by better separation of those co-eluting compounds or by second derivative UV-spectra, which enhances the differences and minimizes the interferences of other UV-bands [7]. In the second derivative spectra, global and local absorbance maxima are featuring sharp minima revealing the fine spectral differences of the conjugated FAs with distinct double bond configurations more clearly (see Suppl. Figure S2). Also, other UV active structural features in conjugated fatty acids modulate the UV-spectra. For instance, an additional isolated double bond next to the conjugated double bond shifts the absorbance maximum slightly to higher wavelengths [8, 41]. However, this additional double bond is associated with retention time and mass shifts which enable their distinction by MS detection. Considering that low energy collisional dissociation (CID) does not provide rich fragmentation of FAs, support of identification of impurities in lipid samples by UV spectral libraries, second order derivative spectra and spectral deconvolution of composite spectra from interfering compounds may be of great utility. Hence, a multi-detector approach combining UV and MS detection is a powerful strategy in impurity profiling of lipid products.

3.1.5.3 [1]D method development for conjugated fatty acid separation

Since the IA-U and IG-U-columns showed superior separation of the individual mixtures of conjugated FAs, they were considered for method development to achieve a complete separation of all investigated fatty acids by one-dimensional LC. Especially the separation of the isomeric fatty acids in each group was of interest because they cannot be differentiated by MS-detection.

Various mobile phases, operating temperatures and gradient profiles were tested (not shown). The chromatograms of the final optimized methods with the IA-U and RP-column are shown in Figure 4. The final optimized IG-U chromatograms can be found in the supplementary information (Figure S3). This column was not further considered because of its higher retention of the analytes without real benefit in terms of selectivity for incompletely resolved isomers.

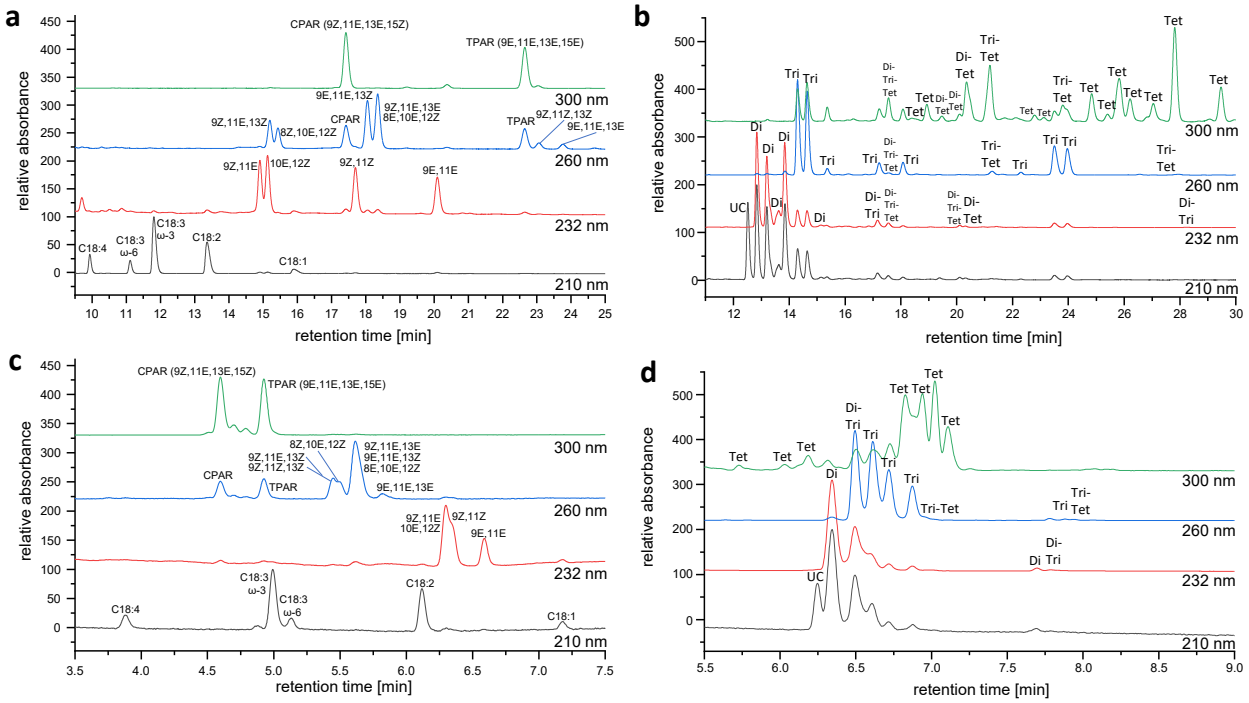

Figure 4: Chromatograms of total-mix (containing unconjugated FAs, conjugated diene, triene, and tetraene FAs) (a,c) and alkaline-treated arachidonic acid (b,d) using different columns; a: total-mix using Chiralpak IA-U; b: alkaline treated arachidonic acid, Chiralpak IA-U; c: total-mix using Acquity CSH C18; d: alkaline treated arachidonic acid, Acquity CSH C18; UC = unconjugated FA 20:4, Di: conjugated diene, Tri: conjugated triene, Tet: conjugated tetraene (for conditions see 3.1.4.4.2).

The separation of the fatty acids was a compromise, because different conditions result in better separation for some of the fatty acids but in worse separation for others. The most problematic separations concerned the critical peak pairs 9Z,11E,13Z-/8Z,10E,12Z-CLNA, 9Z,11Z,13Z-/9E,11E,13E-CLNA and 9Z,11E-/10E,12Z-CLA. They could be resolved by the IA-U-method and

the IG-U-method, resulting in the separation of nearly all of the investigated fatty acids in a single run (Figure 4a). Only the two isomeric compounds 9Z,11E,13E-/8E,10E,12Z-CLNA could not be separated by any of the screened methods. The chiral columns achieved a good separation of the cFA-isomers, but the elution windows of the different groups (conjugated dienes/trienes/tetraenes) overlapped, which in a complex sample results in some co-elutions with convoluted spectra, impairing structural annotation by UV spectra (see Figure S4). To this end, with IA-U and IG-U most of the isobaric C18 fatty acids were resolved except for the peak pair 9Z,11E,13E-CLNA and 8E,10E,12Z-CLNA as well as the peak pair 9Z,11E,13Z-CLNA and 10E,12Z-CLA which were partly coeluting. For the latter peak pair, a differentiation of the co-eluted compounds by their *m/z*-value is possible due to a different double bond number. To further alleviate the problem with coelutions and convoluted UV spectra, we opted for a comprehensive 2D-LC untargeted lipidomics approach combining the optimized chiral LC method with a complementary RPLC separation as presented above. The resolution of co-elutions is particularly mandatory for more complex lipidomics samples (Figure 4b, d) like oxidized/degraded multi-component mixtures of PUFAs (e.g. nutritional supplements, pharmaceutical formulations).

3.1.5.4 Orthogonality evaluation of separations on RP and chiral columns

In order to exploit the highest possible degree of separation capability in a two-dimensional setup, the use of complementary separation dimensions is essential while maintaining mobile phase compatibility [17]. This orthogonality was elucidated by a principal component analysis (PCA). The scatter plot (Figure 5a) reveals a clustering of the different columns based on the type of stationary phase (for loadings plot see Suppl. Figure S4). This correlates with a similar separation-behaviour of the analytes. The only exception is Chiralpak IH-U which is amylose-based but in the cluster of cellulose-based columns, presumably due to the effect from the additional stereocenter of the pendent aralkyl carbamate residues of the chiral selector.

Based on this scatter plot, a hyphenation of two columns from different clusters in the 2D-LC approach would be favourable. The complementarity was further verified by orthogonality plots using the bin-counting method (with normalized retention times) [42, 43]. The orthogonality-plots matched with the clustering of the PCA: (1) the combination of columns from different clusters resulted in a high degree of orthogonality (Figure 5b), (2) combining columns from the same cluster resulted in low orthogonalities (Figure 5c), (3) the combination of amylose-based CSPs with RP-columns gave higher orthogonalities than cellulose-based CSPs with RP-columns (see Table S5).

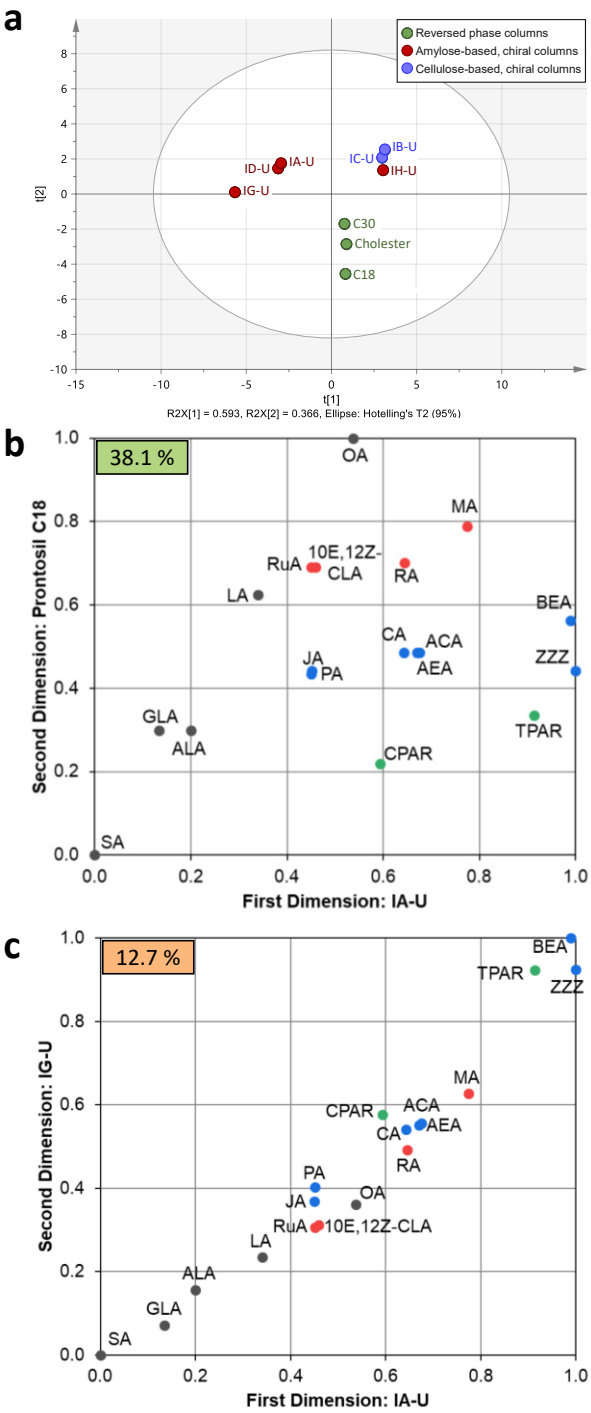

Figure 5: Column orthogonality evaluation: a: principal component analysis (PCA) performed with SIMCA (version 15.0.2, Sartorius Stedim Data Analytics AB, Umeå, Sweden); the scatter plot illustrates the similarity of retention patterns by clustering based on the type of stationary phase. Corresponding loadings plot can be found in the supplementary information. Retention times from the column screening were used and normalized according to Gilar et al. [42]; b: orthogonality plot IA-U vs. C18, orthogonality: 38.1 %; c: orthogonality plot IA-U vs. IG-U, orthogonality: 12.7 %.

3.1.5.5 Full comprehensive chiral RP×RP-DAD-ESI-MS/MS measurements with data-independent SWATH acquisition

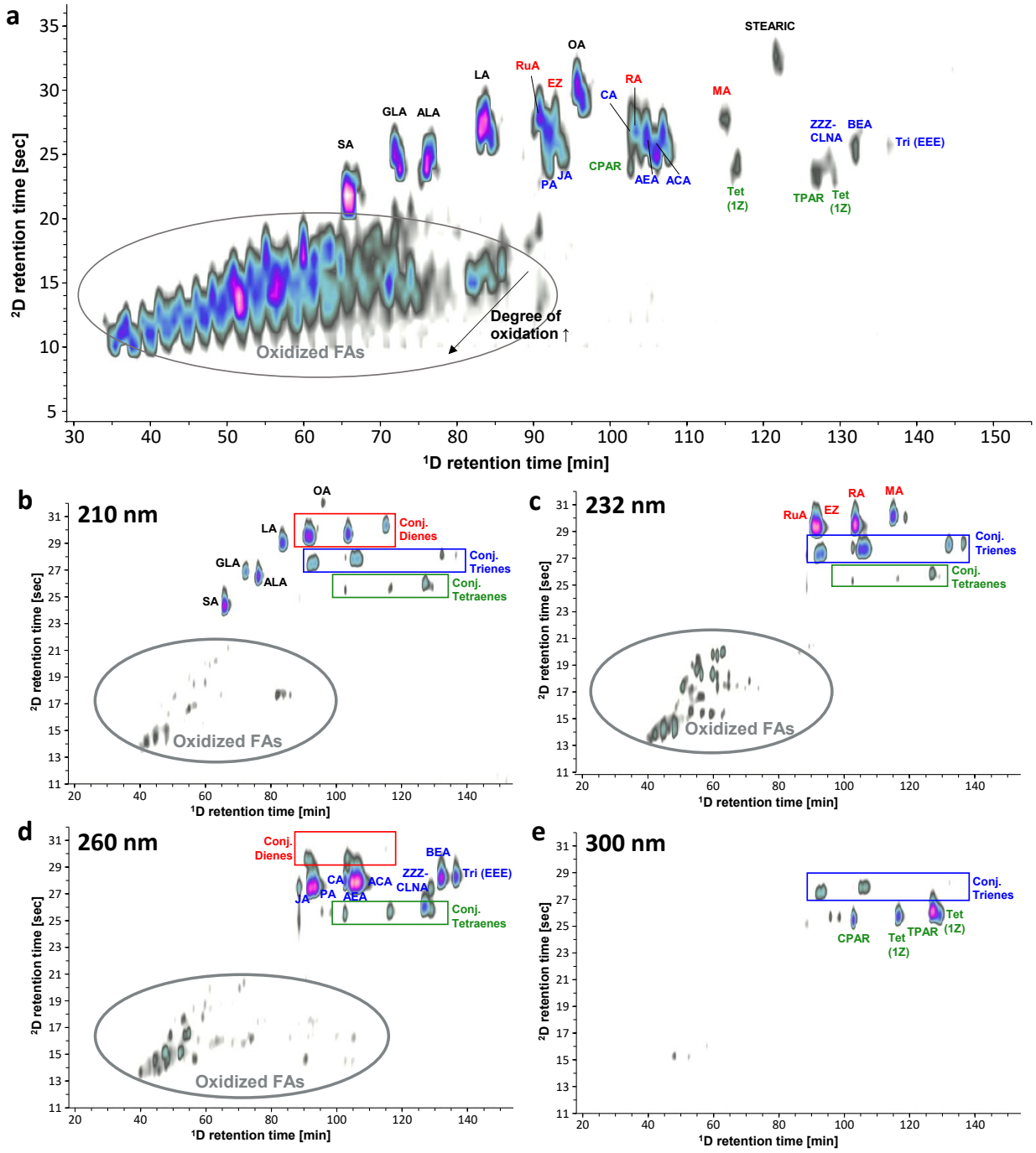

Figure 6: Contour-plot of the full-comprehensive 2D-LC-DAD-MS/MS measurement of the total mix of conjugated FAs. (a) MS detection (MS1 EIC of C18 FAs with 0 to 4 double bonds and 0 to 4 additional oxygen atoms), (b) UV at 210 nm, (c) UV at 232 nm, (d) UV at 260 nm (oxidized impurities generated by air-oxidation during usage of the standards over multiple months). For conditions see 3.1.4.4.3

Because in a full-comprehensive 2D-LC analysis the ^{2}D cycle time equals the sampling time from the first dimension, a short LC-method as the second dimension is necessary to avoid undersampling [17, 18]. Undersampling describes the loss of resolution from the separation of the first dimension through remixing of the analytes during the sampling and can be minimized by sampling 3-4 fractions across 8σ peak width [18]. As shown before, an RP-column as the second dimension can be beneficial, since it allows fast separations, introduces a separation according to the number of double bonds (see Figure 4b, d) and shows high orthogonality values with the Chiralpak IA-U column. Starting from the RP-method (17 min) mentioned in 3.3, the method was shortened by the use of higher flow rates (3.2 mL min^{-1}) and a shorter column (30 mm, same stationary phase) with larger internal diameter (3 mm), while maintaining the eluted column volumes during the gradient. The washing step was removed, the initial focusing step and reequilibration were shortened. The mobile phases and gradient profile were optimized to achieve peak-focusing in the ^{2}D and best possible exploitation of the elution window. For this purpose, a design-of-experiment (DOE) strategy using MODDE was employed and Derringer´s desirability function to rank the screened methods (Figure S6 and S7) [44, 45]. By increasing gradient steepness, the resulting method (1.4 min) was further shortened, which represented the final ^{2}D RPLC method with ^{2}D run time of 0.7 min (including reequilibration, equals ~87 % loop fill; loop fill of 50% only could be beneficial to avoid losses of sample as suggested in ref. [17] but has led to lower desirability in the optimization).

The ^{1}D separation with the chiral IA-U column was also adapted. The column diameter was changed from 3 mm to 2 mm ID. Since such dimension was only available as 3 µm particle column, the packing was changed to Chiralpak IA-3 (150 mm). The final ^{1}D chiral method (see 3.3) was adapted to the Chiralpak IA-3 to achieve the same column volumes during the gradient with a flow rate of 0.05 mL min^{-1}. Although longer gradients may be beneficial for the separation and the unequivocal identification of analytes [46], the gradient length was shortened by 25 % to achieve a reasonable run time without a significant loss of resolution. Reproducibility is, reportedly, one of the weak points of 2D-LC. However, the use of individually optimized methods and well-maintained state-of-the-art equipment ensures robust measurements [47]. Run-to-run repeatability of second dimension retention times were < 0.1% RSD in this work.

While the chiral dimension showed high separation capability for isomers, the introduction of the second (reversed phase) dimension gave the benefit of the separation based on the number of double bonds and degree of oxidation, resulting in a two-dimensional method with high peak capacity (Figure 6a). The combination of the orthogonal columns results also in improved overall

selectivity; i.e. co-elutions on the IA column were resolved on the RP column and vice versa. Although the chiral first dimension yields most of the separations, the second (RP) dimension still adds valuable selectivity (i.e. separation of coelutions from the first dimension, e.g. oxidized/non-oxidized FAs). This leads to UV-spectra with less interferences and easier assignment of MS2-fragments to precursors. The benefit of the two-dimensional approach would become even more evident when analyzing more complex samples with complete PUFA profile and their oxidized derivatives like in food analysis. Both columns were operated under typical hydro-organic RP elution conditions. No mobile phase compatibility problems upon transfer of fractions sampled from ^{1}D into the ^{2}D such as peak splitting or breakthrough were observed.

The method was optimized specifically for conjugated FAs. It was a goal to separate corresponding oxidized lipids from target conjugated FAs, to avoid UV-spectral interferences. A full optimization and characterization of oxidized lipids was beyond the present study. Yet, the current chiral RP×RP 2D-LC method provides preliminary information and its great potential for oxidized FAs is therefore briefly outlined in the following discussion. The information-rich data sets acquired by this chiral RP×RP-DAD-ESI-QTOF-MS/MS method with data independent SWATH acquisition [48] provide multiple layers of selectivity: Chromatographic selectivity from ^{1}D and ^{2}D, accurate mass filtering of the precursor ion (MS1) at TOF-MS mass resolution (providing sum formula), additional selectivity filters by MS2 EIC capability in different SWATH windows and acquisition of UV-spectra across the entire 2D-LC separation enabled the characterization of the analytes regarding their affiliation to one of the groups (conjugated diene, triene, tetraene; see selective 2D-UV-chromatograms in Figure 6b-e) and their double-bond-configurations. The workflow is exemplarily shown in Figure S8 for the tentative structural annotation of an oxoODE. A small peak in the (unmodulated) elution window of the oxidized FAs was detected in front of the peak of rumenic acid (9Z,11E-CLA; Figure S8a). The UV-spectrum and precursor ion in MS1 (*m/z* 293.211) was characteristic for a conjugated “keto-diene”, like 9-oxoODE or 13-oxoODE, with both double bonds in E-configuration [49]. Whilst the fragment with *m/z* 185.119 can be assigned to 9- and 13-oxoODE according to ref. [49], the fragment *m/z* 125.094 seems to be characteristic to 9-oxoODE according to ref. [49-51] but vague here due to too low intensity (Figure S8b). While this preliminary information is not sufficient for an unequivocal identification, it provides valuable evidence for further validation ideally by targeted measurements in comparison to an authentic standard of 9-oxoODE. The information obtained from the UV-spectra is valuable since compounds like 9-HOTrE (9-hydroxy-10,12,15-octadecatrienoic acid) show the same MS1-precursor mass and MS2-fragment, but differ in the UV-spectrum. The same is true for isobaric

epoxy-fatty acids (also common oxidation-products) which can be ruled out due to distinct UV-spectra.

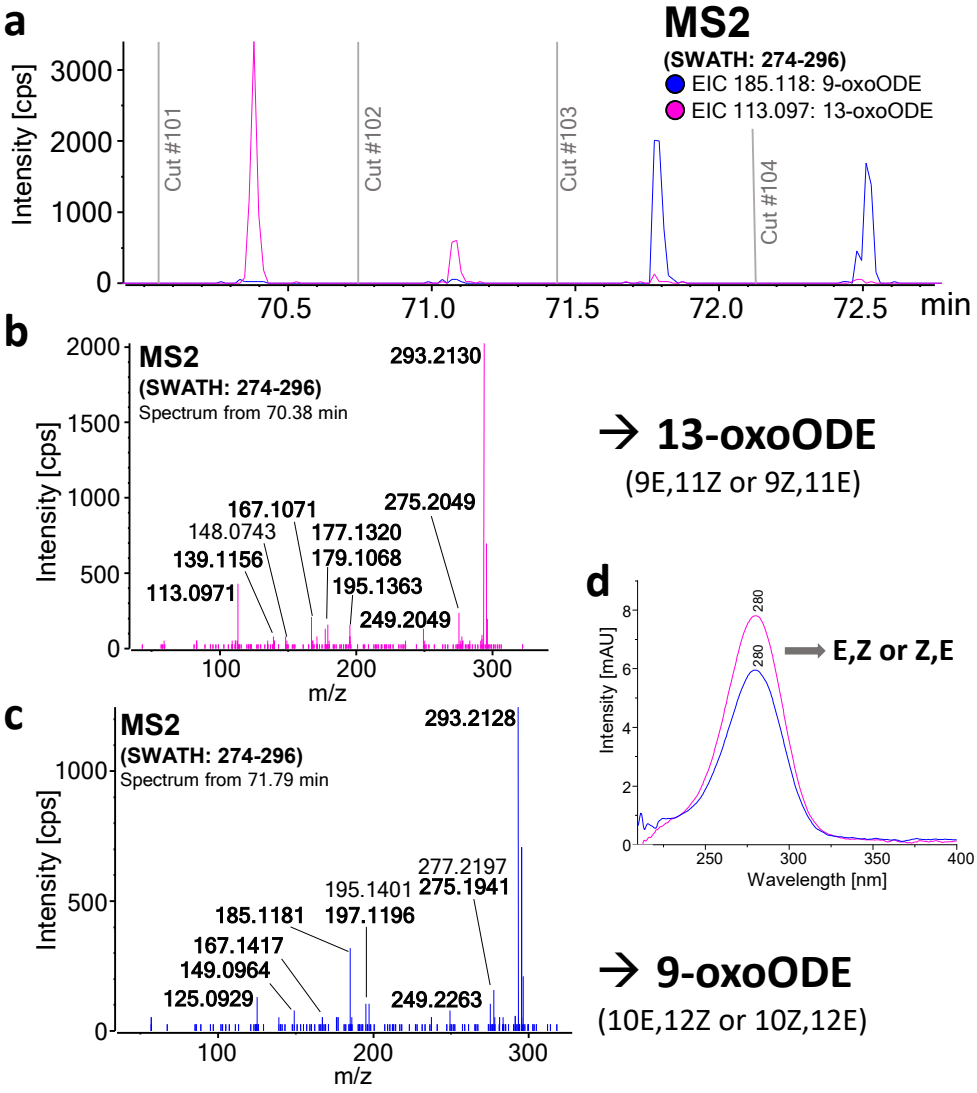

Figure 7: Differentiation of 9-oxoODE and 13-oxoODE by characteristic MS2-fragments; a: EIC from "characteristic" fragments of 9-oxoODE (m/z 185.118) and 13-oxoODE (m/z 113.097) in the SWATH-window (m/z 274-296); b: MS2-spectrum of 70.38 min, which could match the expectation of 13-oxoODE; c: MS2-spectrum of peak at 71.79 min, tentatively assigned as 9-oxoODE, bold MS2-fragments: matching reference spectrum from [50]; d: UV-spectra (characteristic for a conjugated diene with E,Z or Z,E-configuration [49]) of the respective peaks (for conditions see 3.1.4.4.3). MS2-spectra zoomed in.

The SWATH-approach opens up the possibility to generate EICs (extracted ion chromatograms) on MS2-level. This can be used to search for "characteristic" signature fragments that can originate from a subset of isomeric/isobaric compounds only, as shown in Figure 7 for the isomers 9- and 13-oxoODE (for 9-oxoODE the fragment with *m/z* 185 was used for the EIC since it has a higher intensity, although the EIC of the *m/z* 125 would be more specific). For example, in cut #104 (Figure 7a) the peak with *m/z* 185.118 at about 72.5 min (total run time) in the MS2 EIC

shows a second major peak eluting slightly later. As demonstrated in Figure 8, while the first peak can be tentatively annotated as 9-oxoODE, this second eluted peak features the fragment ion of *m/z* 171.103 which is characteristic for 9-HODE [50]. The MS1 EIC for the two peaks and the characteristic spectra provide additional experimental evidence for this tentative annotation. The MS2 EIC of *m/z* 171.103 is selective for 9-HODE and not showing a signal at the retention time of 9-oxoODE (Figure 8a). It is emphasized at this point once more that this structural annotation from an initial 2D-LC screening run is only tentative and needs verification due to several isomers and isobaric compounds giving similar fragment ions.

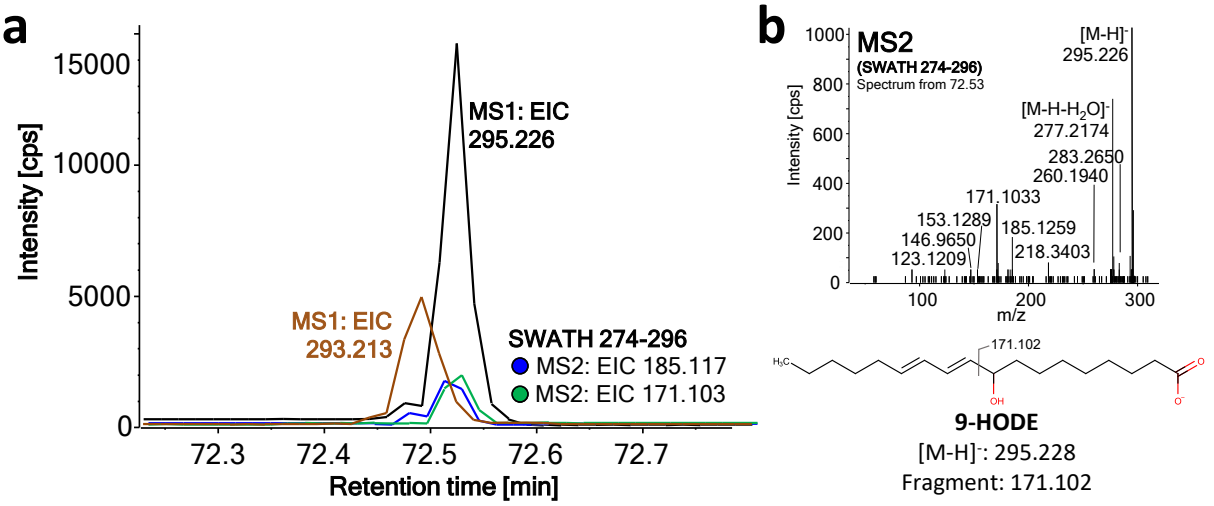

Figure 8: Differentiation and separation of compounds with M+2 isotopologue interference (retention time window of cut #104 from Figure 7); a: MS1 EICs from m/z 293.213 and 295.226, MS2 EICs from the corresponding fragments (m/z 185.117 was assigned to both precursors, while m/z 171.103 only matches the retention time of the precursor with m/z 295.226); b: MS2-spectra at retention time of m/z 295.226 matches the one of 9-HODE [50] (for conditions see 3.1.4.4.3). MS2-spectrum zoomed in.

Figure 9 again documents the advanced benefit of the current LC×LC analysis with combined DAD-UV and data-independent SWATH acquisition. In spite of chromatographic selectivity in two dimensions and high mass resolution (R~37,000) at the MS1 level, the 2D-contour plot generated for MS1 EIC of *m/z* 293.213 is still relatively overcrowded (Figure 9a). The several isomeric species cannot be distinguished at the MS1 level but are mostly chromatographically resolved. On the other hand, the 2D-contour plot generated for the MS2 EIC of *m/z* 113.098 (aligned with MS1 of *m/z* 293.213) is significantly less complex, hence the MS2 EIC is more selective. This fragment ion is characteristic for 13-oxoODE and not present in 9-oxoODE. The UV spectra provide additional information, for instance, that peak 5 belongs to the group of triene and is not a 9-oxoODE isomer (Figure 9b). The MS2 spectra (see Suppl. Figure S9) indicate that peaks 1, 2, 3 and 4 are contaminated with another precursor ion. For more selective analysis and to assign the fragment ions to the respective precursor ion requires reanalysis e.g. by MRM-HR acquisition

mode (not shown). Although this method was developed specifically for conjugated PUFAs and not optimized at all for oxidized lipids, it provides ample preliminary information about the oxidized lipid impurities of the complex E/Z isomer mixture of conjugated PUFAs. For exploiting the full potential of this analytical workflow for oxidized lipids, it must be specifically optimized for oxylipidomics, in particular the chromatographic conditions of the ^{2}D. This preliminary work should demonstrate the great potential and enhanced selectivity of this 2D-LC method.

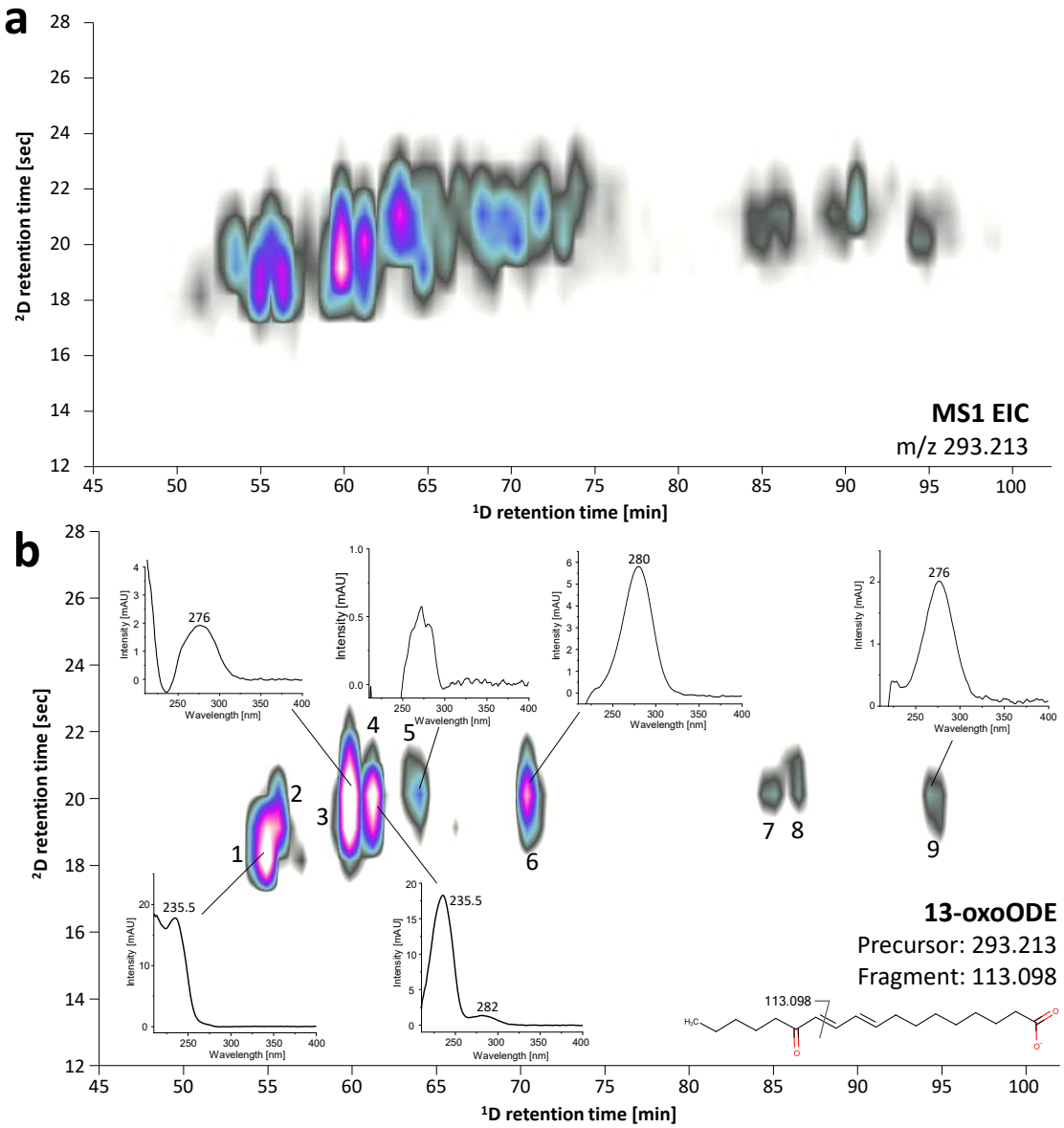

Figure 9: Contour-plots of the full-comprehensive chiral RP×RP 2D-LC-DAD-MS/MS measurement of the total mix; a: MS1-EIC of m/z 293.213 reduces the number of detected peaks significantly, when comparing with Figure 6; b: MS2-EIC filter of m/z 113.098 applied on MS1-precursor ions with m/z 293.213 further reduces the number of peaks; peak filtering of MS1-precursor (m/z 293.213) and the MS2-fragment has been done with MasterView, UV-spectra of the respective peaks are shown, MS2-spectra can be found in the supplementary Fig. S10 (for conditions see 3.1.4.4.3).

3.1.6 Conclusions

A growing number of lipid emulsion formulations are introduced into the pharmaceutical market. They are typically produced from a phospholipid raw material. One typical group of impurities of such pharmaceutical products are fatty acids which originate from hydrolysis of phospholipids. The corresponding polyunsaturated fatty acids can lead to conjugated and oxidized fatty acids as impurities that need to be controlled. Hence, the focus of this research was the development of a method for the comprehensive profiling of saturated, unsaturated (conjugated/unconjugated) and oxidized fatty acids without a derivatization step which could lead to sample-alterations and artefacts in impurity profiling. It was shown that chiral polysaccharide-based columns are able to separate most of the investigated cFA-isomers (amylose- better than cellulose-based columns), although those compounds are achiral. However, chiral columns do also often have enhanced selectivities for other isomers like constitutional isomers or π-diastereomers which was confirmed in this work. One-dimensional LC-methods are not able to sufficiently resolve co-elutions in complex mixtures. The combination of chiral columns (^{1}D) with reversed-phase columns (^{2}D) in a 2D-LC-setup is a powerful option to deal with such problems, since orthogonality and good compatibility of the two dimensions were observed, which is due to the operation of both dimensions under RP-conditions. The first dimension separated mainly isomeric structures, the second dimension separated the co-eluting groups based on number of double bonds and degree of oxidation. UV- and data-independent SWATH-MS-detection complement each other with orthogonal structural information, which makes the determination of conjugated chromophoric systems and double bond-configurations in cFAs as well as substitutions by functional groups feasible and the structural annotation of unknown impurities possible. The present 2D-LC methodology is currently extended to cover the wider (oxy)lipidome.

Conflict of interest statement

The authors declare that they have no known competing financial interest or personal relationships that could have appeared to influence the work reported in this paper.

Acknowledgements

We gratefully acknowledge the financial support of this research by Fresenius Kabi Deutschland GmbH. We are grateful to Agilent Technologies for support of this research by an Agilent Research Award (#4610).

3.1.7 References

[1] A.A. Hennessy, P.R. Ross, G.F. Fitzgerald, C. Stanton, Sources and Bioactive Properties of Conjugated Dietary Fatty Acids, Lipids 51(4) (2016) 377-397. https://doi.org/10.1007/s11745-016-4135-z.

[2] M. Gong, Y. Hu, W. Wei, Q. Jin, X. Wang, Production of conjugated fatty acids: A review of recent advances, Biotechnology Advances 37(8) (2019) 107454. https://doi.org/10.1016/j.biotechadv.2019.107454

[3] A. Mosblech, I. Feussner, I. Heilmann, Oxylipins: Structurally diverse metabolites from fatty acid oxidation, Plant Physiology and Biochemistry 47(6) (2009) 511-517. https://doi.org/10.1016/j.plaphy.2008.12.011.

[4] M. Cebo, X. Fu, M. Gawaz, M. Chatterjee, M. Lämmerhofer, Enantioselective ultra-high performance liquid chromatography-tandem mass spectrometry method based on sub-2µm particle polysaccharide column for chiral separation of oxylipins and its application for the analysis of autoxidized fatty acids and platelet releasates, Journal of Chromatography A 1624 (2020) 461206. https://doi.org/https://doi.org/10.1016/j.chroma.2020.461206.

[5] G. Dobson, Gas Chromatography-Mass Spectrometry of Conjugated Linoleic Acids and Metabolites, in: W.W.C. Jean-Louis Sébédio, Richard Adlof (Ed.), Advances in Conjugated Linoleic Acid Research, AOCS Press2003, pp. 13-36.

[6] J.A.G. Roach, M.M. Mossoba, M.P. Yurawecz, J.K.G. Kramer, Chromatographic separation and identification of conjugated linoleic acid isomers, Analytica Chimica Acta 465(1) (2002) 207-226. https://doi.org/10.1016/S0003-2670(02)00193-9.

[7] A. Lezerovich, Derivative UV spectra of lipid conjugated dienes, Journal of the American Oil Chemists' Society 63(7) (1986) 883-888. https://doi.org/10.1007/BF02540920.

[8] E. Angioni, G. Lercker, N. Frega, G. Carta, M. Melis, E. Murru, S. Spada, S. Banni, UV spectral properties of lipids as a tool for their identification, European Journal of Lipid Science and Technology 104 (2002) 59-64. https://doi.org/10.1002/1438-9312(200201)104:1<59::AID-EJLT59>3.0.CO;2-I.

[9] P. Delmonte, M.P. Yurawecz, M.M. Mossoba, C. Cruz-Hernandez, J.K.G. Kramer, Improved Identification of Conjugated Linoleic Acid Isomers Using Silver-Ion HPLC Separations, Journal of AOAC INTERNATIONAL 87(2) (2019) 563-568. https://doi.org/10.1093/jaoac/87.2.563.

[10] M. Wolter, X. Chen, U. Woiwode, C. Geibel, M. Lämmerhofer, Preparation and characterization of poly(3-mercaptopropyl)methylsiloxane functionalized silica particles and their further modification for silver ion chromatography and enantioselective high-performance liquid chromatography, Journal of Chromatography A 1643 (2021) 462069. https://doi.org/10.1016/j.chroma.2021.462069.

[11] I. Willenberg, A.I. Ostermann, N.H. Schebb, Targeted metabolomics of the arachidonic acid cascade: current state and challenges of LC–MS analysis of oxylipins, Analytical and

Bioanalytical Chemistry 407(10) (2015) 2675-2683. https://doi.org/10.1007/s00216-014-8369-4.

[12] M. Cebo, X. Fu, M. Gawaz, M. Chatterjee, M. Lämmerhofer, Micro-UHPLC-MS/MS method for analysis of oxylipins in plasma and platelets, Journal of Pharmaceutical and Biomedical Analysis 189 (2020) 113426. https://doi.org/10.1016/j.jpba.2020.113426.

[13] F. Ianni, G. Saluti, R. Galarini, S. Fiorito, R. Sardella, B. Natalini, Enantioselective high-performance liquid chromatography analysis of oxygenated polyunsaturated fatty acids, Free Radical Biology and Medicine 144 (2019) 35-54. https://doi.org/https://doi.org/10.1016/j.freeradbiomed.2019.04.038.

[14] K. Nishimura, T. Suzuki, S. Momchilova, K. Miyashita, E. Katsura, Y. Itabashi, Analysis of Conjugated Linoleic Acids as 9-Anthrylmethyl Esters by Reversed-Phase High-Performance Liquid Chromatography with Fluorescence Detection, Journal of chromatographic science 43 (2005) 494-9. https://doi.org/10.1093/chromsci/43.9.494.

[15] F. Ianni, F. Blasi, D. Giusepponi, A. Coletti, F. Galli, B. Chankvetadze, R. Galarini, R. Sardella, Liquid chromatography separation of α- and γ-linolenic acid positional isomers with a stationary phase based on covalently immobilized cellulose tris(3,5-dichlorophenylcarbamate), Journal of Chromatography A 1609 (2020) 460461. https://doi.org/10.1016/j.chroma.2019.460461.

[16] B.W.J. Pirok, D.R. Stoll, P.J. Schoenmakers, Recent Developments in Two-Dimensional Liquid Chromatography: Fundamental Improvements for Practical Applications, Analytical Chemistry 91(1) (2019) 240-263. https://doi.org/10.1021/acs.analchem.8b04841.

[17] B.W.J. Pirok, A.F.G. Gargano, P.J. Schoenmakers, Optimizing separations in online comprehensive two-dimensional liquid chromatography, Journal of Separation Science 41(1) (2018) 68-98. https://doi.org/10.1002/jssc.201700863.

[18] D.R. Stoll, P.W. Carr, Two-Dimensional Liquid Chromatography: A State of the Art Tutorial, Analytical Chemistry 89(1) (2017) 519-531. https://doi.org/10.1021/acs.analchem.6b03506.

[19] E. Lazaridi, H.-G. Janssen, J.-P. Vincken, B. Pirok, M. Hennebelle, A comprehensive two-dimensional liquid chromatography method for the simultaneous separation of lipid species and their oxidation products, Journal of Chromatography A 1644 (2021) 462106. https://doi.org/10.1016/j.chroma.2021.462106.

[20] P.O. Helmer, M.M. Nicolai, V. Schwantes, J. Bornhorst, H. Hayen, Investigation of cardiolipin oxidation products as a new endpoint for oxidative stress in C. elegans by means of online two-dimensional liquid chromatography and high-resolution mass spectrometry, Free Radical Biology and Medicine 162 (2021) 216-224. https://doi.org/10.1016/j.freeradbiomed.2020.10.019.

[21] P. Dugo, T. Kumm, M.L. Crupi, A. Cotroneo, L. Mondello, Comprehensive two-dimensional liquid chromatography combined with mass spectrometric detection in the analyses of triacylglycerols in natural lipidic matrixes, Journal of Chromatography A 1112(1) (2006) 269-275. https://doi.org/10.1016/j.chroma.2005.10.070.

[22] E.J.C. van der Klift, G. Vivó-Truyols, F.W. Claassen, F.L. van Holthoon, T.A. van Beek, Comprehensive two-dimensional liquid chromatography with ultraviolet, evaporative light scattering and mass spectrometric detection of triacylglycerols in corn oil, Journal of Chromatography A 1178(1) (2008) 43-55. https://doi.org/10.1016/j.chroma.2007.11.039.

[23] P. Arena, D. Sciarrone, P. Dugo, P. Donato, L. Mondello, Pattern-Type Separation of Triacylglycerols by Silver Thiolate×Non-Aqueous Reversed Phase Comprehensive Liquid Chromatography, Separations 8(6) (2021) 88. https://doi.org/10.3390/separations8060088.

[24] E.L. Regalado, I.A. Haidar Ahmad, R. Bennett, V. D'Atri, A.A. Makarov, G.R. Humphrey, I. Mangion, D. Guillarme, The Emergence of Universal Chromatographic Methods in the Research and Development of New Drug Substances, Accounts of Chemical Research 52(7) (2019) 1990-2002. https://doi.org/10.1021/acs.accounts.9b00068.

[25] K. Zhang, Y. Li, M. Tsang, N.P. Chetwyn, Analysis of pharmaceutical impurities using multi-heartcutting 2D LC coupled with UV-charged aerosol MS detection, Journal of Separation Science 36(18) (2013) 2986-2992. https://doi.org/10.1002/jssc.201300493.

[26] M. Pursch, S. Buckenmaier, Loop-Based Multiple Heart-Cutting Two-Dimensional Liquid Chromatography for Target Analysis in Complex Matrices, Analytical Chemistry 87(10) (2015) 5310-5317. https://doi.org/10.1021/acs.analchem.5b00492.

[27] P. Dugo, F. Cacciola, T. Kumm, G. Dugo, L. Mondello, Comprehensive multidimensional liquid chromatography: Theory and applications, Journal of Chromatography A 1184(1) (2008) 353-368. https://doi.org/10.1016/j.chroma.2007.06.074.

[28] W.C. Byrdwell, H.K. Kotapati, R. Goldschmidt, P. Jakubec, L. Nováková, Three-dimensional liquid chromatography with parallel second dimensions and quadruple parallel mass spectrometry for adult/infant formula analysis, Journal of Chromatography A 1661 (2022) 462682. https://doi.org/10.1016/j.chroma.2021.462682.

[29] T. Cajka, O. Fiehn, Increasing lipidomic coverage by selecting optimal mobile-phase modifiers in LC–MS of blood plasma, Metabolomics 12(2) (2016) 34. https://doi.org/10.1007/s11306-015-0929-x.

[30] M. Igarashi, T. Miyazawa, Newly recognized cytotoxic effect of conjugated trienoic fatty acids on cultured human tumor cells, Cancer Letters 148(2) (2000) 173-179. https://doi.org/10.1007/s11745-001-0746-0.

[31] H. Ozaki, Y. Nakano, H. Sakamaki, H. Yamanaka, M. Nakai, Basic eluent for rapid and comprehensive analysis of fatty acid isomers using reversed-phase high performance liquid chromatography/Fourier transform mass spectrometry, Journal of Chromatography A 1585 (2019) 113-120. https://doi.org/10.1016/j.chroma.2018.11.057.

[32] H. Tsugawa, T. Cajka, T. Kind, Y. Ma, B. Higgins, K. Ikeda, M. Kanazawa, J. VanderGheynst, O. Fiehn, M. Arita, MS-DIAL: data-independent MS/MS deconvolution for comprehensive metabolome analysis, Nature Methods 12(6) (2015) 523-526. https://doi.org/10.1038/nmeth.3393.

[33] M. Cebo, C. Calderón Castro, J. Schlotterbeck, M. Gawaz, M. Chatterjee, M. Lämmerhofer, Untargeted UHPLC-ESI-QTOF-MS/MS analysis with targeted feature

extraction at precursor and fragment level for profiling of the platelet lipidome with ex vivo thrombin-activation, Journal of Pharmaceutical and Biomedical Analysis 205 (2021) 114301. https://doi.org/10.1016/j.jpba.2021.114301.

[34] S. Strohschein, M. Pursch, D. Lubda, K. Albert, Shape Selectivity of C30 Phases for RP-HPLC Separation of Tocopherol Isomers and Correlation with MAS NMR Data from Suspended Stationary Phases, Analytical Chemistry 70(1) (1998) 13-18. https://doi.org/10.1021/ac970414j.

[35] L.C. Sander, C.A. Rimmer, W.B. Wilson, Characterization of triacontyl (C-30) liquid chromatographic columns, J Chromatogr A 1614 (2020) 460732. https://doi.org/10.1016/j.chroma.2019.460732.

[36] X. Chen, C. Yamamoto, Y. Okamoto, Polysaccharide derivatives as useful chiral stationary phases in high-performance liquid chromatography, Pure and Applied Chemistry 79(9) (2007) 1561-1573. https://doi.org/10.1351/pac200779091561.

[37] R.B. Kasat, S.Y. Wee, J.X. Loh, N.-H.L. Wang, E.I. Franses, Effect of the solute molecular structure on its enantioresolution on cellulose tris(3,5-dimethylphenylcarbamate), Journal of Chromatography B 875(1) (2008) 81-92. https://doi.org/10.1016/j.jchromb.2008.06.045.

[38] M. Lämmerhofer, Chiral recognition by enantioselective liquid chromatography: Mechanisms and modern chiral stationary phases, Journal of Chromatography A 1217(6) (2010) 814-856. https://doi.org/10.1016/j.chroma.2009.10.022.

[39] E. Yashima, C. Yamamoto, Y. Okamoto, NMR Studies of Chiral Discrimination Relevant to the Liquid Chromatographic Enantioseparation by a Cellulose Phenylcarbamate Derivative, Journal of the American Chemical Society 118(17) (1996) 4036-4048. https://doi.org/10.1021/ja960050x.

[40] C.Y. Hopkins, M.J. Chisholm, A survey of the conjugated fatty acids of seed oils, Journal of the American Oil Chemists Society 45(3) (1968) 176-182. https://doi.org/10.1007/BF02915346.

[41] S. Banni, A. Petroni, M. Blasevich, G. Carta, E. Angioni, E. Murru, B.W. Day, M.P. Melis, S. Spada, C. Ip, Detection of conjugated C16 PUFAs in rat tissues as possible partial beta-oxidation products of naturally occurring conjugated linoleic acid and its metabolites, Biochimica et Biophysica Acta (BBA) - Molecular and Cell Biology of Lipids 1682(1) (2004) 120-127. https://doi.org/10.1016/j.bbalip.2004.03.003.

[42] M. Gilar, P. Olivova, A.E. Daly, J.C. Gebler, Orthogonality of Separation in Two-Dimensional Liquid Chromatography, Analytical Chemistry 77(19) (2005) 6426-6434. https://doi.org/10.1021/ac050923i.

[43] M. Gilar, J. Fridrich, M.R. Schure, A. Jaworski, Comparison of Orthogonality Estimation Methods for the Two-Dimensional Separations of Peptides, Analytical Chemistry 84(20) (2012) 8722-8732. https://doi.org/10.1021/ac3020214.

[44] G. Derringer, R. Suich, Simultaneous Optimization of Several Response Variables, Journal of Quality Technology 12(4) (1980) 214-219. https://doi.org/10.1080/00224065.1980.11980968.

[45] C. West, J. Ogden, E. Lesellier, Possibility of predicting separations in supercritical fluid chromatography with the solvation parameter model, Journal of Chromatography A 1216(29) (2009) 5600-5607. https://doi.org/10.1016/j.chroma.2009.05.059.

[46] B.G. Anderson, A. Raskind, H. Habra, R.T. Kennedy, C.R. Evans, Modifying Chromatography Conditions for Improved Unknown Feature Identification in Untargeted Metabolomics, Analytical Chemistry 93(48) (2021) 15840-15849. https://doi.org/10.1021/acs.analchem.1c02149.

[47] R. Karongo, M. Ge, C. Geibel, J. Horak, M. Lämmerhofer, Enantioselective multiple heart cutting online two-dimensional liquid chromatography-mass spectrometry of all proteinogenic amino acids with second dimension chiral separations in one-minute time scales on a chiral tandem column, Analytica Chimica Acta 1180 (2021) 338858. https://doi.org/https://doi.org/10.1016/j.aca.2021.338858.

[48] M. Raetz, R. Bonner, G. Hopfgartner, SWATH-MS for metabolomics and lipidomics: critical aspects of qualitative and quantitative analysis, Metabolomics 16(6) (2020) 71. https://doi.org/10.1007/s11306-020-01692-0.

[49] C. Xia, J. Deng, Y. Pan, C. Lin, Y. Zhu, Z. Xiang, W. Li, J. Chen, Y. Zhang, B. Zhu, Q. Huang, Comprehensive Profiling of Macamides and Fatty Acid Derivatives in Maca with Different Postharvest Drying Processes Using UPLC-QTOF-MS, ACS Omega 6(38) (2021) 24484-24492. https://doi.org/10.1021/acsomega.1c02926.

[50] R.C. Murphy, Fatty Acids, Tandem Mass Spectrometry of Lipids: Molecular Analysis of Complex Lipids, The Royal Society of Chemistry2015, pp. 1-39. https://doi.org/10.1039/9781782626350-00001.

[51] Z.-X. Yuan, S.I. Rapoport, S.J. Soldin, A.T. Remaley, A.Y. Taha, M. Kellom, J. Gu, M. Sampson, C.E. Ramsden, Identification and profiling of targeted oxidized linoleic acid metabolites in rat plasma by quadrupole time-of-flight mass spectrometry, Biomedical Chromatography 27(4) (2013) 422-432. https://doi.org/10.1002/bmc.2809.

3.1.8 Supplementary information

Table S1 Summary of the used fatty acid standards, their abbreviations and suppliers. CLA: conjugated linoleic acid; CLNA: conjugated linolenic acid

	Name		Abbreviation	Supplier
Unconjugated fatty acids	Stearic Acid	C18:0	Stearic	Merck (Darmstadt, Germany)
	Oleic Acid	C18:1 (ω-9)	OA	Fluka Chemie (Steinheim, Germany)
	Linoleic Acid	C18:2 (ω-6)	LA	Sigma-Aldrich (Merck; Darmstadt, Germany)
	α-Linolenic Acid	C18:3 (ω-3)	ALA	
	γ-Linolenic Acid	C18:3 (ω-6)	GLA	Cayman Chemical Company (USA)
	Stearidonic Acid	C18:4 (ω-3)	SA	
	Arachidonic Acid	C20:4 (ω-6)	AA	Sigma-Aldrich (Merck; Darmstadt, Germany)
Conjugated fatty acids	Mangold´s Acid	C18:2 (9E,11E)	MA	Cayman Chemical Company (Ann Arbor, Michigan, USA)
	Rumenic Acid	C18:2 (9Z,11E)	RuA	
	Ricinenic Acid	C18:2 (9Z,11Z)	RA	
	10E,12Z-Octadecadienoic Acid	C18:2 (10E,12Z)	10E,12Z-CLA	
	α-Eleostearic Acid	C18:3 (9Z,11E,13E)	AEA	Biozol (Eching, Germany)
	β-Eleostearic Acid	C18:3 (9E,11E,13E)	BEA	Cayman Chemical Company (Ann Arbor, Michigan, USA)
	Catalpic Acid	C18:3 (9E,11E,13Z)	CA	Biozol (Eching, Germany)
	Punicic Acid	C18:3 (9Z,11E,13Z)	PA	
	9Z,11Z,13Z-Octadecatrienoic Acid	C18:3 (9Z,11Z,13Z)	ZZZ-CLNA	
	α-Calendic Acid	C18:3 (8E,10E,12Z)	ACA	
	Jacaric Acid	C18:3 (8Z,10E,12Z)	JA	
	cis-Parinaric Acid	C18:4 (9Z,11E,13E,15Z)	CPAR	Cayman Chemical Company (Ann Arbor, Michigan, USA)
	trans-Parinaric Acid	C18:4 (9E,11E,13E,15E)	TPAR	

Table S2 Composition of the mixtures used for the initial column screening including the investigated concentrations

Mix	Name	DB-Pos.	Configuration	Concentration
Triene	Punicic Acid	9,11,13	ZEZ	500 ng/mL
	Catalpic Acid		EEZ	500 ng/mL
	alpha-Eleostearic Acid		ZEE	500 ng/mL
	beta-Eleostearic Acid		EEE	500 ng/mL
	ZZZ-CLNA		ZZZ	2000 ng/mL
Diene	Rumenic Acid	9,11	ZE	1250 ng/mL
	Mangolds Acid		EE	1250 ng/mL
	Ricinenic Acid		ZZ	1250 ng/mL
	10E,12Z-CLA	10,12	EZ	1250 ng/mL
FA	Oleic Acid	9	Z	200 µg/mL
	Linoleic Acid	9,12	ZZ	50 µg/mL
	alpha-Linolenic Acid	9,12,15	ZZZ	100 µg/mL
	gamma-Linolenic Acid	6,9,12	ZZZ	40 µg/mL
	Stearidonic Acid	6,9,12,15	ZZZZ	10 µg/mL
Positional	alpha-Calendic Acid	8,10,12	EEZ	500 ng/mL
	Jacaric Acid		ZEZ	500 ng/mL
	Catalpic Acid	9,11,13	EEZ	500 ng/mL
	Punicic Acid		ZEZ	500 ng/mL
Tetraene	cis-Parinaric Acid	9,11,13,15	ZEEZ	50 µg/mL
	trans-Parinaric Acid	9,11,13,15	EEEE	1 µg/mL

Table S3 Composition and concentrations of the individual fatty acids of the total FA mix, used for the method development

Compound	DB-Pos.	Configuration	Concentration [µg/mL]
Punicic Acid	9,11,13	ZEZ	0.50
Catalpic Acid		EEZ	0.50
alpha-Eleostearic Acid		ZEE	0.50
beta-Eleostearic Acid		EEE	0.50
ZZZ-CLNA		ZZZ	2.00
Rumenic Acid	9,11	ZE	1.25
Mangolds Acid		EE	1.25
Ricinenic Acid		ZZ	1.25
10E,12Z-CLA	10,12	EZ	1.25
Oleic Acid	9	Z	200.00
Linoleic Acid	9,12	ZZ	50.00
alpha-Linolenic Acid	9,12,15	ZZZ	100.00
gamma-Linolenic Acid	6,9,12	ZZZ	40.00
Stearidonic Acid	6,9,12,15	ZZZZ	10.00
alpha-Calendic Acid	8,10,12	EEZ	0.50
Jacaric Acid		ZEZ	0.50
cis-Parinaric Acid	9,11,13,15	ZEEZ	5.00
trans-Parinaric Acid	9,11,13,15	EEEE	0.20

Table S4 Number of MS experiments and used SWATH-windows for the isolation and fragmentation of the compounds in the *m/z* range of the respective SWATH window

Experiment	MS Type	Min *m/z*	Max *m/z*
0	SCAN	35	1000
1	SWATH	50	170
2	SWATH	169	191
3	SWATH	190	212
4	SWATH	211	233
5	SWATH	232	254
6	SWATH	253	275
7	SWATH	274	296
8	SWATH	295	317
9	SWATH	316	338
10	SWATH	337	359
11	SWATH	358	380
12	SWATH	379	401
13	SWATH	400	422
14	SWATH	421	443
15	SWATH	442	464
16	SWATH	463	485
17	SWATH	484	506
18	SWATH	505	600
19	SWATH	599	700

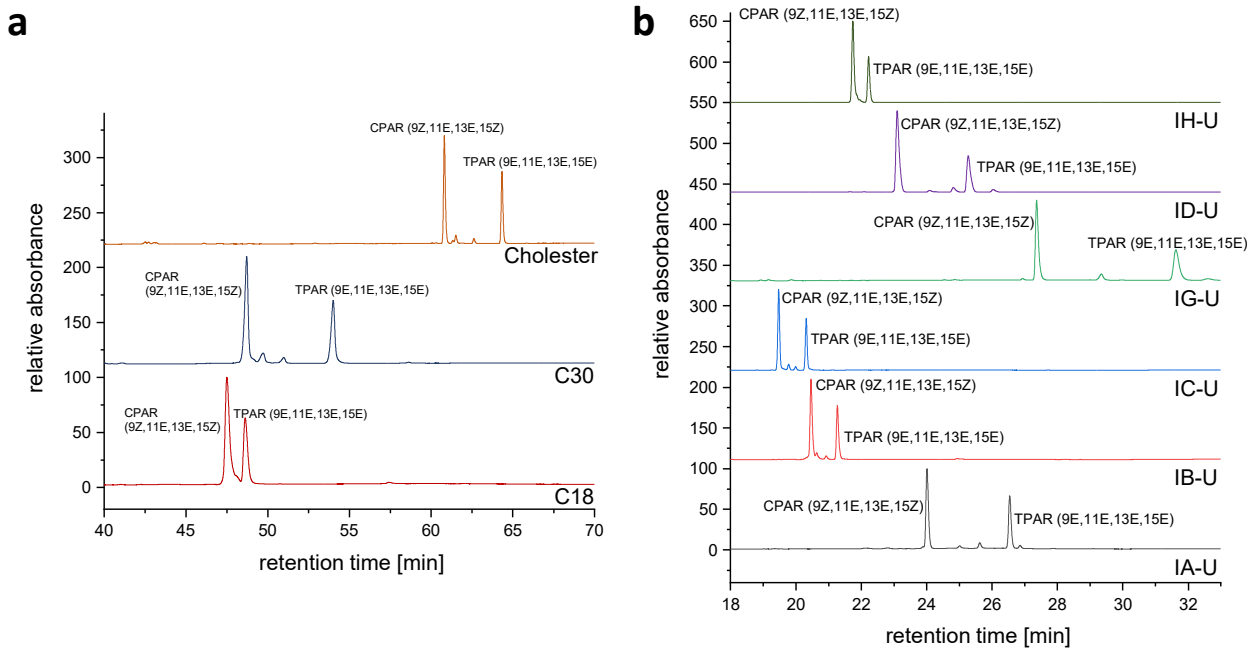

Figure S1 Chromatograms of the tetraene mix from the column screening, a: RP-columns, b: chiral columns (for conditions see 3.1.4.4.1).

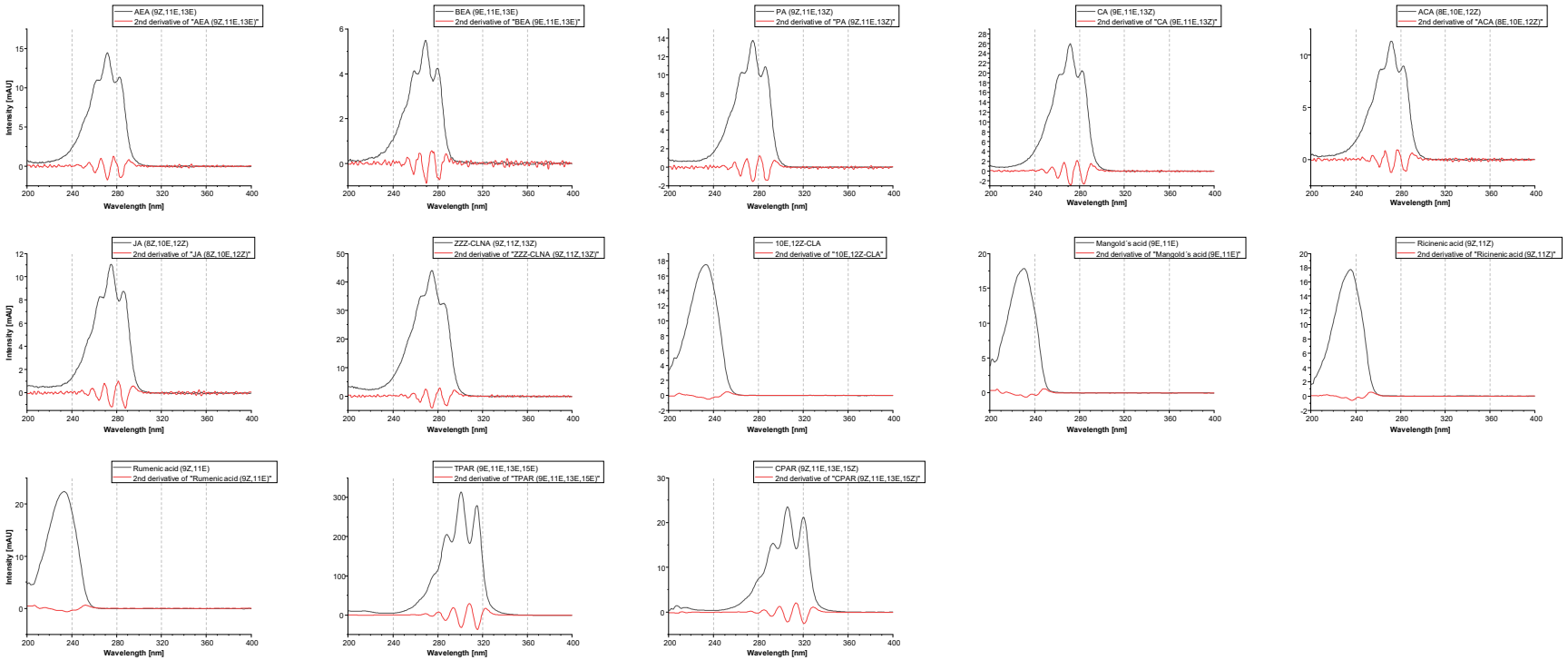

Figure S2 UV-spectra of the conjugated triene, diene and tetraene standards and their second derivation (smoothed)

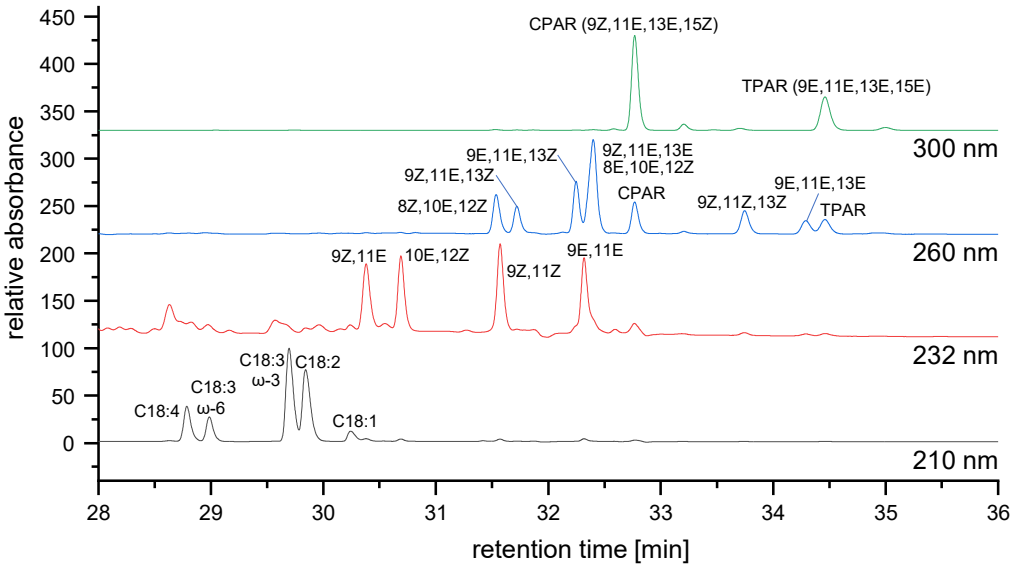

Figure S3 Chromatogram of the total mix with the final method using the IG-U-column (for conditions see 3.1.4.4.2)

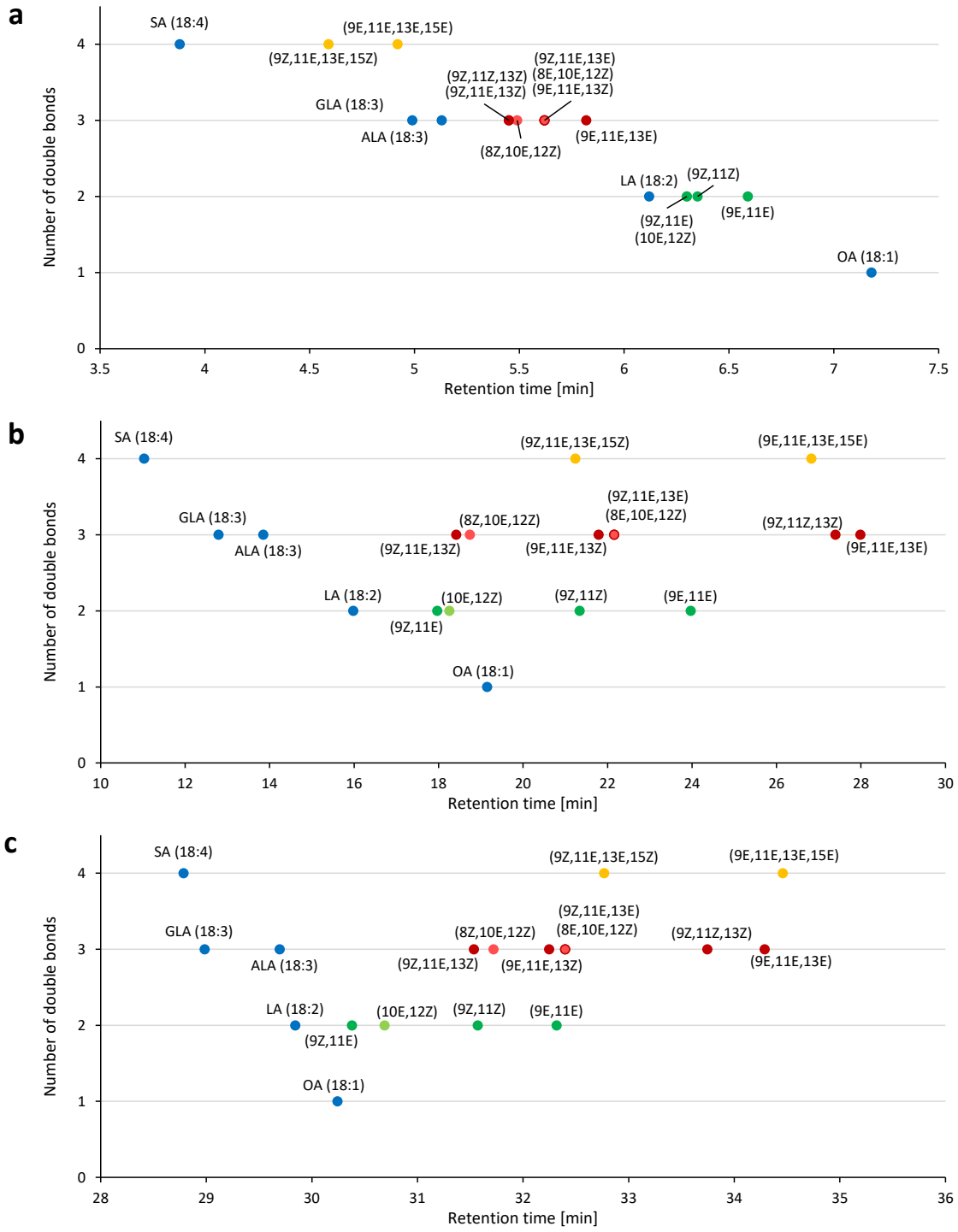

Figure S4 Schematic representation of the retention times in dependence of the DB number of the compounds in the total FA mix using the final optimized 1D-LC method of the respective column; a: Acquity CSH C18, b: Chiralpak IA-U, c: Chiralpak IG-U; blue: unconjugated FAs, green: conjugated dienes, red: conjugated trienes, yellow: conjugated tetraenes (for conditions see 3.1.4.4.2)

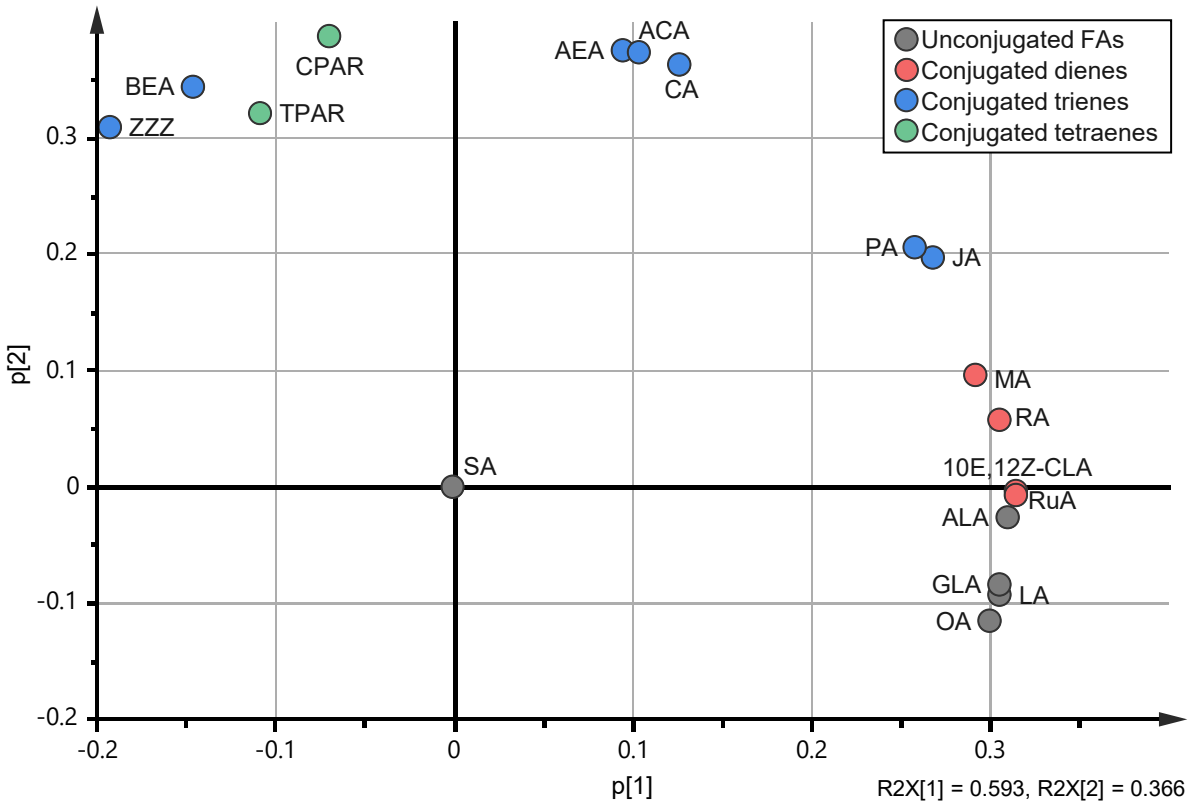

Figure S5 Loadings plot of the principal component analysis (PCA) performed with SIMCA. Retention time data set of the column screening was normalized according to Gilar et al. [1].

Table S5 Orthogonality values, based on the column screening, calculations made as described by Gilar et al. [1]. Maximal orthogonality that can be achieved (18 occupied bins, since 18 analytes were used) is 82.5 %.

Orthogonality [%]		¹D columns								
		IA-U	IB-U	IC-U	IG-U	ID-U	IH-U	Prontosil C18	Prontosil C30	Cholester
²D columns	IA-U	0.0%	31.8%	31.8%	12.7%	0.0%	31.8%	38.1%	44.4%	44.4%
	IB-U	31.8%	-6.4%	0.0%	25.4%	31.8%	6.4%	25.4%	6.4%	19.1%
	IC-U	31.8%	0.0%	0.0%	31.8%	38.1%	6.4%	25.4%	6.4%	19.1%
	IG-U	12.7%	25.4%	31.8%	0.0%	19.1%	31.8%	38.1%	38.1%	38.1%
	ID-U	6.4%	31.8%	38.1%	19.1%	0.0%	31.8%	44.4%	50.8%	50.8%
	IH-U	31.8%	6.4%	6.4%	31.8%	38.1%	0.0%	25.4%	19.1%	12.7%
	Prontosil C18	38.1%	25.4%	25.4%	38.1%	44.4%	19.1%	0.0%	25.4%	19.1%
	Prontosil C30	44.4%	6.4%	6.4%	38.1%	50.8%	19.1%	25.4%	0.0%	19.1%
	Cholester	44.4%	19.1%	19.1%	38.1%	50.8%	12.7%	19.1%	19.0%	0.0%

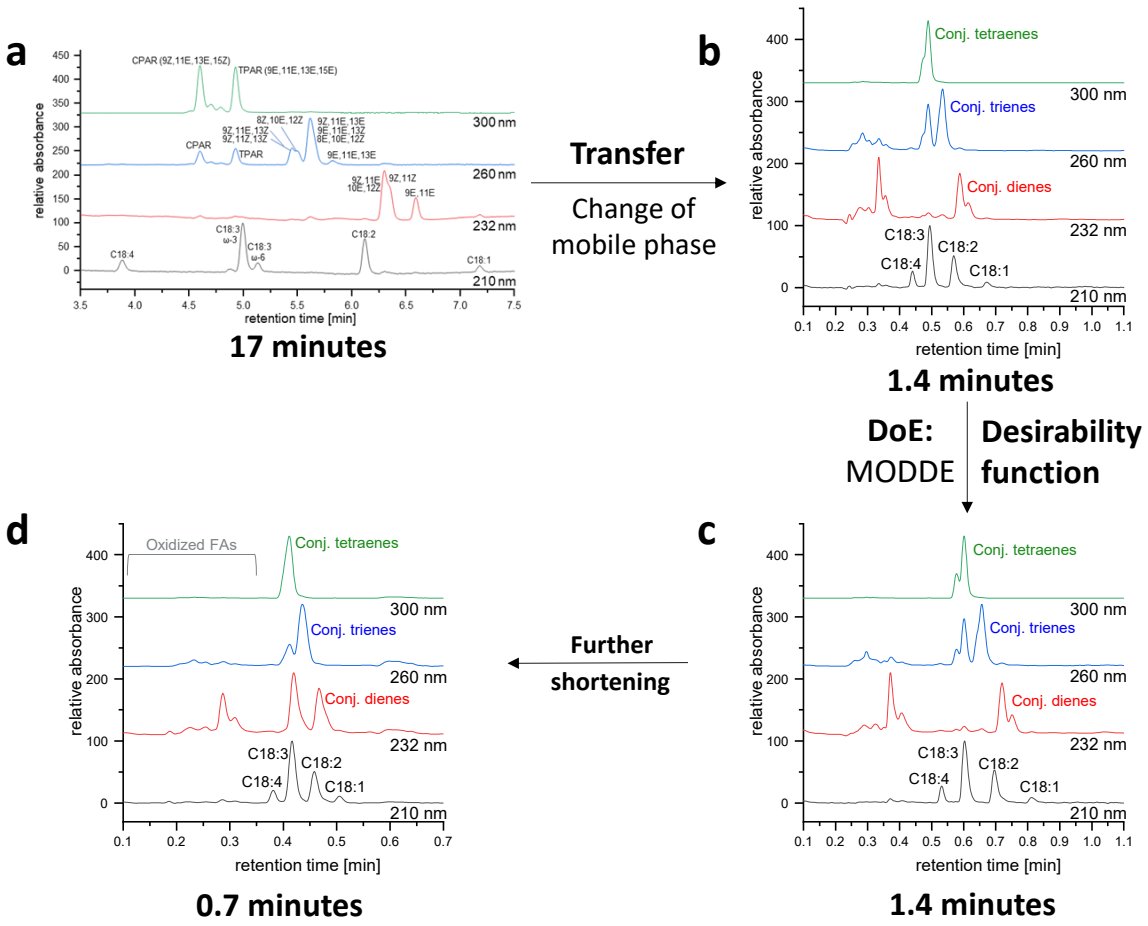

Figure S6 Workflow applied for the development of a short second (reversed phase) dimension, starting with the original one-dimensional method (a).

The starting method (Figure S6a, see 3.1.4.4.2) was transferred to the shorter column (Acquity UPLC CSH C18, 30 x 3 mm, 1.7 µm) and the mobile phase was exchanged to achieve a focusing with mobile phase A in the beginning of the method and to reduce the elution strength of mobile phase B (Figure S6b; for mobile phases see final method in 3.1.4.4.3 of the main document). Afterwards design of experiment using MODDE was employed for optimization of the factors: percentage of organic modifier in mobile phase A (5 %, 10 %, 20 %), step to X% B (50, 60, 70, 80) and injection volume (20µL, 40µL, 60µL). The following responses were observed: number of peaks, resolution, elution during gradient. Responses were converted with Derringer´s desirability function and added to total-desirability (ranging from 0 to 1, where 1 is the most desirable event). The chromatogram using the most desirable method is shown in Figure S6c (20 % organic in mobile phase A, step to 60 % mobile phase B, 40 µL injection volume. This resulting method was further shortened to achieve a total analysis time of 0.7 min in the 2D (Figure S6d).

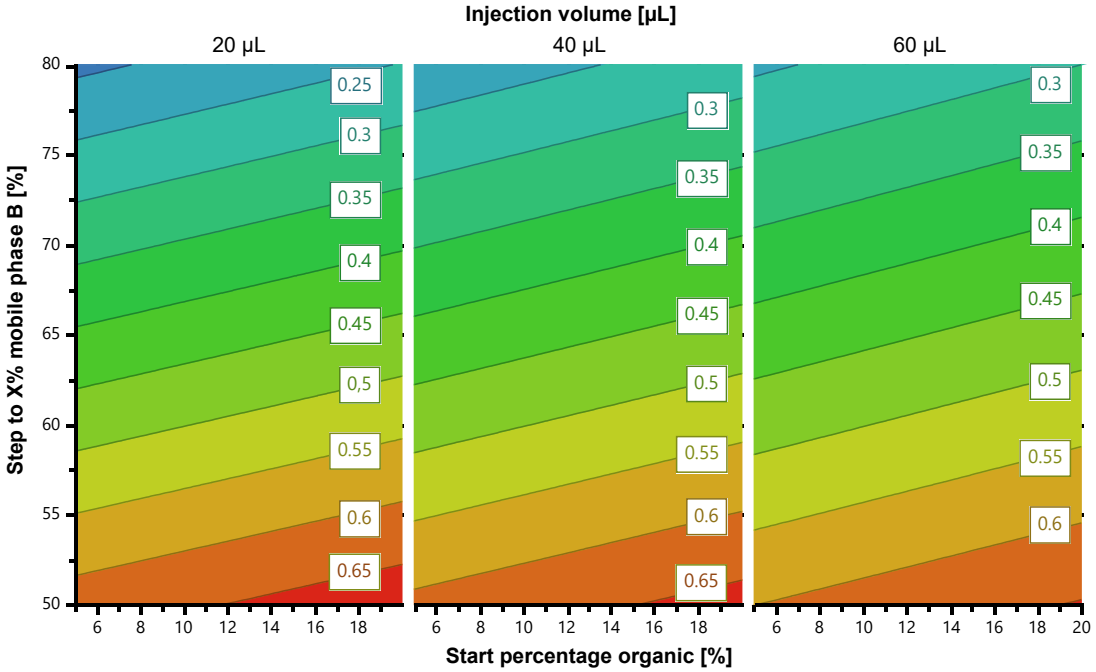

Figure S7 Visualization of the total-desirability with MODDE; factors: Start with X% organic (5 %, 10 %, 20 %), Step to X% B (50 %, 60 %, 70 %, 80 %), Injection volume (20 µL, 40 µL, 60 µL); responses: total desirability.

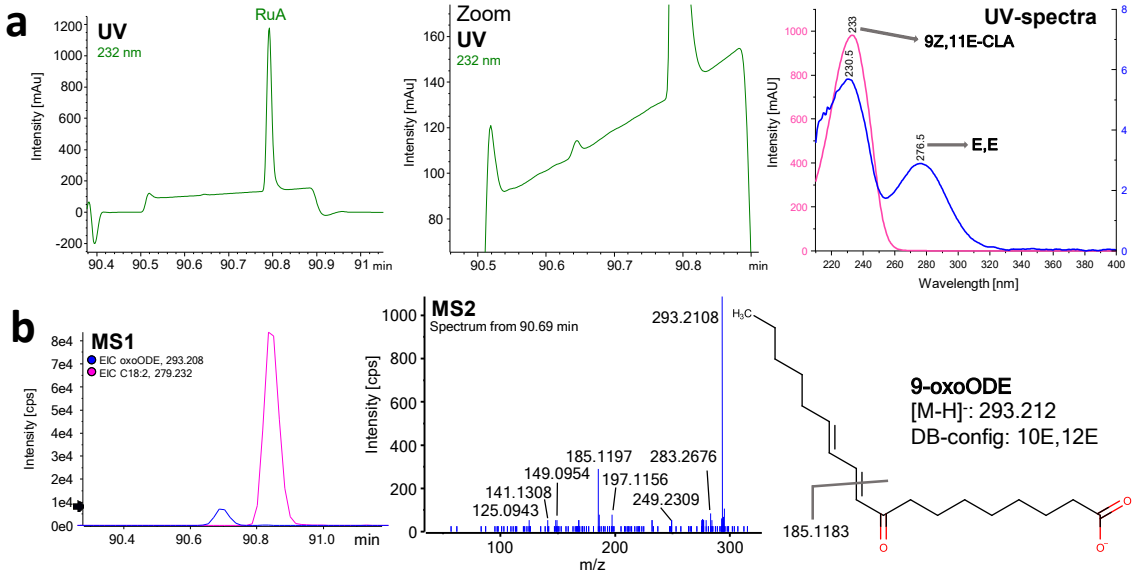

Figure S8 Workflow for the tentative structural annotations of 9-oxoODE (10E,12E); a: UV-signal from DAD at 232 nm and the respective UV-spectra (pink: rumenic acid, blue: unknown oxidation product); b: MS1-EIC from rumenic acid and the precursor ion of the unknown, MS2-spectrum from peak-maximum of the unknown (SWATH 274-296), structural formula of 9-oxoODE (10E,12E). UV-maximum from Xia et al. [2]; for conditions see 3.1.4.4.3 in the main document. MS2-spectrum zoomed in.

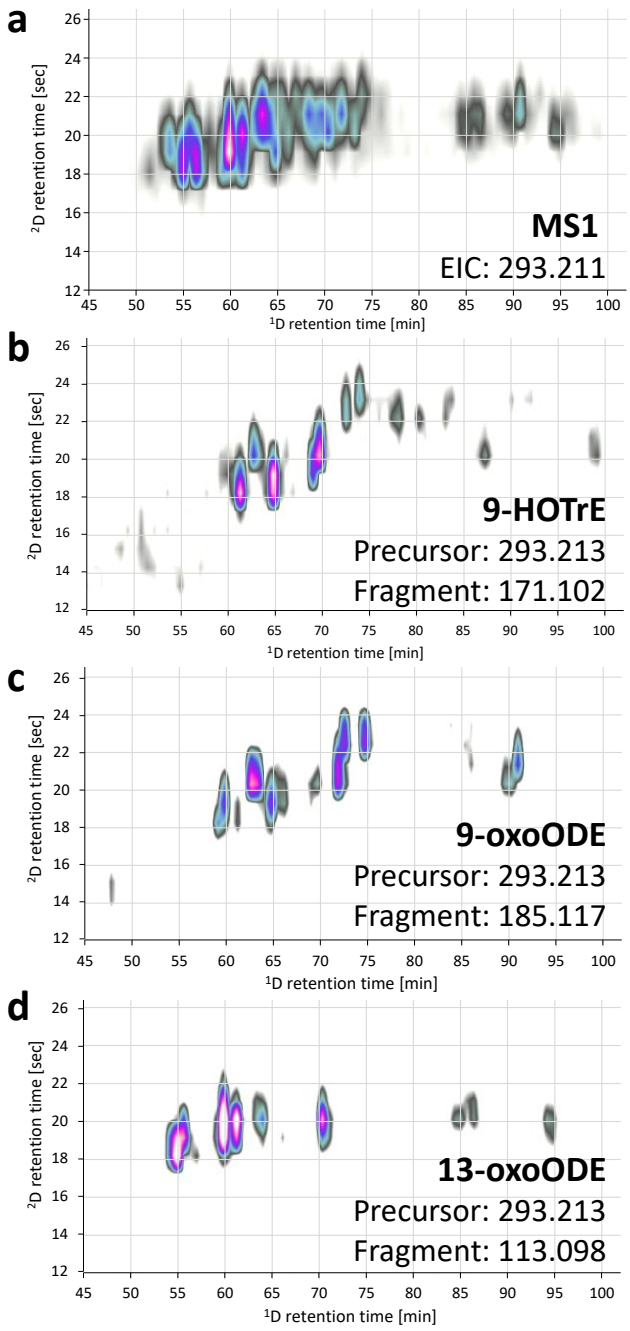

Figure S9 Contour plots of the full-comprehensive 2D-LC-DAD-MS/MS measurement of the total mix at MS1 level (a) and with tentative annotations of 9-HOTrE (b), 9-oxoODE (c), and 13-oxoODE (d). a: MS1 EIC from the precursor with *m/z* 293.211 shows a large number of peaks; peak picking by filtering of characteristic precursor and fragment ions using MasterView further delimits the number of peaks and allows a straightforward tentative identification of the unknown peaks (see b, c, d). Although differences between the three plots (b, c, d) are clearly visible, some of the peaks exist in more than one of the plots. This can either be a result of co-elution (since the method is yet not optimized for oxidized FAs) or the "characteristic" fragments can result from multiple isobaric compounds with the same precursor.

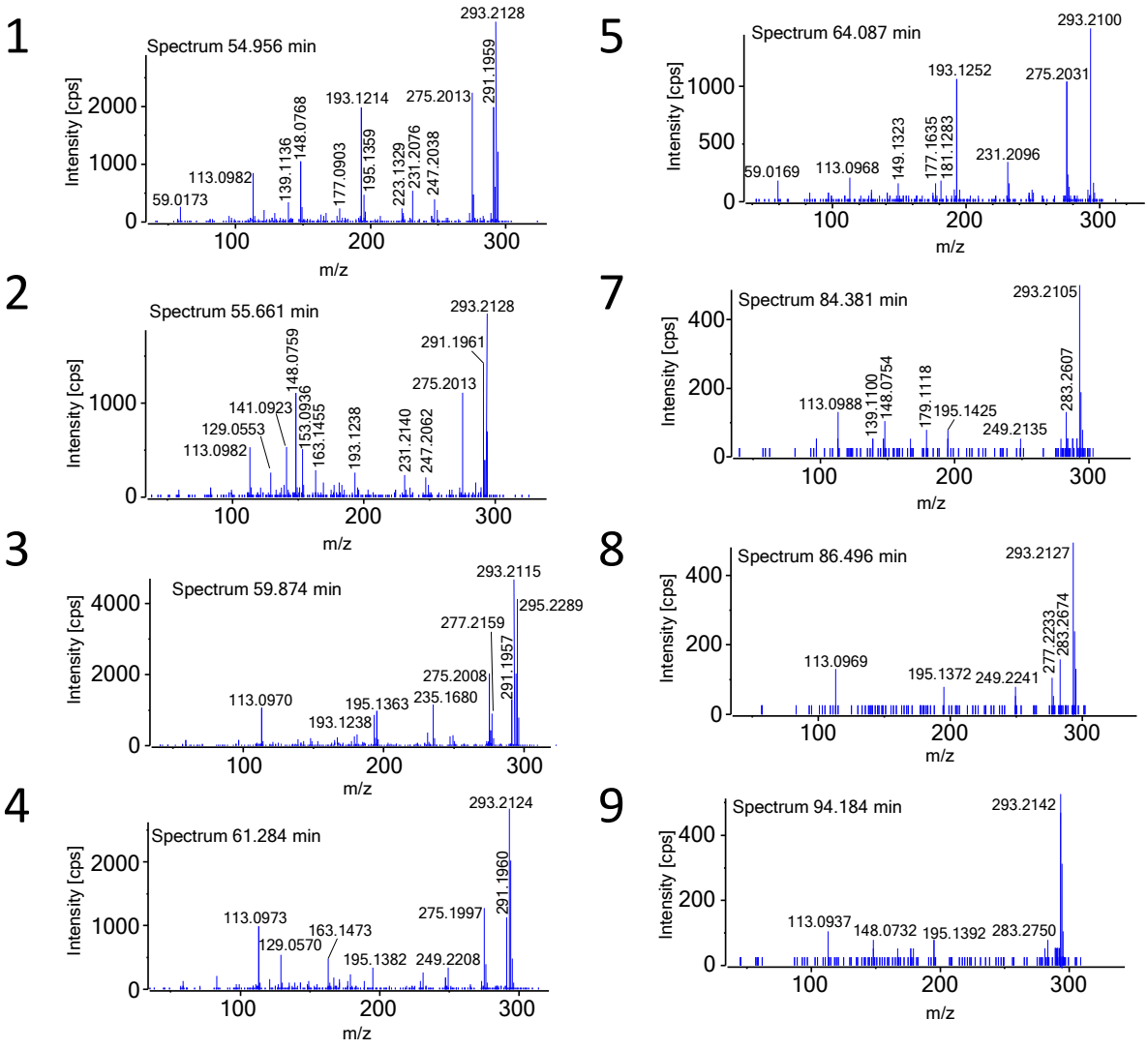

Figure S10 MS2 spectra from the peaks shown in Figure 11 of the main document. Some of the here displayed spectra represent composite spectra (1,2,3, and 4) from two or three precursors. Precursors: spectrum 1: *m/z* 291.196, 293.213; spectrum 2: *m/z* 291.196, 293.211; spectrum 3: *m/z* 291.196, 293.212, 295.229; spectrum 4: *m/z* 291.196, 293.212; spectrum 5: *m/z* 293.210; spectrum 6: *m/z* 293.213 (see Figure 9b of main document); spectrum 7: *m/z* 293.213; spectrum 8: *m/z* 293.214. All spectra are zoomed in.

3.1.8.1 References

[1] M. Gilar, P. Olivova, A.E. Daly, J.C. Gebler, Orthogonality of Separation in Two-Dimensional Liquid Chromatography, Analytical Chemistry 77(19) (2005) 6426-6434. https://doi.org/10.1021/ac050923i.

[2] C. Xia, J. Deng, Y. Pan, C. Lin, Y. Zhu, Z. Xiang, W. Li, J. Chen, Y. Zhang, B. Zhu, Q. Huang, Comprehensive Profiling of Macamides and Fatty Acid Derivatives in Maca with Different Postharvest Drying Processes Using UPLC-QTOF-MS, ACS Omega 6(38) (2021) 24484-24492. https://doi.org/10.1021/acsomega.1c02926.

3.2 Publication II

Branched medium-chain fatty acid profiling and enantiomer separation of anteiso-forms of teicoplanin fatty acyl side chain RS3 using UHPLC-MS/MS with polysaccharide columns

Christian Geibel[1], Matthias Olfert[1], Cornelius Knappe, Kristian Serafimov, Michael Lämmerhofer*

Institute of Pharmaceutical Sciences, Pharmaceutical (Bio-)Analysis, University of Tübingen, Auf der Morgenstelle 8, 72076 Tübingen, Germany

[1] These authors contributed equally

* Author for correspondence:
Prof. Dr. Michael Lämmerhofer
michael.laemmerhofer@uni-tuebingen.de

This article was published in Journal of Pharmaceutical and Biopharmaceutical Analysis, Volume 224 (2023), DOI: 10.1016/j.jpba.2022.115162

3.2.1 Abstract

This work reports on targeted UHPLC-tandem mass spectrometry methods for the chiral separation of *anteiso*-methyl branched fatty acids (*ai*FAs). The methods involve precolumn derivatization with 1-naphthylamine and chiral separation on Chiralpak IG-U. *anteiso*-Methyl branched fatty acids with up to eight carbons can be separated. A method was used for the assignment of the absolute configuration of an *ai*FA present as fatty acyl residue of the teicoplanin mixture, namely teicoplanin RS3. Furthermore, the excellent methylene selectivity and improved selectivity for constitutional isomers of the polysaccharide columns was exploited for the elucidation and structural confirmation of previously unknown fatty acyl residues in teicoplanin. This shows the versatility and practical applicability of polysaccharide columns as orthogonal stationary phases to reversed-phase for structural elucidation of natural compounds. The developed methods are useful tools for related subdisciplines such as targeted metabolomics and lipidomics.

3.2.2 Introduction

Teicoplanin is a glycopeptide antibiotic that is bactericide in the treatment of gram-positive bacteria, being effective among others against Clostridium difficile and methicillin-resistant Staphylococcus aureus (MRSA). It inhibits the cell wall synthesis by interfering in the late-stage synthesis, namely by inhibiting murein (peptidoglycan) synthesis [1]. It shares its mode of action as well as its general chemical structure with vancomycin. Biosynthetically, teicoplanin is generated from the bacterium *Actinoplanes teichomyceticus* [2]. Of note, teicoplanin is not a single substance, but a mixture of multiple substances (Fig. 1) which can be classified into three subgroups with the major subgroup being the A2 group. In the approved drug, this group comprises at least 80% of the total component, while the subgroup A3 must be less than 15% according to the Ph. Eur. Minor related substances, assigned by RS, are abundant up to 5% according to European Medicines Agency (EMA) [3]. As can be seen from Fig.1, teicoplanin features besides the glycopeptide core structure N-acetyl and N-acyl moieties on two distinct glucosamine residues, the latter revealing distinct chain lengths mainly responsible for its molecular dispersity. Of vital importance is the fatty acid residue which was shown to have impact on the antibacterial efficiency [4]. Two substances of the A2 group show chiral fatty acid moieties due to methyl branching, namely the major compound teicoplanin A2-4 (8-methyldecanoic acid) and the minor compound teicoplanin RS3 (6-methyloctanoic acid). On the contrary, all other compounds are either linear or *iso*-branched, thus achiral. Despite being in clinical use since 1984 (respectively 1988 in Germany) [5] after its first description in 1978 [2], the chirality of those side-

chains have to our knowledge not been determined up to now. In general, however, the determination or assignment of absolute configurations should be part of a full structure elucidation of natural compounds.

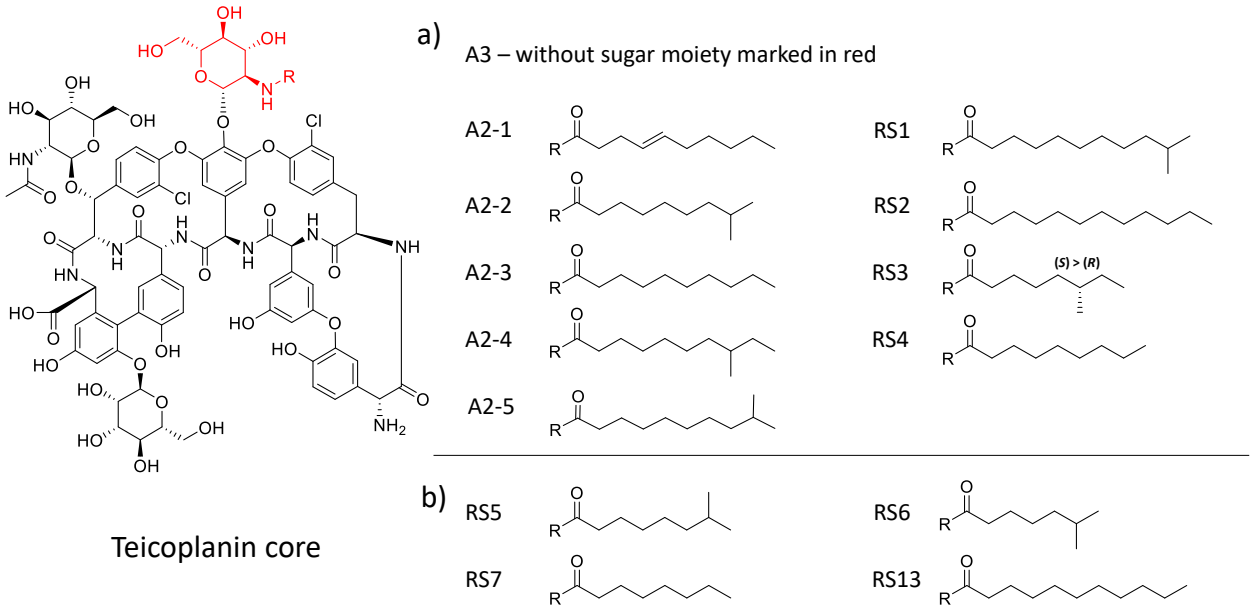

Fig. 1: Molecular diversity of Teicoplanin which consists of a variety of structural analogues with the same core but distinct fatty acyl residues. The core consists of the peptide aglycon and carries 3 carbohydrate residues, an α-D-mannose, a N-acetyl–β-D-glucosamine and the N-acyl–β-D-glucosamine indicated in red which is missing in teicoplanin A3 but is present in all other teicoplanin subspecies which differ in their N-acyl residue (R) of this glucosamine (shown on the right in a) and b)). The fatty acyl structures depicted in a) were elucidated already earlier, but were lacking the description of the chirality (in the case of A2-4 and RS3). The fatty acyl residues shown in b) are the newly confirmed minor substances discussed in this work. Nomenclature follows the suggestion of Ref. [13].

For this reason, we develop herein a new enantioselective UHPLC-MS/MS method based on sub-2µm polysaccharide-type chiral stationary phases (CSPs) for methyl-branched fatty acid enantiomer separation. We recently published a work for the systematic separation of branched short-chain fatty acids as 1-naphthylamine derivatives on chiral polysaccharide phases [6] (based on prior work which was mainly focused on the LC separation of N-protected amino acids, arylpropionic acids and phenoxypropionic acids as 1-naphthylamine derivatives [7]). Fatty acids with a length up to eight carbon atoms (octanoic acid) and branching between the second to fourth carbon atom were successfully separated. The longest *anteiso*-fatty acid, thus carrying the branching on the penultimate carbon atom, was 4-methylhexanoic acid, that was successfully separated into enantiomers. As the carbon chain gets longer and the methyl-branching moves farther away from the tentative primary interaction site of the analyte, i.e. the naphthylamide group, the baseline separation of the enantiomers becomes more challenging. Hence, herein we extend our previous enantioselective UHPLC method for the longer *anteiso*-fatty acids which are part of teicoplanin RS3. Existing methods for chiral separation of medium or long chain *anteiso*-

FAs usually either indirect enantiomer separation methods with chiral derivatization agent in LC [8, 9] or are gas chromatographic methods [10, 11]. Besides, the separation of constitutional isomers of these branched fatty acids (FAs), i.e. between *anteiso*-, *iso*-, and n-FAs, should be evaluated in the present work. Recently, new minor compounds have been discovered in teicoplanin (based on HRMS-analysis of the intact teicoplanin molecule), but were structurally not fully elucidated [12, 13]. It was raised the question whether they are due to other, hitherto unknown, fatty acyl residues which should be clarified in this work as well. Our work is based on new sub-2µm polysaccharide derivatives immobilized on silica support. These polysaccharide phases were introduced by Okamoto and coworkers in 1984 [14-16] and are the most widely used chiral stationary phases for LC enantiomer separations. Recently, various publications showed their exceptional applicability in lipidomics [17-20]. To this end, the current work should widen its scope of application in isomer selective metabolomics, introducing a new targeted lipidomics assay for fatty acid profiling and give important information on the composition of teicoplanin fatty acyl residues.

3.2.3 Experimental

3.2.3.1 Materials

Teicoplanin (order number T0578), magnesium turnings, copper bromide, ammonium chloride, sodium hydroxide, hydrochloric acid, 2-propanol (technical), (S)-(+)-1-bromo-2-methylbutane, toluene (anhydrous), N-methyl-2-pyrrolidone, 1-naphthylamine, N-ethyl-N'-(3-dimethylamino-propyl)carbodiimide (EDC) and n-undecanoic acid were supplied by Sigma Aldrich (Merck, Munich, Germany). Racemic 6-methyloctanoic acid, racemic 8-methyldecanoic acid, n-octanoic acid, n-nonanoic acid, 6-methylheptanoic acid, 7-methyloctanoic acid, ethyl 4-bromobutanoate and ethyl 6-bromohexanoate were purchased by BLD Pharm (Kaiserslautern, Germany). Acetonitrile (ACN) (MS grade) was purchased from Carl Roth (Karlsruhe, Germany). Purified water for MS measurements was produced by Elga Purelab Ultra system (Celle, Germany).

3.2.3.2 Instrumentation

Pretests were run on an Agilent 1260 LC system from Agilent Technologies (Waldbronn, Germany), equipped with a quaternary pump, a degasser, an autosampler and a UV-DAD detector. LC-MS/MS experiments were performed by an Agilent 1290 Infinity UHPLC system equipped with a binary pump with included degasser and a column oven, coupled to a CTC PAL HTC autosampler (CTC Analytics AG, Zwingen, CH) hyphenated to an API 4000 triple quadrupole mass spectrometer with TurboIonSpray (SCIEX, Concord, Ontario, Canada). High resolution mass spectrometry analysis was performed using a TripleToF 5600+ mass spectrometer with a TurboIonSpray Source (SCIEX, Concord, Ontario, Canada) which was coupled to an Agilent 1290 Infinity I UHPLC system and a PAL-HTX xt DLW autosampler (CTC Analytics). Chiral columns Chiralpak IA-U, IB-U, IC-U, ID-U, IG-U and IH-U (1.6 µm fully porous particles) from Daicel (Osaka/Tokyo, Japan) were supplied by Chiral Technologies Europe (Illkirch, France) and had the dimensions of 3.0 x 100 mm (i.d. x l.).

3.2.3.3 Synthesis of enantiopure (S)-6-methyloctanoic acid

Enantiopure standard substance for the assignment of the elution order was synthesized in a modified form of the procedure reported previously [21]. The standards was prepared from (2*S*)-1-bromo-2-methylbutane and ethyl 4-bromobutanoate by a Cu-catalyzed cross-coupling reactions with Grignard's reagents. THF was distilled over sodium and *N*-methyl-2-pyrrolidone over phosphorus pentoxide. Both were stored over a 5Å molecular sieve. Under vacuum/argon atmosphere in a Schlenk line, to 48 mg (2 mmol) of Mg turnings in dry THF (0.72 g), 250 mg (1.655 mmol) of (*S*)-1-bromo-2-methylbutane was added dropwise at 30°C. After 3 hours, the

resultant mixture was added dropwise to a mixture of ethyl 4-bromobutanoate (1.38 mmol; 269.17 mg) and CuBr (5 mg, 0.034 mmol) in *N*-methyl-2-pyrrolidone (547 mg, 5.52 mmol) and stirred for 3 h at 10 °C. After quenching with aqueous ammonium chloride (20% aq.), the product was extracted with hexane. After evaporation to dryness, the residue was reconstituted in 5 mL THF, 5 mL NaOH (20% aq.) added, and the mixture refluxed for 5 h. Afterwards, the aqueous layer was separated and acidified with 1 M HCl and extracted with hexane. The product was then concentrated under reduced pressure and not further purified.

(S)-6-Methyloctanoic acid ($C_9H_{18}O_2$): HRMS: calculated (negative mode, $[M-H]^-$): *m/z* 157.1234, found: *m/z* 157.1244. ^{1}H NMR ($CDCl_3$, 400 MHz): δ 0.84 (3H, d, *J* = 6.4), 0.86 (3H, t, *J* = 7.3), 1.06 – 1.18 (2H, m), 1.25 – 1.40 (5H, m), 1.57 – 1.67 (2H, m), 2.36 (2H, t, *J* = 7.5), 10.6 (1H, broad); ^{13}C NMR ($CDCl_3$, 100 MHz): δ 11.59, 19.35, 25.22, 26.78, 29.64, 34.19, 34.43, 36.37, 179.70. Purity > 95%.

3.2.3.4 Derivatization

Derivatization was performed as described in Ref. [6] and depicted in Fig. 2. The respective fatty acid (0.31 mmol), 1-naphthylamine (0.42 mmol), and EDC (0.42 mmol) were dissolved in 1 ml 2-propanol and allowed to react on a shaker at 30°C for 16 h. Afterwards, the product was dried in a high-performance evaporator (Genevac EZ2, Ipswich, UK). The resulting 1-naphthylamide derivative was reconstituted in ACN to a concentration of 1 mg/mL. For MS measurements, this product was diluted 1:100.000 in MS-grade ACN.

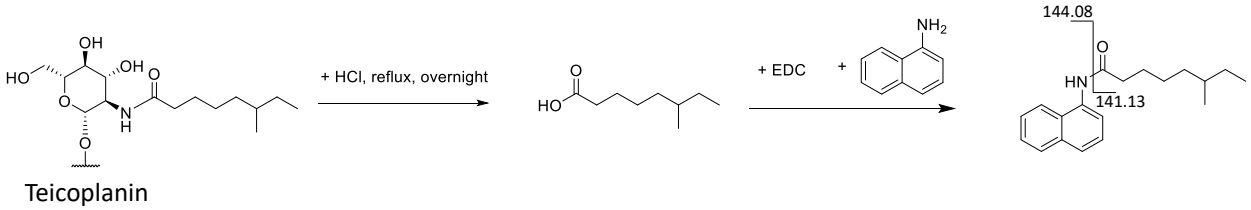

Fig. 2: Exemplary workflow of acyl moiety hydrolysis (in this case: teicoplanin RS3) and derivatization of the fatty acid using EDC and 1-naphthylamine. The cut in the product indicates the found fragments in MS, with 144.08 being the tag for all derivatized carboxylic acids.

3.2.3.5 Hydrolysis and isolation of fatty acid residues from teicoplanin

To release the fatty acid residues from teicoplanin, 50 mg of teicoplanin were dissolved in 5 mL 6N HCl. The mixture was left under stirring and boiling at reflux overnight. Afterwards, the mixture was allowed to cool down to room temperature. Subsequently a liquid-liquid extraction using 5 mL hexane was performed twice to extract the free fatty acids into the organic phase. The organic solvent was evaporated and derivatized as described in section 3.2.3.4.

3.2.3.6 Separation methods

Fatty acids with 8 carbon atoms C8 (n-octanoic acid FA 8:0, 6-methylheptanoic acid FA 7:0;6Me) and 9 carbon atoms, C9 (n-nonanoic acid FA 9:0, 7-methyloctanoic acid FA 8:0;7Me, 6-methyloctanoic acid FA 8:0;6Me) were either separated on a Chiralpak IB-U (achiral separation for fatty acid profiling) or on a Chiralpak IG-U (chiral separation of FA 8:0;6Me). Conditions for runs on Chiralpak IB-U were as follows: 0°C, flow rate 0.2 mL/min, Mobile phase A: water containing 0.1% (v/v) acetic acid, mobile phase B: ACN containing 0.1% (v/v) acetic acid. Gradient profile: 0.00 min: 55.0% B, 60.00 min: 60% B, 60.01 min 55.0% B. Conditions for chiral profiling of FA 8:0;6Me on Chiralpak IG-U were as follows: 0°C, flow rate 0.15 mL/min, Mobile phase A: water containing 0.1% (v/v) acetic acid, mobile phase B: ACN containing 0.1% (v/v) acetic acid. Gradient profile: 0.00 min: 70.0% B, 60.00 min: 85% B, 60.01 min 100% B, 70.00 min: 100% B, 70.01 min: 70.0% .MS detection with QqQ was run in multiple reaction monitoring (MRM) mode with transitions *m/z* 270.2 → 144.1 (FA 8:0 and isomers) and *m/z* 284.2 → 144.1 (FA 9:0 and isomers). Ion source parameters (for all experiments) were as follows: nebulizer gas (GS1) 50 psi, heater gas (GS2) 40 psi, curtain gas (CUR) 30 psi, temperature (TEM) 450°C, ion source voltage 5500 V, collision energy (CE) in MS2 was 30 V, declustering potential (DP) 80V.

Chromatographic separation for fatty acids with 11 carbon atoms C11 (n-undecanoic acid FA 11:0, 8-methyldecanoic acid FA 10:0;8Me) was performed on a Chiralpak IA-U at 0°C at a flow rate of 0.2 mL/min. Mobile phase A: water with 0.1% (v/v) acetic acid, mobile phase B: ACN with 0.1% (v/v) acetic acid. Gradient: 0.00 min: 90.0% B, 60.00 min: 100% B, 80.0 min: 100% B, 80.01 min: 90.0% B. MS was run in multiple reaction monitoring (MRM) mode with transition *m/z* 312.2 → 144.1 (C11). For ion source settings, see above. Achiral separation for the assignment of n-undecanoic acid was performed on a Chiralpak IA-U column at 20°C at a flow rate of 0.2 mL/min. Mobile phase A: water containing 0.1% (v/v) acetic acid, mobile phase B: ACN containing 0.1% (v/v) acetic acid. Gradient: 0.00 min: 10.0% B, 45.0 min: 90.0% B, 60.0 min: 90.0% B, 60.01 min 10.0% B, MRM transition *m/z* 312.2 → 144.1. For ion source settings, see above. Injection volume in all samples was 2.5 µL. MS was run in positive mode only. All chromatograms were gaussian smoothed (20.0 pt).

3.2.4 Results and discussion

3.2.4.1 Chiral separation and absolute configuration assignment of the fatty acyl side chain (6-methyloctanoic acid) of teicoplanin RS3

Racemic 6-methyldecanoic acid could be baseline separated after derivatization using the Chiralpak IG-U column (Fig. 3) using the method mentioned in section 3.2.3.6. Hereby, an elution order of R before S could be determined (Fig. 3a) by injecting racemic 6-methyloctanoic acid standard (black trace), synthesized (S)-6-methyloctanoic acid reference (blue trace) and rac-6-methyloctanoic acid spiked with the S-enantiomer (red trace). Cellulose with its almost linear β(1 → 4) glycosidic bonds resulting in a left-handed helicity of 3/2 was previously shown to exhibit excellent separation abilities for short and medium chain branched fatty acids [23, 24], while amylose shows a stronger left-handed helicity (helicity of 4/3 as effect of the α(1 → 4) glycosidic bonds [16, 22]) – which appears to be detrimental for the S/MCBFAs. Amylose based columns seem to have beneficial separation abilities for longer branched fatty acids. Interestingly, the injection of fatty acyl residue isolated from teicoplanin (Fig. 3b, purple trace) showed presence of both enantiomers of 6-methyloctanoic acid, but the S-form in significant excess. Injection of a corresponding sample spiked with racemate (green trace) and with the S-form (orange trace) confirmed that the 6-methyloctanoic acid residue in teicoplanin RS3 has primarily S configuration and to less extent R-enantiomer. This is in line with the expectation, as feeding of isoleucine led to a higher yield of the *anteiso*-fatty acid bearing teicoplanin A2-4, the feeding of leucine to a higher yield of the *iso*-fatty acid bearing derivative A2-5 [25]. Since L-Isoleucine carries S configuration in the side chain at the methyl branching position, teicoplanin RS3 was expected to be in S-configuration, if it is derived from the branched chain amino acid, Ile. The peak eluting shortly before the R peak of FA 8:0;6Me could be identified to be the achiral FA 8:0;7Me. Interestingly, the elution pattern differs here from the elution pattern on the cellulose based IB-U column as shown in Fig. 5. This indicates once again the difficulty of elution pattern prediction of polysaccharide phases as underlying interaction mechanisms between analyte and stationary phase are complex and not yet fully elucidated. While the elution pattern strictly followed the *ai*<i<n-FA pattern in shorter fatty acids (C6) using IG-U [6], this seems not to be valid for longer fatty acids (C9) as shown here – this could be an effect either of the longer carbon chain or of the lower temperature used in this case.

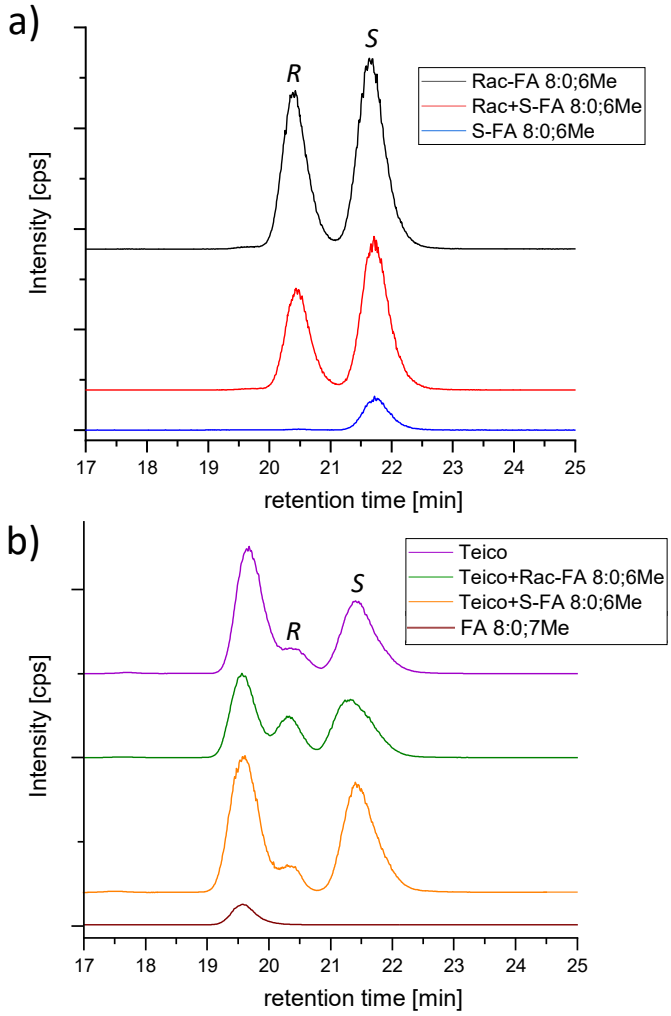

Fig. 3: Determination of the absolute configuration of the branched fatty acyl residue of Teicoplanin RS3 (as 1-naphthylamine derivative). (a) 6-Methyloctanoic acid standards (*rac*, *S*, *rac* spiked with *S*) and (b) isolated FA from Teicoplanin RS3 as well as spike with *rac* and *S*-enantiomer of 6-methyloctanoic acid and standard of 7-methyloctanoic acid. Experimental conditions: Chiralpak IG-U at 0°C (flow rate: 0.15 mL/min, for gradient: see section 3.2.3.6). Elution order could be determined to be *R* before *S*, (see blue trace, *S* enantiomer and black trace, racemate as well as red trace, racemate + *S* enantiomer). FA residue of Teicoplanin RS3 (purple trace) reveals to be of mostly *S* configuration, which could be confirmed by spiking experiments with racemic 6-methyloctanoic acid (green trace) and the *S* enantiomer (orange trace). The first eluting peak in all chromatograms displayed in b) could be shown to be 7-methyloctanoic acid (dark red trace).

Teicoplanin uses the tailoring of acyl moieties for the anchoring of itself into the membrane of gram-positive bacterium [26, 27], and the hydrophobic acyl chain was found to be responsible for the increased antibiotic potency of teicoplanin in comparison to vancomycin and for a reduced likelihood of resistances against teicoplanin [28]. Biosynthetically, an N-acetylglucosamine is connected with the teicoplanin A3, which, after deacetylation, will be armed with a new fatty acid [27]. Here, the acyltransferase gene orf (open reading frame) 11, the acyl-CoA synthetase gene orf13 and the type II thioesterase gene orf30 seem to be responsible for the biosynthesis and linkage of the fatty acid [29, 30]. In this step, different lengths of acyl chains are possible, with

preference of the acyltransferase for carbon chain lengths of C10 – C12, but also shorter and longer carbon chains are possible extending this window to C6 – C14; they can fit the binding requisites and be built in to transform the glycopeptide into a lipoglycopeptide [31]. It was found in this work that shorter acyl chains lower the antibiotic potency, whilst no statement about the chirality of the branched fatty acid side chain was made. Interestingly, it could be shown that teicoplanin RS3 is neither only S configurated nor racemic, but exhibits a small but significant amount of R. The origin of the small amount of R configuration in RS3 is not clear. However, it has been shown that R-configuration of branched chain FAs can be obtained from S-enantiomer by racemase activity of α-methyl acyl-CoA racemase (AMACR) [32]. This enzyme is also responsible for the inversion of S-ibuprofen to its R-enantiomer. Here, the racemization of 2-methylbutyryl-CoA (originating from Ile) would need to take place before chain elongation. Fatty acid synthetase can also produce methyl-branched FAs if propionyl-CoA instead of acetyl-CoA is used as building block via methyl-malonyl-CoA [33]. The stereochemical preference of thus derived branched chain FAs are to our knowledge not clarified yet. Furthermore, it has been reported an unexpected formation of low quantities of R-configurated *anteiso*-fatty acids in rumen fluid [34]. Introduction of uncommon FAs via media could be another source for this unexpected FA. Overall, this is not the first stereochemical inconsistency found in teicoplanin, though the inconsistencies prior known are related to the formation of the heptapeptide core by non-ribosomal peptide synthases (NRPSs) [30]. In conclusion, the determined S configuration is in line with the anticipated chirality. Polymyxin B, a natural product clinically used as polypeptide antibiotic and produced in *Paenibacillus polymyxa*, was also proven to show S configuration in its 6-methyloctanoic acid side chain [35], potentially hinting towards a similar biosynthesis way in these two bacteria strains resp. using the same precursor for the biosynthesis, namely isoleucine. In any case, it remains remarkable that a significant amount of R is present in teicoplanin RS3 the origin of which is unclear at this point.

As a summary of the enantiomer separations achieved so far for branched short- and medium-chain FAs as 1-naphthylamides, Fig. 4 gives an overview of columns and conditions which provided the best resolution under tested conditions. Apparently, methyl-*ai*FAs with up to eight carbons in its chain (nine carbons in total) seems to be the longest FA which can be separated into enantiomers under the chosen mild circumstances with 1-naphthylamine derivatization using polysaccharide phases. None of the used columns could separate 8-methyldecanoic acid (teicoplanin A2-4). To be able to elucidate the chirality of teicoplanin A2-4, the indirect method described in Ref. [8, 9], could be used.

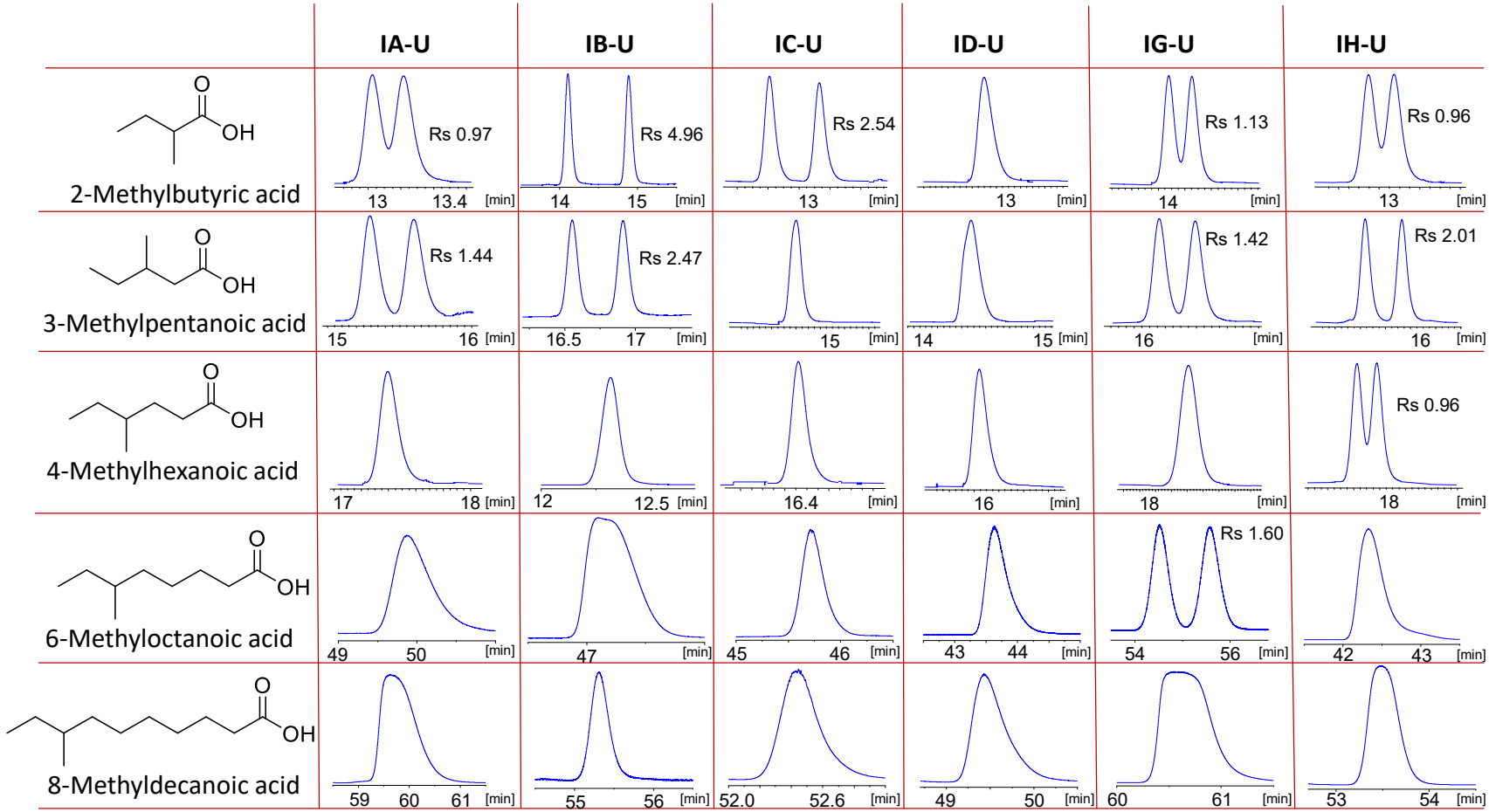

Fig. 4: Gradient separation of five different *anteiso*-fatty acids is shown, data for 2-methylbutyric acid, 3-methylpentanoic acid and 4-methylhexanoic acid was taken from Ref. [6] and was analysed by applying the following gradient: A: water + 0.1% acetic acid, B: ACN + 0.1% acetic acid; gradient profile: 20% to 90% B in 20 min, 90% to 10% B 20–20.01 min, 10% B 20.01–24 min; flow rate: 0.3 ml/min; column T: 10°C; injection volume: 1 µl; detection: UV 215 nm. 6-Methyloctanoic acid and 8-methyldecanoic acid were analysed by applying the following gradient: A: water + 0.1% acetic acid, B: ACN + 0.1% acetic acid; gradient profile: 20% to 90% B in 60 min, 90% to 20% B 60–60.01 min, 20% B 60.01–90 min; flow rate: 0.15 ml/min; column T: 0°C; injection volume: 1 µl; detection: UV 215 nm. While a partly separation of 6-methyloctanoic acid could further be optimized on Chiralpak IG-U, no separation could be achieved for 8-methyldecanoic acid. A carbon chain length of 8 seems to be the limit for the developed method under chosen circumstances. Elution order was determined for all separated substances except 3-methylpentanoic acid.

3.2.4.2 General profiling of teicoplanin unknown fatty acyl residues on chiral column

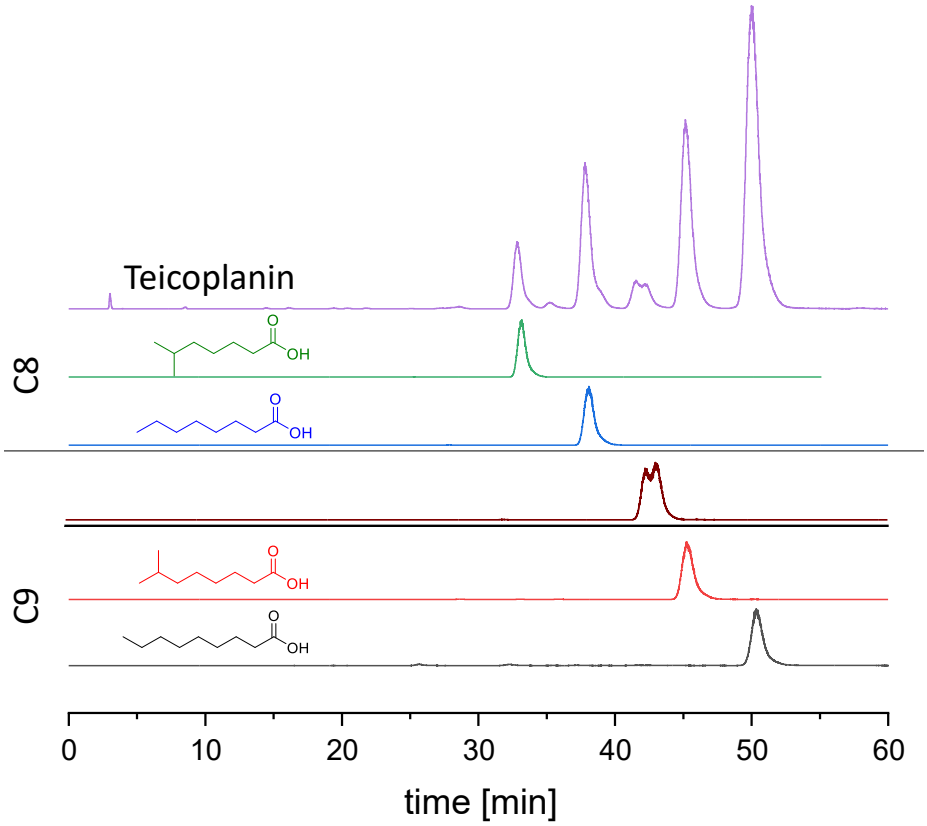

Fig. 5: 1-Naphthylamine derivatized FAs from hydrolysate of teicoplanin analyzed at 0°C on Chiralpak IB-U column (flow rate: 0.2 mL/min, for gradient: see section 3.2.3.6), MRM for C8 FAs (*m/z* 270.2 → 144.1) and C9 FAs (*m/z* 284.2 → 144.1). Teicoplanin hydrolysate (purple trace; summed MRM), 7-methyloctanoic acid (green trace), 6-methyloctanoic acid (wine red trace), n-octanoic acid (blue trace), 7-methyloctanoic acid (red trace) and n-nonanoic acid (black trace).

In the course of above screening further unknown peaks corresponding to FAs with 9 carbons (C9) were detected in the teicoplanin hydrolysate sample. For this reason, the extracted FA sample was screened for previously unknown fatty acyl chains that are not listed in the dossier of the EMA [3]. Exhibiting a remarkable methylene selectivity as shown in Ref. [6], polysaccharide columns are due to their orthogonal selectivity to RP useful for separation of constitutional isomers, apart from their original scope as chiral columns for stereoisomer separation. For a better overview thus a cleaner chromatogram, only C8 transitions to the naphthylamine tag (*m/z* 270.2 → 144.1) and C9 transitions (*m/z* 284.2 → 144.1) were measured on a Chiralpak IB-U column. The resulting chromatogram is shown in Fig. 5 (purple trace). Here, all major peaks could be assigned to distinct molecules using reference compounds. The largest peak eluting at 50 min could be assigned to n-nonanoic acid (see black trace for standard substance chromatogram), referred to as teicoplanin RS4 residue by the EMA. The second to last peak is also a C9 FA,

namely 7-methyloctanoic acid (red trace), i.e. an achiral *iso*-fatty acid. The split peak at ~42 min was assigned to 6-methyloctanoic acid (RS3) and is shown in wine red here. FAs with 8 carbons (C8) could be found at lower retention times than 40 minutes, n-octanoic acid (blue trace) and 6-methylheptanoic acid (green trace) as second and first eluting peaks. This confirms the characteristic elution pattern for methyl branched fatty acids, with larger selectivities for polysaccharide columns in comparison to RP columns, as shown already previously for branched short chain FAs [6]. The farther away the branching from the functional (naphthylamide) group, the later the substance elutes – with linear carboxylic acid showing the highest retention times (i.e. *ai*FA<*i*FA<nFA). Furthermore, this analysis reveals three previously unknown fatty acids being part of the teicoplanin family. While Yushchuk et al. [29] observed a (not further specified) C8 chain in teicoplanin and Tengattini et al. [12] found two C8 species, García-Gómez et al. [13] proposed them to be linear and branched, suggesting the branching in *iso*- or *anteiso*-position. Our method could be used for the determination of the branched C8 FA to be 6-methylheptanoic acid, thus an *iso*-branched fatty acid. We would like to keep the proposed nomenclature by García-Gómez et al. [13] and refer to teicoplanin with FA 8:0 (nFA carrying the linear C8 chain) as teicoplanin RS7, and to teicoplanin carrying 6-methylheptanoic acid as teicoplanin RS6.

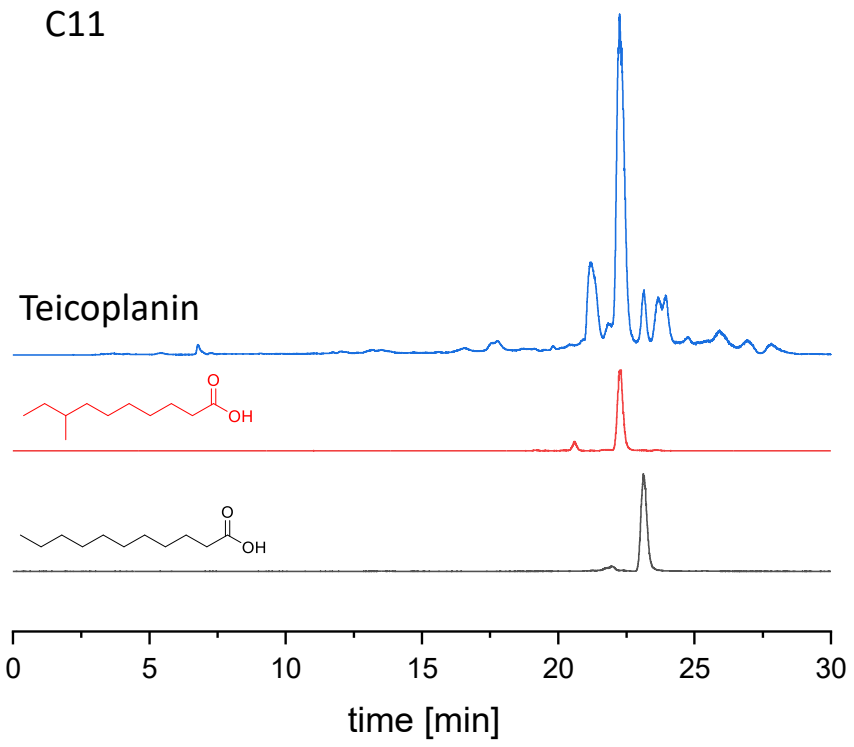

Fig. 6: 1-Naphthylamine derivatized FAs from hydrolysate of teicoplanin analyzed at 20°C on Chiralpak IA-U column (flow rate: 0.2 mL/min, for gradient: see section 3.2.3.6), MRM for C11 FAs (*m/z* 312.2 → 144.1). Teicoplanin hydrolysate (blue trace), 8-methyldecanoic acid (red trace) and n-undecanoic acid (black trace).

Teicoplanin with C9-fatty acyl residue, which was not yet described in the EMA dossier, was referred to as RS5 by García-Gómez et al. [13]. Based on the similarity of the fragmentation pattern with known *iso*- and *anteiso*-fatty acids (namely A2-4 and A2-5), they suggested RS5 to be the *iso*-form, namely 7-methyloctanoic acid. We could indeed confirm this assumption by our experiments.

The same workflow was applied for the elucidation of FAs with C11 residues, using a Chiralpak IA-U column at 20°C. The resulting chromatogram can be seen in Fig. 6. Several peaks were detected. Two of them could be annotated based on reference substances. The largest peak could be assigned to the 8-methyldecanoic acid, A2-4. The later eluting peak could be annotated as the linear n-undecanoic acid. In Ref. [12], a substance referred to as “A2-4/5 isomer” (and proposed to be n-undecanoic acid (RS13) in Ref. [13]) was found. This could be confirmed to be FA11:0 by our work.

3.2.5 Conclusion

This work extends a previously reported concept of enantioselective UHPLC-ESI-MS/MS based on polysaccharide columns and multiple reaction monitoring (MRM) for the enantiomer separation of branched short-chain fatty acids [6] to branched medium-chain fatty acids widening its applicability for targeted lipidomics. The straightforward derivatization using 1-naphthylamine and EDC gives access to relatively generic liquid chromatographic methods for substances that – because of their volatility – were previously preferentially analyzed by gas chromatographic methods as FAMEs. The introduced naphthylamide group not only supports isomer selectivity, but also features a mass tag for favourable ionization in positive ion mode and an MS2 signature ion for convenient programming of MRM transitions for targeted lipidomics of fatty acids. While our previously reported method could reliably enantioseparate branched fatty acids up to eight carbon atoms (with a branching up to the fourth position) and *anteiso*-branched fatty acids up to six carbon atoms, the method presented in this work can separate *anteiso*-branched fatty acids up to eight carbon atoms chain length. This UHPLC-ESI-MS/MS method using Chiralpak IG-U was used for the elucidation of the fatty acyl side chain chirality of therapeutically relevant antibiotic teicoplanin. It could be shown that the related substance teicoplanin RS3 (6-methyloctanoic acid) is mainly S configurated but shows also a significant amount of R configurated FA 8:0;6Me. Furthermore, the excellent methylene selectivity of the polysaccharide-based columns Chiralpak IA-U and IB-U were used for the structural elucidation of previously unknown minor compounds in teicoplanin. Overall, it could be demonstrated that polysaccharide-based columns are powerful tools for structural elucidation of natural compounds, not only for assignment of absolute configurations but also for the differentiation of constitutional isomers.

Conflict of interest statement

The authors declared no conflicts of interest.

3.2.6 References

[1] P.E. Reynolds, Structure, biochemistry and mechanism of action of glycopeptide antibiotics, European Journal of Clinical Microbiology and Infectious Diseases, 8 (1989) 943-950.

[2] F. Parenti, G. Beretta, M. Berti, V. Arioli, Teichomycins, new antibiotics from Actinoplanes teichomyceticus Nov. Sp. I. Description of the producer strain, fermentation studies and biological properties, The Journal of antibiotics, 31 (1978) 276-283.

[3] European Medicines Agency: EMA/194668/2013, Assessment report, Review under Article 5(3) of Regulation (EC) No 726/2004, Teicoplanin, Procedure no: EMEA/H/A-5(3)/1315, https://www.ema.europa.eu/en/documents/referral/assessment-report-article-53-procedure-teicoplanin-containing-medicinal-products_en.pdf, Accessed July 2022.

[4] H.-M. Jung, M. Jeya, S.-Y. Kim, H.-J. Moon, R. Kumar Singh, Y.-W. Zhang, J.-K. Lee, Biosynthesis, biotechnological production, and application of teicoplanin: current state and perspectives, Applied Microbiology and Biotechnology, 84 (2009) 417-428.

[5] M. Trautmann, M. Oethinger, R. Marre, H. Wiedeck, M. Ruhnke, Teicoplanin: 10 years of clinical experience, Infection, 22 (1994) 430-436.

[6] C. Geibel, L. Zhang, K. Serafimov, H. Gross, M. Lämmerhofer, Towards enantioselective ultrahigh performance liquid chromatography–mass spectrometry-based metabolomics of branched-chain fatty acids and *anteiso*-fatty acids under reversed-phase conditions using sub-2-µm amylose- and cellulose-derived chiral stationary phases, Chirality, 34 (2022) 484-497.

[7] M.F. Islam, S. Adhikari, M.-J. Paik, W. Lee, Liquid chromatographic enantiomer separation of 1-naphthylamides of chiral acids using several amylose- and cellulose-derived chiral stationary phases, Arch. Pharm. Res., 40 (2017) 350-355.

[8] K. Akasaka, H. Meguro, H. Ohrui, Enantiomeric separation of carboxylic acids having chiral centers remote from the carboxyl group by labelling with a chiral fluorescent derivatization reagent, Tetrahedron Lett., 38 (1997) 6853-6856.

[9] K. Akasaka, H. Ohrui, Enantiomeric Separation of Branched Fatty Acids after Conversion with trans-2-(2,3-Anthracenedicarboximido)cyclohexanol, a Highly Sensitive Chiral Fluorescent Conversion Reagent, Biosci. Biotechnol. Biochem., 63 (1999) 1209-1215.

[10] S. Hauff, W. Vetter, Exploring the fatty acids of vernix caseosa in form of their methyl esters by off-line coupling of non-aqueous reversed phase high performance liquid chromatography and gas chromatography coupled to mass spectrometry, J. Chromatogr. A, 1217 (2010) 8270-8278.

[11] S. Hauff, G. Hottinger, W. Vetter, Enantioselective analysis of chiral *anteiso* fatty acids in the polar and neutral lipids of food, J. Lipids, 45 (2010) 357-365.

[12] S. Tengattini, F. Corana, D. Bianchi, G. Marrubini, R. Colombo, S. Furlanetto, M. Terreni, C. Temporini, Application of an HPLC-MS/MS method for Teicoplanin drug substance and related impurities, part 2: Identity assignment of related impurities, J. Pharm. Biomed. Anal., 168 (2019) 38-43.

[13] D. García-Gómez, B. Alonso Díaz, E. Rodríguez-Gonzalo, LC-HRMS based on mixed-mode chromatography for the separation of teicoplanin and the unravelment of its composition, J. Pharm. Biomed. Anal., 186 (2020) 113308.

[14] Y. Okamoto, M. Kawashima, K. Hatada, Chromatographic resolution. 7. Useful chiral packing materials for high-performance liquid chromatographic resolution of enantiomers: phenylcarbamates of polysaccharides coated on silica gel, J. Am. Chem. Soc., 106 (1984) 5357-5359.

[15] Y. Okamoto, M. Kawashima, K. Yamamoto, K. Hatada, Useful chiral packing materials for high-performance liquid chromatographic resolution. Cellulose triacetate and tribenzoate coated on macroporous silica gel, Chem. Lett., 13 (1984) 739-742.

[16] B. Chankvetadze, Recent developments on polysaccharide-based chiral stationary phases for liquid-phase separation of enantiomers, J. Chromatogr. A, 1269 (2012) 26-51.

[17] P. Li, M. Lämmerhofer, Isomer selective comprehensive lipidomics analysis of phosphoinositides in biological samples by liquid chromatography with data independent acquisition tandem mass spectrometry, Anal. Chem., 93 (2021) 9583-9592.

[18] M. Cebo, X. Fu, M. Gawaz, M. Chatterjee, M. Lämmerhofer, Enantioselective ultra-high performance liquid chromatography-tandem mass spectrometry method based on sub-2µm particle polysaccharide column for chiral separation of oxylipins and its application for the analysis of autoxidized fatty acids and platelet releasates, J. Chromatogr. A, 1624 (2020) 461206.

[19] R. Karongo, J. Jiao, H. Gross, M. Lämmerhofer, Direct enantioselective gradient reversed-phase ultra-high performance liquid chromatography tandem mass spectrometry method for 3-hydroxy alkanoic acids in lipopeptides on an immobilized 1.6 µm amylose-based chiral stationary phase, J. Sep. Sci., 44 (2021) 1875-1883.

[20] F. Ianni, G. Saluti, R. Galarini, S. Fiorito, R. Sardella, B. Natalini, Enantioselective high-performance liquid chromatography analysis of oxygenated polyunsaturated fatty acids, Free Radic. Biol. Med., 144 (2019) 35-54.

[21] Y. Ohkubo, K. Akasaka, Y. Masuda, S. Konishi, C.Y. Yang, H. Takikawa, K. Mori, Pheromone synthesis. Part 265: Synthesis and stereochemical composition of two pheromonal compounds of the female Korean apricot wasp, Eurytoma maslovskii, Tetrahedron, 76 (2020) 131410.

[22] C. Yamamoto, E. Yashima, Y. Okamoto, Structural analysis of amylose tris(3,5-dimethylphenylcarbamate) by NMR relevant to its chiral recognition mechanism in HPLC, J. Am. Chem. Soc., 124 (2002) 12583-12589.

[23] M. Lämmerhofer, Chiral recognition by enantioselective liquid chromatography: mechanisms and modern chiral stationary phases, J. Chromatogr. A, 1217 (2010) 814-856.

[24] P. Peluso, V. Mamane, R. Dallocchio, A. Dessì, S. Cossu, Noncovalent interactions in high-performance liquid chromatography enantioseparations on polysaccharide-based chiral selectors, J. Chromatogr. A, 1623 (2020) 461202.

[25] A. Borghi, D. Edwards, L.F. Zerilli, G.C. Lancini, Factors affecting the normal and branched-chain acyl moieties of teicoplanin components produced by Actinoplanes teichomyceticus, Microbiology, 137 (1991) 587-592.

[26] D.H. Williams, B. Bardsley, The Vancomycin Group of Antibiotics and the Fight against Resistant Bacteria, Angew. Chem. Int. Ed., 38 (1999) 1172-1193.

[27] Y. Zou, J.S. Brunzelle, S.K. Nair, Crystal Structures of Lipoglycopeptide Antibiotic Deacetylases: Implications for the Biosynthesis of A40926 and Teicoplanin, Chem. Biol., 15 (2008) 533-545.

[28] S.D. Dong, M. Oberthür, H.C. Losey, J.W. Anderson, U.S. Eggert, M.W. Peczuh, C.T. Walsh, D. Kahne, The Structural Basis for Induction of VanB Resistance, J. Am. Chem. Soc., 124 (2002) 9064-9065.

[29] O. Yushchuk, B. Ostash, T.H. Pham, A. Luzhetskyy, V. Fedorenko, A.W. Truman, L. Horbal, Characterization of the Post-Assembly Line Tailoring Processes in Teicoplanin Biosynthesis, ACS Chem. Biol., 11 (2016) 2254-2264.

[30] T.-L. Li, F. Huang, S.F. Haydock, T. Mironenko, P.F. Leadlay, J.B. Spencer, Biosynthetic Gene Cluster of the Glycopeptide Antibiotic Teicoplanin: Characterization of Two Glycosyltransferases and the Key Acyltransferase, Chem. Biol., 11 (2004) 107-119.

[31] R.G. Kruger, W. Lu, M. Oberthür, J. Tao, D. Kahne, C.T. Walsh, Tailoring of Glycopeptide Scaffolds by the Acyltransferases from the Teicoplanin and A-40,926 Biosynthetic Operons, Chem. Biol., 12 (2005) 131-140.

[32] G. Kong, H. Lee, Q. Tran, C. Kim, J. Park, S.H. Kwon, S.-H. Kim, J. Park, Current knowledge on the function of α-methyl acyl-CoA racemase in human diseases, Front. Mol. Biosci, 7 (2020).

[33] J.P. Dewulf, S. Paquay, E. Marbaix, Y. Achouri, E. Van Schaftingen, G.T. Bommer, ECHDC1 knockout mice accumulate ethyl-branched lipids and excrete abnormal intermediates of branched-chain fatty acid metabolism, J. Biol. Chem., 297 (2021) 101083.

[34] D. Eibler, H. Abdurahman, T. Ruoff, S. Kaffarnik, H. Steingass, W. Vetter, Unexpected formation of low amounts of (R)-configurated *anteiso*-fatty acids in rumen fluid experiments, PLOS ONE, 12 (2017) e0170788.

[35] S. Wilkinson, Crystalline Derivatives of the Polymyxins and the Identification of the Fatty Acid Component, Nature, 164 (1949) 622-622.

3.3 Publication III

Determination of double bond positions in unsaturated fatty acids by pre-column derivatization with dimethyl and dipyridyl disulfide followed by LC-SWATH-MS analysis

Matthias Olfert, Cornelius Knappe, Adrian Sievers-Engler, Benedikt Masberg, Michael Lämmerhofer *

Institute of Pharmaceutical Sciences, Pharmaceutical (Bio-)Analysis, University of Tübingen, Auf der Morgenstelle 8, 72076 Tübingen, Germany

* Author for correspondence:
Prof. Dr. Michael Lämmerhofer
michael.laemmerhofer@uni-tuebingen.de

This article was published in Analytical and Bioanalytical Chemistry as Paper in Forefront in the collection “Metabolomics for Clinical Applications” (Springer Nature, 2024)
DOI: 10.1007/s00216-024-05542-z

3.3.1 Graphical Abstract

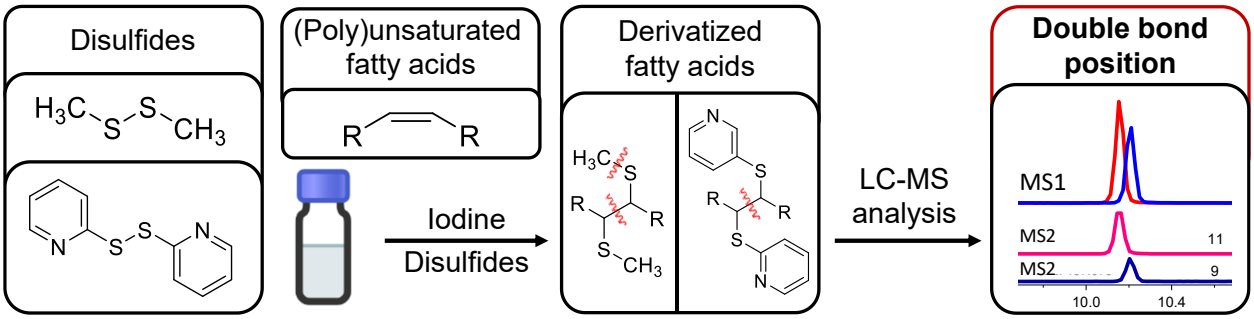

3.3.2 Abstract

Comprehensive in-depth structural characterization of free monounsaturated and polyunsaturated fatty acids often requires the determination of double bond positions due to their impact on physiological properties and relevance in biological samples or during impurity profiling of pharmaceuticals. In this research, we report on the evaluation of disulfides as suitable derivatization reagents for the determination of double bond positions of unsaturated free fatty acids by UHPLC-ESI-QTOF-MS/MS analysis and SWATH (sequential windowed acquisition of all theoretical mass spectra) acquisition. Iodine-catalyzed derivatization of C=C-double bonds with dimethyl disulfide (DMDS) enabled detection of characteristic carboxy-terminal MS2-fragments for various fatty acids in ESI negative mode. The determination of double bond positions of fatty acids with up to three double bonds, the transfer of the method to plasma samples and its limitations have been shown. To achieve charge-switching for positive ion mode MS-detection, derivatization with 2,2'-dipyridyldisulfide (DPDS) was investigated. It enabled detection of both corresponding characteristic omega-end- and carboxyl-end-fragments for fatty acids with up to two double bonds in positive ion mode. It provides a straightforward strategy for designing MRM transitions for targeted LC-MS/MS assays. Both derivatization techniques represent a simple and inexpensive way for the determination of double bond positions in fatty acids with low number of double bonds. No adaptations of MS hardware is required and the specific isotopic pattern of resulting sulfur-containing products provides additional structural confirmation. This reaction scheme opens up the avenue of structural tuning of disulfide reagents beyond DMDS and DPDS using reagents like cystine and analogs to achieve enhanced performance and sensitivity.

3.3.3 Introduction

Fatty acids are a diverse group of molecules and the main building blocks for lipids in the human body [1]. They are typically characterized by their carbon number, their degree and position of unsaturation. Whilst carbon number and degree of unsaturation are readily obtained by high-resolution mass spectrometry, the determination of the carbon-carbon-double bond (DB) position represents an analytical challenge due to the isobaric nature of such constitutional isomers and limited fragmentation in MS2 of commonly employed collisional induced dissociation (CID) [2, 3]. Knowledge of DB positions, however, is of prime importance, as they have a major influence on the physiological and pathophysiological properties of fatty acids. (Poly-)Unsaturated fatty acids of physiological interest can be differentiated in ω-3-, ω-6- and ω-9-fatty acids. From biological viewpoint, the balance of ω-3- and ω-6-fatty acids plays a critical role in the prevention of several diseases [1, 4, 5].

Structural lipidomics requires the full elucidation of molecular characteristics including DB positions. The complete structural elucidation is also necessary to get a deeper understanding regarding physiological properties of lipids but also as part of the identification of unknowns in the pharmaceutical and food industry. During quality control of starting materials and finished lipid-containing products unspecified fatty acid isomers could be considered as impurity and proper identification is required once the respective threshold is exceeded [6, 7].

Numerous methods have been reported recently for the determination of DB positions. For instance, for GC-MS (gas chromatography-mass spectrometry) analysis the derivatization with dimethyl disulfide (DMDS), enabling characteristic cleavage of the derivatized C-C bond by electron ionization (EI) was suggested [8-10]. Its applicability has been shown especially for mono-unsaturated fatty acids but also polyunsaturated fatty acids (PUFAs) can be derivatized efficiently by using lower temperatures [11]. This approach involved also derivatization of free fatty acids to e.g. methylesters or amides as an additional step in the sample preparation to achieve volatility for GC-MS-analysis [12]. There is a certain risk that the required derivatization-conditions alter the sample-composition, especially in multi-component samples.

For liquid chromatography (LC)-MS analysis, various derivatization approaches for DB position determination have been established. For a brief overview, the reader is referred to recent reviews on this subject [13-17]. One of the most commonly used methods appears to be Paternò-Büchi reaction [18] and modified versions [19]. The original method is based on the formation of oxetane rings at the original DB position by addition of acetone during in-source online-derivatization with

nanoESI-tip and activation with UV-light [18]. This type of reaction can be used as a platform technology tuned with different ketones/aldehydes to achieve higher yields, fewer side reactions (e.g. for trifluoroacetophenone) [13, 20] and detection in positive ion mode by charge switching (e.g. in-source derivatization with acetylpyridine) [13, 21]. Besides these in-source derivatizations, also “pre-source” (e.g. with inline bare fused silica capillary) [22] and pre-column derivatizations [20] have been proposed. The derivatization allows fragmentation by collision-induced dissociation (CID), generating two characteristic MS2 fragments by cleavage at the original DB position [18]. Downsides of this method include specific hardware requirements (e.g. low-pressure mercury lamps, fused-silica-capillaries) and possible generation of side-products and positional isomers, leading to more complex chromatograms if performed pre-column [13, 20]. The application of Paternò-Büchi reaction has been shown to be effective as part of double derivatization techniques [23] and in combination with ion mobility MS analysis [24]. Other derivatization approaches involve the introduction of stable epoxides at DB positions with low-temperature plasma [25], mCPBA (meta-chloroperoxybenzoic acid) [26, 27], oxone (potassium peroxymonosulfate) [28] or urea hydrogen peroxide [29], aza-Prilezhaev aziridination [30], derivatization with N-Alkylpyridinium [31] and derivatization of the carboxylic function inducing alkyl chain fragmentation with characteristic product ions allowing to pinpoint the DB position [32]. In a modified version of the mCPBA derivatization, an analytical strategy for relative quantification of FAs, carbon–carbon double-bond localization, and cis-/trans-geometry differentiation was proposed by isobaric multiplex labeling reagents for carbonyl-containing compound tag conjugation and m-CPBA epoxidation (isobaric tagging) [33]. The typical Diels-Alder-reaction has been utilized for conjugated FAs [34], while Cerrato et al. recently described the inverse-electron-demand Diels-Alder reaction for positional determination of isolated DBs in free fatty acids and other lipids [35]. Various ozonolysis-based approaches for DB localization have been proposed, in which the formed ozonides decomposed into characteristic fragments; such ozonolysis reactions have been performed off-line [36], in the ion source (OzESI-MS) [37] and in the collision cell (ozone-induced dissociation, ozID) [38]. Other gas phase approaches include the use of electron-activated dissociation (EAD) [39, 40] and ultraviolet photo-dissociation (UVPD) instead of CID for fragmentation [15].

Our research focused on extending the analyst´s toolbox for determination of DB positions in unsaturated fatty acids. First, the applicability of the DMDS-derivatization protocol for LC-MS analysis of fatty acids was evaluated for the first time. Second, the suitability of disulfide-reagents as a tunable platform for DB position determination in lipids was investigated to elucidate whether i) ionizable residues allow charge reversal, leading to detectability in positive ion mode and thus

improving ionization efficiency, ii) confirmative product ions of both ω- and carboxy-terminal ends can be designed into the concept, and iii) such confirmative product ions from both sides of the double bond would be suitable to design in silico MRM transitions for targeted HPLC-QqQ-ESI-MS/MS analysis.

3.3.4 Experimental

3.3.4.1 Materials

Mass-spectrometry-grade (Rotisolv, Ultra LC-MS grade) methanol, acetonitrile and n-hexane were purchased from Carl Roth (Karlsruhe, Germany). Dimethyl disulfide (DMDS), 2,2´-Dipyridyl disulfide (DPDS), Palmitoleic acid (PAL, C16:1n-7), Oleic acid (OA; C18:1n-9), cis-Vaccenic acid (VA; C18:1n-7), Linoleic acid (LA; C18:2n-6,9), γ-Linolenic acid (GLA; C18:3n-6,9,12), NIST SRM 1950, Iodine, Diethyl ether and Sodium thiosulfate were obtained from Sigma-Aldrich (Taufkirchen, Germany). α-Linolenic acid (ALA; C18:3n-3,6,9), Ricinenic acid (9Z,11Z-CLA; C18:2n-7,9), 10E,12Z-octadecadienoic acid (10E,12Z-CLA; C18:2n-6,8) and "Polyunsaturated Fatty Acid MaxSpec LC-MS Mixture" were from Cayman Chemical Company (Ann Arbor, USA). Ultrapure water was produced by additional purification of demineralized water using an Elga LabWater Ultra purification system (Celle, Germany). Acetic acid (Rotipuran > 98 %) was obtained from Carl Roth (Karlsruhe, Germany). Nomenclature and abbreviations of the fatty acids in accordance with LIPID MAPS [41] and Lipidomics Standard Initiative [42] can be found in Table S1. The reversed phase column Kinetex C8 (3.0 x 50 mm, 2.6 µm, 100 Å) was obtained from Phenomenex (Aschaffenburg, Germany).

3.3.4.2 Instrumentation and software

The HPLC-system consisted of an Agilent 1290 Infinity series UHPLC system with a thermostated column compartment and binary pump (Agilent Technologies, Santa Clara, United States) and an PAL HTC-xt autosampler (CTC Analytics AG, Zwingen, Switzerland). The HPLC-system was hyphenated by a diverter valve and AB Sciex CDS (calibrant-delivery-system) to a Sciex TripleTOF 5600+ system with DuoSpray source for electrospray-ionization from Sciex (Framingham, MA, USA). The system was controlled by Analyst TF 1.8.1 and the data evaluation was performed with PeakView 2.2 and Multiquant 3.0. OriginPro 2022 (version 9.9) from OriginLab Corporation (Northampton, USA) was used for data visualization. Graphical abstract was created with Chemix (https://chemix.org).

3.3.4.3 Derivatization method

The derivatization method followed previous works with DMDS for GC-MS with some modifications [43, 44]. The following solutions were prepared: fatty acids in n-hexane (50 µg/mL), Iodine in diethyl ether (60 mg/mL), DMDS as neat solution, DPDS in n-hexane (3 mg/mL), 10 % sodium thiosulfate in water. The samples were prepared by mixing 200 µL fatty acid solution with 200 µL Iodine solution and 400 µL DMDS or DPDS-solution. The incubation was carried out at 35

°C and various time points (Figures were created at the apex of the kinetic curves). To remove the excess iodine and stop the reaction the sodium thiosulfate solution was added until discoloration of the hexane phase. After removing the hexane phase into a new vial, n-hexane was added to the sample and shaken to extract remaining fatty acids. Again, the hexane-phase was pipetted into the new vial. The combined hexane fractions were evaporated in a Genevac EZ-2 evaporator (Ipswich, UK) under nitrogen and reconstituted with methanol to achieve a concentration of 1 µg/mL for LC-MS measurements. The workflow is schematically depicted in Figure S1.

3.3.4.4 LC-MS method

Kinetex C8, 3.0 x 50 mm, 2.6 µm was used as column. Mobile phase A consisted of water with 0.1 % (v/v) acetic acid and mobile phase B of acetonitrile with 0.1 % (v/v) acetic acid. The column temperature was set to 40 °C and the flow rate to 0.5 mL min^{-1}. The following gradient profile was applied: 10 to 100 % B in 13 min, 100 % B for 3 min, 100 to 10 % B in 0.1 min, 10 % B for 3.9 min. The first 5 minutes were directed into the waste by a diverter valve.

Mass spectrometer settings were as follows: Curtain gas: 30 psi, source gas 1: 50 psi, source gas 2: 40 psi, ion-spray voltage floating: -4500 V (negative mode), 5500 V (positive mode), ion source temperature: 550 °C, declustering potential: -80 V (negative mode), 80 V (positive mode).

Data were recorded by data-independent acquisition with SWATH technology: A TOF-MS full scan with 200 ms accumulation time scan range from *m/z* 50-1000, collision energy of -5 V (negative mode), SWATH-MS accumulation time of 50 ms and collision energy of -45 V (negative mode). The design of the SWATH-windows can be found in the Supplementary information (Table S2).

Targeted product ion experiments (MRM-HR) consisted of a TOF-MS full scan experiment with 200 ms accumulation time, scan range from *m/z* 50-1000, collision energy of -5 V (negative mode) and 5 V (positive mode), respectively. Collision energy was screened for all single-standards from -20 to -60 V in negative ion mode (DMDS) or 20 to 60 V in positive ion mode (DPDS) in 5 V steps, whereas 45 V (positive ion mode) and -45 V (negative ion mode) showed the best results. Subsequently, product ion scans were performed with an accumulation time of 100 ms and collision energy of -45 V (negative ion mode) and 45 V (positive ion mode).

3.3.5 Results and discussion

3.3.5.1 Double bond derivatization with disulfides

The reaction of disulfides, like dimethyl disulfide (DMDS), with the double bond needs iodine catalysis. Iodine initially forms an iodonium ion by electrophilic addition to the double bond. The resulting iodide anion reacts in a nucleophilic substitution with the DMDS, forming thiomethyl anions, which react in an anti-addition with the iodonium-ion. The resulting sulfonium ring is further attacked by thiomethyl anions yielding bis-methylthio derivatives at the initial DB position. This mechanism has been recently proposed by Richter et al. [45] and can be found in Figure S2. The bis-methylthio substituents activate the C-C bond corresponding to the original DB for fragmentation by CID affording characteristic fragments for pinpointing the DB location in the unsaturated lipid. The generation of characteristic fragments in LC-MS was also shown by Deng et al. for mono-methylthio-derivatives of diacylglycerides, although the exact chemistry of the formation of mono-methylthio-derivatives remains unclear and could not be confirmed in our study [46].

Limitations of DMDS in LC-MS based fatty acid DB position determination include restriction to negative mode, detection of solely carboxy-terminal fragments and lack of corresponding confirmative fragments from ω-terminal tail. To overcome this, a charge-switching concept in which the methyl-groups of the disulfide were exchanged for an ionizable group, like pyridines, to enable detection in positive mode was envisaged by use of 2,2'-dipyridyl disulfide (DPDS) as derivatization reagent. It was envisioned that this concept allows extension of DB position determination to volatile analytes such as aldehydes which are difficult to analyse by LC-MS without proper derivatization [47].

Various MUFAs and PUFAs were selected as model lipids to systematically study the reactivity and reaction products as well as product ions formed. For every single-standard (DMDS or DPDS-derivatized) in each mass spectrometric cycle the following MS-experiments were performed: (i) time-of-flight (TOF)--MS scan for MS1-precursor measurement; (ii) PIS (product ion scans, MRM-HR) of the mono-derivatized product for fragmentation and recording of the respective MS2-spectra. Hereby, it was possible to simultaneously detect mono-derivatized products for DMDS and DPDS and bis-derivatized and cyclic products for DMDS on MS1-level. The summarized experimentally observed fragments for DMDS can be found in Table S3 and suggested transitions for targeted MRM-experiments in Table S4. For DPDS the respective fragments and transitions can be found in Table S5 and Table S6.

3.3.5.1.1 Oleic acid (C18:1n-9) and Vaccenic acid (C18:1n-7)

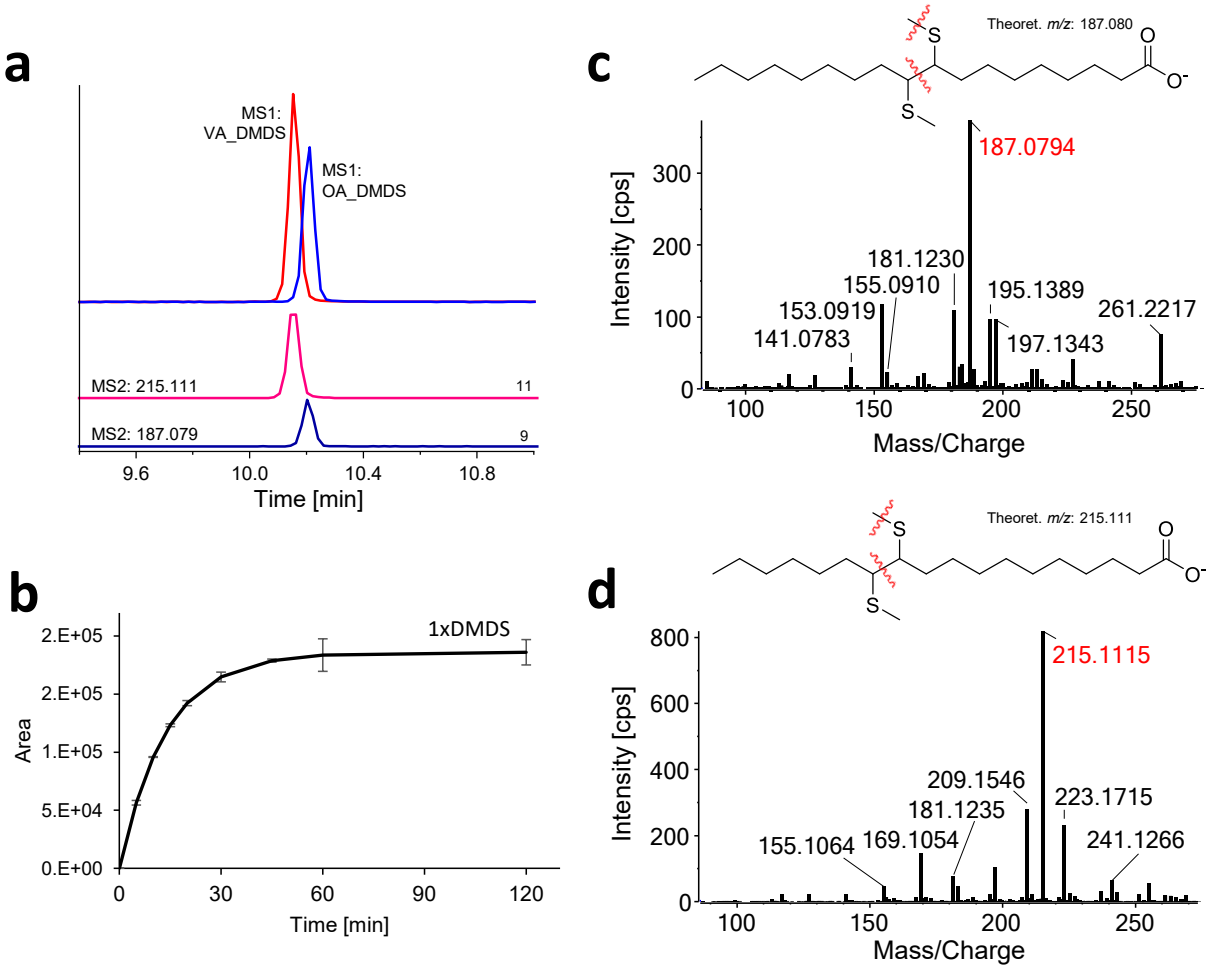

Figure 1: DMDS-derivatized mono-unsaturated fatty acids; a: MS1-EIC of derivatized oleic acid (blue; *m/z* 375.240 ± 0.01 Da) and cis-vaccenic acid (red, *m/z* 375.240 ± 0.01 Da) from TOF-MS scans, MS2-EIC of characteristic fragments (*m/z* 215.111 ± 0.01 Da, *m/z* 187.080 ± 0.01 Da; intensity multiplied with 20 for better visibility) from PIS (MRM-HR) of respective mono-derivatized products; b: derivatization kinetics of mono-derivatized oleic acid (fitted, pseudo 1st order, BoxLucas1); c: MS2 spectrum (CE: 45 V) of derivatized oleic acid with tentative fragmentation pattern leading to fragment with *m/z* 187.080; d: MS2 spectrum (CE: 45 V) of derivatized cis-vaccenic acid with tentative fragmentation pattern leading to fragment *m/z* 215.111

Oleic acid and vaccenic acid were selected as model MUFAs with different DB position. Initial experiments were performed with individual standard solutions. As shown in Figure 1a DMDS successfully reacted with both MUFAs yielding a significant peak of mono-DMDS derivatized oleic and vaccenic acid (yielding bis-methylthio-derivatives) by negative ESI ion mode LC-MS. DMDS-derivatized vaccenic acid (VA) with double bond position at C11 (Δ11; ω7) elutes before oleic acid (OA) with its double bond at C9 (Δ9; ω9). It is striking that there is no separation of diastereomers (2 chiral centers, 4 stereoisomers) that obviously coelute which is favorable from viewpoint of sensitivity. The slight shift in retention time between VA and OA can be explained by the hindered tight interaction between the alkyl strands of C18 phase and analyte due to the

methylthio substituents like in branched chain fatty acids. In case of the oleic acid a longer alkyl tail can still tightly interact with the C18 chain leading to stronger retention. Next, the derivatization kinetics was measured over 120 min (Figure 1b). The peak area for the oleic acid derivative steeply increased exponentially until a plateau was reached after approximately 45 min. A pseudo-first order rate model provided a good fit (reaction rate constant k: 0.0723 min^{-1}, half time $t_{1/2}$: 9.58 min). Differentiation between the constitutional isomers (OA & VA) is possible on MS2-level based on the characteristic carboxy-terminal fragments obtained by C-C bond cleavage and additional demethylation of the thioether (OA: *m/z* 187.080; VA: *m/z* 215.111, Figure 1c and 1d). The fragment with *m/z* 215.111 was negligible in oleic acid, especially when compared to the fragment *m/z* 187.080. The correct assignments can be confirmed by other additional fragments with smaller intensities (*m/z* 153.092, 213.095 for oleic acid or *m/z* 243.142, 241.127 for vaccenic acid) which, however, are all related to the carboxy-terminal head that carries the negative charge (see Figure S3 and S4). DMDS-derivatized palmitoleic acid (C16:1n-7), which shows a double bond in position 9, exhibits the same fragmentation behavior as oleic acid with the product ion of *m/z* 187.080 being the most intensive characteristic fragment (Figure S5 and S6). The successful implementation of DMDS derivatization to the above discussed MUFAs confirms the general applicability of this double bond reagent for LC-MS and CID fragmentation.

All experiments with 2,2'-dipyridyl disulfide (DPDS) were performed in positive ion mode. In Figure 2a the MS1-EICs of mono-derivatized oleic acid (OA) and vaccenic acid (VA) show for both fatty acids a major double peak between 8.5 and 9 min and one minor peak eluting significantly later than the two major peaks (at around 10.5 min). However, only the first two peaks have an MS2-spectrum which can be assigned to the derivatized fatty acids. The double peak can be explained by the formation of diastereomers which are chromatographically separated. This is unfavorable since the signal intensity is divided into two peaks and increases complexity of the chromatogram. The derivatization kinetics (Figure 2b; reaction rate constant k: 0.0681 min^{-1}, half time $t_{1/2}$: 10.18 min), under the same MS-conditions (as DMDS), is comparable to the one from oleic acid and DMDS (Figure 1b), but the MS2-spectra show reduced intensities of the fragments compared to the derivatization with DMDS (mobile phase was optimized for DMDS-derivatives in negative ESI mode but not specifically for DPDS-derivatives in positive ESI mode). Nevertheless, characteristic product ions obtained by cleavage of the C-C bond, which corresponds to the former C=C-DB, were found and exhibited good intensities: *m/z* 248.110, 266.121 and 236.127 for position 9 (OA); *m/z* 276.142, 294.152 and 208.115 for position 11 (VA). By the introduction of pyridine-rings as ionizable group the fragments of the omega-end were also detectable in positive mode. Interestingly, for palmitoleic acid (PAL, C16:1n-7, double bond position 9) only one major peak

was detected, i.e. the diastereomers coeluted although the carbon chain was only by 2 methylene groups shorter (see Figure S7). DB position determination was possible by the same carboxy-terminal fragments as for oleic acid: *m/z* 266.120, 248.110 (COOH-end). However, it also shares one fragment with vaccenic acid (*m/z* 208.116, omega-end). This enables the discrimination of PAL from OA and VA on MS1-level and on MS2-level (for MS2-spectra see Figure S8).

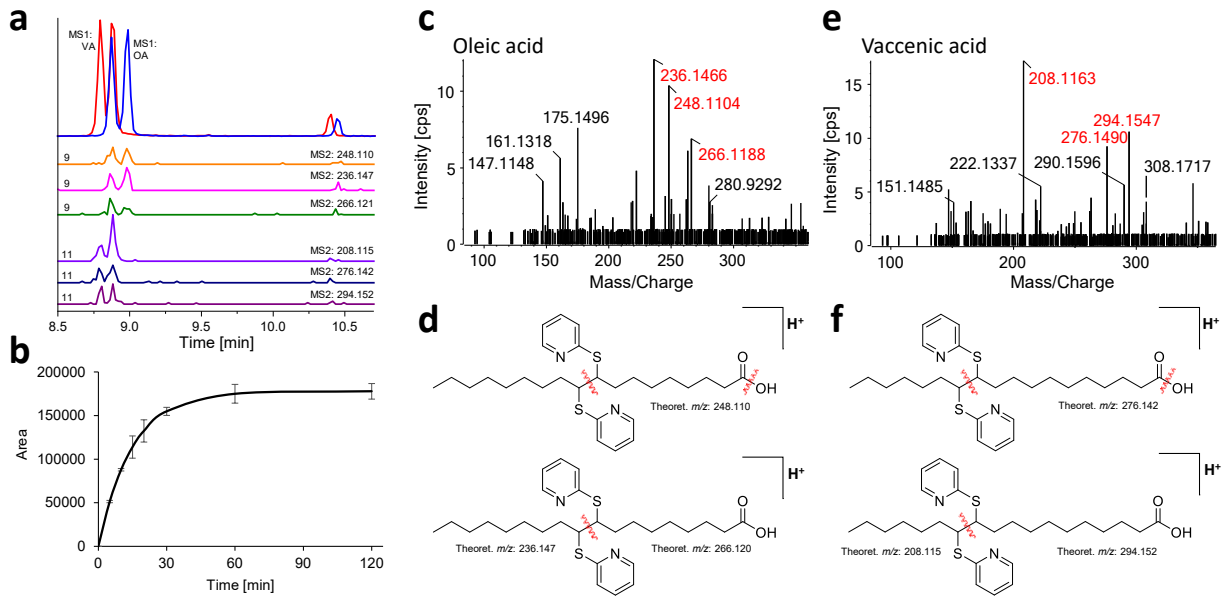

Figure 2: DPDS-derivatized mono-unsaturated fatty acids, detected as $[M+H]^+$; a: MS1-EIC of derivatized oleic acid (blue; *m/z* 503.276 ± 0.01 Da) and cis-vaccenic acid (red, *m/z* 503.276 ± 0.01 Da) from TOF-MS scans, MS2-EICs of characteristic fragments (40-fold multiplied for visibility; derived from OA: *m/z* 248.110, 236.147, 266.121; derived from VA: *m/z* 208.115, 276.142, 294.152) from PIS (MRM-HR) of respective mono-derivatized products; b: derivatization kinetics of mono-derivatized oleic acid (fitted, pseudo 1st order, BoxLucas1); c: MS2 spectrum (CE: 45 V) of derivatized oleic acid; d:tentative fragmentation patterns of oleic acid e: MS2 spectrum (CE: 45 V) of derivatized cis-vaccenic acid; f: tentative fragmentation patterns of cis-vaccenic acid

3.3.5.1.2 Linoleic acid (C18:2n-6,9)

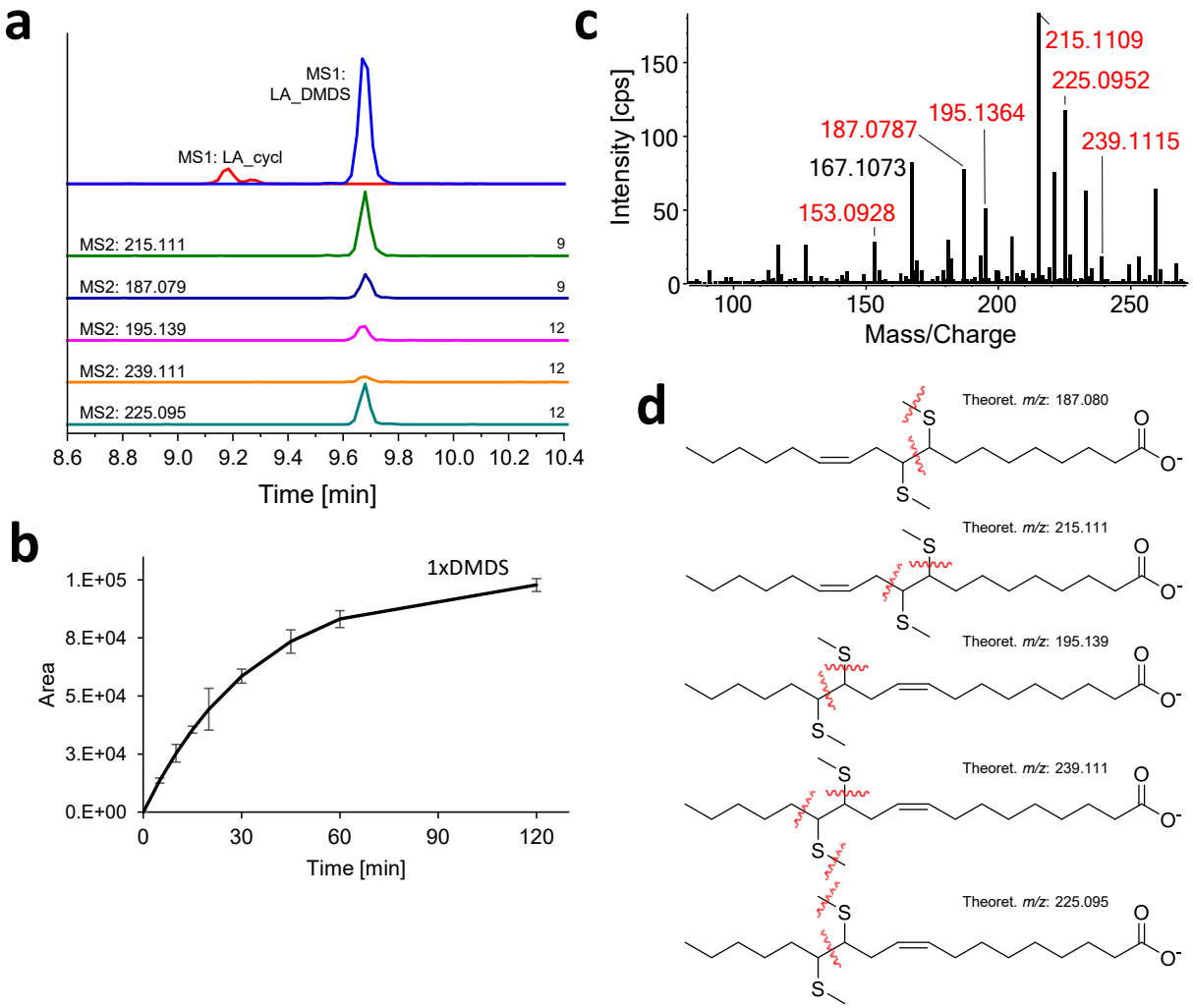

Figure 3: DMDS-derivatized linoleic acid (C18:2n-6,9); a: MS1-EIC of derivatized linoleic acid (blue; *m/z* 373.224 ± 0.01 Da), cyclic products of linoleic acid (red, *m/z* 405.197 ± 0.01 Da) from TOF-MS scan and MS2-EIC of fragmentation products (40-fold increased for visibility) from PIS (MRM-HR) of mono-derivatized linoleic acid; b: derivatization kinetics of linoleic acid (fitted, pseudo 1st order, BoxLucas1); c: MS2 spectrum (CE: 45 V) of derivatized linoleic acid; d: tentative fragmentation patterns leading to characteristic fragments (position 9: *m/z* 187.080, 215.111; position 12: *m/z* 195.139, 239.111, 225.095)

Due to multiple DBs, the situation gets more complicated for PUFAs. DMDS-derivatization of linoleic acid (C18:2n-6,9) leads to mono-derivatized products (Figure 3a). In spite of isolated DBs, poly-derivatized products were not observed, probably due to the steric hindrance once one DB has been derivatized. This confirms previous observations from GC-MS studies [48, 49]. A small, earlier eluting double-peak with the mass of cyclic products was detected. The generation of this unwanted side product is quite low with the used conditions, since short reaction times and low temperature slow down the generation of cyclic products [11]. The determination of DB positions by cyclic products is difficult due to their more complex MS2 spectra [10].

When comparing the derivatization kinetics of oleic acid with linoleic acid, it becomes obvious that linoleic acid needs significantly longer to reach the plateau (Figure 3b, reaction rate constant k: 0.0289 min^{-1}, half time $t_{1/2}$: 23.97 min).

The MS2-spectrum in Figure 3c features the fragments for double bond position 9 (*m/z* 187.080, 153.092 and 215.111) and for double bond position 12 (*m/z* 195.139, 239.111 and 225.095). The fragment with *m/z* 187.080 was expected since OA and LA both share a DB at position 9. On the other hand, the fragment with *m/z* 215.111 resulting from α-cleavage on the ω-terminal side is observed with high intensity and must belong to derivatization at position 9 instead of 11 as described for vaccenic acid. Nevertheless, linoleic acid and vaccenic acid can be differentiated by their precursor *m/z* and the presence of fragments with *m/z* 187.080 and 225.095 which are absent in the latter.

DPDS derivatized linoleic acid shows multiple major peaks with the respective mass (see P1, P2, P3 in Figure S9), which is due to diastereoisomerism and two derivatization sites (double bond position 9 and 12). The derivatization kinetics exhibits an exponential increase until 15 min followed by a significant decrease in derivatization product with quite high standard deviations (Figure S10). The proposed fragmentation patterns are shown in Figure S9b and S9c for position 9 and 12 and MS2-spectra can be found in Figure S11 and S12. Double bond position 9 can be assigned by fragments with *m/z* 280.136, 266.121 and 262.126, whereas double bond position 12 can be assigned by fragments with *m/z* 288.142, 208.115 and 194.100. This differentiation can be visualized by overlay of MS1-EIC of the precursor with the MS2-EICs of the fragments: Compounds of P1 and P3 are derivatized at double bond position 12, while P2 is derivatized at double bond position 9 (see Figure S9a). Especially the MS2-EICs allow unequivocal assignments. Nevertheless, the separation of diastereomers and positional isomers of the derivatives leads to increased complexity of the chromatogram and loss of sensitivity. The detection of omega-end fragments allows a differentiation of double bond-position 9 in LA from analytes like OA and PAL on MS2-level, as their omega-fragments differ by the additional DB in LA compared to OA.

The further transfer of the DPDS-derivatization to analytes with three DBs was unfortunately not successful due to limited sensitivity and needs further method optimization. The screening of 4,4'-DPDS as reagent was not successful, as it unexpectedly only generated an insignificant amount fatty acid derivatives.

3.3.5.1.3 Conjugated Linoleic acid (C18:2)

Conjugated fatty acids, like conjugated linoleic acids (CLAs) are isomeric with respect to their unconjugated counterparts (in this case linoleic acid). UV-detection enables the differentiation of such isomers based on their UV-spectra and even enables the identification of double-bond configurations [3]. Nevertheless, an unequivocal identification of DB positions without respective standard substances by UV is difficult. However, it is a highly relevant analytical problem since CLAs can be produced during oxidation reactions e.g. in pharmaceutical formulations [50, 51]. As a proof of principle, 9Z,11Z-CLA (C18:2n-7,9) and 10E,12Z-CLA (C18:2n-6,8), bearing their double bonds in position 9 and 11 and in position 10 and 12, respectively, were analyzed.

Interestingly, unlike linoleic acid both conjugated linoleic acid isomers show two peaks. Since both peaks show the same MS2 spectrum, it can be assumed that diastereomers are separated (Figure S13). The presence of the DB next to the stereogenic center with the methylthio group seems to favor diastereoselectivity, while the isolation of the two structural elements (DB and methylthio group) by a methylene group in linoleic acid presumably introduces conformational flexibility which prohibits the diastereomer separation. The differentiation of linoleic acid from its conjugated LA isomers is less straightforward since they show similar fragmentation patterns. Nevertheless, 9Z,11Z-CLA can be differentiated from linoleic acid by the absence of the fragment ion with *m/z* 215.111 and the presence of fragment ion with *m/z* 213.095 (Figure S14a). As expected, the fragments with *m/z* 187.080 and 153.092 are present and allow to pinpoint one double bond in position 9, as discussed for oleic acid and linoleic acid. A possible fragmentation pattern leading to the identification of double bond position 11 is shown in Figure S14b. It is based on the characteristic product ion with *m/z* 213.095 and additional presence of the less characteristic fragments with *m/z* 225.095 and 239.111.

The DB locations of 10E,12Z-CLA are easier to assign. The double peak elutes slightly earlier (Figure S13) and shows the fragment ions with *m/z* 227.111 and 239.111 indicating position 12 and the fragment ion with *m/z* 201.095 which is characteristic for position 10 (Figure S14, c and d). On contrary, the fragments with *m/z* 187.080 and 153.092 are absent. It was reported in the literature for DMDS-derivatization of unconjugated C18:2 fatty acids with one cis and one trans configured (isolated) double bond that only the cis double bond will be derivatized, probably due to steric hindrance [48, 49]. Obviously, this is not the case for conjugated fatty acids since 10E,12Z-CLA is trans,cis-configured and DMDS reacted with both DBs.

3.3.5.1.4 α- and γ-Linolenic acid (C18:3)

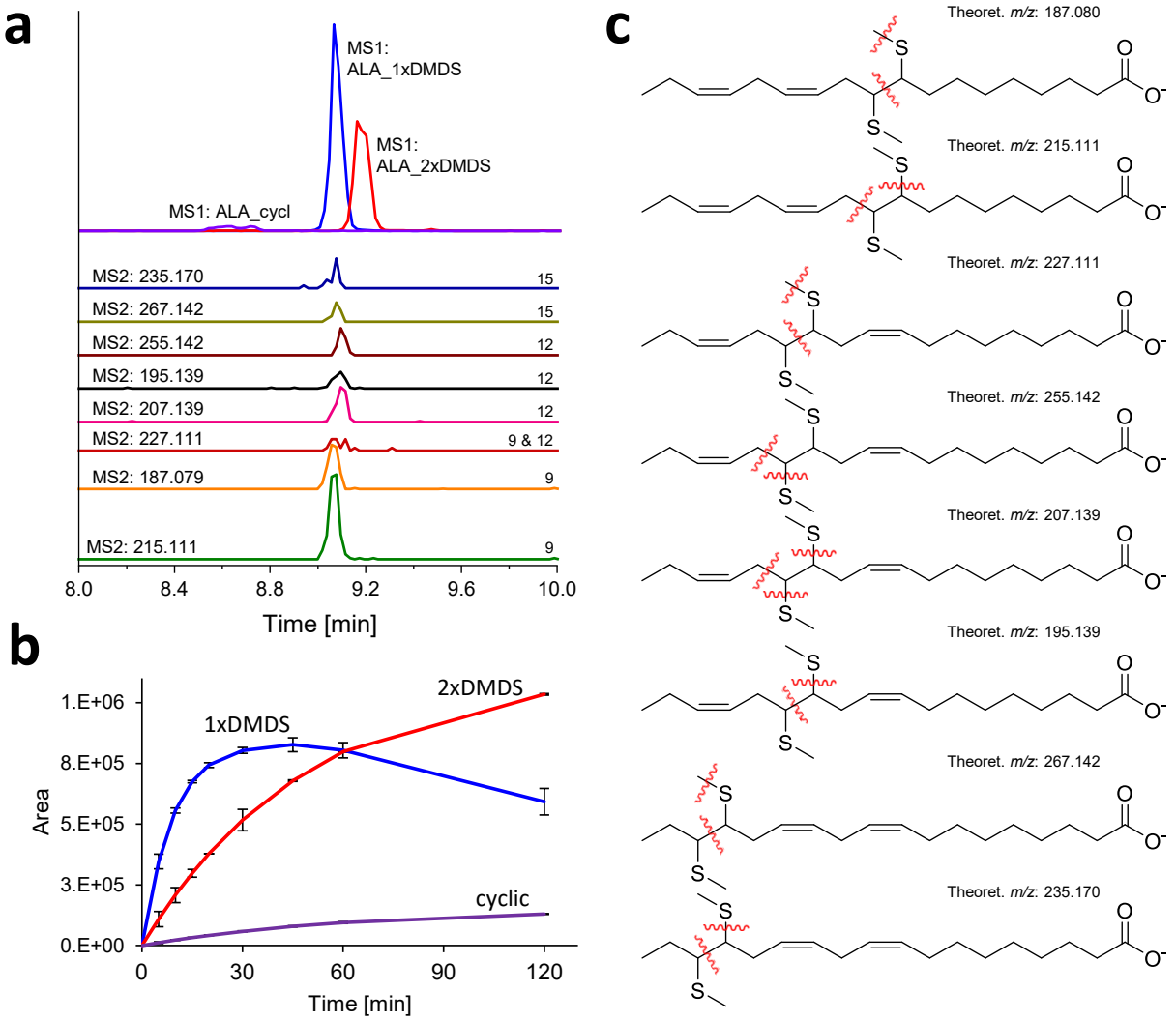

Figure 4: DMDS-derivatized α-linolenic acid (C18:3n-3,6,9); a: MS1-EIC of mono-derivatized α-linolenic acid (blue; *m/z* 371.208 ± 0.01 Da), bis-derivatized α-linolenic acid (red; *m/z* 465.200 ± 0.01 Da) and cyclic products (purple, *m/z* 403.178 ± 0.01 Da) from TOF-MS scan, MS2-EICs (CE: 45 V) of fragments (300-fold increased: *m/z* 227.111, 235.170, 255.142, 267.142; 100-fold multiplied: *m/z* 195.139, 215.111, 187.080, 207.139) from PIS (MRM-HR) of mono-derivatized α-linolenic acid; b: derivatization kinetics (fitted, mono-derivatized: ExpGrowDec, di-derivatized: BoxLucas1, cyclic product: BoxLucas1); c: proposed fragmentation patterns leading to characteristic fragments

α-Linolenic acid (ALA, C18:3n-3,6,9) is one of the most important (essential) ω-3 fatty acids, bearing its DBs on position 9, 12 and 15. After DMDS-derivatization the mono-derivatized product was used for the assignment of DB positions, but also bis-derivatized and cyclic products were observed (Figure 4a). The reaction kinetics displays a slow decrease of mono-derivatized products after an initial exponential increase, mainly due to increasing formation of bis-derivatized products (Figure 4b). DMDS-mono-derivatives of all three double bonds can be found. Double bond position 9 can be determined by presence of fragment ions with *m/z* 187.080, 153.092 and

215.111, of which the main fragment ion is *m/z* 215.111 like for linoleic acid. Double bond position 12 is characterized by the fragments with *m/z* 207.139, 195.139, 225.095 and 213.095, while the derivative at the double bond position 15 exhibits fragment ions of *m/z* 267.142 and 235.170. Tentative fragmentation patterns can be seen in Figure 4c. It must be considered that the fragments for double bond position 15 can also be found in the discussed conjugated linoleic acids and only in low intensities which could be due to steric hindrance during the derivatization reaction. Therefore, for the unequivocal assignment of the fragments to the respective precursor, a chromatographic separation could be helpful which is achieved in the present case, e.g. for α- and γ-Linolenic acid and other PUFAs like mentioned CLAs.

Nevertheless, a differentiation between α- and γ-Linolenic acid by their MS2 spectra or MS2-EICs of characteristic fragments is possible, since they exhibit completely different fragment ions. γ-Linolenic acid (C18:3n-6,9,12) with double bond position 6, 9 and 12 shows a significantly faster decrease in mono-derivatized product (Figure S15b) and a double peak in its MS1-EIC, which can be explained with different attachment-sites of the DMDS reagent. All 3 DBs can be derivatized to mono-derivatized products. MS2-fragment ions with *m/z* 197.064 and 183.048 can be assigned to double bond position 9, while *m/z* 185.067, 223.079 and 237.095 are presumably derived from derivatives at position 12 (see Figure S15). For position 6 derivative, some fragments (like *m/z* 142.083) were found to correlate with the first eluting MS1-peak, but a fragmentation pattern could not be suggested. MS2 spectra for derivatized α-and γ-Linolenic acid can be found in Figure S16, S17 and S18.

3.3.5.1.5 Mixture of polyunsaturated fatty acids

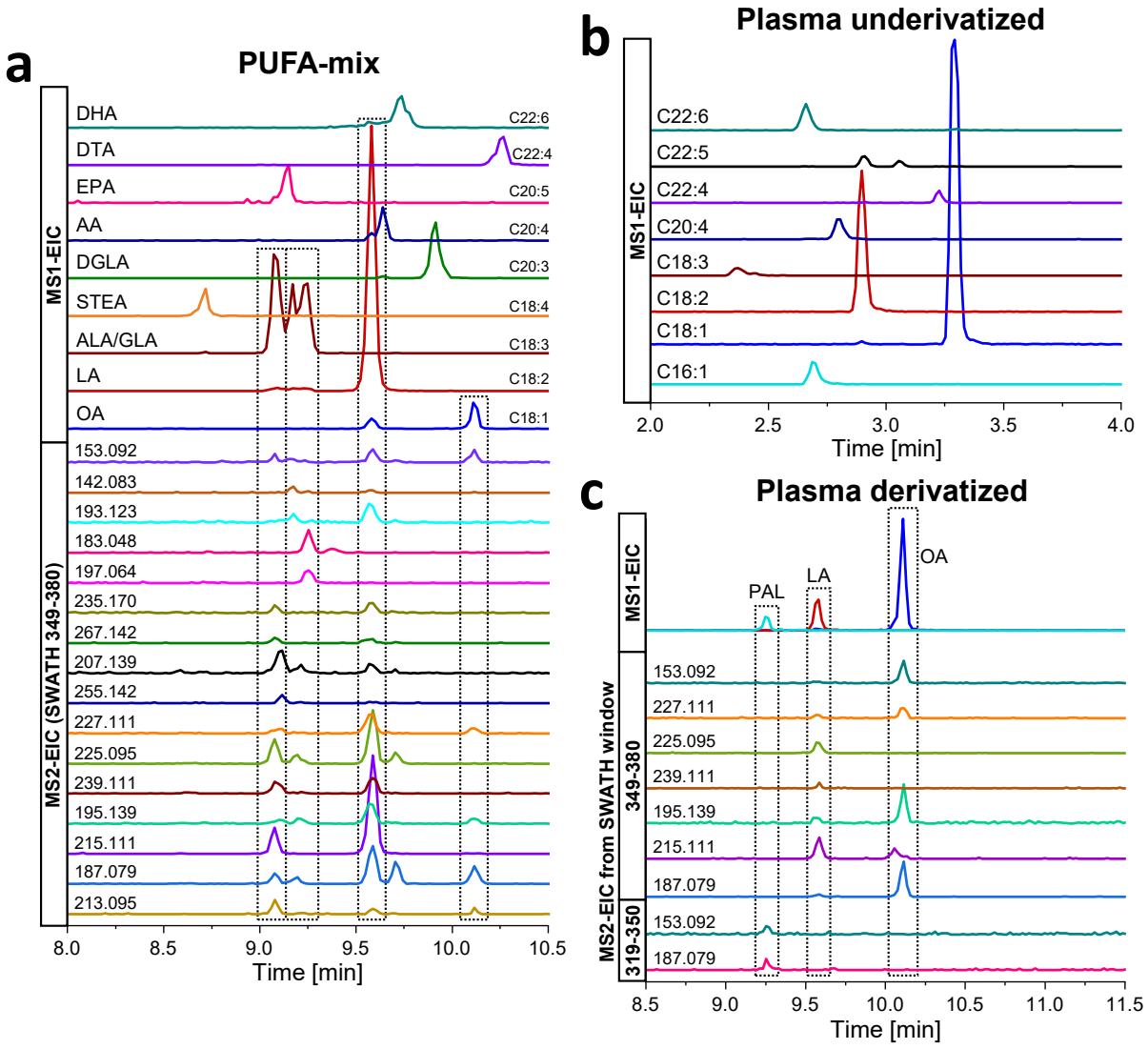

Figure 5: SWATH-MS measurements of DMDS-derivatized PUFA-mix (a), underivatized plasma extract (b) and DMDS-derivatized plasma extract (c); a: MS1-EIC of mono-derivatized oleic acid (OA, *m/z* 375.239 ± 0.01 Da), linoleic acid (LA, *m/z* 373.224 ± 0.01 Da), α-/γ-linolenic acid (ALA/GLA, *m/z* 371.208 ± 0.01 Da), stearidonic acid (STEA, *m/z* 369.193 ± 0.01 Da), dihomo-γ-linolenic acid (DGLA, *m/z* 399.240 ± 0.01 Da), arachidonic acid (AA, *m/z* 397.224 ± 0.01 Da), eicosapentaenoic acid (EPA, *m/z* 395.208 ± 0.01 Da, multiplied with 10 for better visibility), docosatetraenoic acid (DTA, *m/z* 425.255 ± 0.01 Da, multiplied with 2 for better visibility) and docosahexaenoic acid (DHA, *m/z* 421.224 ± 0.01 Da, multiplied with 2 for better visibility); MS2-EICs (CE: 45 V) of characteristic fragments from SWATH window *m/z* 349-380 (20-fold multiplied: *m/z* 187.080, 215.111, 195.139, 225.095; 50-fold multiplied: *m/z* 239.111, 227.111, 255.142, 207.139, 267.142, 235.170, 197.064, 183.048, 193.123); b: Underivatized plasma extract: MS1-EICs of underivatized C16:1, C18:1, C18:2, C18:3, C20:4, C22:4, C22:5 and C22:6 (assigned with MS-Dial, but does not allow a statement about double bond positions); c: Derivatized plasma extract: MS1-EIC of derivatized FAs with assigned double bond positions: palmitoleic acid (C16:1), oleic acid (C18:1) and linoleic acid (C18:2). And corresponding MS2-EICs (CE: 45 V) of their characteristic fragments (60-fold multiplied (SWATH window *m/z* 319-350): *m/z* 153.092, 187.080; 40-fold multiplied (SWATH window *m/z* 349-380): *m/z* 227.111, 225.095, 239.111, 195.139, 215.111; 10-fold-multiplied (SWATH window *m/z* 349-380): *m/z* 187.080). All MS1-EICs are extracted from the TOF-MS scans and MS2-EIC from respective SWATH-MS windows

Above experiments were carried out with single standard mixtures. To evaluate applicability to samples in which multiple MUFAs and PUFAs are present simultaneously, it is required that there is adequate specificity of the process, either by LC or MS selectivity. Data were recorded by SWATH-acquisition which is a preferential measurement technique in untargeted mass spectrometric analysis for detection of isomers of unknowns in complex samples (as MS2 EICs may be isomer selective) and/or when there is interest in the detection of multiple analytes by targeted MS2-experiments. This is often the case for lipid- or PUFA-containing samples due to their susceptibility to oxidation and further complex degradation reactions [3, 52, 53]. Herein, SWATH-MS was selected to study the reaction products as it allows to enable the extraction of EICs both from precursor and product ions. Retention time overlapping of the EICs of a specific peak group is a good evidence supporting the structural annotations. Overall, the availability of MS2-EIC chromatograms turned out to be helpful for the processing of the data and interpretation of the results.

A commercially available mixture of MUFA and PUFA standards (Polyunsaturated Fatty Acid MaxSpec LC-MS Mixture from Cayman Chemical Company) was derivatized with DMDS and analyzed by the same method (for composition see Figure 5a plus docosapentaenoic acid). As discussed above, the different derivatization kinetics suggests varying incubation time optima for different fatty acids, therefore 30 min was selected as a compromise. The results are depicted in Figure 5a. The DMDS-derivatization of the PUFA-mix showed mono-derivatized products for all contained fatty acids (docosapentaenoic acid (DPA) only shown in Figure S19 due to very low intensity). It becomes evident from Figure 5a that the fatty acids with lower number of DBs (LA, ALA/GLA) were observed with higher signal intensities. Although derivatization products of fatty acids with more than three DBs were observed, the unequivocal determination of DB positions was not easily possible due to lack of characteristic fragments and low intensities in MS2-spectra. This might be due to low intensities of mono-derivatized and very high intensities of bis-derivatized products (see Figure S19), which maybe could be optimized in the future to achieve higher yields of mono-derivatized products.

For C18:1/C18:2/C18:3 the DB positions could be assigned based on MS2-EICs of the characteristic fragments discussed in the chapters above. Figure 5a depicts overlays of MS1 EICs (mono-derivatized FAs) with the MS2-EICs of the respective fragments found in the SWATH-window (Q1 precursor isolation window *m/z* 349-380). MS1-EIC of C18:3 showed three peaks, of which the first peak can be assigned to ALA based on aligned MS2 peaks in EICs for the fragments of *m/z* 187.080 and 215.111 for position 9, *m/z* 207.139 and 213.095 for position 12 and *m/z* 235.170 and 267.142 for position 15. The second and third peak, on contrary, can be

assigned to GLA based on retention time of MS2-EICs of fragments with *m/z* 142.083, 183.048 and 197.064. Unfortunately, fragments with *m/z* 223.080 and 237.096 for position 12 are missing which could be e.g. due to incomplete derivatization or insufficient sensitivity. The presence of linoleic acid (LA) was confirmed by occurrence of fragment ion with *m/z* 187.080 and 215.111 for position 9 and *m/z* 195.139, 239.111 and 225.095 for position 12. The peak of C18:1 was assigned to oleic acid due to the occurrence of the *m/z* 187.080 fragment and absence of any additional fragment peak of *m/z* 215.111 which would correlate to the isomer vaccenic acid.
Dihomo-γ-linolenic acid (C20:3n-6,9,12; double bond position 8, 11, 14) similarly to ALA and GLA exhibits mono- and bis-derivatized products, whereby the assessment of DB position was made with the mono-derivatized product. Although the intensities were lower when compared to ALA/GLA, a possible assignment of characteristic fragments and MS2-spectra can be found in Figure S20, S21 and S22.

3.3.5.1.6 Plasma extract

Practical applicability was then tested with plasma. Prior to derivatization with DMDS, the plasma extract was measured underivatized and its free fatty acid profile was determined with MS-DIAL (Figure 5b). C18:1 and C18:2 fatty acids were observed in high amounts while C16:1, C18:3, C20:4, C22:4, C22:5 and C22:6 fatty acids were only detected at lower levels. After derivatization, mono-derivatized products for C16:1, C18:1 and C18:2 were found (Figure 5c). C16:1 was assigned to palmitoleic acid due to presence of the fragment with *m/z* 187.079 and 153.092 for position 9 in the SWATH-window of *m/z* 319-350. The C18:2 fatty acid was assigned to linoleic acid by occurrence of fragments with *m/z* 215.111, 187.080 (position 9) and *m/z* 225.095, 195.139, 239.111 (position 12) in the SWATH-window of *m/z* 349-380. C18:1 is mainly assigned to oleic acid due to the major fragment ion of *m/z* 187.080, characteristic for position 9. However, there is a slight fronting which together with the occurrence of fragment ion of *m/z* 215.111 might indicate the presence of vaccenic acid in the plasma extract. This possibility to distinguish isobaric interferences by MS2-EIC in untargeted LC-MS analysis emphasizes the benefits of SWATH-acquisition.

3.3.5.2 Discussion

Impressive amounts of publications exist which utilize Paternò-Büchi reactions for the determination of DB positions shown in various applications and matrices [13, 15]. Therein, the performance of those methods strongly depends on the selected derivatization reagent and was subsequently optimized, reducing the disadvantages of the initially used reagent (acetone: side reactions, low yield and *m/z* overlap) [13]. Therefore, we believe that disulfide reagents can be further optimized in a similar manner to allow wider applicability in LC-MS.

The usage of disulfide-reagents allows a relatively fast, simple and cost-effective workflow, due to independence from specific hardware, typically used in some of the other methods for DB position determination (e.g. UVPD, OzID, EAD [17]). Additionally, due to the introduction of sulfur in the derivatized target analytes characteristic isotope patterns due to ^{34}S isotope provide additional information for structural annotation. Further, this method does not need UV-light to enable the reaction, which was in the focus for side reactions and potential health risks [17, 54].

DMDS as double bond derivatization agent in LC-MS in combination with SWATH-acquisition is a viable strategy to pinpoint DB positions of fatty acids with up to 3 double bonds. However, the assignment of fragment ions and evaluation of MS2-spectra gets more difficult with increasing number of DBs. Double bond positions of conjugated fatty acids are less straightforward to distinguish from their unconjugated counterparts. DMDS-derivatization of fatty acids is limited to the negative ion mode and provides only characteristic fragment ions from the carboxy-terminal tail. It was shown that DPDS is a viable option to solve this issue, as it allows detection in positive mode and therefore leads to predictable fragmentation which allows straightforward design of two preferred MRM transitions with a characteristic fragment ion from either end of the original DB. The concept can therefore be easily transferred to targeted UHPLC-ESI-QqQ-MS/MS technology with MRM acquisition. The application to fatty acids with more than three double bonds and real samples needs further optimization like the methodology with DPDS as reagent. Further screening of distinct disulfide derivatives like cystine derivatives could be promising as well. Cystine or other functional disulfides allow tuning of the MS properties via amino and/or carboxy group as well as the introduction of specific tags via those reactive groups.

3.3.6 Conclusion

In this research, we presented the transfer of an established simple and cost-effective method for positional determination of C=C-DBs in fatty acids from GC-MS to LC-MS to extend the analyst´s "toolbox" for the comprehensive profiling of fatty acid containing samples. The derivatization with DMDS in combination with targeted product ion scan (MRM-HR) or untargeted SWATH (MS/MS) detection allowed the straightforward differentiation of DB positions in fatty acids with up to three double bonds. With higher number of double bonds the differentiation is less straightforward. The applicability of this workflow was also documented for a mixture of PUFAs and for a plasma sample. Derivatization with DPDS introduced pyridine rings into the fatty acids, allowing LC-MS measurements in positive ion mode. It also delivered clearer MS2-spectra, simplifying the evaluation and allowed a better differentiation of LA (double bond position 9) from OA and PAL (double bond position 9) on MS2-level due to detectable fragments of the omega-end. The methodology with DPDS, however, needs further optimization. Derivatization of fatty acids with more than three double bonds was not possible in this preliminary proof-of-principle evaluation. However, the approach with DPDS indicated the potential for use of tailor-made disulfide-based derivatization reagents to achieve higher derivatization efficiencies, optimized ionization and specific fragmentation, and applicability to fatty acids with more than two double bonds. The applicability of the presented derivatization reagents on larger lipid groups (e.g. glycerolipids, glycerophospholipids) was not tested in this study, but should be possible. Especially DPDS can be advantageous for mono-unsaturated lipids since it is not dependent on the ionization properties of the target molecule. We presented here a proof of principle study on the reactivity of the disulfide agents and their characteristic fragmentations. A follow up study will address the further optimization in view of real sample application and validation of the methodology.

Conflict of interest statement

The authors declare that they have no known competing financial interest or personal relationships that could have appeared to influence the work reported in this paper.

3.3.7 References

[1] U.N. Das, Essential fatty acids: biochemistry, physiology and pathology, Biotechnology Journal 1(4) (2006) 420-439. https://doi.org/10.1002/biot.200600012.

[2] S. Takashima, K. Toyoshi, T. Yamamoto, N. Shimozawa, Positional determination of the carbon–carbon double bonds in unsaturated fatty acids mediated by solvent plasmatization using LC–MS, Scientific Reports 10(1) (2020) 12988. https://doi.org/10.1038/s41598-020-69833-y.

[3] M. Olfert, S. Bäurer, M. Wolter, S. Buckenmaier, E. Brito-de la Fuente, M. Lämmerhofer, Comprehensive profiling of conjugated fatty acid isomers and their lipid oxidation products by two-dimensional chiral RP×RP liquid chromatography hyphenated to UV- and SWATH-MS-detection, Analytica Chimica Acta 1202 (2022) 339667. https://doi.org/10.1016/j.aca.2022.339667.

[4] M. Asif, Health effects of omega-3,6,9 fatty acids: Perilla frutescens is a good example of plant oils, Oriental Pharmacy & Experimental Medicine 11(1) (2011) 51-59. https://doi.org/10.1007/s13596-011-0002-x.

[5] A.P. Simopoulos, N.G. Bazán, Omega-3 Fatty Acids, the Brain and Retina, Karger2009.

[6] International Conference on Harmonisation of Technical Requirements for Registration of Pharmaceuticals for Human Use, ICH Harmonised Tripartite Guideline: Impurities in New Drug Substances Q3A (R2), 2006. https://database.ich.org/sites/default/files/Q3A%28R2%29%20Guideline.pdf. (Accessed 14th May 2024).

[7] International Conference on Harmonisation of Technical Requirements for Registration of Pharmaceuticals for Human Use, ICH Harmonised Tripartite Guideline: Impurities in New Drug Products Q3B (R2), 2006. https://database.ich.org/sites/default/files/Q3B%28R2%29%20Guideline.pdf. (Accessed 15th May 2024).

[8] C. Pepe, P. Dizabo, J. Dagaut, N. Balcar, M.F. Lautier, Letter: Determination of Double Bond Position in Di-Unsaturated Alkadienes by Means of Mass Spectrometry of Dimethyl Disulfide Derivatives, European Mass Spectrometry 1(2) (1995) 209-211. https://doi.org/10.1255/ejms.127.

[9] E. Koch, A. Löwen, N. Kampschulte, K. Plitzko, M. Wiebel, K.M. Rund, I. Willenberg, N.H. Schebb, Beyond Autoxidation and Lipoxygenases: Fatty Acid Oxidation Products in Plant Oils, Journal of Agricultural and Food Chemistry 71(35) (2023) 13092-13106. https://doi.org/10.1021/acs.jafc.3c02724.

[10] S. Liao, G. Sherman, Y. Huang, Elucidation of double-bond positions of polyunsaturated alkenes through gas chromatography/mass spectrometry analysis of mono-dimethyl disulfide derivatives, Rapid Communications in Mass Spectrometry 36(3) (2022) e9228. https://doi.org/10.1002/rcm.9228.

[11] S. Liao, Y. Huang, Preferential formation of mono-dimethyl disulfide adducts for determining double bond positions of poly-unsaturated fatty acids, Journal of the American Oil Chemists' Society 99(4) (2022) 279-288. https://doi.org/10.1002/aocs.12561.

[12] S.J.K.A. Ubhayasekera, J. Staaf, A. Forslund, P. Bergsten, J. Bergquist, Free fatty acid determination in plasma by GC-MS after conversion to Weinreb amides, Analytical and Bioanalytical Chemistry 405(6) (2013) 1929-1935. https://doi.org/10.1007/s00216-012-6658-3.

[13] C. Chen, R. Li, H. Wu, Recent progress in the analysis of unsaturated fatty acids in biological samples by chemical derivatization-based chromatography-mass spectrometry methods, Journal of Chromatography B 1215 (2023) 123572. https://doi.org/10.1016/j.jchromb.2022.123572.

[14] L. Yang, J. Yuan, B. Yu, S. Hu, Y. Bai, Sample preparation for fatty acid analysis in biological samples with mass spectrometry-based strategies, Analytical and Bioanalytical Chemistry 416(9) (2024) 2371-2387. https://doi.org/10.1007/s00216-024-05185-0.

[15] W. Zhang, R. Jian, J. Zhao, Y. Liu, Y. Xia, Deep-lipidotyping by mass spectrometry: recent technical advances and applications, Journal of Lipid Research 63(7) (2022) 100219. https://doi.org/10.1016/j.jlr.2022.100219.

[16] T.W. Mitchell, S.H.J. Brown, S.J. Blanksby, Structural Lipidomics, Lipidomics2012, pp. 99-128. https://doi.org/https://doi.org/10.1002/9783527655946.ch6.

[17] H. Lu, H. Zhang, S. Xu, L. Li, Review of Recent Advances in Lipid Analysis of Biological Samples via Ambient Ionization Mass Spectrometry, Metabolites 11(11) (2021) 781.

[18] X. Ma, Y. Xia, Pinpointing Double Bonds in Lipids by Paternò-Büchi Reactions and Mass Spectrometry, Angewandte Chemie International Edition 53(10) (2014) 2592-2596. https://doi.org/10.1002/anie.201310699.

[19] A. Cerrato, A.L. Capriotti, C. Cavaliere, C.M. Montone, S. Piovesana, A. Laganà, Novel Aza-Paternò-Büchi Reaction Allows Pinpointing Carbon–Carbon Double Bonds in Unsaturated Lipids by Higher Collisional Dissociation, Analytical Chemistry 94(38) (2022) 13117-13125. https://doi.org/10.1021/acs.analchem.2c02549.

[20] J. Zhao, X. Xie, Q. Lin, X. Ma, P. Su, Y. Xia, Next-Generation Paternò–Büchi Reagents for Lipid Analysis by Mass Spectrometry, Analytical Chemistry 92(19) (2020) 13470-13477. https://doi.org/10.1021/acs.analchem.0c02896.

[21] P. Esch, S. Heiles, Charging and Charge Switching of Unsaturated Lipids and Apolar Compounds Using Paternò-Büchi Reactions, Journal of the American Society for Mass Spectrometry 29(10) (2018) 1971-1980. https://doi.org/10.1007/s13361-018-2023-x.

[22] R.C. Murphy, T. Okuno, C.A. Johnson, R.M. Barkley, Determination of Double Bond Positions in Polyunsaturated Fatty Acids Using the Photochemical Paternò-Büchi Reaction with Acetone and Tandem Mass Spectrometry, Analytical Chemistry 89(16) (2017) 8545-8553. https://doi.org/10.1021/acs.analchem.7b02375.

[23] S.-l. Xu, B.-f. Wu, M. Orešič, Y. Xie, P. Yao, Z.-y. Wu, X. Lv, H. Chen, F. Wei, Double Derivatization Strategy for High-Sensitivity and High-Coverage Localization of Double Bonds in Free Fatty Acids by Mass Spectrometry, Analytical Chemistry 92(9) (2020) 6446-6455. https://doi.org/10.1021/acs.analchem.9b05588.

[24] H. Shi, Y. Xia, Shotgun Lipidomic Profiling of Sebum Lipids via Photocatalyzed Paternò–Büchi Reaction and Ion Mobility-Mass Spectrometry, Analytical Chemistry 96(14) (2024) 5589-5597. https://doi.org/10.1021/acs.analchem.4c00141.

[25] Y. Zhao, H. Zhao, X. Zhao, J. Jia, Q. Ma, S. Zhang, X. Zhang, H. Chiba, S.-P. Hui, X. Ma, Identification and Quantitation of C═C Location Isomers of Unsaturated Fatty Acids by Epoxidation Reaction and Tandem Mass Spectrometry, Analytical Chemistry 89(19) (2017) 10270-10278. https://doi.org/10.1021/acs.analchem.7b01870.

[26] Y. Feng, B. Chen, Q. Yu, L. Li, Identification of Double Bond Position Isomers in Unsaturated Lipids by m-CPBA Epoxidation and Mass Spectrometry Fragmentation, Analytical Chemistry 91(3) (2019) 1791-1795. https://doi.org/10.1021/acs.analchem.8b04905.

[27] T.-H. Kuo, H.-H. Chung, H.-Y. Chang, C.-W. Lin, M.-Y. Wang, T.-L. Shen, C.-C. Hsu, Deep Lipidomics and Molecular Imaging of Unsaturated Lipid Isomers: A Universal Strategy Initiated by mCPBA Epoxidation, Analytical Chemistry 91(18) (2019) 11905-11915. https://doi.org/10.1021/acs.analchem.9b02667.

[28] C. Song, D. Gao, S. Li, L. Liu, X. Chen, Y. Jiang, Determination and quantification of fatty acid C=C isomers by epoxidation reaction and liquid chromatography-mass spectrometry, Analytica Chimica Acta 1086 (2019) 82-89. https://doi.org/10.1016/j.aca.2019.08.023.

[29] R. Sun, W. Tang, P. Li, B. Li, Development of an Efficient On-Tissue Epoxidation Reaction Mediated by Urea Hydrogen Peroxide for MALDI MS/MS Imaging of Lipid C═C Location Isomers, Analytical Chemistry 95(43) (2023) 16004-16012. https://doi.org/10.1021/acs.analchem.3c03262.

[30] Y. Li, Y. Wang, K. Guo, K.-f. Tseng, X. Zhang, W. Sun, Aza-Prilezhaev Aziridination-Enabled Multidimensional Analysis of Isomeric Lipids via High-Resolution U-Shaped Mobility Analyzer–Mass Spectrometry, Analytical Chemistry 96(18) (2024) 7111-7119. https://doi.org/10.1021/acs.analchem.4c00481.

[31] Y. Li, J. Bai, K. Tseng, X. Zhang, L. Zhang, J. Zhang, W. Sun, Y. Guo, Intramolecular Ring–Chain Equilibrium Elimination Strategy for Pinpointing C═C Positional and Geometric Isomers of N-Alkylpyridinium Unsaturated Fatty Acid Derivatives via Ion Mobility-Mass Spectrometry, Analytical Chemistry 96(5) (2024) 1977-1984. https://doi.org/10.1021/acs.analchem.3c04320.

[32] K. Yang, B.G. Dilthey, R.W. Gross, Identification and Quantitation of Fatty Acid Double Bond Positional Isomers: A Shotgun Lipidomics Approach Using Charge-Switch Derivatization, Analytical Chemistry 85(20) (2013) 9742-9750. https://doi.org/10.1021/ac402104u.

[33] Y. Feng, Y. Lv, T.-J. Gu, B. Chen, L. Li, Quantitative Analysis and Structural Elucidation of Fatty Acids by Isobaric Multiplex Labeling Reagents for Carbonyl-Containing Compound (SUGAR) Tags and m-CPBA Epoxidation, Analytical Chemistry 94(38) (2022) 13036-13042. https://doi.org/10.1021/acs.analchem.2c01917.

[34] T. Higashi, M. Takekawa, J.Z. Min, T. Toyo'oka, Diels–Alder derivatization for sensitive detection and characterization of conjugated linoleic acids using LC/ESI-MS/MS, Analytical and Bioanalytical Chemistry 403(2) (2012) 495-502. https://doi.org/10.1007/s00216-012-5819-8.

[35] A. Cerrato, C. Cavaliere, A. Laganà, C.M. Montone, S. Piovesana, A. Sciarra, E. Taglioni, A.L. Capriotti, First Proof of Concept of a Click Inverse Electron Demand Diels–Alder Reaction for Assigning the Regiochemistry of Carbon–Carbon Double Bonds in Untargeted Lipidomics, Analytical Chemistry 96(26) (2024) 10817-10826. https://doi.org/10.1021/acs.analchem.4c02146.

[36] K.A. Harrison, R.C. Murphy, Direct Mass Spectrometric Analysis of Ozonides: Application to Unsaturated Glycerophosphocholine Lipids, Analytical Chemistry 68(18) (1996) 3224-3230. https://doi.org/10.1021/ac960302c.

[37] M.C. Thomas, T.W. Mitchell, D.G. Harman, J.M. Deeley, R.C. Murphy, S.J. Blanksby, Elucidation of Double Bond Position in Unsaturated Lipids by Ozone Electrospray Ionization Mass Spectrometry, Analytical Chemistry 79(13) (2007) 5013-5022. https://doi.org/10.1021/ac0702185.

[38] M.C. Thomas, T.W. Mitchell, D.G. Harman, J.M. Deeley, J.R. Nealon, S.J. Blanksby, Ozone-Induced Dissociation: Elucidation of Double Bond Position within Mass-Selected Lipid Ions, Analytical Chemistry 80(1) (2008) 303-311. https://doi.org/10.1021/ac7017684.

[39] J.L. Campbell, T. Baba, Near-Complete Structural Characterization of Phosphatidylcholines Using Electron Impact Excitation of Ions from Organics, Analytical Chemistry 87(11) (2015) 5837-5845. https://doi.org/10.1021/acs.analchem.5b01460.

[40] P.H. Mueller, Gérard, De-Novo Structural Elucidation of Acylglycerols by Collision-Induced Dissociation of Odd-Electron Ion Precursors and by Electron Activated Dissociation of Even-Electron Ion Precursors, ChemRxiv, This content is a preprint and has not been peer-reviewed. (2024). https://doi.org/10.26434/chemrxiv-2024-2xh03.

[41] V.B. O'Donnell, E.A. Dennis, M.J.O. Wakelam, S. Subramaniam, LIPID MAPS: Serving the next generation of lipid researchers with tools, resources, data, and training, Science Signaling 12(563) (2019) eaaw2964. https://doi.org/doi:10.1126/scisignal.aaw2964.

[42] G. Liebisch, J.A. Vizcaíno, H. Köfeler, M. Trötzmüller, W.J. Griffiths, G. Schmitz, F. Spener, M.J.O. Wakelam, Shorthand notation for lipid structures derived from mass spectrometry, Journal of Lipid Research 54(6) (2013) 1523-1530. https://doi.org/https://doi.org/10.1194/jlr.M033506.

[43] H.R. Buser, H. Arn, P. Guerin, S. Rauscher, Determination of double bond position in mono-unsaturated acetates by mass spectrometry of dimethyl disulfide adducts, Analytical Chemistry 55(6) (1983) 818-822. https://doi.org/10.1021/ac00257a003.

[44] E. Dunkelblum, S.H. Tan, P.J. Silk, Double-bond location in monounsaturated fatty acids by dimethyl disulfide derivatization and mass spectrometry: Application to analysis of fatty acids in pheromone glands of four lepidoptera, Journal of Chemical Ecology 11(3) (1985) 265-277. https://doi.org/10.1007/BF01411414.

[45] N. Richter, J.T. Dillon, D.M. Rott, M.A. Lomazzo, C.T. Seto, Y. Huang, Optimizing the yield of transient mono-dimethyl disulfide adducts for elucidating double bond positions of long chain alkenones, Organic Geochemistry 109 (2017) 58-66. https://doi.org/10.1016/j.orggeochem.2017.02.003.

[46] P. Deng, D. Zhong, X. Wang, Y. Dai, L. Zhou, Y. Leng, X. Chen, Analysis of diacylglycerols by ultra performance liquid chromatography-quadrupole time-of-flight mass spectrometry: Double bond location and isomers separation, Analytica Chimica Acta 925 (2016) 23-33. https://doi.org/https://doi.org/10.1016/j.aca.2016.04.051.

[47] M. Eggink, M. Wijtmans, A. Kretschmer, J. Kool, H. Lingeman, I.J.P. de Esch, W.M.A. Niessen, H. Irth, Targeted LC–MS derivatization for aldehydes and carboxylic acids with a new derivatization agent 4-APEBA, Analytical and Bioanalytical Chemistry 397(2) (2010) 665-675. https://doi.org/10.1007/s00216-010-3575-1.

[48] S. Shibamoto, T. Murata, W. Lu, K. Yamamoto, Preparation of Dimethyl Disulfide Adducts from the Mono-Trans Octadecadienoic Acid Methyl Esters, Lipids 53(6) (2018) 653-659. https://doi.org/10.1002/lipd.12047.

[49] S. Shibamoto, T. Murata, K. Yamamoto, Determination of Double Bond Positions and Geometry of Methyl Linoleate Isomers with Dimethyl Disulfide Adducts by GC/MS, Lipids 51(9) (2016) 1077-1081. https://doi.org/10.1007/s11745-016-4180-7.

[50] H. Yin, L. Xu, N.A. Porter, Free Radical Lipid Peroxidation: Mechanisms and Analysis, Chemical Reviews 111(10) (2011) 5944-5972. https://doi.org/10.1021/cr200084z.

[51] M. Gong, Y. Hu, W. Wei, Q. Jin, X. Wang, Production of conjugated fatty acids: A review of recent advances, Biotechnology Advances 37(8) (2019) 107454. https://doi.org/10.1016/j.biotechadv.2019.107454

[52] M. Cebo, C. Calderón Castro, J. Schlotterbeck, M. Gawaz, M. Chatterjee, M. Lämmerhofer, Untargeted UHPLC-ESI-QTOF-MS/MS analysis with targeted feature extraction at precursor and fragment level for profiling of the platelet lipidome with ex vivo thrombin-activation, Journal of Pharmaceutical and Biomedical Analysis 205 (2021) 114301. https://doi.org/10.1016/j.jpba.2021.114301.

[53] M. Cebo, J. Schlotterbeck, M. Gawaz, M. Chatterjee, M. Lämmerhofer, Simultaneous targeted and untargeted UHPLC-ESI-MS/MS method with data-independent acquisition for quantification and profiling of (oxidized) fatty acids released upon platelet activation by thrombin, Analytica Chimica Acta 1094 (2020) 57-69. https://doi.org/10.1016/j.aca.2019.10.005.

[54] G. Feng, Y. Hao, L. Wu, S. Chen, A visible-light activated [2 + 2] cycloaddition reaction enables pinpointing carbon–carbon double bonds in lipids, Chemical Science 11(27) (2020) 7244-7251. https://doi.org/10.1039/D0SC01149E.

3.3.8 Supporting Material

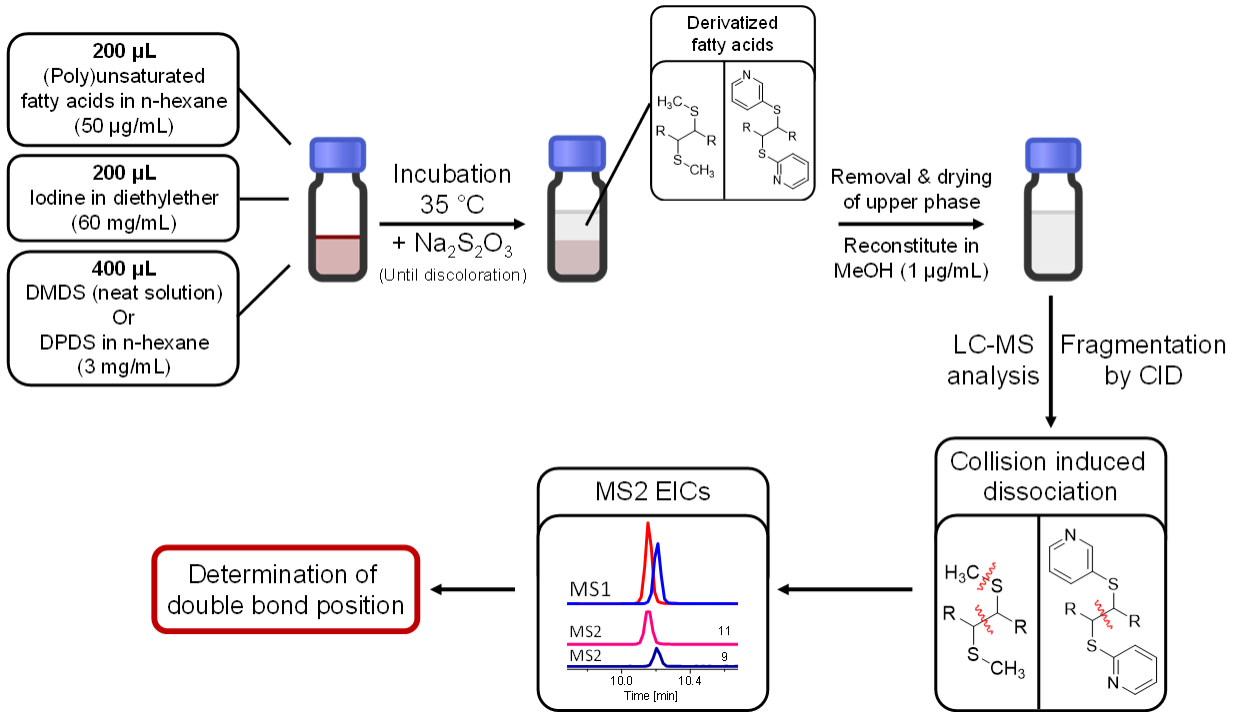

Figure S1: Utilized workflow for DMDS and DPDS sample preparation, followed by LC-MS analysis for double bond position determination. Figure was created with Chemix (https://chemix.org).

Table S1: Nomenclature and abbreviations of fatty acids used in this study. Information obtained from LIPID MAPS [1] and „LIPID MAPS Fatty acyl structure level" based on Liebisch et al. [2].

Common Name	Abbreviation	Systematic name	Short-hand	LIPID MAPS Fatty acyl structure level
Palmitoleic acid	PAL	9Z-hexadecenoic acid	C16:1n-7	FA 16:1 (9Z)
Oleic acid	OA	9Z-octadecenoic acid	C18:1n-9	FA 18:1 (9Z)
cis-Vaccenic acid	VA	11Z-octadecenoic acid	C18:1n-7	FA 18:1 (11Z)
Linoleic acid	LA	9Z,12Z-octadecadienoic acid	C18:2n-6,9	FA 18:2 (9Z,12Z)
Ricinenic acid	9Z,11Z-CLA	9Z,11Z-octadecadienoic acid	C18:2n-7,9	FA 18:2 (9Z,11Z)
10E,12Z-octadecadienoic acid	10E,12Z-CLA	10E,12Z-octadecadienoic acid	C18:2n-6,8	FA 18:2 (10E,12Z)
alpha-Linolenic acid	ALA	9Z,12Z,15Z-octadecatrienoic acid	C18:3n-3,6,9	FA 18:3 (9Z,12Z,15Z)
gamma-Linolenic acid	GLA	6Z,9Z,12Z-octadecatrienoic acid	C18:3n-6,9,12	FA 18:3 (6Z,9Z,12Z)
Stearidonic acid	STEA	6Z,9Z,12Z,15Z-octadecatetraenoic acid	C18:4n-3,6,9,12	FA 18:4 (6Z,9Z,12Z,15Z)
Dihomo-gamma-linolenic acid	DGLA	8Z,11Z,14Z-eicosatrienoic acid	C20:3n-6,9,12	FA 20:3 (8Z,11Z,14Z)
Arachidonic acid	AA	5Z,8Z,11Z,14Z-eicosatetraenoic acid	C20:4n-6,9,12,15	FA 20:4 (5Z,8Z,11Z,14Z)
EPA	EPA	5Z,8Z,11Z,14Z,17Z-eicosapentaenoic acid	C20:5n-3,6,9,12,15	FA 20:5 (5Z,8Z,11Z,14Z,17Z)
Adrenic acid	DTA	7Z,10Z,13Z,16Z-docosatetraenoic acid	C22:4n-6,9,12,15	FA 22:4 (7Z,10Z,13Z,16Z)
DPA	DPA	7Z,10Z,13Z,16Z,19Z-docosapentaenoic acid	C22:5n-3,6,9,12,15	FA 22:5 (7Z,10Z,13Z,16Z,19Z)
DHA	DHA	4Z,7Z,10Z,13Z,16Z,19Z-docosahexaenoic acid	C22:6n-3,6,9,12,15,18	FA 22:6 (4Z,7Z,10Z,13Z,16Z,19Z)

Table S2: Used SWATH-windows in untargeted measurements of MUFA/PUFA-mix and Plasma extract

SWATH-Experiment	Start *m/z*	Stop *m/z*
1	199	230
2	229	260
3	259	290
4	289	320
5	319	350
6	349	380
7	379	410
8	409	440
9	439	470
10	469	500
11	499	530
12	529	560
13	559	590
14	589	620
15	619	650
16	649	680
17	679	710
18	699	730
19	729	760
20	759	790

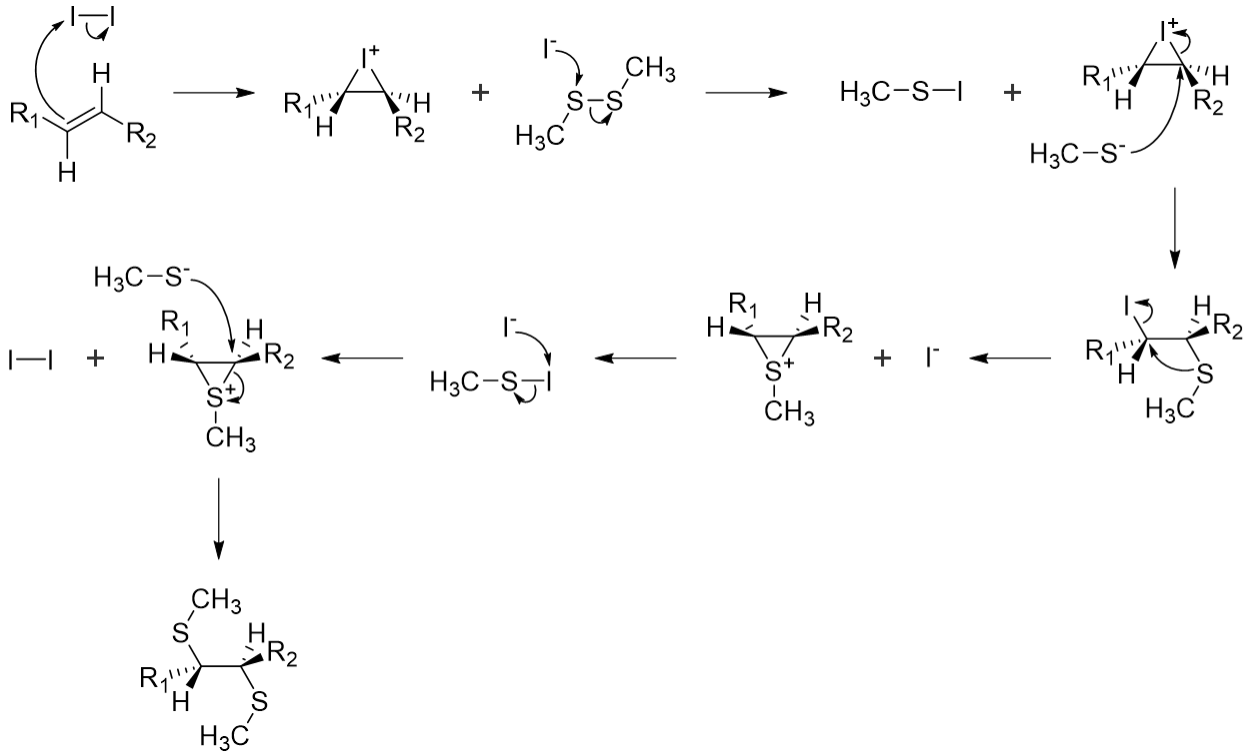

Figure S2: Mechanism for the derivatization of carbon-carbon double bonds with dimethyldisulfide, proposed by Richter et al. [3].

Table S3: Overview of experimentally observed fragments (*m/z*) and their occurrence for the different DMDS-derivatized fatty acids palmitoleic acid (PAL), oleic acid (OA), cis-vaccenic acid (VA), linoleic acid (LA), α-linolenic acid (ALA), γ-linolenic acid (GLA), 9,11-octadecadienoic acid (9,11-CLA) and 10,12-octadecadienoic acid (10,12-CLA). Here the intensity in the respective sample is visualized in decreasing order: +++ > ++ > + > -. Fields with no entry equal no occurrence of the fragment. Color code: blue: double bond position 6, yellow: double bond position 9, violet: double bond position 10, green: double bond position 11, orange: double bond position 12, red: double bond position 15

		C16:1n-7	C18:1n-9	C18:1n-7		C18:2n-6,9	C18:2n-7,9	C18:2n-6,8		C18:3n-3,6,9	C18:3n-6,9,12
	Precursor $[M-H]^-$	347.208	375.240	375.240	Precursor $[M-H]^-$	373.224	373.224	373.224	Precursor $[M-H]^-$	371.208	371.208
	DB-position	9	9	11	DB-position	9, 12	9, 11	10, 12	DB-position	9, 12, 15	6, 9, 12
Indicated DB-Position	Fragment m/z	PAL	OA	VA	Indicated DB-Position	LA	9,11-CLA	10,12-CLA	Indicated DB-Position	ALA	GLA
	142.083								6		++
9	153.092	++	++		9	+	++		9	+	-
	183.049								9		+++
9	187.079	+++	+++		9	++	++		9	++	
	195.139	++	++		12	++	+	+	12	+	
	197.064								9		+++
	201.095				10			++			
	207.139			-		-	+	+	12	++	-
	213.095	-	-		11	-	+		12	++	
11	215.111	-	-	+++	9	+++			9	+++	
	223.080								12		++
11	225.095			+	11 or 12	+++	+++	+	12	+++	+
	227.111	+	+	-	12	+		++	12	-	
	235.17					-	+	++	15	+	
	237.096								12		++
	239.111				11 or 12	+	+	+++	12	+	
11	241.127	-	-	+							
11	243.142			-							
11	255.142			+							
	267.142					-	+	+	15	+	

Table S4: Suggested transitions (*m/z*) for targeted MRM-Experiments of DMDS-derivatized fatty acids. Color code: blue: double bond position 6, yellow: double bond position 9, violet: double bond position 10, green: double bond position 11, orange: double bond position 12, red: double bond position 15

	PAL	OA	VA	LA	9Z,11Z-CLA	10E,12Z-CLA	ALA	GLA
	C16:1n-7	C18:1n-9	C18:1n-7	C18:2n-6,9	C18:2n-7,9	C18:2n-6,8	C18:3n-3,6,9	C18:3n-6,9,12
Precursor $[M-H]^-$	347.208	375.240	375.240	373.224	373.224	373.224	371.208	371.208
DB-Pos.	9	9	11	9, 12	9, 11	10, 12	9, 12, 15	6, 9, 12
6								142.083
9	153.092	153.092		187.079	153.092		187.079	183.049
	187.079	187.079		215.111	187.079		215.111	197.064
10						201.095		
11			215.111		213.095			
			241.127		225.095			
12				195.139		227.111	207.139	223.080
				227.111		239.111	213.095	237.096
15							235.170	
							267.142	

Table S5: Overview of experimentally observed fragments (*m/z*) and their occurrence for the different DPDS-derivatized fatty acids palmitoleic acid (PAL), oleic acid (OA), cis-vaccenic acid (VA) and linoleic acid (LA). Here the intensity in the respective sample is visualized in decreasing order: +++ > ++ > +. Fields with no entry equal no occurrence of the fragment. Color code: yellow: double bond position 9, orange: double bond position 11, blue: double bond position 12.

			C16:1n-7	C18:1n-9	C18:1n-7	C18:2n-6,9
		Precursor [M+H]$^+$	475.245	503.276	503.276	501.260
Which end?	**Indicated DB-Position**	**DB-position**	9	9	11	9, 12
		Fragment	**PAL**	**OA**	**VA**	**LA**
COOH	9	266.120	+++	++		+++
COOH	9	248.110	+++	+++		+++
omega-6 or -7	9, 11 or 12	208.116	+++	+	+++	+++
omega-9	9	236.147	+	+++		
COOH	11	276.142			++	
COOH	11	294.152			+++	
omega-6	12	194.099	+		+	+++
COOH	12	288.145				+
omega-9	9	234.131				++
COOH	9	262.127	+	+	+	+++
COOH	9	280.137	+	++		+++

Table S6: Suggested transitions (*m/z*) for targeted MRM-Experiments of DPDS-derivatized fatty acids. Color code: yellow: double bond position 9, orange: double bond position 11, blue: double bond position 12.

		C16:1n-7	C18:1n-9	C18:1n-7	C18:2n-6,9
	Precursor [M+H]$^+$	475.245	503.276	503.276	501.260
	DB-position	9	9	11	9, 12
DB-Pos.	**Which end?**	**PAL**	**OA**	**VA**	**LA**
9	COOH	248.11	248.11		248.11
	omega	208.116	236.147		234.131
11	COOH			294.152	
	omega			208.116	
12	COOH				288.145
	omega				208.116

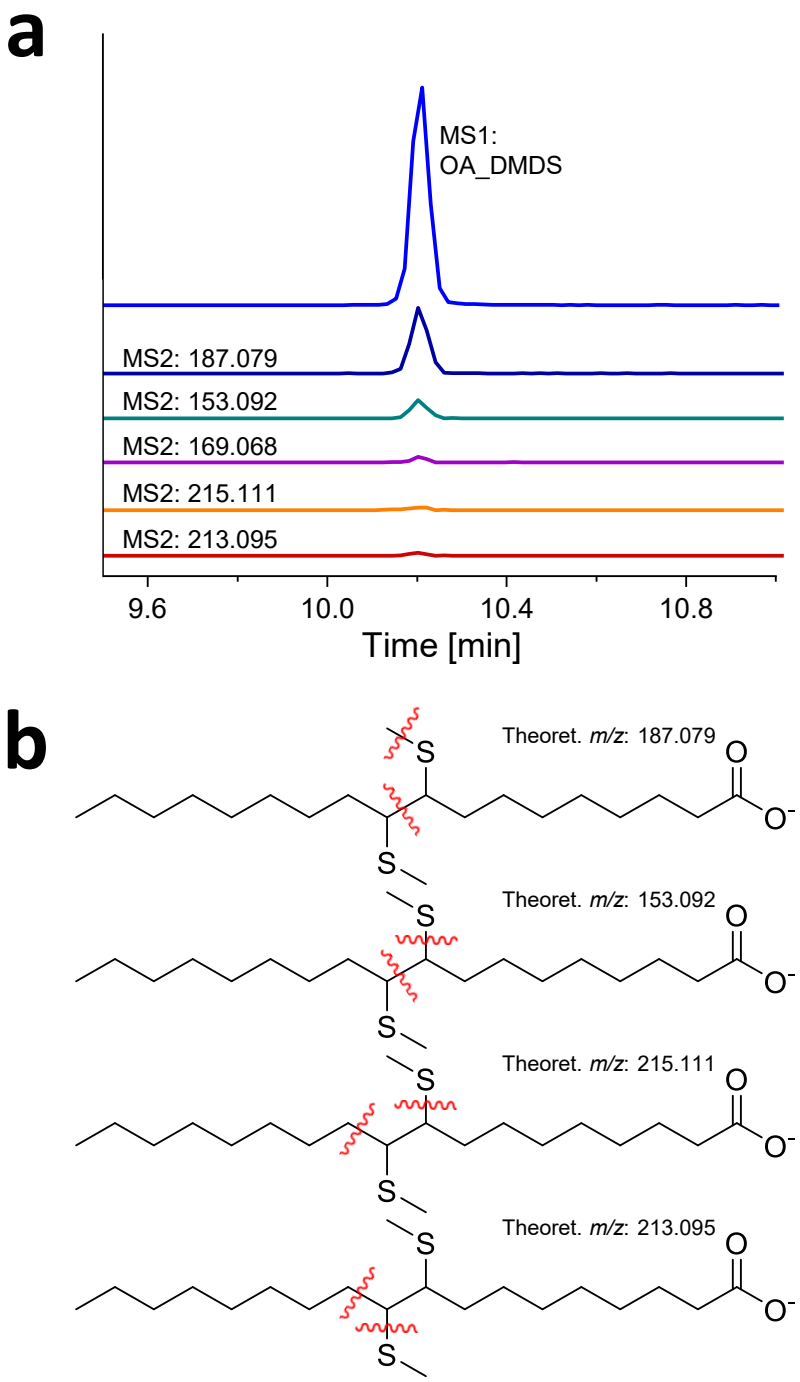

Figure S3: DMDS-derivatized oleic acid; a: MS1-EIC of mono-derivatized oleic acid (OA) (*m/z* 375.240 ± 0.01 Da) and MS2-EIC of characteristic fragments (for visibility 20-fold increased: *m/z* 187.079, 153.092; 40-fold increased: *m/z* 169.068, 215.111, 213.095); b: proposed fragmentation patterns

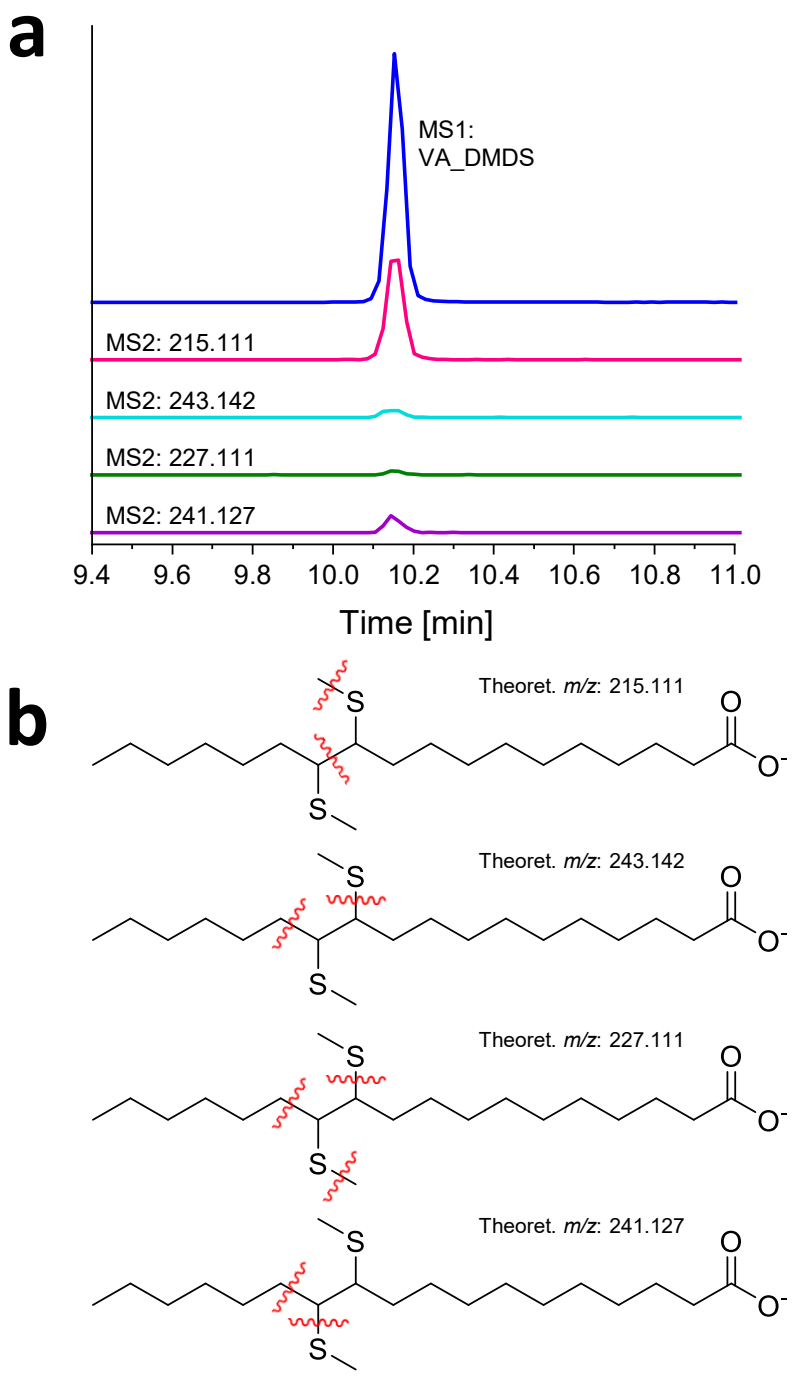

Figure S4: DMDS-derivatized cis-vaccenic acid; a: MS1-EIC of mono-derivatized cis-vaccenic acid (VA) (*m/z* 375.240 ± 0.01 Da) and MS2-EIC of characteristic fragments (for visibility 20-fold increased: *m/z* 215.111; 60-fold increased: *m/z* 243.142, 227.111, 241.127); b: proposed fragmentation patterns.

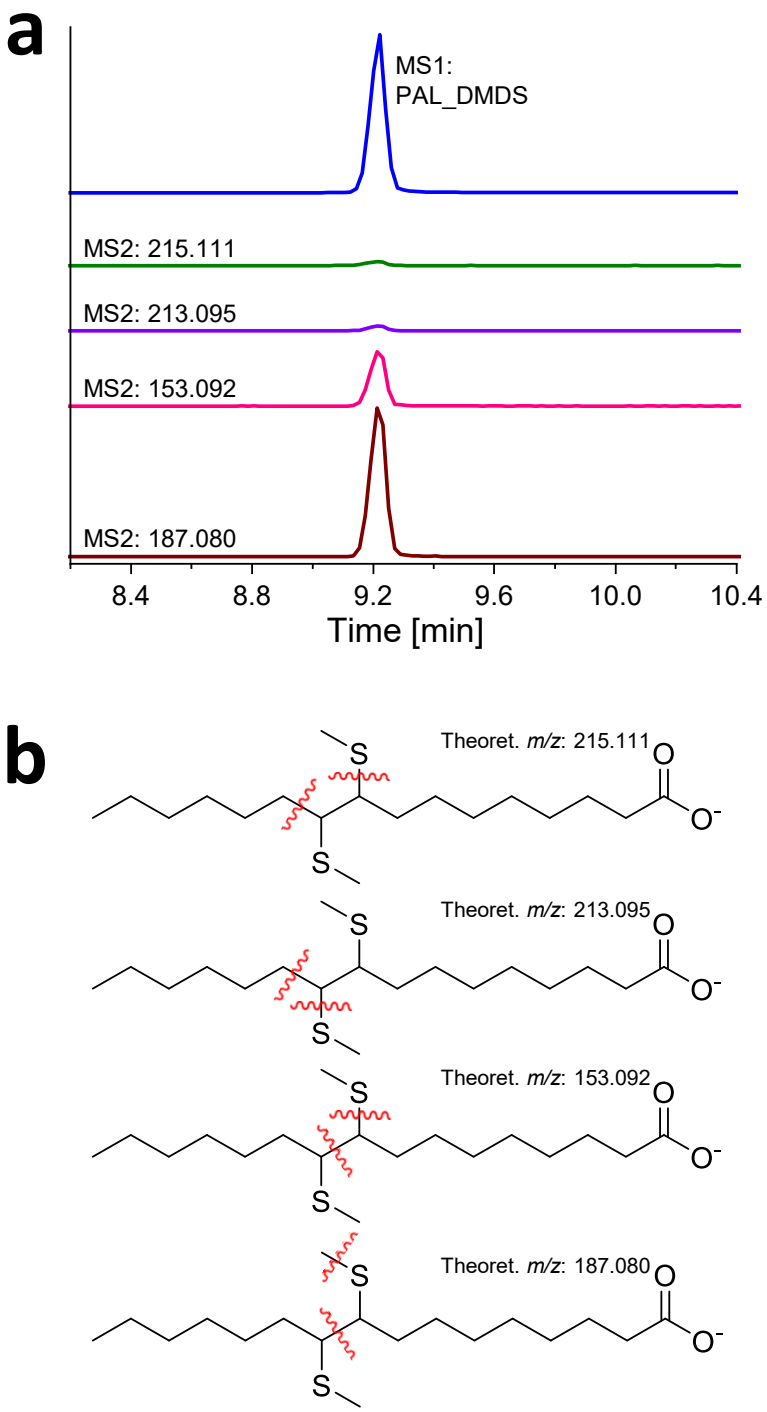

Figure S5: DMDS-derivatized palmitoleic acid; a: MS1-EIC of mono-derivatized palmitoleic acid (PAL) (*m/z* 347.208 ± 0.01 Da) and MS2-EIC of characteristic fragments (for visibility 100-fold increased: *m/z* 215.111, 213.095, 153.092, 187.068); b: proposed fragmentation patterns.

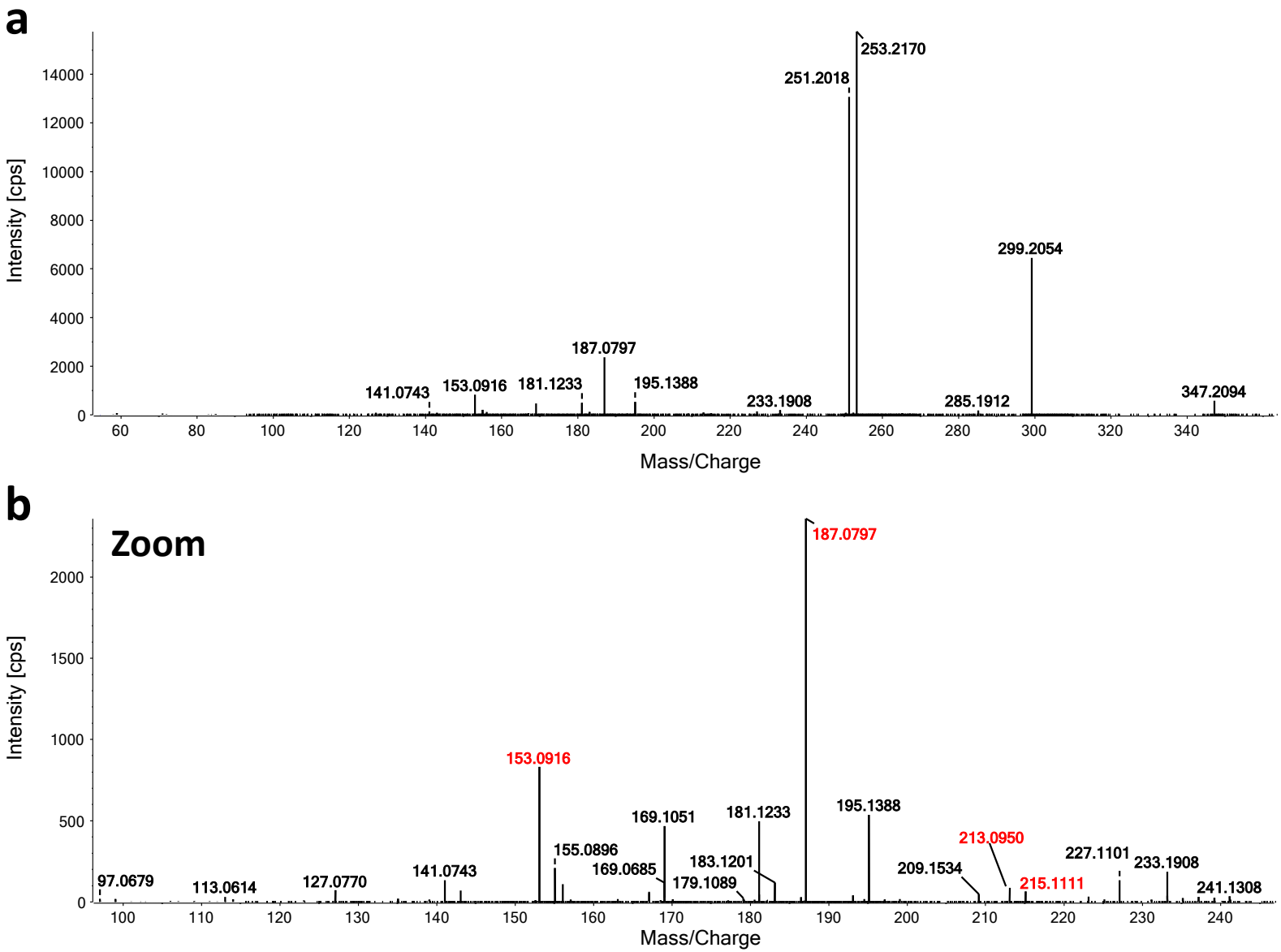

Figure S6: MS2-spectra of DMDS derivatized palmitoleic acid, a: without zoom, b: with zoom in the relevant section

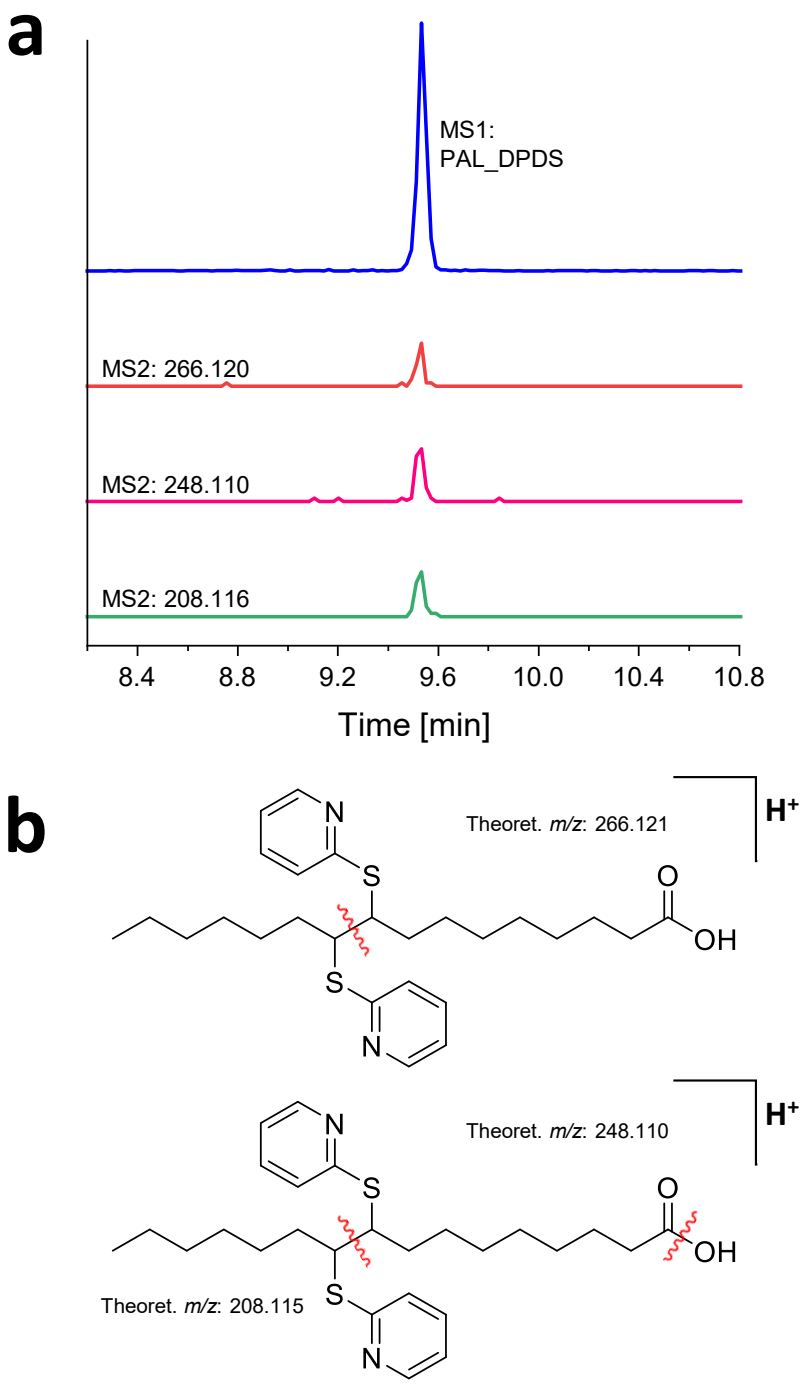

Figure S7: DPDS-derivatized palmitoleic acid (PAL), detected as $[M+H]^+$; a: MS1-EIC of mono-derivatized palmitoleic acid (PAL, *m/z* 475.245 ± 0.01 Da) and MS2-EIC of possible fragmentation products (60-fold increased for visibility); b: Structure of PAL-DPDS derivates and proposed fragmentation patterns.

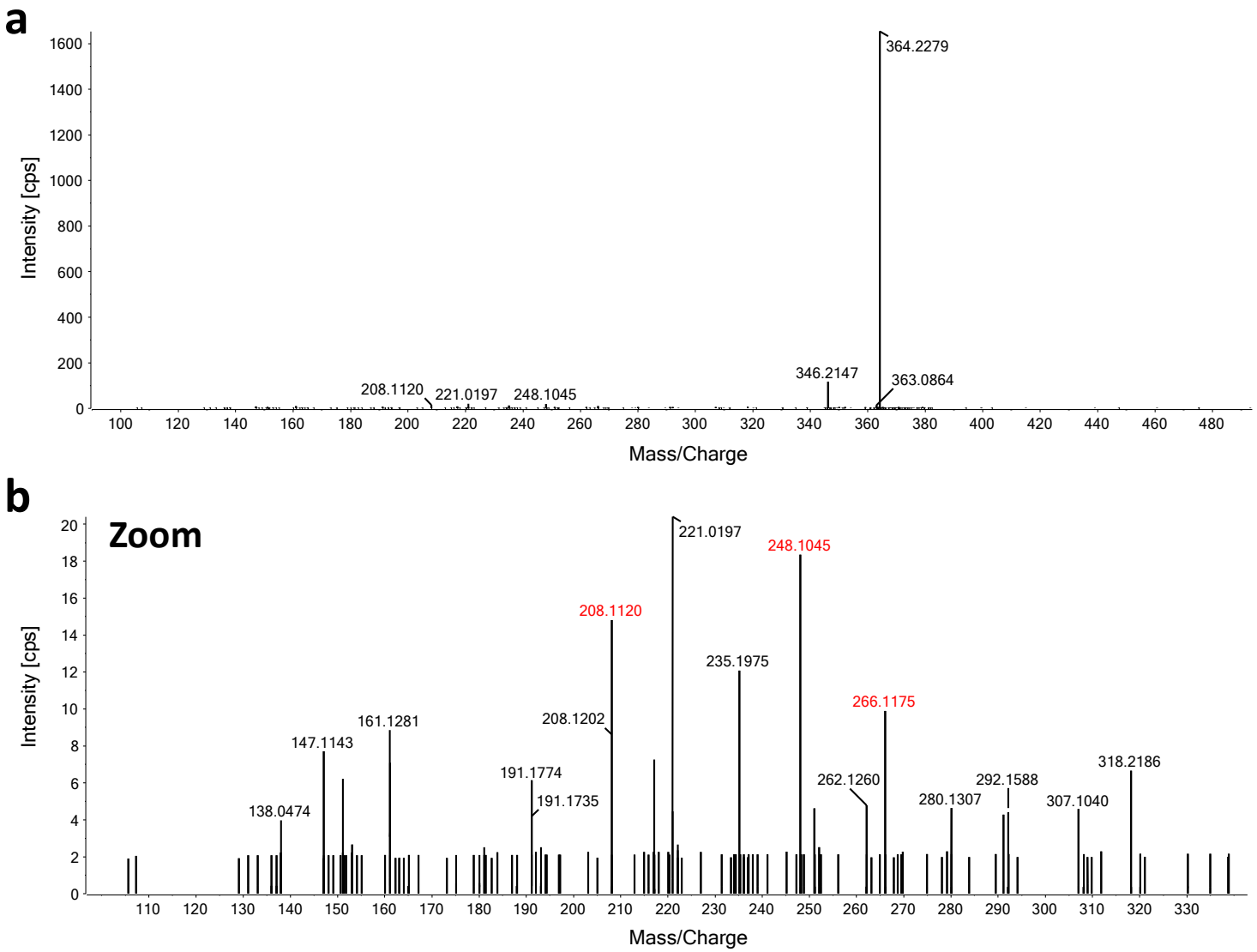

Figure S8: MS2-spectra of DPDS derivatized palmitoleic acid, a: without zoom, b: with zoom in the relevant section

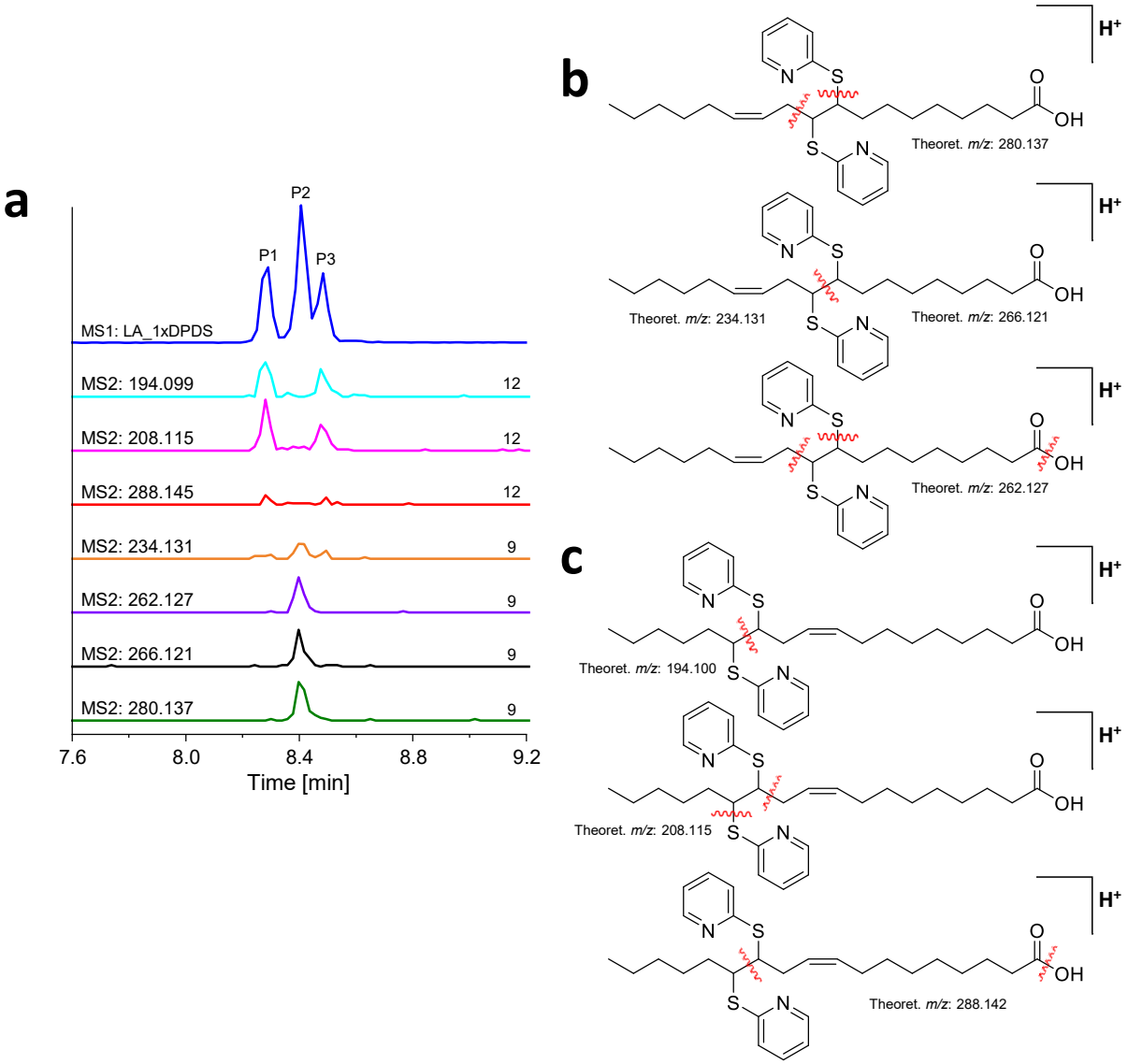

Figure S9: DPDS-derivatized linoleic acid (C18:2n-6,9), detected as $[M+H]^+$; a: MS1-EIC of mono-derivatized linoleic acid (blue; *m/z* 501.260 ± 0.01 Da) from TOF-MS scan and MS2 EICs (CE: 45 V) of its fragments (50-fold multiplied for visibility) from PIS (MRM-HR) of mono-derivatized linoleic acid; b: tentative fragmentation patterns for double bond position 9; c: tentative fragmentation patterns for double bond position 12

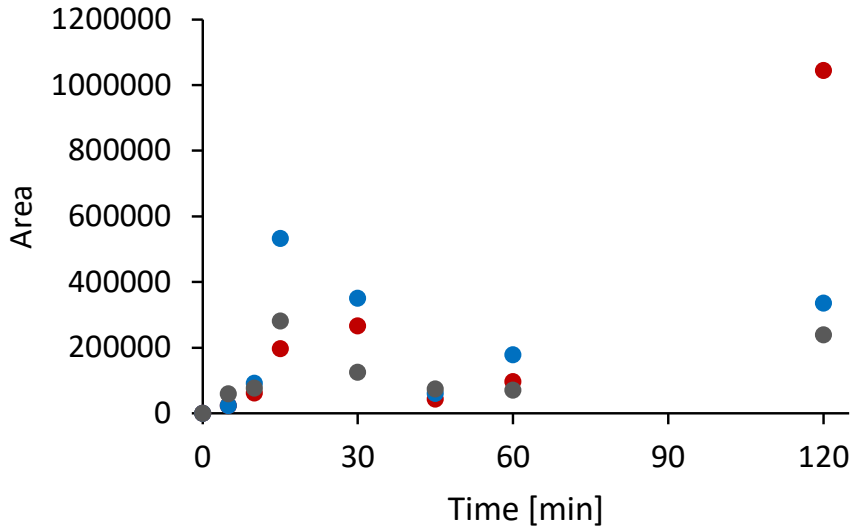

Figure S10: DPDS-derivatized linoleic acid; kinetic study (n=3) displays fluctuations between the replicates and different timepoints.

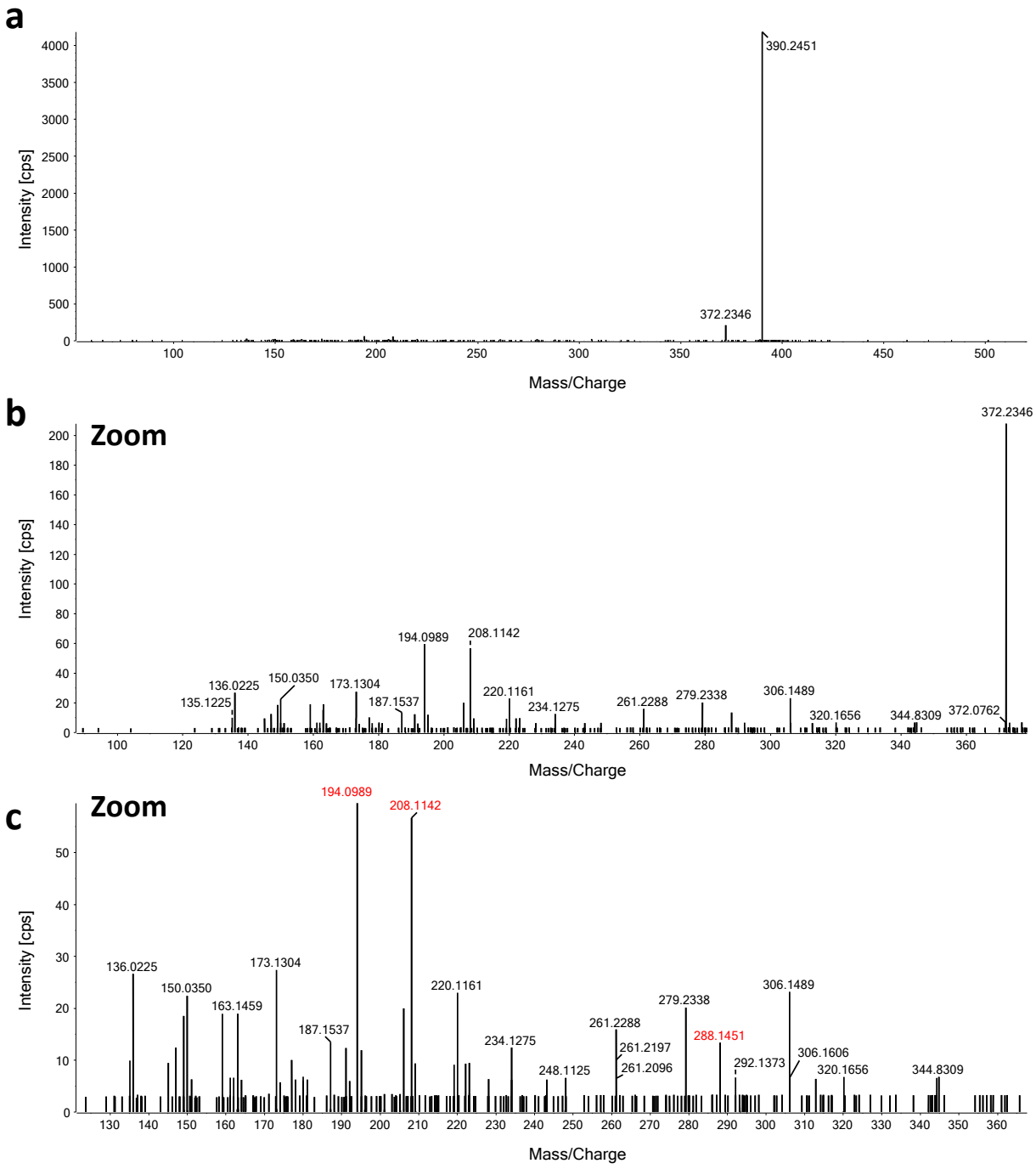

Figure S11: MS2-spectra of DPDS derivatized linoleic acid (first eluting peak, equals the one of the third eluting peak), a: without zoom, b: with zoom in the relevant section, c: with zoom in the relevant section (smaller mass range).

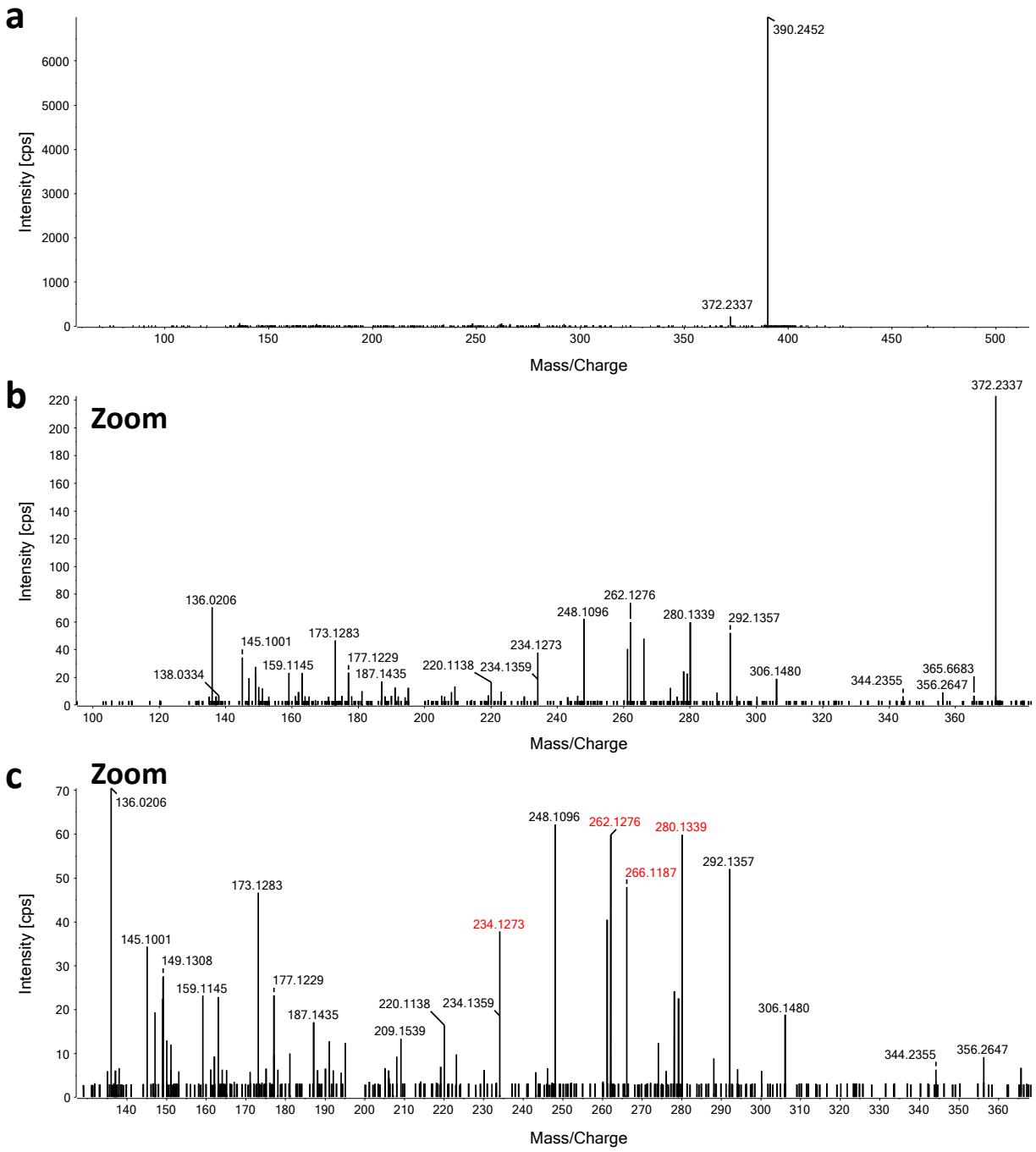

Figure S12: MS2-spectra of DPDS derivatized linoleic acid (second eluting peak), a: without zoom, b: with zoom in the relevant section, c: with zoom in the relevant section (smaller mass range).

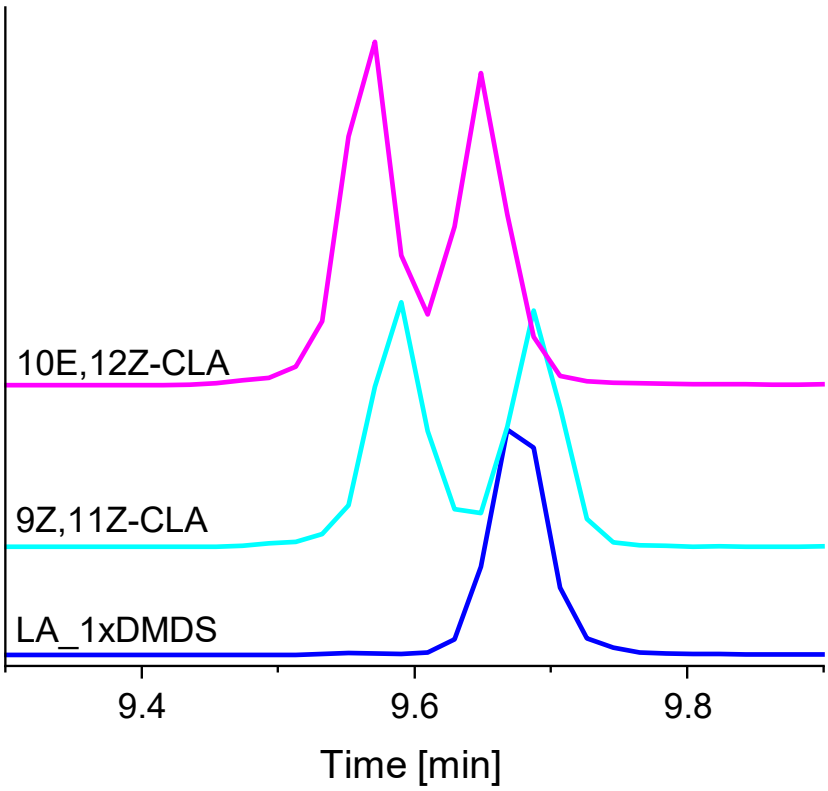

Figure S13: MS1-EIC of DMDS-derivatized 10E,12Z-conjugated linoleic acid (CLA), 9Z,11Z-conjugated linoleic acid (*m/z* 373.224 ± 0.01 Da) and linoleic acid (double bonds position 9 and 12, *m/z* 373.224 ± 0.01 Da)

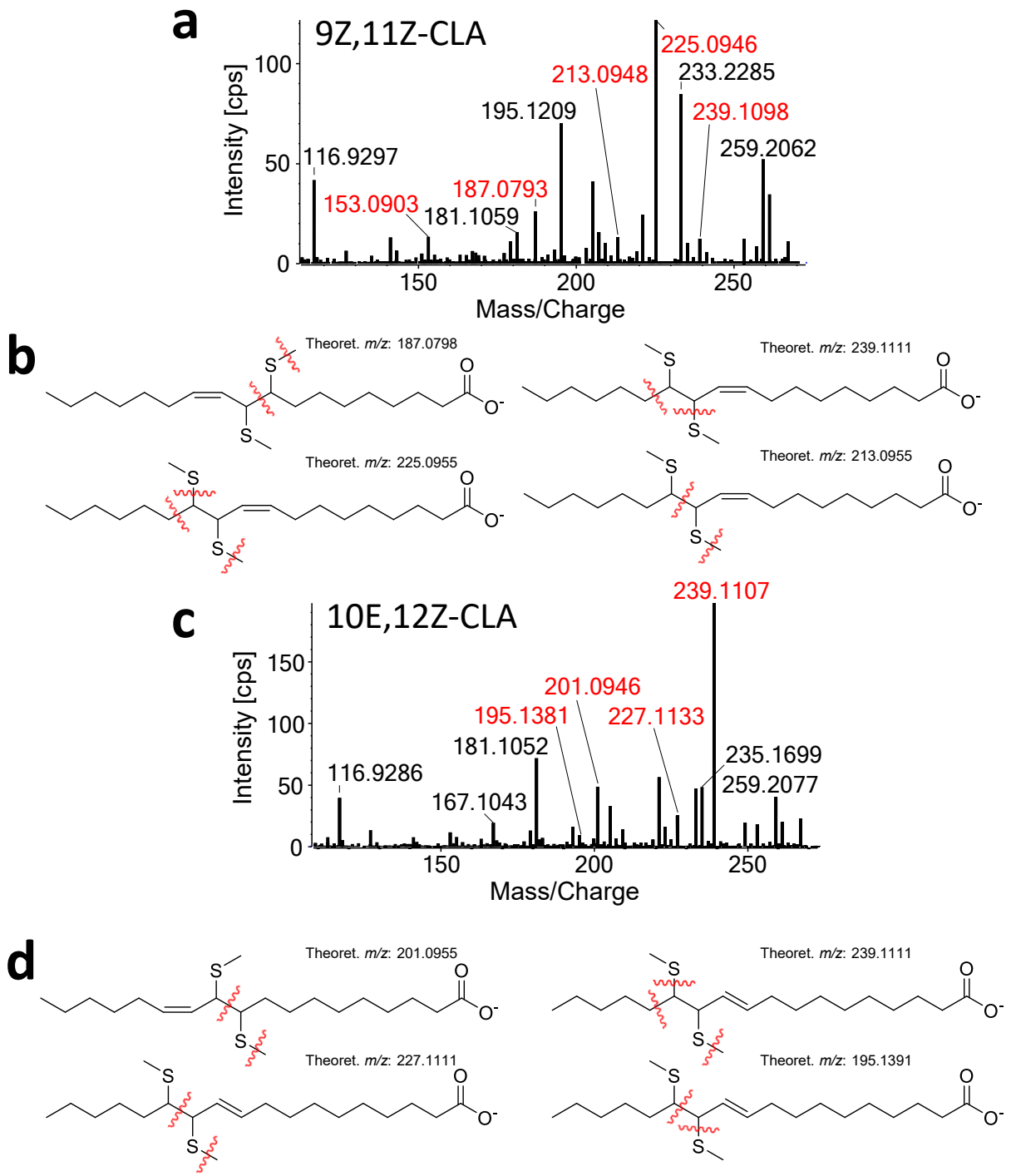

Figure S14: DMDS-derivatized conjugated linoleic acids (9Z,11Z-CLA; 10E,12Z-CLA); a: MS2 spectrum of derivatized 9Z,11Z-CLA (*m/z* 373.224 ± 0.01 Da); b: tentative fragmentation patterns of 9Z,11Z-CLA leading to characteristic fragments (position 9: *m/z* 187.079, 153.090; position 12: *m/z* 213.095, 239.111, 225.095); c: MS2 spectrum of derivatized 10E,12E-CLA (*m/z* 373.224 ± 0.01 Da); d: tentative fragmentation patterns of 10E,12Z-CLA leading to characteristic fragments (position 10: *m/z* 201.095; position 12: *m/z* 195.139, 227.111, 239.111).

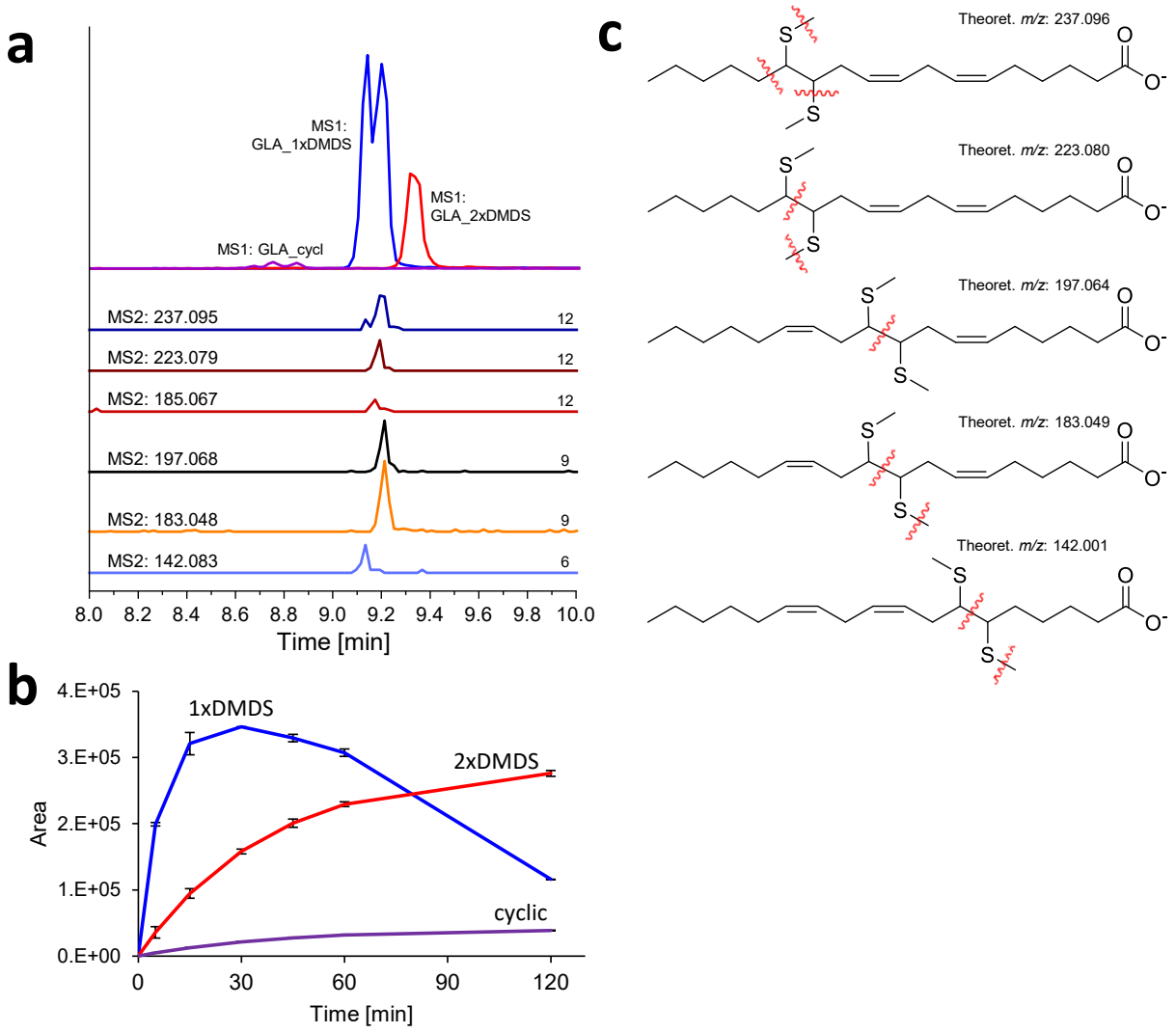

Figure S15: DMDS-derivatized γ-linolenic acid (C18:3n-6,9,12); a: MS1-EIC of mono-derivatized γ-linolenic acid (blue; *m/z* 371.208 ± 0.01 Da), bis-derivatized γ-linolenic acid (red; *m/z* 465.200 ± 0.01 Da) and cyclic products (purple, *m/z* 403.178 ± 0.01 Da) from TOF-MS scan, MS2-EICs (CE: 45 V) of fragments (for visibility 100-fold increased: *m/z* 197.068, 183.048; 300-fold increased: *m/z* 142.083, 185.067, 223.079, 237.095) from PIS (MRM-HR) of mono-derivatized γ-linolenic acid; b: derivatization kinetic (fitted, mono-derivatized: ExpGrowDec, bis-derivatized: BoxLucas1, cyclic product: BoxLucas1); c: tentative fragmentation patterns leading to characteristic fragments

.

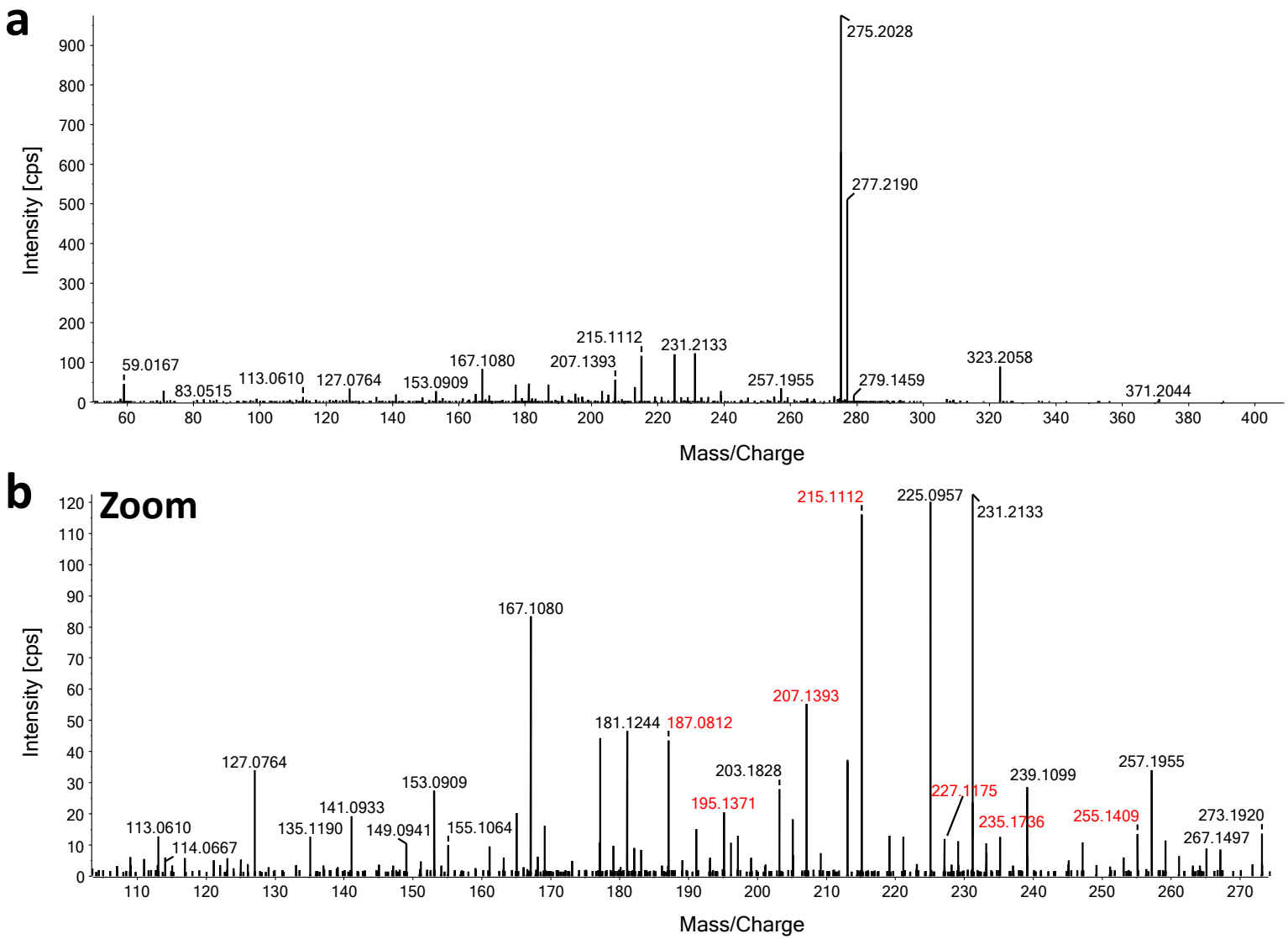

Figure S16: MS2-spectra of DMDS derivatized α-linolenic acid, a: without zoom, b: with zoom in the relevant section.

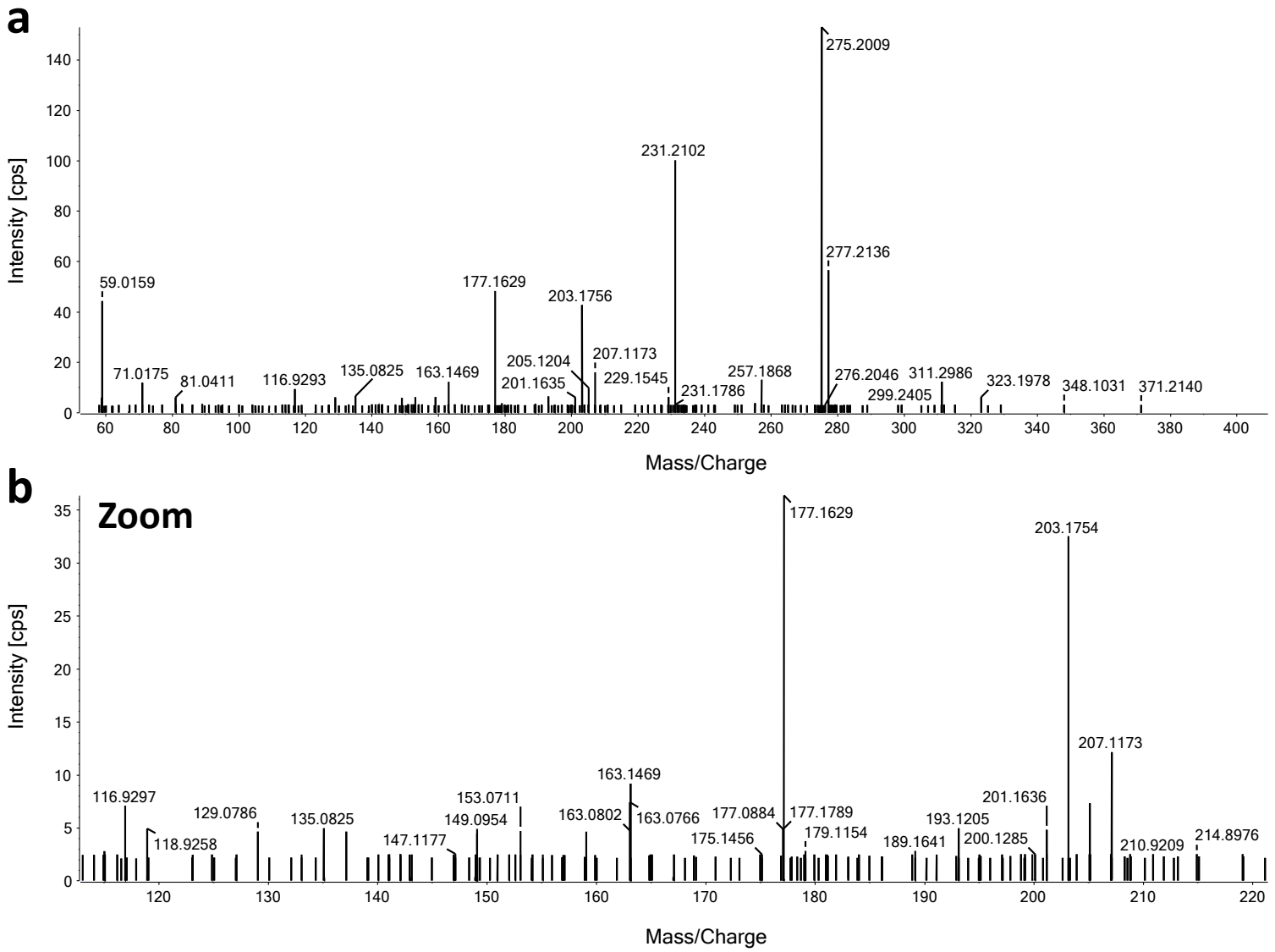

Figure S17: MS2-spectra of DMDS derivatized γ-linolenic acid (first eluting peak), a: without zoom, b: with zoom in the relevant section.

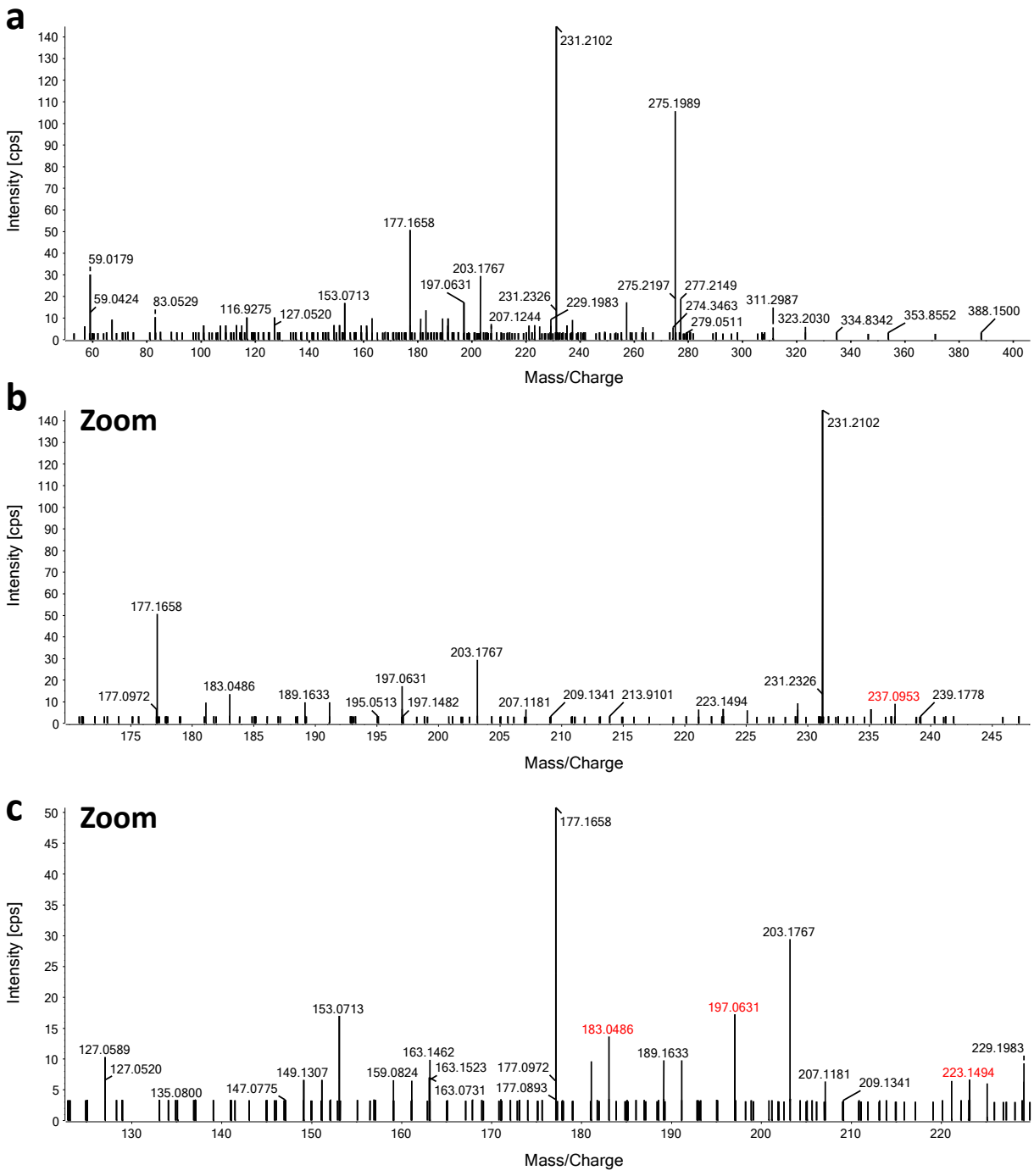

Figure S18: MS2-spectra of DMDS derivatized γ-linolenic acid (second eluting peak), a: without zoom, b: with zoom in the relevant section, c: with zoom in the relevant section (smaller mass range).

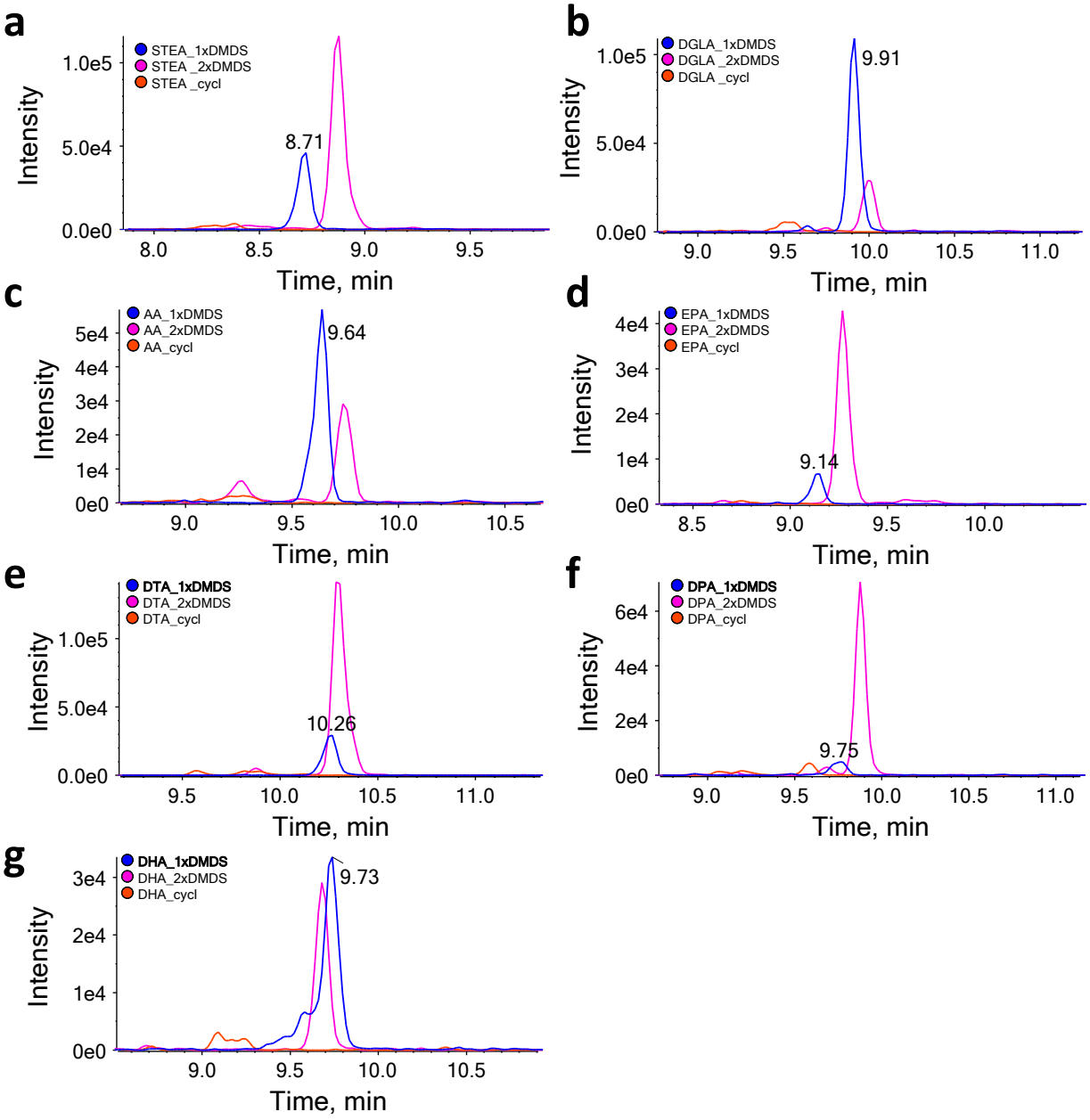

Figure S19: EICs of DMDS mono-/bis-derivatized and cyclic products of polyunsaturated fatty acids, from SWATH measurement of PUFA-Mix; a: Stearidonic acid (STEA, mono: *m/z* 369.193, bis: *m/z* 463.184, cyclic: *m/z* 401.163); b: Dihomo-γ-linolenic acid (DGLA, mono: *m/z* 399.240, bis: *m/z* 493.231, cyclic: *m/z* 431.210); c: Arachidonic acid (AA, mono: *m/z* 397.224, bis: *m/z* 491.215, cyclic: *m/z* 429.194); d: Eicosapentaenoic acid (EPA, mono: *m/z* 395.208, bis: *m/z* 489.200, cyclic: *m/z* 427.178); e: Docosatetraenoic acid (DTA, mono: *m/z* 425.255, bis: *m/z* 519.246, cyclic: *m/z* 457.225); f: Docosapentaenoic acid (DPA, mono: *m/z* 423.240, bis: *m/z* 517.231, cyclic: *m/z* 455.210); g: Docosahexaenoic acid (DHA, mono: *m/z* 421.224, bis: *m/z* 515.215, cyclic: *m/z* 453.194); Gaussian smoothed..

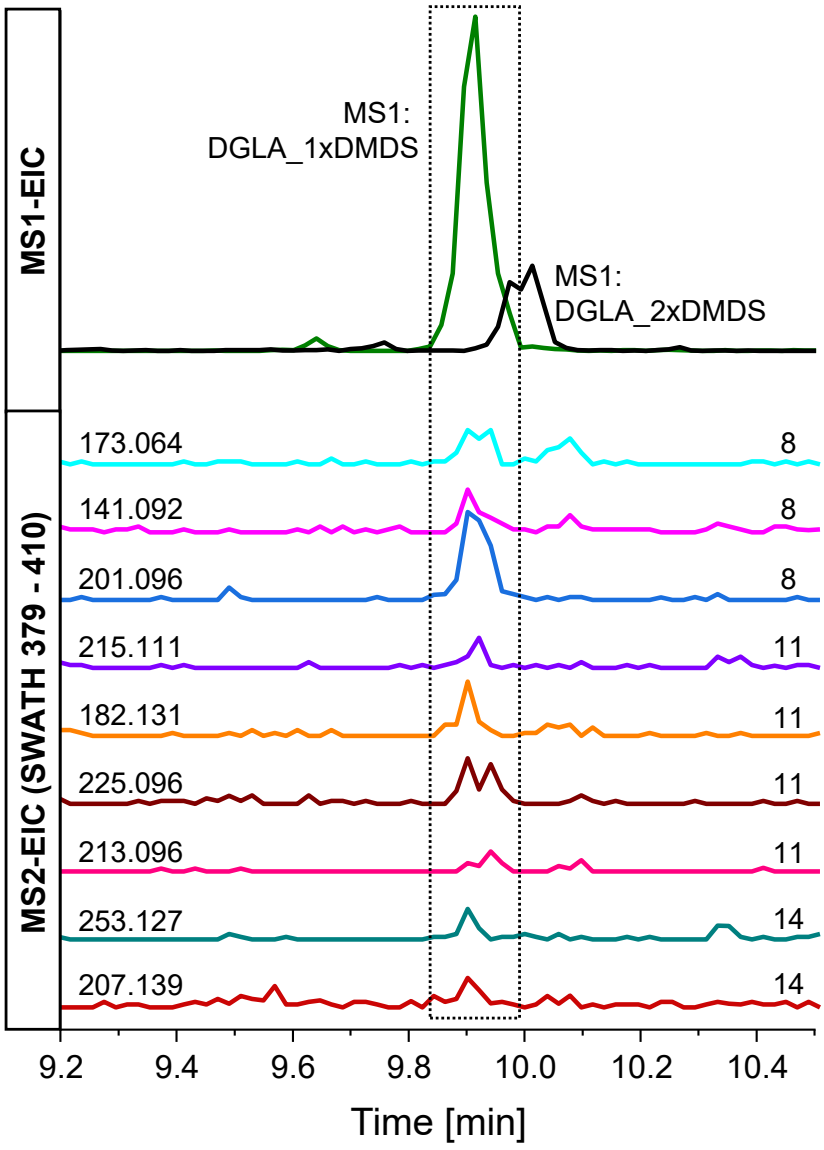

Figure S20: DMDS-derivatized dihomo-γ-linolenic acid (DGLA; C20:3n-6,9,12); MS1-EIC of mono-derivatized (*m/z* 399.239 ± 0.01 Da) and di-derivatized DGLA (*m/z* 493.231 ± 0.01 Da) and MS2-EIC of possible characteristic fragments from SWATH-window *m/z* 379-410 (60-fold increased for visibility).

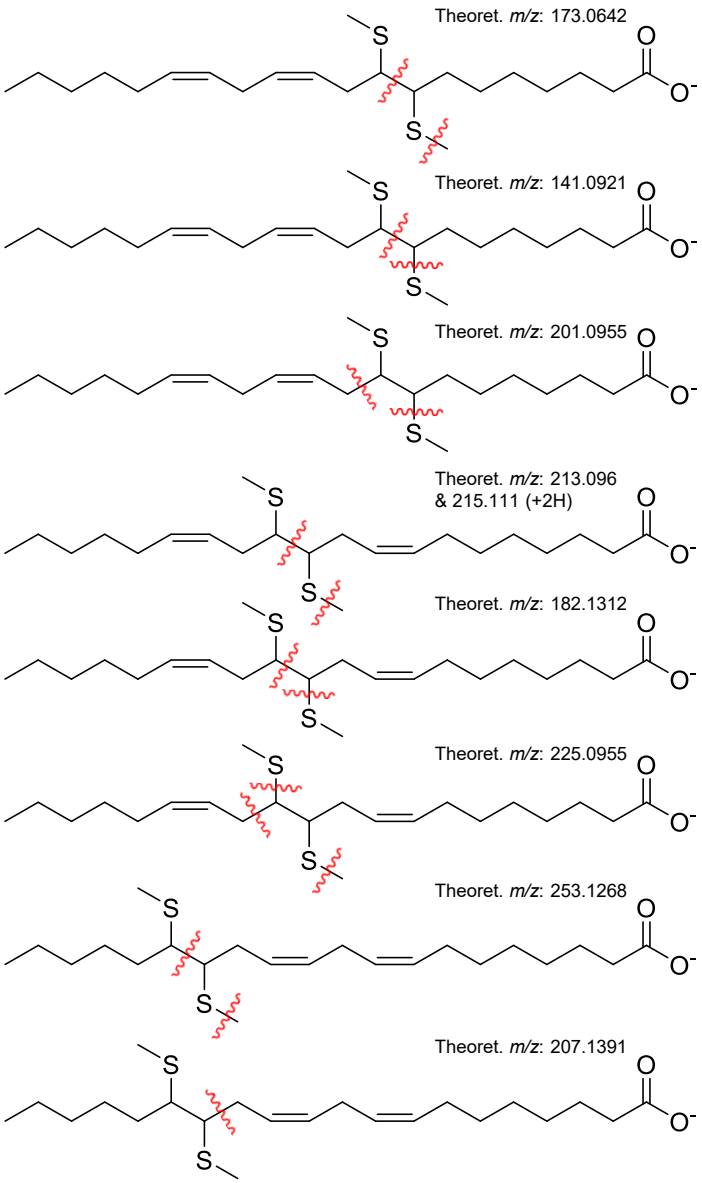

Figure S21: Proposed fragmentation patterns of mono-derivatized dihomo-γ-linolenic acid (DGLA; C20:3n-6,9,12).

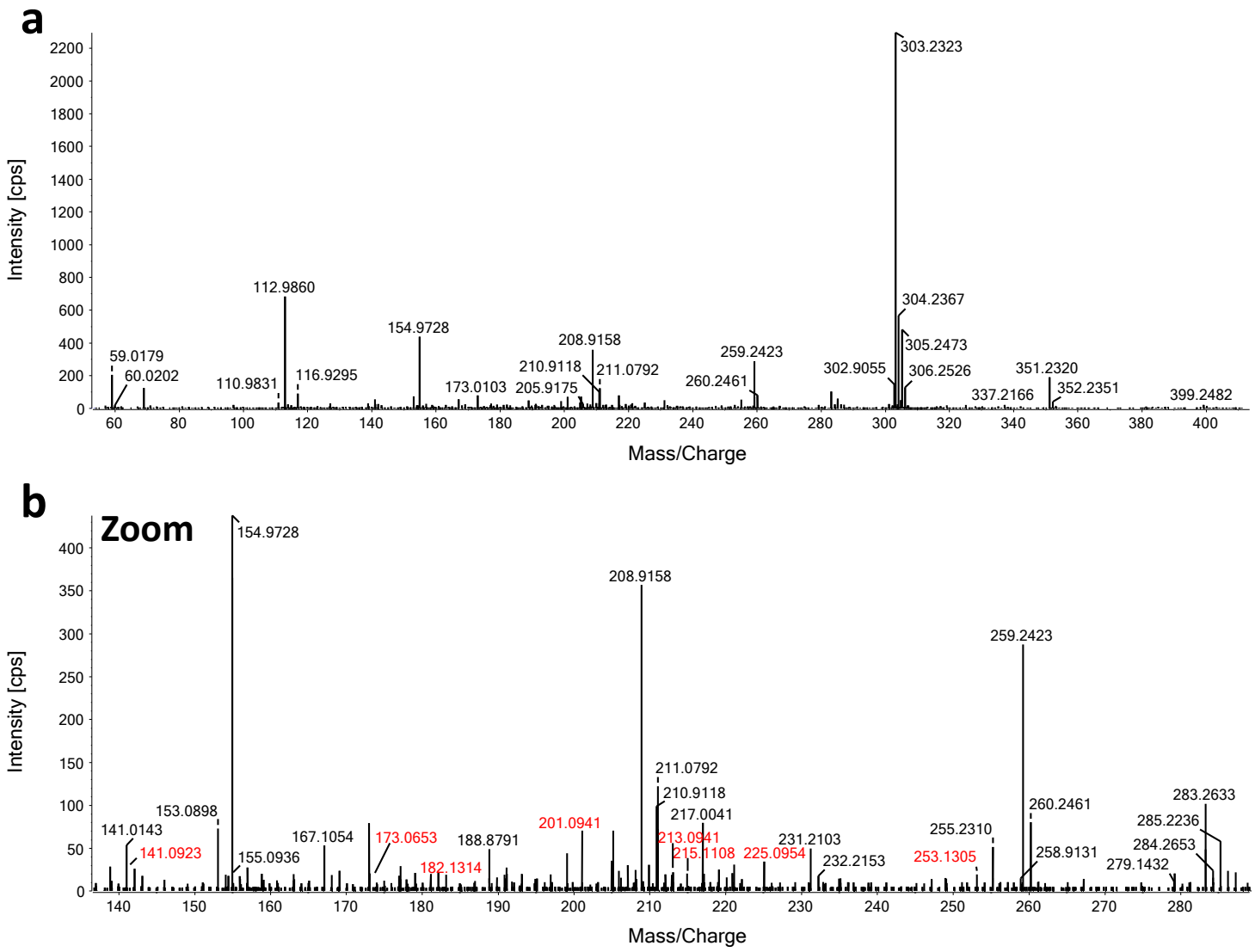

Figure S22: MS2-spectra of DMDS derivatized dihomo-γ-linolenic acid (DGLA; C20:3n-6,9,12), a: without zoom, b: with zoom in the relevant section

Table S7: Equations used in Origin for curve fitting of the derivatization kinetic curves.

Analyte and derivatization agent	Used equation for curve fitting	Variables
OA, DMDS derivatized	$f(x) = a * (1 - e^{-k*x})$	*a:* 186065.7 *k:* 0.0723 min^{-1}
LA, DMDS derivatized	$f(x) = a * (1 - e^{-k*x})$	*a:* 100918 *k:* 0.0289 min^{-1}
ALA, 1xDMDS derivatized	$f(x) = y_0 + A_d + A_g * \left(e^{-\frac{x_c}{t_g}} - e^{-\frac{x}{t_g}}\right); if\ x \leq x_c$ $f(x) = y_0 + A_d * e^{-\frac{x-x_c}{t_d}}; if\ x > x_c$	y_0: 888570 x_c: 45 min A_g:855765 t_g: 8.85 min A_d: -61657.5 t_d: -47.8 min
ALA, 2x DMDS derivatized	$f(x) = a * (1 - e^{-k*x})$	*a:* 1133333 *k:* 0.0203 min^{-1}
ALA, cyclic DMDS product	$f(x) = a * (1 - e^{-k*x})$	*a:* 150829 *k:* 0.0164 min^{-1}
GLA, 1xDMDS derivatized	$f(x) = y_0 + A_d + A_g * \left(e^{-\frac{x_c}{t_g}} - e^{-\frac{x}{t_g}}\right); if\ x \leq x_c$ $f(x) = y_0 + A_d * e^{-\frac{x-x_c}{t_d}}; if\ x > x_c$	y_0: 397412.9 x_c: 30 min A_g: 348496.6 t_g: 5.9 min A_d: -51081.2 t_d: -52.7 min
GLA, 2x DMDS derivatized	$f(x) = a * (1 - e^{-k*x})$	*a:* 287989.3 *k:* 0.0265 min^{-1}
GLA, cyclic DMDS product	$f(x) = a * (1 - e^{-k*x})$	*a:* 40696.9 *k:* 0.0251 min^{-1}
OA, DPDS derivatized	$f(x) = a * (1 - e^{-k*x})$	*a:* 177910 *k:* 0.0681 min^{-1}

3.3.8.1 References

[1] V.B. O'Donnell, E.A. Dennis, M.J.O. Wakelam, S. Subramaniam, LIPID MAPS: Serving the next generation of lipid researchers with tools, resources, data, and training, Science Signaling 12(563) (2019) eaaw2964. https://doi.org/doi:10.1126/scisignal.aaw2964.

[2] G. Liebisch, J.A. Vizcaíno, H. Köfeler, M. Trötzmüller, W.J. Griffiths, G. Schmitz, F. Spener, M.J.O. Wakelam, Shorthand notation for lipid structures derived from mass spectrometry, Journal of Lipid Research 54(6) (2013) 1523-1530. https://doi.org/https://doi.org/10.1194/jlr.M033506.

[3] N. Richter, J.T. Dillon, D.M. Rott, M.A. Lomazzo, C.T. Seto, Y. Huang, Optimizing the yield of transient mono-dimethyl disulfide adducts for elucidating double bond positions of long chain alkenones, Organic Geochemistry 109 (2017) 58-66. https://doi.org/10.1016/j.orggeochem.2017.02.003.

Danksagung

Hier möchte ich gerne noch die Gelegenheit nutzen um den vielen Menschen zu danken die mich auf dem Weg zur Erarbeitung dieser Dissertation über die vergangen Jahre begleitet und unterstützt haben.

Zu allererst möchte ich Prof. Dr. Michael Lämmerhofer danken für die Möglichkeit dieses Dissertationsprojekt während meiner Promotionszeit bearbeiten zu dürfen. Danke für die vielen wissenschaftlichen Diskussionen, die Unterstützung mit deiner analytischen Expertise und die Möglichkeit mich wissenschaftlich und zwischenmenschlich weiter zu entwickeln. Ebenso möchte ich mich bedanken für die vielen Möglichkeiten an (internationalen) Konferenzen teilzunehmen, spannende Industrieprojekte zu bearbeiten und international Kontakte zu knüpfen.

Dankeschön an Prof. Matthias Gehringer für die Unterstützung bei chemischen Fragen und für die Übernahme des Zweitgutachtens dieser Arbeit.

Danke auch an Eveline Wachendorfer, Michaela Friedrichs und Ingrid Straub für die schönen Gespräche und dass ihr dafür gesorgt habt, dass ich im Bürokratiedschungel nicht untergehe.

Ein großes Dankeschön an alle ehemaligen und aktuellen Doktoranden und Mitarbeitern des Arbeitskreises für die Wegbegleitung in den letzten Jahren: Adrian Brun, Dr. Bernhard Drotleff, Dr. Carlos Calderón Castro, Dr. Feiyang Li, Dr. Kristina Dittrich, Dr. Malgorzata Cebo, Dr. Peng Li, Dr. Ryan Karongo, Dr. Simon Jaag, Dr. Stefan Neubauer, Dr. Xiaoqing Fu, Dr. Ece Aydin, Franz Fießinger, Kristian Serafimov, Min Su, Mirna Maalouf, Philipp Seyfried, Yachao Hao, Zijing Xu. Ein besonders großes Dankeschön an Dr. Stefanie Bäurer, Dr. Christian Geibel, Marc Wolter und Dr. Adrian Sievers-Engler für die schöne Einführung in die Analytik, Massenspektrometrie und die private und berufliche Unterstützung. Dankeschön an Cornelius Knappe für die technische Expertise, viele spannende Diskussionen und geteilte Kaffeeleidenschaft. Danke an Benedikt Masberg, Tamara Janker und Niklas Carstensen für nette Gespräche bei vielen Tassen Kaffee und das gemeinsame Bouldern. Dankeschön an Prof. Sylwia Studzińska und Ina Varfaj die mir die polnische und italienische Kultur näher gebracht haben. Es hat mich sehr gefreut euch kennenzulernen.

Ebenso möchte ich allen Doktoranden und Professoren der anderen Arbeitskreisen danken für die schöne Zeit in der Lehre und gemeinsamen Projekten. Hier möchte ich besonders AK Böckler, AK Laufer und AK Lunter hervorheben.

Aus meinem privaten Umfeld möchte ich herzlich all meinen Freunden danken für die zahlreichen gemeinsamen Abende, Konzerte und schönen Erlebnisse.

Friedi möchte ich besonders herzlich danken: dafür dass du an meiner Seite bist, mich unaufhörlich unterstützt und immer ein offenes Ohr selbst in stressigen Situationen hast.

Zu guter Letzt möchte ich meinen Eltern Marina, Peter und meinem Bruder Martin für die unendliche Unterstützung danken. Ohne euch wäre das alles nicht möglich gewesen!